Supramolecular aspects of some quinone derivatives and coordination polymer of flexible dicarboxylic acids

A Dissertation submitted to the
Indian Institute of Technology Guwahati as
partial fulfillment for the Degree of
Doctor of Philosophy
in Chemistry

Submitted by

Wangkheimayum Marjit Singh

Department of Chemistry

Indian Institute of Technology Guwahati

July 2010

Dedicated to My Beloved Sisters

Statement

I hereby declare that this thesis entitled "**Supramolecular aspects of some quinone derivatives and coordination polymer of flexible dicarboxylic acids**" is the outcome of research work carried out by me under the supervision of Prof. Jubaraj B. Baruah, at the Department of Chemistry, Indian Institute of Technology Guwahati, India.

In keeping with the general practice of reporting scientific observations, due acknowledgement has been made whenever work described here has been based on the findings of other investigators.

IIT Guwahati
July 14, 2010

Wangkheimayum Marjit Singh

Certificate

This is to certify that Wangkheimayum Marjit Singh has been working under my supervision since July, 2006 as a regular registered Ph. D. student. I am forwarding his thesis entitled "**Supramolecular aspects of some quinone derivatives and coordination polymer of flexible dicarboxylic acids**" being submitted for the Ph. D. (Science) Degree of this Institute.

I certify that he has fulfilled all the requirements according to the rules of this Institute regarding the investigations embodied in his thesis and this work has not been submitted elsewhere for a degree.

IIT Guwahati
July 14, 2010

Prof. Jubaraj B. Baruah

Acknowledgements

The enlightening experience of doing science under the guidance of Prof. Jubaraj B. Baruah can hardly be described in words. It is my immense pleasure to express my sincere gratitude to my guide, for his precious suggestion, incisive guidance and decisive insights during the entire course of Ph.D. research. The numerous discussions and interactions I had with him expanded my horizons to hitherto unknown frontiers of science and knowledge. I am indebt to this wonderful person for all that he has given me and above all for motivating me towards scientific research.

I would like to acknowledge my sincere gratitude to all my doctoral committee members, Dr. Anil Kumar Saikia, Dr. Biplab Mondal, and Dr. Mihir Kumar Purkait for their insightful advices, earnest suggestions and corrections for nourishment of the work. I am also grateful to the entire faculty and staff in the Department of Chemistry, Indian Institute of Technology Guwahati for providing a wonderful work atmosphere throughout this period.

I would like to thank my group members Rupam Sarma, Devendra Singh, Dipjyoti Kalita, Babulal Das, Bigyan Ranjan Jali, Bhaskar Nath, Himansu Deka and other group members, department of chemistry for their timely help, support and for the wonderful time we shared during this period. I would like to give my special thanks to my lab seniors Dr. Rupam Jyoti Sarma, Dr. Nilotpal Barooah and Dr. Anirban Karmakar with whom I had an opportunity to work.

I acknowledge the Indian Institute of Technology Guwahati and the Department of Chemistry for offering me the state of art facilities. I also thank Central Instrument Facility, IIT Guwahati for providing the instrumental facility. The financial support from Council of Scientific and Industrial Research (CSIR), New Delhi is duly acknowledged.

Finally, my Ph. D. endeavor could not be completed without the endless love, unending support, tolerance and blessings from my family. I wish to express my sincere gratitude to my parents, my brothers and sisters. They are the main soul and inspiration for each and every step that I achieve in my life.

Preview

The chemistry of quinones and its derivatives is one of the important aspects of synthetic organic and medicinal chemistry. Quinone compounds have various applications which may involve some simple molecules or complex macromolecules containing quinones. The thesis entitled as "**Supramolecular aspects of some quinone derivatives and coordination polymer of flexible dicarboxylic acids**" deals with the synthesis, characterization, properties and supramolecular aspects of a few quinone derivatives. It also deals with the functionalization of quinone derivatives to flexible dicarboxylic acids for the synthesis and characterization of coordination polymers. The structural aspects are investigated with objectives to understand their self-assembly processes. Another importance of this research is that some quinone compounds presented in the thesis can be having pharmacological and therapeutic uses.

The content of the thesis is divided into six chapters which are described below.

Chapter 1: Introduction

With view to define the above study we introduce a brief review of the state of art of the existing literature of quinone and its derivatives and various aspects related to synthesis, structure, properties and applications in chapter 1. The structural and optical properties of topologically interesting molecules are also discussed from the viewpoint of the electron acceptor nature of the quinone motif. The polymorphism, co-ordination chemistry and supramolecular assemblies of quinone and its derivatives are also analyzed with suitable examples.

Chapter 2: Carbon-sulphur and carbon-nitrogen bond formation reactions of quinones

This chapter describes some of important aspects related to the synthesis of quinone derivatives through carbon-sulphur and carbon-nitrogen bond formation reactions. Several new quinone derivatives are synthesized and characterized (**fig. 1**).

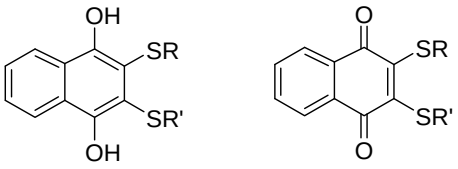

Fig. 1

We also extend our study to synthesize molecules containing two units of quinones connected by different aliphatic and aromatic spacers. Comparative reactivity of amine, thiol and phenolic groups towards quinone is presented. It is observed that the thiols are more reactive than amines and than phenols. We also synthesized various 2,5-bis (alkyl/arylamino)-1,4-benzoquinones from the reaction of various amines with 1,4-benzoquinone in methanol. Some of these compounds were tested for their cell viability against the cancerous pancreatic cancer cell lines Panc-1 and MiaPaCa with thymoquinone molecule as reference; are found to have superior activity against the mention cancerous cell lines.

Chapter 3: Polymorphism in quinone derivatives

Chapter 3 contains polymorphism and structural studies of various quinone derivatives (**fig. 2**). The polymorphism of these quinone derivatives was studied to understand their crystallization conditions and process. The molecular conformations, hydrogen bonding, packing arrangements and their supramolecular behaviour are found to be responsible in giving rise to polymorphs.

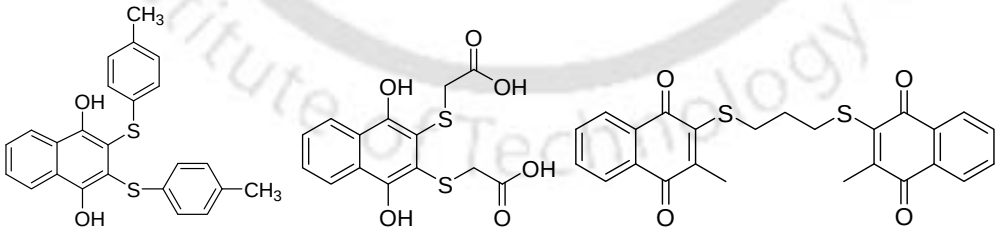

Fig. 2

The conformational polymorphism in these molecules arises due to the orientation of lone pair of electron on sulphur atom, which provides possible orientations across two directly bonded sulphur atoms or two sulphur atoms separated by intervening carbon atoms. The polymorphs also arise due to the difference in weak interactions with

oxygen atom of the quinone as well as, due to the presence of the different orientations of the substituents in the rigid quinone ring and also arise due to differences in crystal packing.

Chapter 4: Structural studies on co-crystals and salt of quinonic carboxylic acids

This chapter 4 describes the synthesis, characterization and structural features of co-crystal and salt of quinonic carboxylic acids (**fig. 3**). This study is done to unearth various weak interactions of quinonic carboxylic acids with different cyclic aromatic amines such as 4,4′-bipyridine and 1,10-phenanthroline and triphenylphosphin oxide. It gives rise to self assembly extended hydrogen bonded networks through the carboxylic acid end groups and the oxygen atoms of quinone motif.

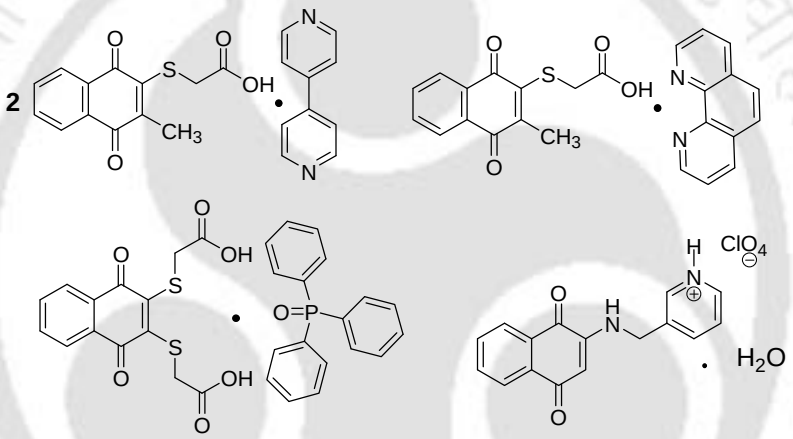

Fig. 3

Based on the hydrogen bond acceptor properties and a strong tendency of the carboxylic acid group to adopt different hydrogen bonded structures, we are able to construct supramolecular assembly governed by various non-covalent interactions such as weak O···H−O and O−H···N C−H···O and C−H···π interactions.

Chapter 5: Carbon-sulphur bond breaking reaction of carboxylic acids attached to quinone to form the metal complexes

Chapter 5 enumerate the carbon-sulphur bond breaking reaction of quinonic carboxylic acid for in situ formation of metal complexes and their utility are described. To understand the synthetic and supramolecular behaviour, the copper(II) complexes $[Cu_2(L_1)_2(bipy)_2]$ and $[Cu_2(L_1)_2(phen)_2][Cu(L_1)(phen)].5H_2O$ of 2-(1,4-dihydro-2-

hydroxy 1,4-dioxonaphthalen-3-ylthio)acetic acid **LH_2** (**scheme 1**) are synthesised and characterized by different spectroscopic techniques.

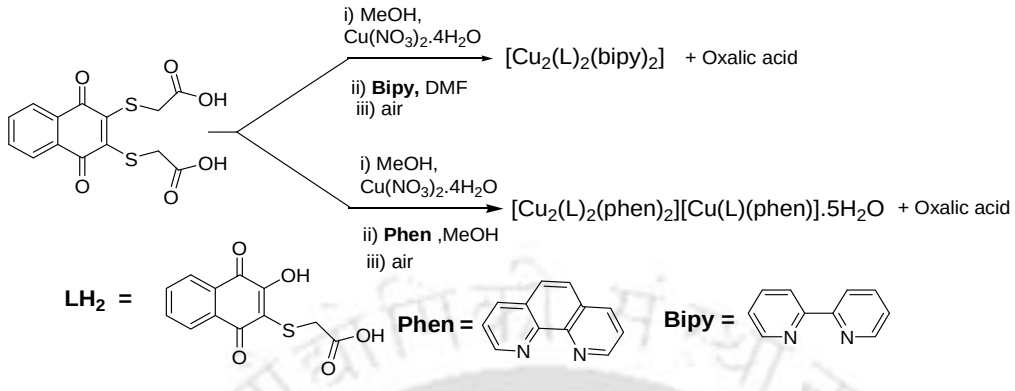

Scheme 1

These copper(II) complexes are synthesized from the carbon-sulphur bond breaking reactions of (3-carboxymethylsulfanyl 1,4-dioxo-1,4-dihydronaphthalen-2-ylsulfanyl)-acetic acid with copper(II) nitrate tetrahydrate in the presence of 2,2'-bipyridine and 1,10-phenanthroline respectively. The synthesis of such type of copper(II) complexes having quinone motif are important as the quinones are good candidates for the electron transfer reactions. In molecular systems electron transfer reactions are fundamental components of life processes. We also described the carbon-sulphur bond cleavage reaction of compound 2-(3-methyl-1,4-dihydronaphthalen-2-yl-sulfanyl)nicotinic acid in the presence of metal ions such as Fe^{+2} and Mn^{+2}. These reactions give S-S bond containing compound **LH_2** and lead to the in situ formation of metal complexes $\{[Fe(phen)_3](L)(LH_2)(7H_2O)\}$ and $[Mn(L)(py)_2(MeOH)_2]_n$ as illustrated in **scheme 2**.

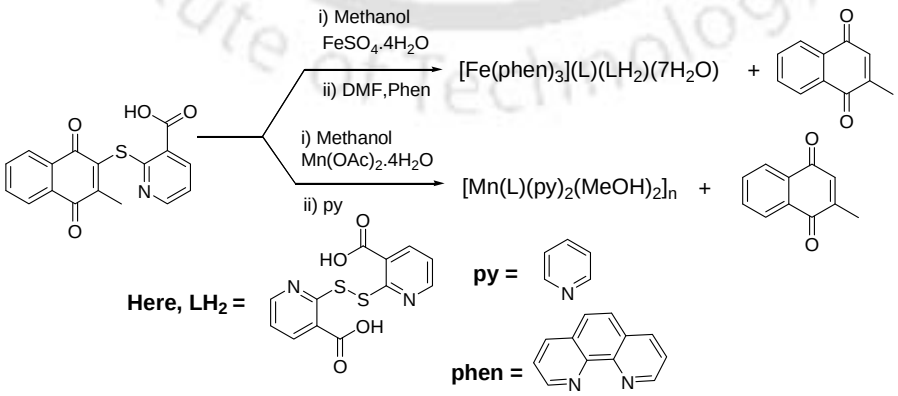

Scheme 2

We also demonstrated the catalytic activity of the iron complex {[Fe(phen)$_3$](L)(LH$_2$)(7H$_2$O)} for epoxidation of alkenes in presence of hydrogen peroxide (**scheme 3**)

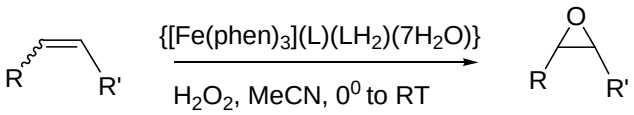

Scheme 3

Various olefinic compounds are converted to corresponding epoxide by catalytic amount of iron(II) complex in very good yields.

Chapter 6: Coordination polymers of flexible dicarboxylic acids

This chapter deals with the synthesis and structure of various coordination polymers of flexible dicarboxylic acids with different metal ions. We describe the synthesis and structure of a one dimensional coordination polymer of manganese(II) carboxylate that contains repeated units of aqua-bridged binuclear manganese carboxylate and the core has close structurally analogy to biological aqua-bridged metal carboxylate (**scheme 4**).

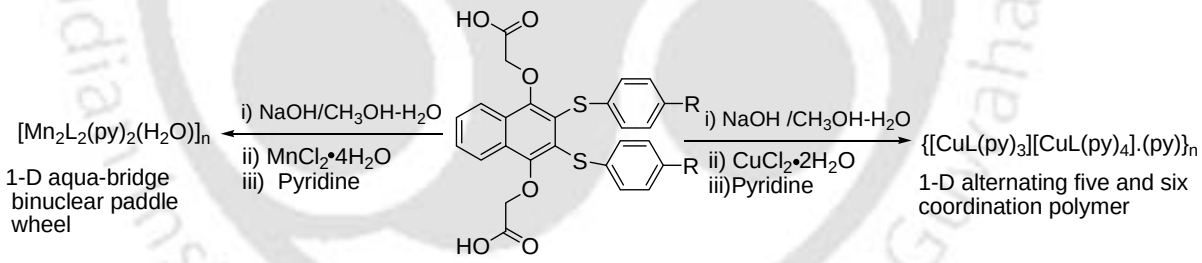

Scheme 4

We could also describe the synthesis and structure of a one dimensional coordination polymer of copper(II) carboxylate that contains repeated units of alternating five and six co-ordination geometry and one pyridine molecule occupies the interstitial position between the two polymeric helical structures (scheme 4). We extended our study to the reactions of zinc(II) acetate dihydrate with 2,2′-(2,3-*bis*-arylsulfanylnaphthalene-1,4-yloxy)acetic acid which leads to many polymeric

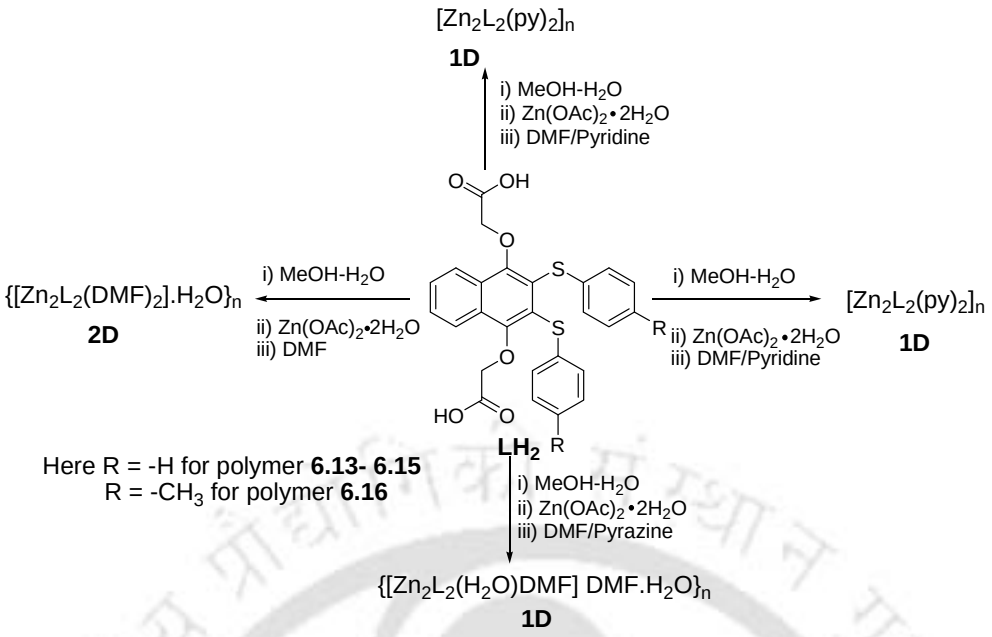

Scheme 5

complexes (**scheme 5**). These coordination polymers can bind to different ancillary ligands and depending on them they adopt different dimensional structures. The complexes having pyridine ancillary ligands are 1-D coordination polymers while the complex having *N*,*N*′-dimethylformamide is 2-D dimension coordination polymers (**fig 4**).

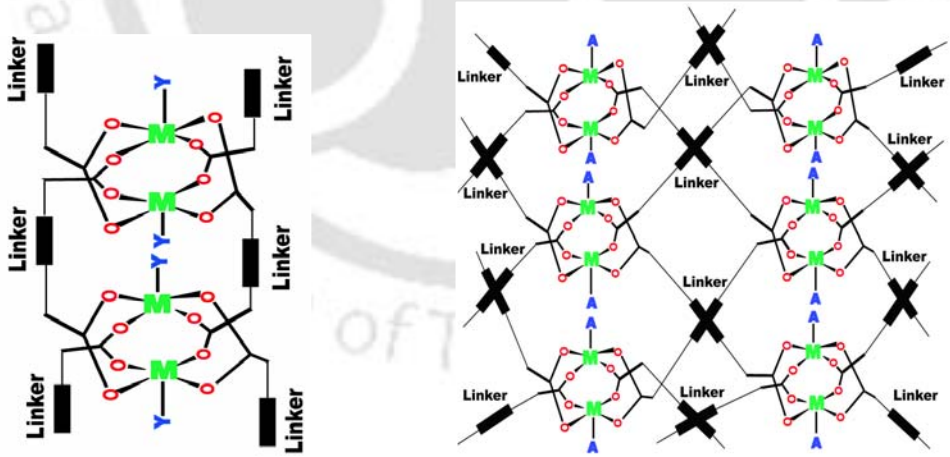

Fig. 4

We also enumerate the change in the dimensionality of coordination polymers with weak interactions. In the 1-D and 2-D coordination polymers the spatial arrangement of the naphthalene rings plays a major role in changing the dimension. The differences in the directional C–H···π and π···π interactions in the two cases makes the disposition of

the naphthalene rings different. We also describe the synthesis and structural studies of 1-D, 2-D and 3-D coordination polymers of cadmium. We also investigate the structural variations in coordination polymer of cadmium by providing steric factors of ancillary ligands and substituents due to the multiple possibilities of coordination numbers of cadmium ions.

The cumulative references are listed towards the end of the thesis.

Contents

Chapter 1

Introduction

1.1 General features of Quinones

Quinones are an important class of organic compounds commonly used either as reactant[1-5] or as catalyst[6] in organic synthesis and in coordination chemistry.[7-11] Quinone compounds have the properties of redox-switch,[12] fluorescence switch,[13] electron transfer agent,[14] non-linear optical materials.[15] In solid state some of the quinonic compounds show polymorphism.[16] The redox properties of quinonic compounds play important role in electrochemistry and biochemistry.[17-19] Quinone units are found in many biologically relevant molecules[20-22] and have important role in biological system as electron acceptors in respiration and photosynthesis.

1.2 Synthesis of quinones and their derivatives

Quinones are generally synthesized by oxidizing phenols or their derivatives. Varieties of oxidizing agents such as oxygen, hydrogen peroxide, silver oxide, etc. are used for such reactions. For example 1,4-benzoquinone **1.1** or 1,4-naphthoquinone **1.2** derivatives are prepared by oxidizing corresponding phenol or 1-naphthol derivatives by hydrogen peroxide in the presence of titanium silicate as catalyst[23] (**scheme 1.1**). It may be noted that in these reactions functional groups like primary alcohol groups attached to quinone do not get oxidized.

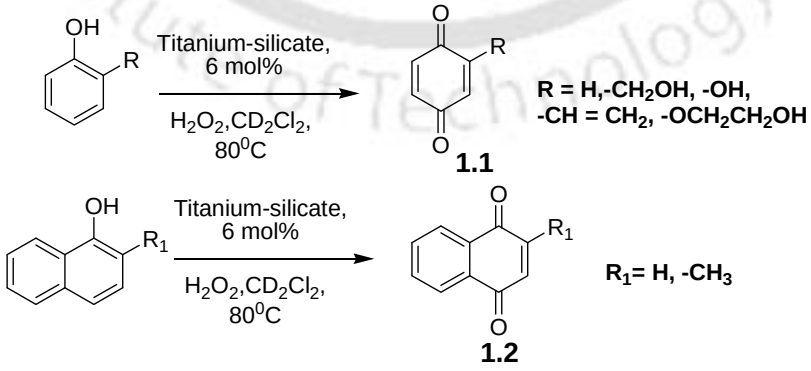

Scheme 1.1

Carbon-carbon coupling reactions cum oxidation reactions of various 1-naphthol derivatives by stannic chloride in the presence of oxygen to give dimeric naphthoquinone are reported.[24] In these reactions, the side reaction to form carbon-oxygen bond takes place, which leads to formation of side product such as **1.4**. However, the side product **1.4** gets converted to the naphthoquinone derivative **1.3** when excess stannic chloride is used (**scheme 1.2**).

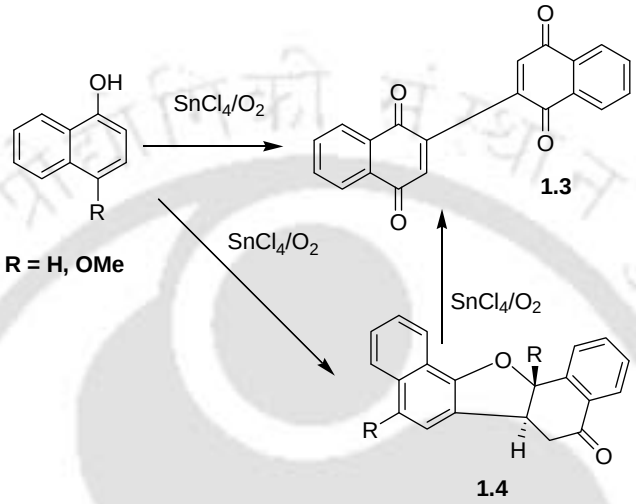

Scheme 1.2

Quinones act as dienophile for many [4+2] cyclo-addition reactions.[25-30] For example, the reaction of thiazole derivatives **1.5** with 1,4-naphthoquinone, leads to an intermediate product which further aromatises to form **1.6** through 1,3-hydrogen shift in moderate yields[31] (**scheme 1.3**).

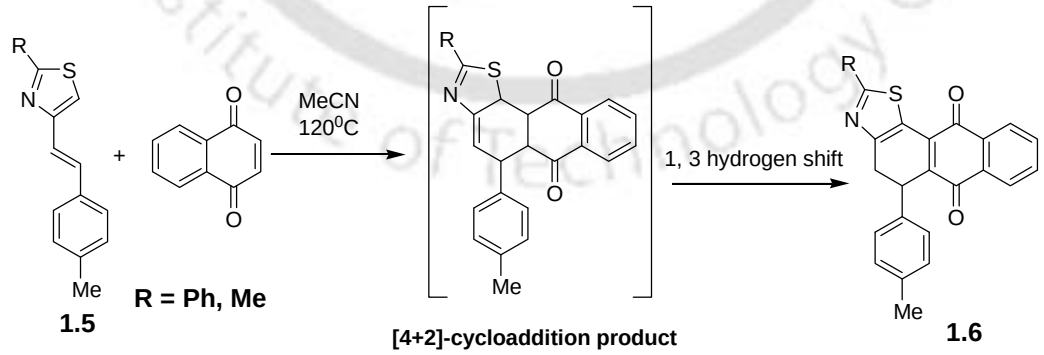

Scheme 1.3

The reactions of equimolar mixture of 1,4-benzoquinone derivatives with myrcene in aqueous sodium dodecylsulfate (SDS) lead to compounds **1.7**[32] (**scheme 1.4**).

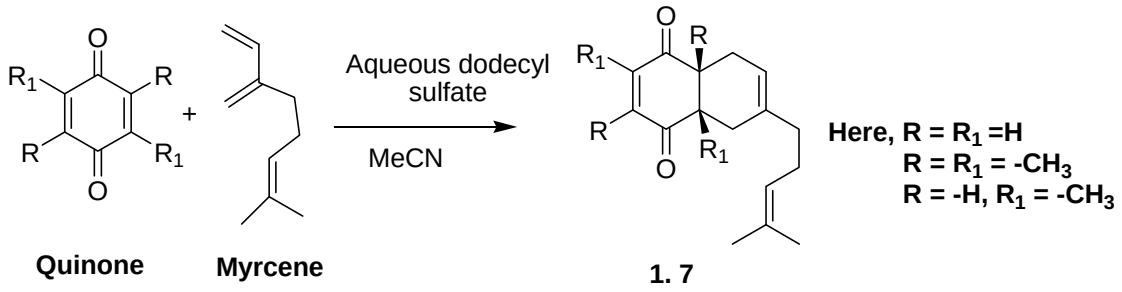

Scheme 1.4

The 2,3-di-allyl benzoquinones **1.9** are synthesized from the O-allylated compounds **1.8** by Claisen rearrangement[33-35] (**scheme 1.5**) under solvent free conditions[36] on silica support.

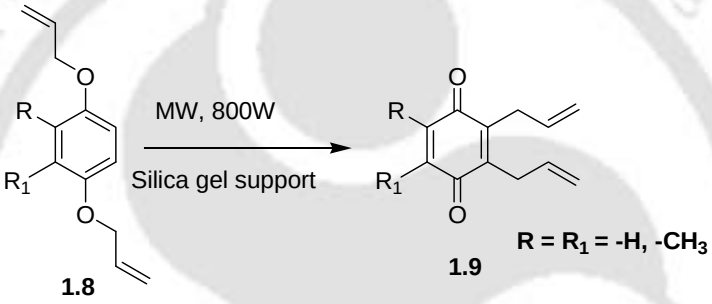

Scheme 1.5

Irradiation of light to compounds **1.10** possessing photolabile protecting group**,** such as, 2,5-dihydroxybenzyl group results[37] in the formation of 4-hydroxyquinone-2-methide **1.11** (**scheme 1.6**) as intermediate product. These intermediates undergo rapid tautomerization to form methyl *p*-quinone **1.12**. The formation of the *o*-quinone methide intermediate is very fast.

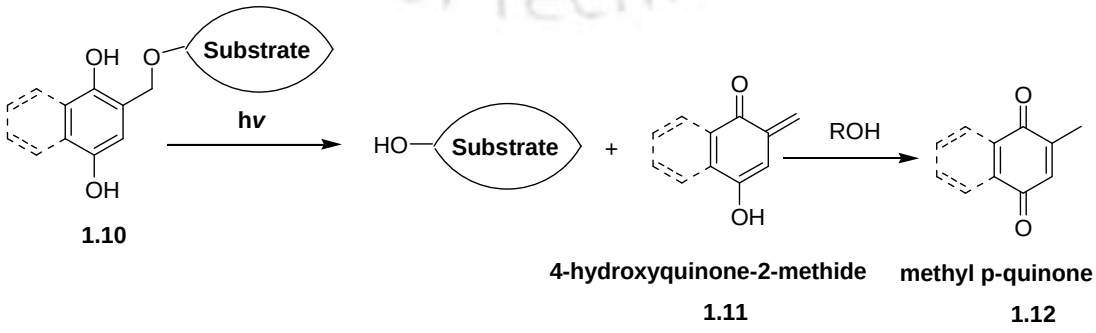

Scheme 1.6

A series of naphthoquinone thiol-crown ethers and thiol-crowned bis-naphthoquinone[38] are prepared from the reaction of 2,3-dichloro1,4-naphthoquinone and 1,4-naphthoquinone with β, β′-dimercaptodiethyl ether respectively as shown in the **scheme 1.7**.

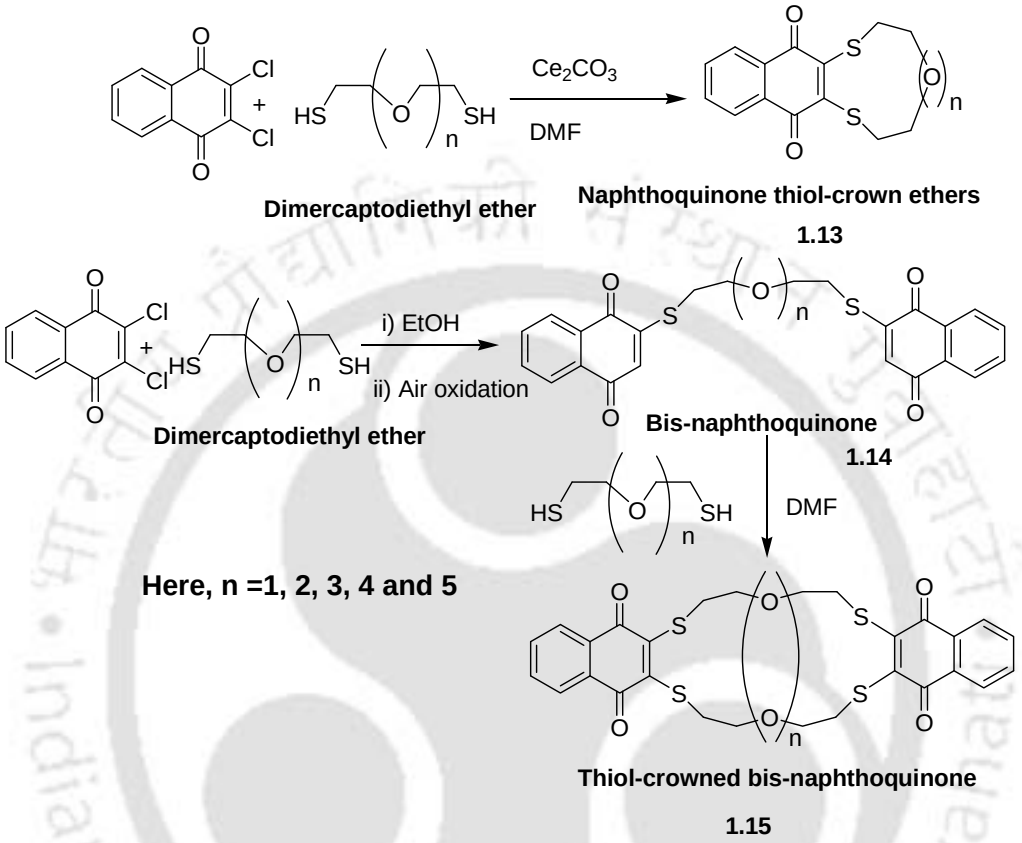

Scheme 1.7

Hydroxy group containing naphthoquinone derivatives **1.20** were prepared from 2-allyl or 2-methylallyl-1-naphthol[39-40] **1.16**. The reaction starts with hydroboration of **1.16** to form **1.17** followed by two successive oxidation reactions using Fremy's salt $\{Na_2NO(SO_3)_2\}$ to form **1.18** and by 2,6-dichloro-3,5-dicyano-1,4-benzoquinone (DDQ, **1.19**). Hydrolysis of **1.19** in basic medium gives naphthoquinone alcohols **1.20**. Naphthoquinone esters were obtained by esterification of naphthoquinone alcohols with 2-naphthoic acid in the presence of 1,1′-carbodiimidazole (CDI) in tetrahydrofuran[41] (THF) as shown in **scheme 1.8**. The corresponding diester was formed in moderate yield.

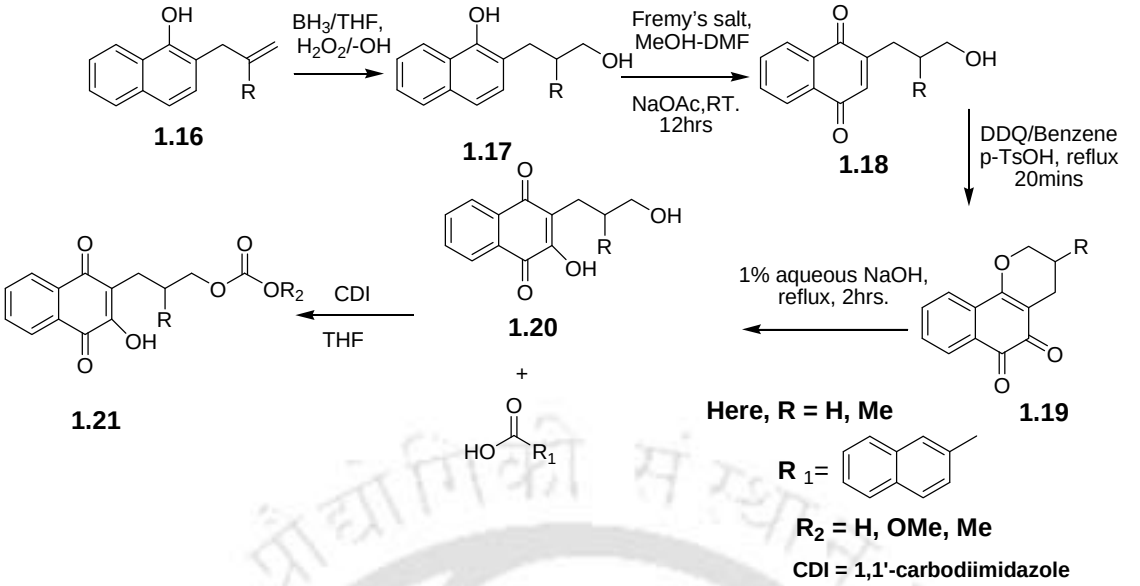

Scheme 1.8

The synthesis of triad acceptor-donor-acceptor (A-D-A) **1.28** was carried out via intermediate 2-oxo-1,3-dithiole derivative **1.26** (**scheme 1.9**).[42-43] The intermediate 2-oxo-1,3-dithiole derivative **1.26** can be obtain from the compound **1.22**. The compound **1.22** can be oxidized by using *p*-benzoquinone. The oxidised product cyclizes upon treatment with glacial acetic acid leading to iminium salt **1.23**.

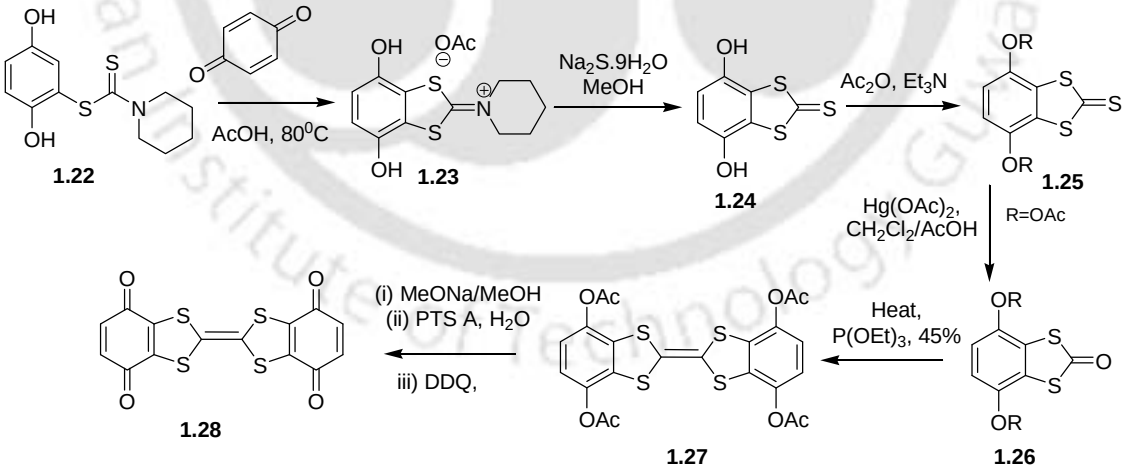

Scheme 1.9

The iminium salt gets converted to the corresponding 2-thioxo-1,3-dithiol **1.24** on reaction with sodium sulfide. The dihydroxy aromatic compound thus formed on protection leads to the acetyl derivatives **1.25**. The transchalcogenation of the

compounds **1.25** with mercuric acetate results in the 2-oxo-1,3-dithiol derivatives **1.26**. The compound **1.26** reacts with triethylphosphite to form the tetrathiafulvalene **1.27**. The compound **1.27** on subsequent methanolysis and treatment with *p*-toluene sulfonic acid (PTSA) and DDQ gives the A-D-A triad **1.28**.

Quinones are easily derivatized with nucleophiles such as aromatic and aliphatic amines and thiols.[44-48] For example, 2,3-diamino-1,4-naphthoquinone derivatives **1.32** are synthesized from the reaction of 2-chloro-3-(2,4-dinitrophenylamino)-1,4-naphthoquinone **1.31** with aromatic and aliphatic amines.[49] The compound 2-chloro-3-(2,4-dinitrophenylamino)-1,4-naphthoquinone **1.31** is prepared by reaction of aniline derivative with quinone (**scheme 1.10**). The strong electron withdrawing nature of the dinitrophenylamino group makes the quinone system electron deficient so that the second chlorine is easily displaced by various secondary amines.

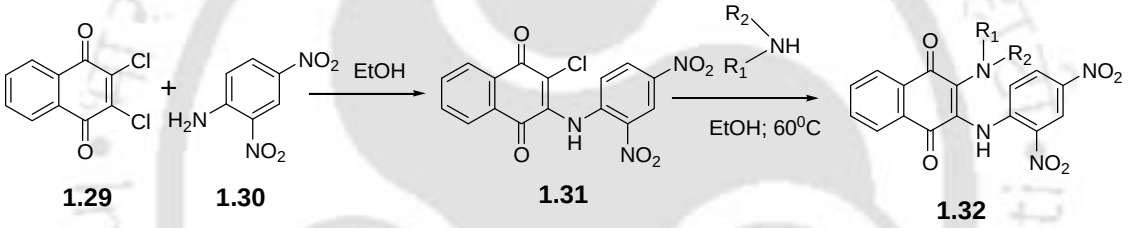

1.29 **1.30** **1.31** **1.32**

Scheme 1.10

The reaction of 2,6-dimethylbenzoquinone with varieties of thiols in water gives the corresponding thioethers of the corresponding hydroquinone **1.33** (**scheme 1.11**).[50]

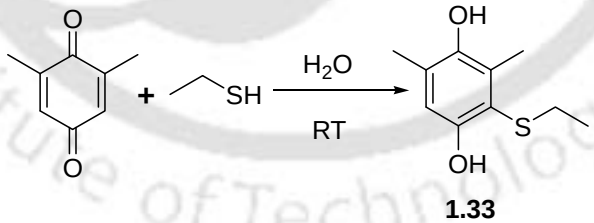

1.33

Scheme 1.11

Presumably water molecules in this reaction accelerates the reaction through hydrogen bond formation with the carbonyl oxygen atom of the 2,6-dimethylbenzoquinone. Such interactions enhance the electrophilic character at the carbon center, which is attacked by the thiol.

1.3 Electrochemical properties of quinones and their derivatives

Quinones are important redox species; play important role in electrochemistry and have been utilized in supramolecular electrochemical devices.[51] The quinone shows two step reduction processes through the equilibrium shown in **scheme 1.12**.

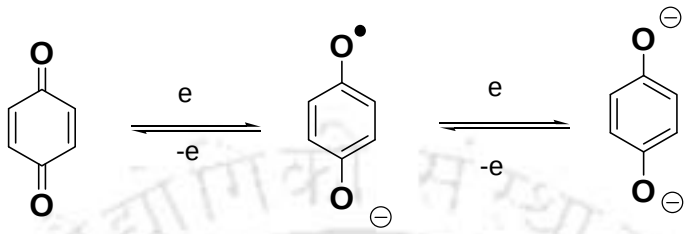

Scheme 1.12

The potentials of these reductions depend on parameters such as solvent,[52] supporting electrolyte.[53] Quinones can also possess hydrogen bonding interactions; redox process in such cases gets slightly modified.[54] There are many examples of quinone compounds that involved the redox processes. For example the 4-hydroxycoumarine1,4-benzoquinone[55] **1.34** (**fig. 1.1**) shows a reversible redox couple with $E_{1/2}$ value of approximately 0.053 V corresponding to the two consecutive electron transfers.

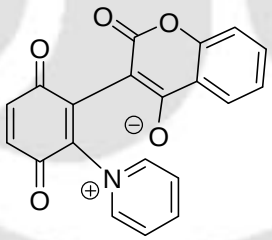

1.34

Fig. 1.1

Hydrogen bonded quinonic systems lead to synthetic receptor-substrate systems.[56-57] For example 9,10-phenanthrenequinone in the presence of 1,3-diphenylurea[58] shows reversible one-electron reduction in aprotic media to form radical anion as illustrated in **scheme 1.13**.

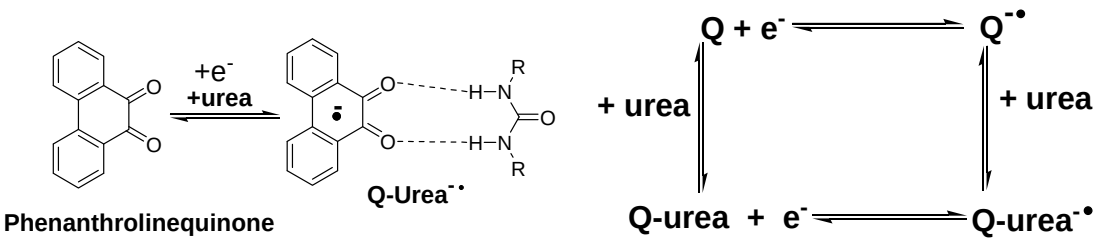

Scheme 1.13 Redox process of hydrogen bonded quinonic system

In this case with increasing amount of 1,3-diphenylurea, the half-wave potential ($E_{1/2}$) of 9,10-phenanthrenequinone significantly shifts to the positive side of the original potential. The reduction process essentially is an on/off switch for *o*-quinone/urea binding in DMF. Binding is "off" in the oxidized state and "on" in the reduced state. The role of carboxylate groups as proton accepting groups in an electrochemical reaction of the 2,5-dicarboxy1,4-benzoquinone/2,5-dicarboxylate1,4-hydrobenzo-quinone[59] couple is investigated by means of a cyclic voltametry in *N*,*N*′-dimethylformamide. It shows several redox processes as shown in **scheme 1.14**.

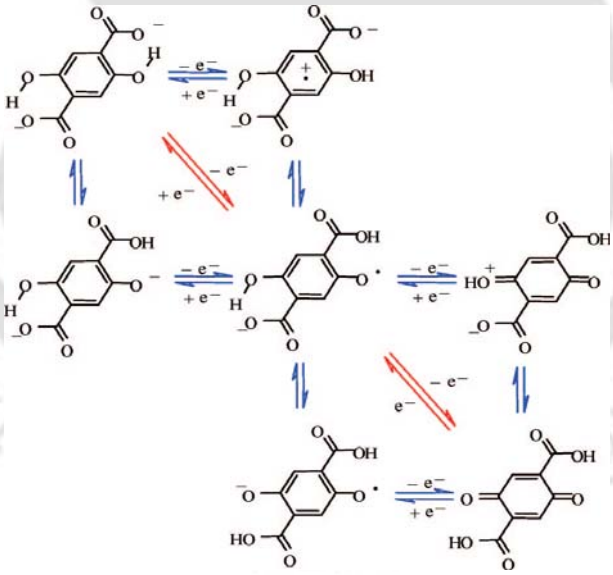

Scheme 1.14: Electrochemical reactions of the 2,5-dicarboxy 1,4-benzoquinone/2,5-dicarboxylate 1,4-hydrobenzoquinone couple.

There are two types of mechanisms that are put forward to explain these electrochemical changes. A mechanism in which the two reactions occur in a stepwise manner (in blue in the **scheme 1.14**), with proton transfer first, followed by electron transfer (PET) or, vice versa, electron transfer first, followed by proton transfer (EPT).

Alternatively, another mechanism in which proton and electron transfer occurs in a concerted manner (CPET) is also put forward (red in the **scheme 1.14**). These studies are important in biological quinone-based couples as electron-proton transfer agents in the oxidative phosphorylation of ADP to ATP, or photosynthesis.[60-61]

1.4 Electron transfer in quinones and their derivatives

The photosynthesis is characterized by a series of electron transfer events in the reaction center producing long lived charge-separated states.[62] The initial step in this series of electron transfer processes is the transfer of an electron from one photoexcited chlorophyll to the adjacent quinone.[63] A large number of porphyrin-quinone systems for the photo induced charge separation in photosynthetic reaction centers have been reported. Most of them consist of porphyrin covalently linked to electron acceptor quinones.[64-67] Spectroscopic study of these materials have revealed much about the dependence of electron-transfer rates on donor-acceptor coupling, thermodynamic driving force, solvent, and temperature. The hydroquinone-appended porphyrin, [5,10,15-triphenyl-20-(2,5-dihydroxyphenyl)porphyrinato] zinc(II)[68] **1.35** is prepared by condensing pyrole 2,5-dihydroxybenzaldehyde, and benzaldehyde in propionic acid, followed by zinc(II) insertion[69]. With the addition of hydroquinone to a solution of tetraphenyl-porphyrin functionalized with a hydroquinone moiety results in the formation of hydroquinone-quinone complex **1.35** (**fig. 1.2**).

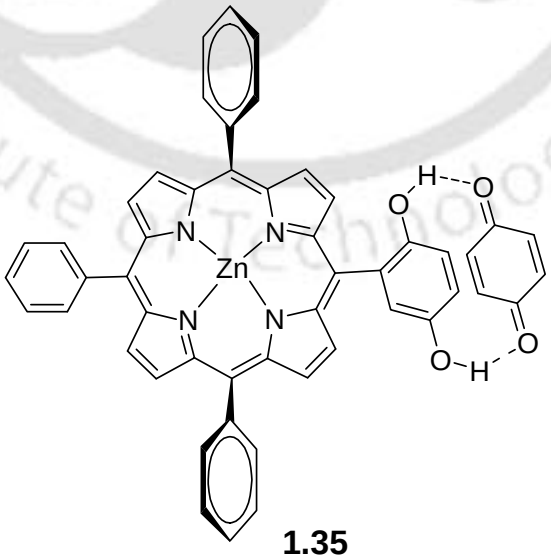

1.35

Fig. 1.2

The synthesis of *meso*-polyarylporphyrin and quinone triad[70] **1.36** was done by the modification of MacDonald [2+2] cycloaddition[71-72] (**fig. 1.3**). The quenching was investigated by time-resolved fluorescence studies and found that the quinone moieties contribute to the quenching. In this system the first excited singlet state of the porphyrin bearing quinone moiety is strongly quenched and found to be due to photo induced electron transfer that yields a porphyrin radical cation and quinone radical anion.

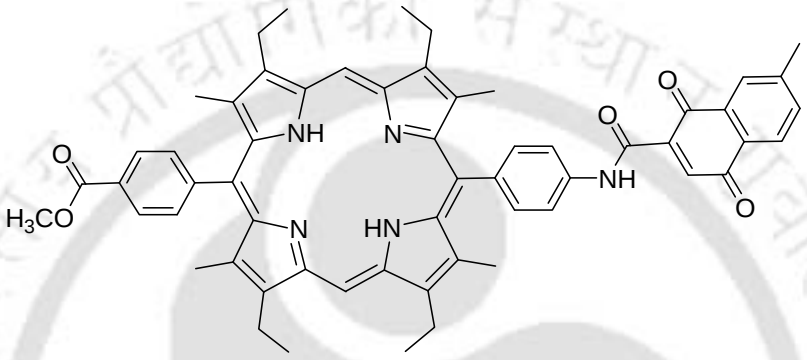

1.36

Fig. 1.3

1.5 Quinone derivatives in fluorescence switch

Quinones covalently linked to chromophores and fluorophores act as donor-acceptor systems with reversible redox functions and potential 'switching' properties. Covalent linking of quinones to strong fluorophores results in efficient quenching of the donor emissive state via intramolecular electron transfer from the excited fluorophores to the adjacent quinone acceptor, or by transfer of excitation energy to a low-lying non-emissive charge-transfer state. In such type of system, the quinone/hydroquinone redox couple[73] can interconvert reversibly by exchanging two protons and two electrons, thus it can serve as the 'antenna' or 'control' subunit, which affects absorption or emission properties.

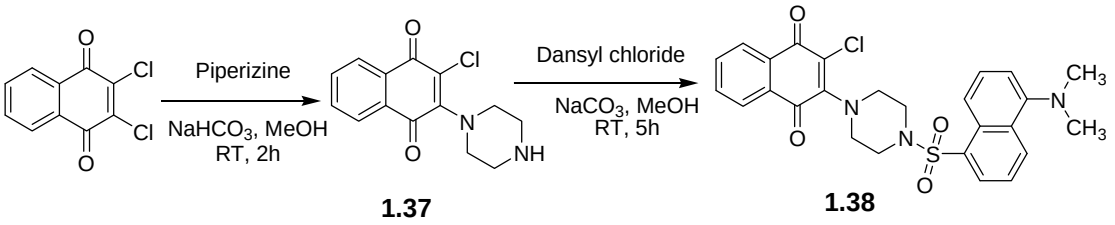

Scheme 1.15

Fluorescent switching device systems find use as probes for the determination of local environmental redox properties and as bio-sensor elements to study electron and energy transfer mechanisms.[74-75] 2-Chloro-1,4-naphthoquinone when covalently attached to 5-dimethylaminonaphthalene via a non-conjugating piperizine[76] leads to **1.38**; which has property of a molecular switch (**scheme 1.15**).

Addition of one drop of sodium borohydride to the red solution of compound **1.38** leads to spontaneous chemical reduction to **1.39** and instant chemical 'on' fluorescence switching occurs (excitation wavelength = 360 nm; emission wavelength = 532 nm in DMSO and 522 nm in MeOH). The electron transfer process is reversible (**scheme 1.16**).

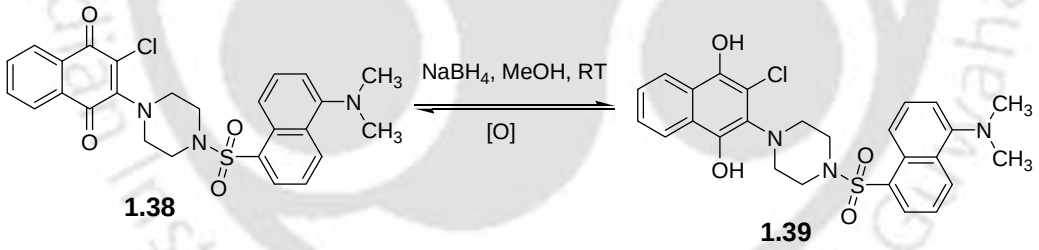

Scheme 1.16

Another example of quinone containing fluorophore synthesis is the synthesis of *N*-dansyl-carbazoloquinone[77] **1.43** as shown in **scheme 1.17**. The fluorescence emission from the excited state of the dansyl group is totally quenched (off) in compound **1.43** but instant 'on' fluorescence occurs upon chemical reduction of the quinone (**1.44**) with sodium borohydride (excitation wavelength = 336 nm; emission wavelength = 528 nm; quantum yield = 0.018).

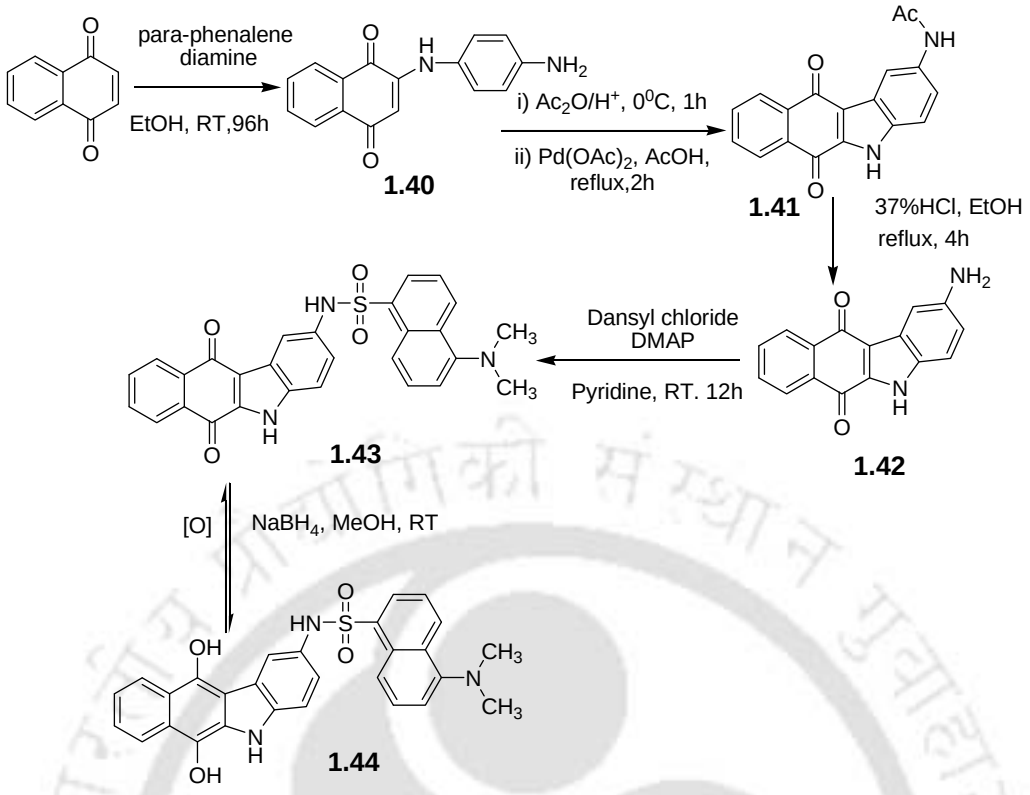

Scheme 1.17

The fluorescence properties of transition metal complexes containing quinone or hydroquinone ligands are interesting.[78] The complex **1.46** has square pyramidal geometry with the pyridine ligand at the apical coordination site a shown in (**fig. 1.4**). The complex **1.46** exhibits intense fluorescence[79] at 535 nm upon excitation at 350 nm in DMSO solution.

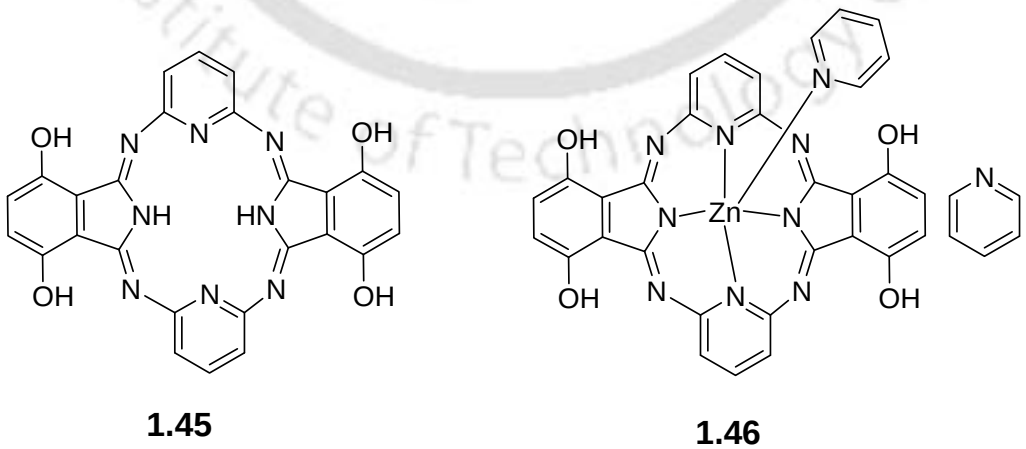

1.45 **1.46**

Fig. 1.4

Recently, the synthesis and properties of a series of quinonic compounds **1.47-1.49** with integrated chromophores, redox-active moieties, and hydrogen bond donors are reported[80] (**fig. 1.5**).

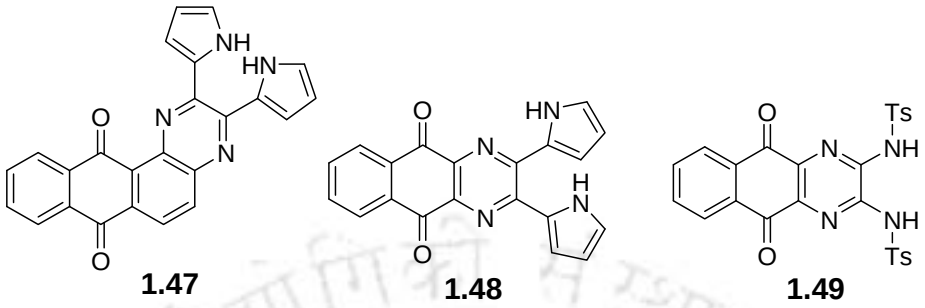

Fig. 1.5

UV-visible spectroscopy and visual inspection of solutions of **1.47-1.49** before and after addition of anion such as fluoride, cyanide, acetate, and pyrophosphate in the form of salts show dramatic changes in color. This suggests the strong hydrogen bonding interactions between the receptors and the anions.

1.6 Quinone derivatives in photochemistry

The quinone derivatives are considered to be the critical intermediates in the DNA-cleaving reactions.[81-82] Quinone linked to peptide[83] **1.50** leads to 2,5-substitution by amines.[84-86] Irradiation of peptide **1.50** gives the cyclization product **1.51** (**scheme 1.18**).

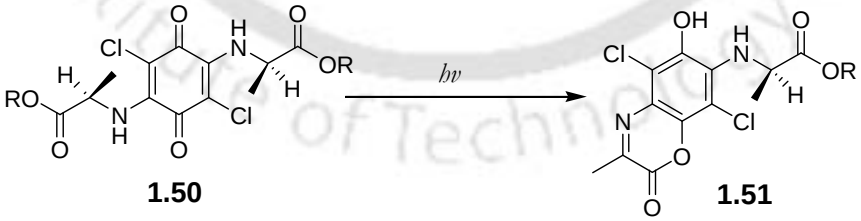

Scheme 1.18

2-Pyrrolidino-1,4-benzoquinone **1.52** undergoes photocyclization with visible light, results in the formation of **1.53**.[87] Visible light activates the photoremovable protecting group of **1.53** to release or unmask them to form the product **1.54** as illustrated in **scheme 1.19**. Elimination of benzoic acid affords *o*-quinone methide **1.54**.

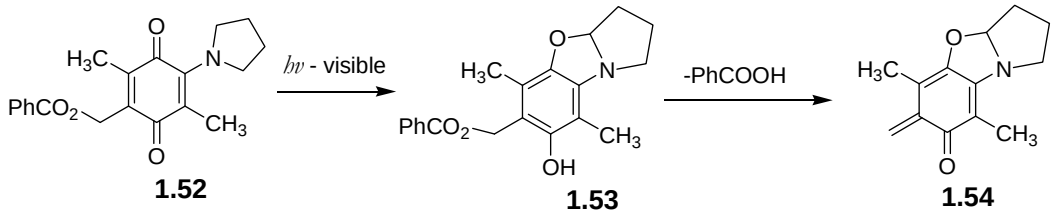

1.52 **1.53** **1.54**

Scheme 1.19

1.7 Quinone derivatives in nonlinear optics

Organic materials possessing nonlinear optical properties have attracted attention for their great potential in storing devices.[88-90] For the demonstration of optical switching operation,[91-92] push-pull materials, in which electron donor acceptor moieties are attached to the structure are of interest as second and third order nonlinear optical materials. The 2-amino-1,2,3-triazole-quinone[93-94] **1.55** has coplanar donor-acceptor and it produces push-pull system with potentially large nonlinearities. This compound **1.55** (**fig. 1.6**) have third-order nonlinearities.

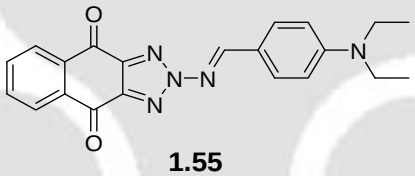

1.55

Fig. 1.6

The nonlinearity of compounds, quinone-tetrathiafulvalene dyads **1.56** and triads **1.57** are studied[95] (**fig. 1.7**). These two compounds show third order nonlinear optical properties and second-order nonlinear optical hyperpolarizability. Such properties are attributed to their highly delocalized π-electrons and their ability to easily donate or accept electrons. The excitations in these cases were done by 30 ps laser pulses at λ = 532 nm generated by an amplified mode-locked Quantel Nd:YAG laser operating with a 1 Hz repetition rate.

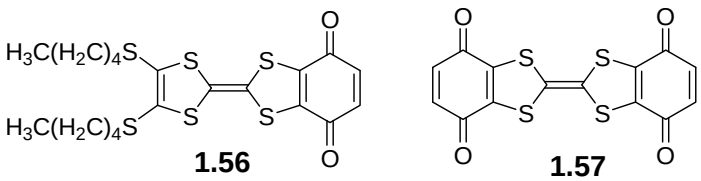

1.56 **1.57**

Fig. 1.7

1.8 Quinones in organofullerene

A structurally simple type of electron acceptor organofullerene is [60] fullerene-*p*-benzoquinone system **1.62**. This organofullerene **1.62** can be prepared from substituted *o*-quinodimethane by reaction with C_{60}.[96-97] These organofullerenes are prepared from *o*-quinodimethane[98-99] intermediate **1.59**. The intermediate **1.59** can be prepared by heating 'sultines' **1.58** under mild condition through several steps as shown in **scheme 1.20**.

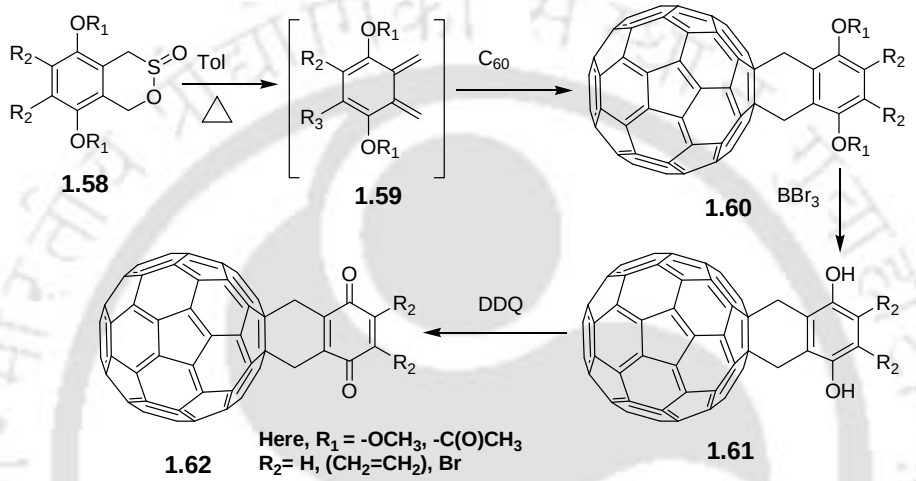

Scheme 1.20

1.9 Quinones and its derivatives in catalysis

Reaction of *E*-isomer of compound **1.63** with catalytic amount of Li_2PdCl_4 in the presence of *p*-benzoquinone and LiCl in acetone-acetic acid gives a mixture of two isomeric allylic chlorides **1.64** and **1.65** (**scheme 1.21**). Under the same reaction condition *Z*-isomer of compound **1.63** reacts to give the same product with different ratios.[100] In this nucleophilic addition reaction the quinone replaces chloride attached to the palladium and facilitates attack of chloride on (η^3-allyl) palladium complex.

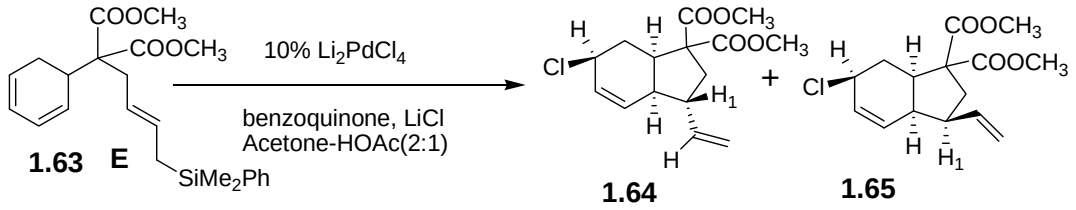

Scheme 1.21

The 1,4-oxidation reactions of 1,3-cyclohexadiene is catalyzed by zerovalent palladium in the presence of *p*-benzoquinone **1.66** (5 mol%) to give 1,4-diacetoxy-2-cyclohexene **1.67**[101] (**scheme 1.22**). In this reaction benzene is formed as a side product. In this palladium-catalyzed 1,4-oxidation reactions, *p*-benzoquinone causes reoxidation of Pd (0)[102] to palladium(II) for making the reversible catalytic cycle.

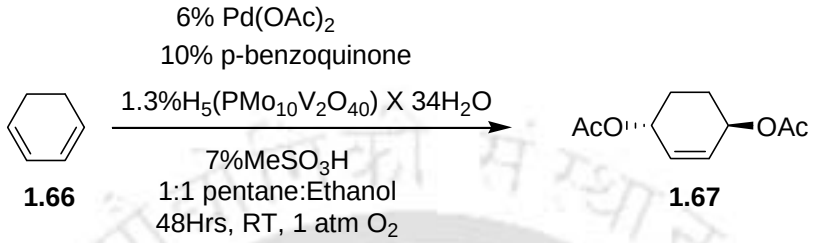

Scheme 1.22

The mechanism for this palladium catalyzed reaction in the presence of quinone is illustrated by the catalytic cycle shown in **scheme 1.23**. The quinone induces the nucleophilic attack on the (η^3-allyl) palladium complex as well as it mediates the reoxidation of the Pd(0).

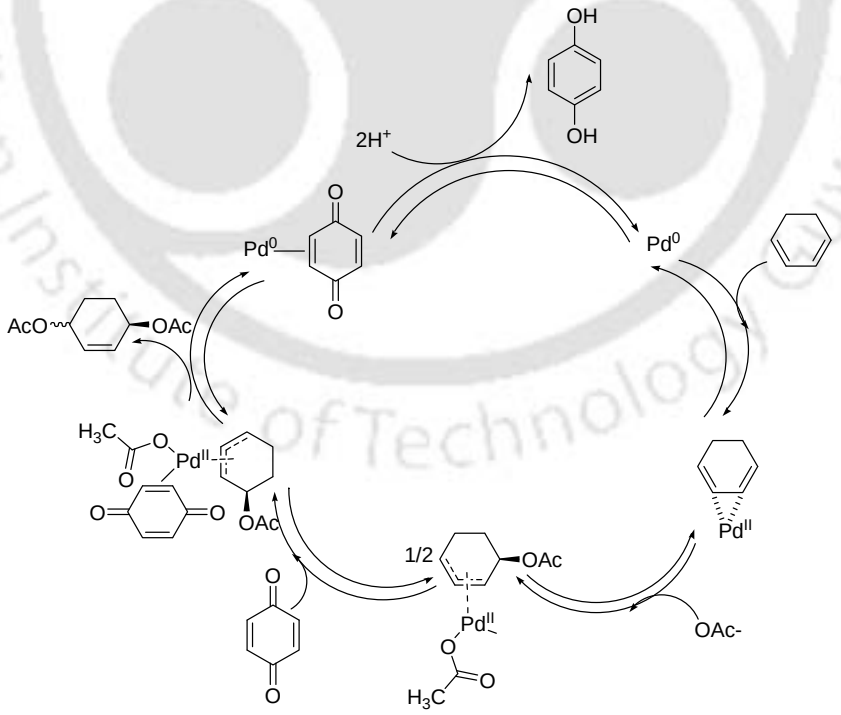

Scheme 1.23

1.10 Pharmaceutical application of quinone derivatives

Quinone derivatives are well known for their pharmacological and therapeutic uses.[103] It includes the antifungal,[104-106] antibacterial,[107-109] antivirial,[110] anticancer[111-120] activities. For example, anthracycline antibiotics, which are highly functionalized glycosides containing quinonoid chromophores. Thee have been extensively used for more than four decades and currently constitute the second largest class of anticancer drugs in clinical application.[121-122]

Lagopodin A, **1.68a-c** and Enokipodins A, **1.69a-b** (**fig. 1.8**) are fungal sesquiterpene and exhibit significant antimicrobial activity against the fungus *Cladosporium herbarum* and the gram-positive bacteria *Staphylococcus aureus* and *Bacillus subtilis*.[123]

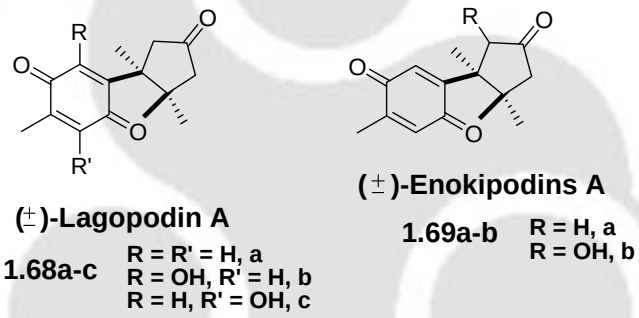

Fig. 1.8

Kinamycins antibiotics contain a diazo-substituted benzofluorenes.[124-125] Two other such examples of antibiotics are prekinamycin **1.70** and ketoanhydrokinamycin **1.71** (**fig. 1.9**). Due to their antibiotic values, the biosynthesis of kinamycin antibiotics has been studied at the structural level as well as at the biochemical and molecular genetic levels.

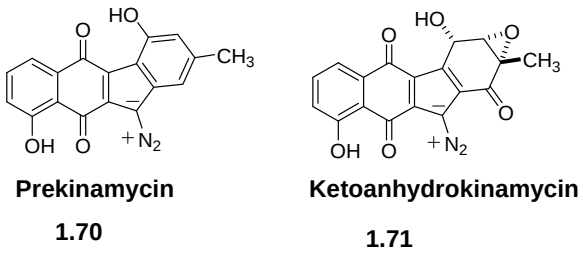

Fig. 1.9

Juglomycins A (**1.72**) and B (**1.73**), act as bioreductive alkylating agents.[126] They are isolated from the culture filtrate of the fungus Streptomyces species.[127] These anbiotics (**fig. 1.10**) have inhibitory action against a variety of microorganisms.[128]

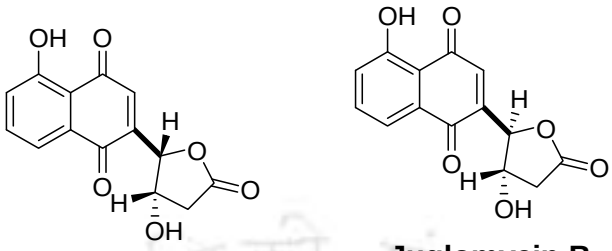

Fig. 1.10

Many clinically important anticancer drugs such as anthracyclines, mitoxantrones, and saintopin, contain quinone nucleus.

A novel quinonoid plant product, glycoconjugates of diospyrin was synthesized and cytotoxicity against human malignant melanoma (A375) and laryngeal carcinoma (Hep2).[129] were evaluated. Some of the diosporin anticancer drugs (**1.74-1.77**) are shown in **fig. 1.11**.

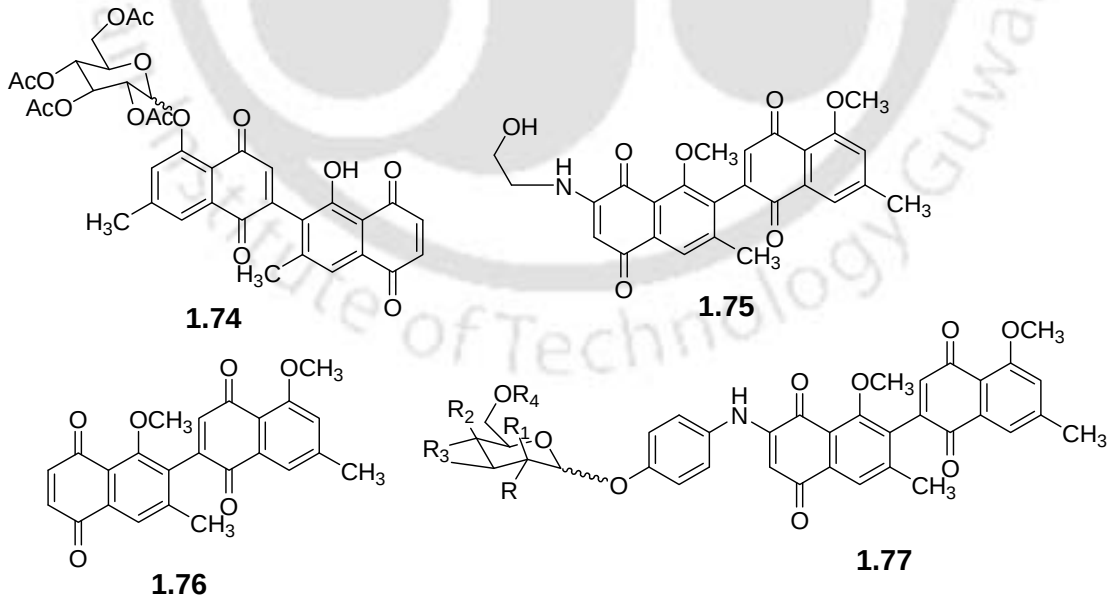

Fig. 1.11

When the A375 cells treated with diosporin **1.76** and **1.77**, cytotoxicity properties against human malignant melanoma (A375) were found.

Rhinacanthins are naphthoquinone ester derivative which were isolated from the methanolic extract of the roots of the medicinal plant *Rhinacanthus nasutus*. A few of these compounds have been reported to exhibit cytotoxicity against P388, A-549, HT-29, and HL-60 cell lines.[130] Rhinacanthin-M, -N, -Q (**1.78-1.80** respectively)[131] and related naphthoquinone esters (**fig.1.12**) were also studied for their cytotoxicities against human carcinoma cell lines, KB (oral human epidermoid carcinoma), HeLa (human cervical carcinoma), and HepG2 (human hepatocellular carcinoma).

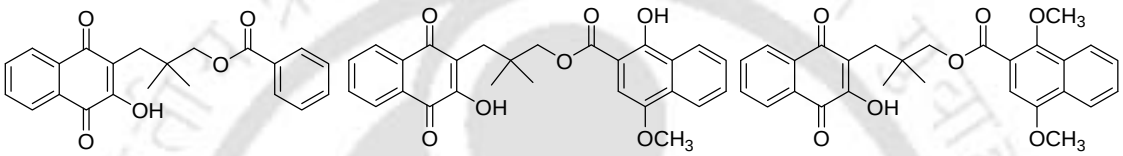

Fig. 1.12

Saframycins A, B, C, D, and E (compound **1.81**, **fig. 1.13**) were isolated from *Streptomyces lavendulae*.[132] These were the first of many saframycins to be subsequently isolated from natural source. All of the saframycins have been found to display antitumor activity.[133]

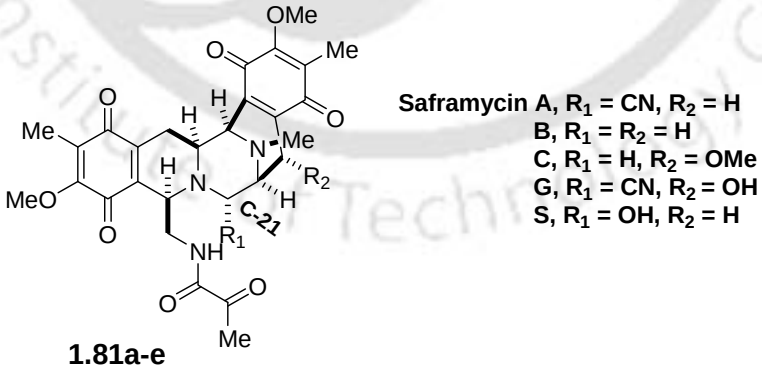

Fig. 1.13

The saframycins possessing nitrile or hydroxyl group at C-21 shows the highest activities. Saframycin S displays the most potent antitumor activity,[134] while

saframycins R[135]and A[136] exhibited potent antitumor and antimicrobial activities but less than Saframycin S.

1.11 Polymorphism in quinone derivatives

In the case of molecular solids, polymorphism is a phenomenon of a substance having several different crystal forms or modifications.[137-143] As a consequence of their different crystal structures; the polymorphs are chemically identical but they differ in their physical properties, such as density, vibrational spectra, and diffraction patterns. So the studies of polymorphic systems represent an ideal opportunity for understanding structure-property relationships. In recent years, there have been discovery of many polymorphs of active drugs such as barbiturates, sulfa drugs, steroids etc.[144-146] The studies on the polymorphism in quinone and their derivatives are of great interest as many of the quinone derivatives are drugs. The polymorphism in quinone derivatives arises due to the structural features such as *syn* and *anti* conformation across directly bonded atoms or groups of the quinone ring. Depending on the availability of the acceptor two –C=O of quinones, the different C-H···O interactions and close packing motifs decides the number of polymorphic structures in quinone. In recent year many polymorph of quinone derivatives are reported.[147-150] Polymorphism in fuchsones[151] such as, 4-(α,α′-diphenylmethylene)1,4-benzoquinone [152-153] **1.82a-d** (R= Me, *i*-Pr, *t*-Bu and Cl) is well studied.

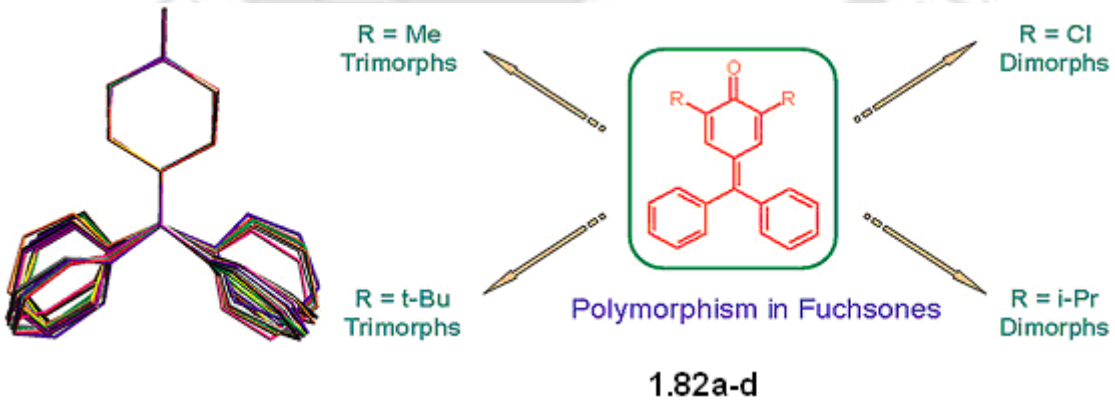

Fig. 1.14

The chloro and isopropyl derivatives of this class of compounds are dimorphic while methyl and *t*-butyl compounds are trimorphic as shown in **fig. 1.14**. This polymorphism

is related to the difference in conformations adopted by the exodiphenylmethylene group at the 4-position of the benzoquinone ring. Depending on the availability of the acceptor fuchsones C=O and the conformation of the phenyl ring at the 4-position, different C-H···O interactions, and close packing motifs are optimized in these crystal structures of polymorphs.

The zinc porphyrin complexes covalently linked to benzoquinone with a cyclohexanediyl bridge in *cis* and *trans* configuration (**1.83**) are reported in literature.[155] These two porphyrin quinone complexes undergo electron transfer from porphyrin to quinone at comparable rates (**fig 1.15**).

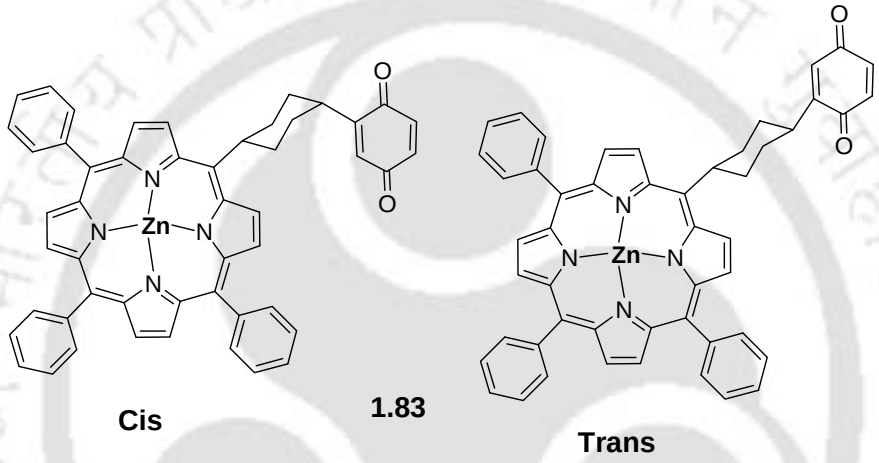

Fig. 1.15

The structures of porphyrin-quinone cyclophanes with one or two quinones covalently attached above and below the porphyrin plane are also reported.[156-157] Porphyrin compounds with a quinone unit directly bonded at *meso* position are extensively studied.[158]

1.12 Quinone in supramolecular chemistry and metal complexes

A charge-transfer complex or electron donor-acceptor complex is a chemical association of two or more molecules, such that a fraction of electronic charge is transferred between the molecular entities. The resulting electrostatic attraction provides a stabilizing force to the molecular complex. Quinones are also capable of engaging in charge-transfer complexes and intermolecular interactions through the formation of hydrogen bonds (C-H···O, N-H···O etc).[159-164]

The ability to coordinate a metal to the π-system in hydroquinone and catechol constitutes one of the basis for developing metal organometallic coordination networks (MOMNs).[165-169] The attachment of a metal fragment to the π-system significantly influence the proton and electron transfer occurring in the formation of the semiquinone and quinone oxidation products.[170-173]

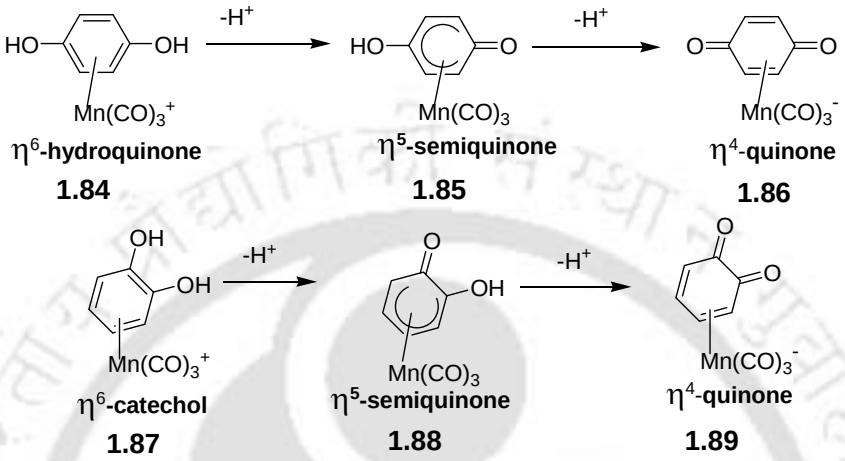

Scheme 1.24

One such example is the thermally stable π-complex (η^6-hydroquinone)$Mn(CO)_3^+$, **1.84** as well as the *o*-hydroquinone analogues[175] **1.87** as shown in **scheme 1.24**. These serve as the manganese tricarbonyl transfer reagents. The neutral η^5-semiquinone complex **1.85** has a linear polymeric array like structure dictated by strong intermolecular hydrogen bonding.[175] Similar catechol analogue **1.88** exists as discrete hydrogen-bonded dimer. X-ray structural studies have revealed that the complexes possess strong hydrogen-bonding interactions as shown in **fig. 1.16**.

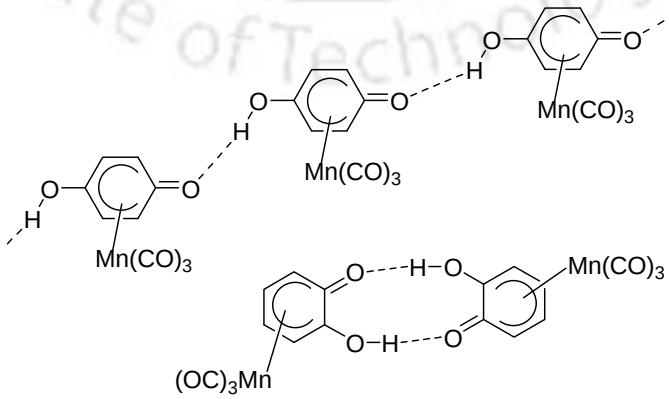

Fig. 1.16

The *p*-benzoquinone complex **1.86** serves as a bifunctional ligand in the presence of appropriate metal ions by *σ*-bonding through both oxygen atoms[176] resulting in the formation of neutral coordination networks **1.90** (**fig. 1.17**).

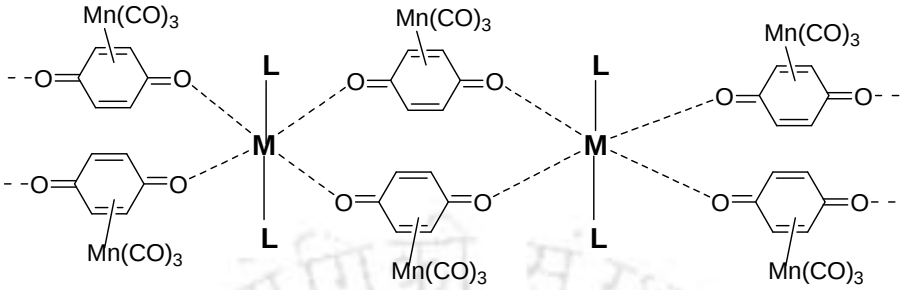

1.90 (M = Mn, Co, Cd; L = DMSO, Py)

Fig. 1.17

By axial ligand variation with the aid of bifunctional organic spacer ligands, the 1D polymer **1.90** can be tied together to give the 2D metal organometallic coordination network (MOMN) **1.91** (**fig. 1.18**). The 1D string in **1.90** could be linked together by 4,4′-bipyridine. The 2D MOMN systems **1.90** are structurally characterized (M = Mn and Ni) and have the structure shown in **fig. 1.18**.

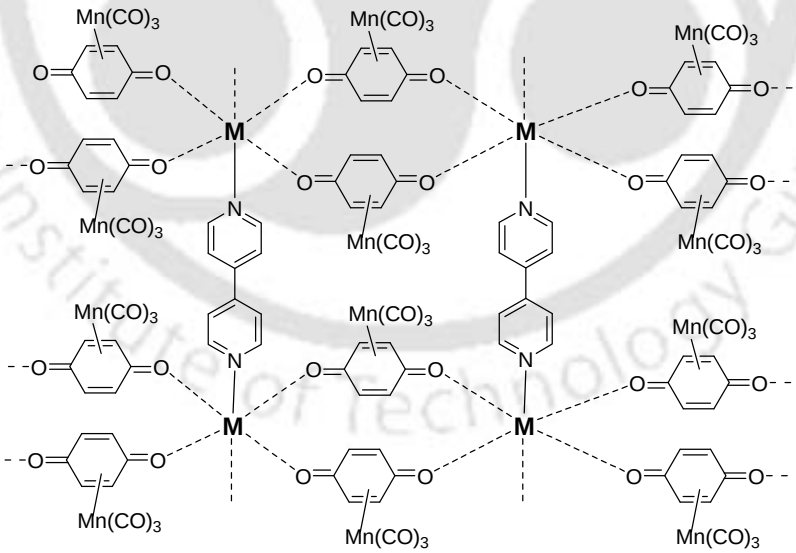

MOMN 1.91 (M = Mn and Ni)

Fig. 1.18

1,2-Benzoquinone forms three different types of coordination complexes, namely quinolate, semiquinolate and catecholate[177] (**scheme 1.25**). These complexes are

associated with the redox activity of the quinone ligands and exist in a number of electronic states due to the combined electrochemical properties of metal ion and quinone ligands.[178-180]

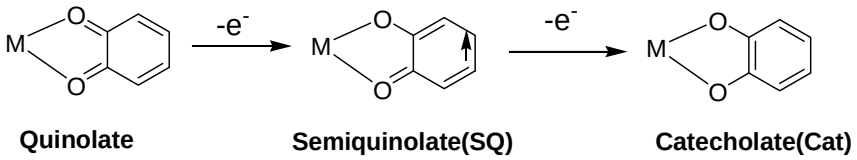

Scheme 1.25

The reaction between 3,5-di-*tert*-butyl-1,2-benzoquinone (3,5-DBBQ) and $Co_2(CO)_8$ and followed by treatment with 2,2′-bipyridine (bpy) gives the Co^{III}(bpy)(3,5-DBSQ)(3,5-DBCat),[181] **1.92** (where 3,5-DBSQ = 3,5-di-*tert*-butyl-semiquinolate, 3,5-DBCat = 3,5-di-*tert*-butyl-catecholate). The structure of this compound is characterized by single X-ray crystallography. From the electronic, electron paramagnetic resonance, ^{1}H NMR spectra and magnetic characterization it observed to occur the Co(III) and Co(II) redox isomers of the complex and were together in thermal equilibrium[182] as shown in **scheme 1.26**.

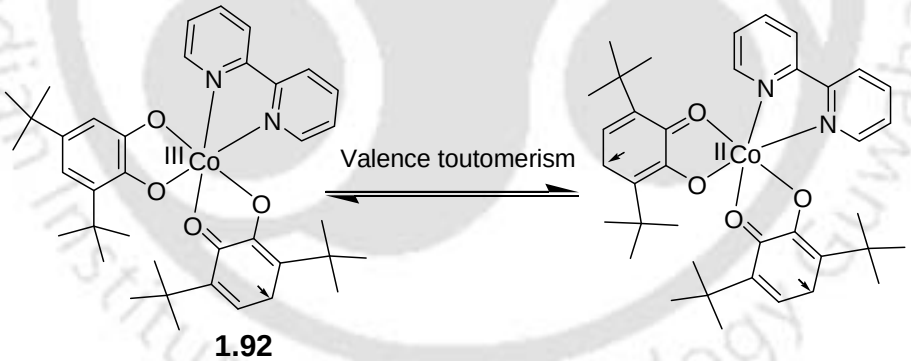

1.92

Scheme 1.26

There are also examples of one dimensional coordination polymer of ortho-benzoquinone derivatives. One such polymer is manganese [*trans*-Mn(μ-pyz)(3,6-DBSQ)(3,6-DBCat)]$_n$ **1.93** (Here Pyr = pyrazine, DBSQ = *t*-dibutyl semiquinone, DBCat = *t*-dibutylcatecholate).[183] This polymer **1.93** was prepared by irradiating a mixture of $Mn_2(CO)_{10}$, pyrazine and 3,6-di-*tert*-butyl-1,2-benzoquinone (3,6-DBBQ). This coordination polymer encapsulates hexane molecules between the two polymeric

chains. In this complex of manganese, three redox isomers are possible. The equilibria occur in two steps (**eqns 2.1** and **2.2**, **scheme 1.27**) showing the valence tautomerism among the isomers.[184-185] Polymeric cobalt complex [Co(μ-pyz)(3,6-DBSQ)(3,6-DBCat)]$_n$ **1.94** are reported[186] along with large numbers of similar semiquinolate, catecholate metal complexes.[187-193]

$Mn^{IV}(N\text{-}N)(Cat)_2 \leftrightarrow Mn^{III}(N\text{-}N)(SQ)(Cat)$ (2.1) where cat = catecholate

$Mn^{III}(N\text{-}N)(SQ)(Cat) \leftrightarrow Mn^{II}(N\text{-}N)(SQ)_2$ (2.2) N-N = pyrazine, SQ = semiquinolate

Scheme 1.27

Metal complexes of 1,4-naphthoquinone-SALEN type ligand are also reported. Such type of complexes of quinone-functionalized chelating ligands is used for multiple electron/proton transfer reduction reactions[194] (**fig. 1.19**)

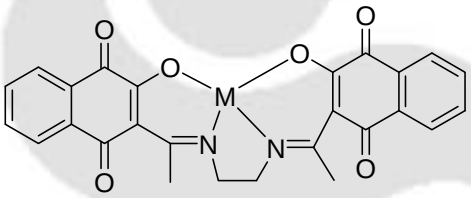

Here M = Ni and Cu

1.95

Fig. 1.19

Novel metal complex[195] assemblies are constructed from the flexible hinge-like ligand 2,2′-bi-(3-hydroxy-1,4-naphthoquinone) **1.96** (**1.96** = H_2bhnq, **fig. 1.20**).

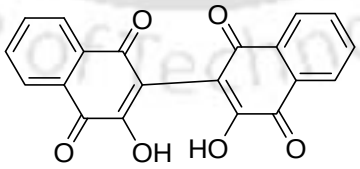

1.96

Fig. 1.20

The H_2bhnq **1.96** is capable of adjusting itself sterically owing to the flexible hinge-like ligand. The two naphthoquinone groups in H_2bhnq are linked by a single bond and it allows the rotation about the single bonds. This rotation allows the conformational

flexibility in H_2bhnq. The ligand possesses skewed conformation. There are at least four possible architectures of the assemblies that might reasonably exist with skewed conformation, they are namely; zigzag, helix, square, and dimer. Four types of architectures from this ligand are accessible with different metal ions. In the case of copper(II) ions, the chelating bhnq^{2-} ions bridge copper(II) centers to form one-dimensional zigzag chains **1.97**. These chains are arranged by hydrogen-bonding interactions and stacking interactions to produce porous structures. Secondly, cobalt(II) and zinc(II) ions form one dimensional helical chains **1.98**. The crystal packing of these helical chains induces spontaneous resolution of the helical chains with chiral cavities formed perpendicular to the helices.

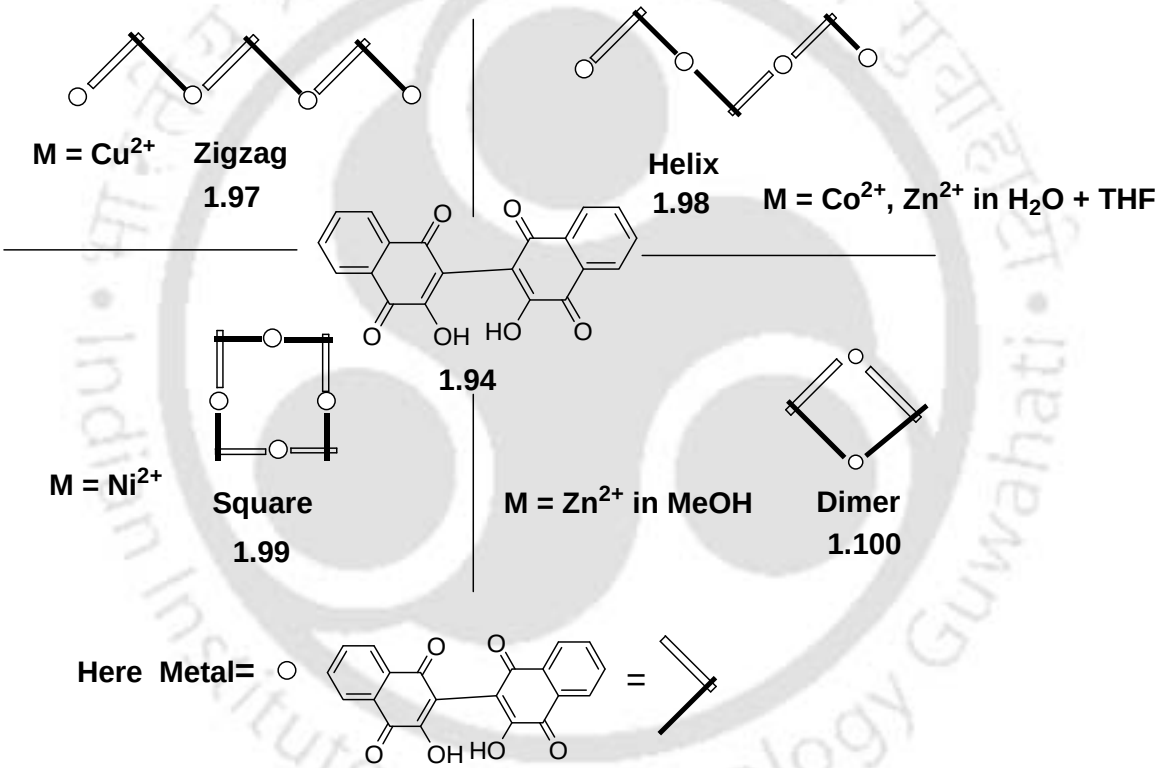

Fig. 1.21

Thirdly, nickel(II) ions form cyclic tetramers **1.99**. The fourth architecture, a dimer **1.100** is obtained by the reaction of zinc(II) ions and H_2bhnq in methanol. In these two compounds **1.99** and **1.100**, change the dihedral angles and the metal-coordination mode of the bhnq^{2-} ion induce the structural versatility. The complete reaction scheme and the structure of the complexes **1.97**-**1.100** are shown in **fig. 1.21**.

1.13 Scope of the present work

Foregoing discussion has clearly shown the vast dimension of chemistry related to quinone derivatives. Further to these amino quinone derivatives[196] are used for the preparation of the modified Au electrode.[197-98] For example the modified Au electrode of naphthoquinone derivatives **1.101** was used for ‘‘Write–Read–Erase’’ information processing system with integration of hydrophobic magnetic nanoparticles in water-toluene two phase assembly (**fig. 1.22**).[199] The different electrochemical properties of the quinone monolayer in the presence of the aqueous solution or the hydrophobic layer

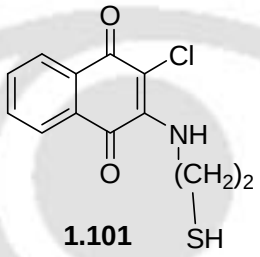

1.101

Fig. 1.22

generated by the magnetic nanoparticles (NPs) enable the encoding of information, its storage and erasure. Firstly, the ‘‘Write’’ process occurs in the aqueous environment when the magnetic NPs are retracted from the electrode. Secondly, the ‘‘Read’’ process occurs in the non-aqueous environment when the magnetic NPs are attracted to the electrode and lastly, the ‘‘Erase’’ process also occurs in the non-aqueous environment when the magnetic NPs are attracted to the electrode.

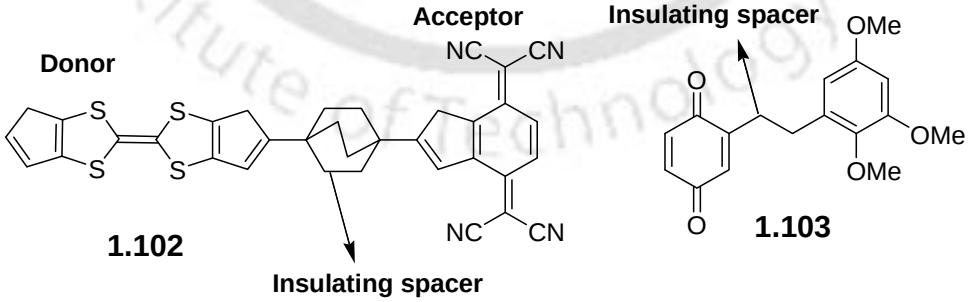

1.102 **1.103**

Fig. 1.23

The compounds **1.102** and **1.103** have an σ-bond insulating framework with donor and acceptor components and can be compared to an anode and cathode with insulating

spacer. These molecules are attractive system for the supramolecular components of molecular rectifier.[200] Electrons from the cathode are transferred into acceptor as soon as the potential is large enough to cause overlap of donor and acceptor orbitals.[201] The insulating spacer is used to tunnel the electron in this space.

The new substituted tetrathiofulvalene-quinone dyad **1.104** has a long oligoethylene glycol chain as spacer[202] (**fig. 1.24**) observed binds with metal ions (Pb^{2+}, Zn^{2+}, and Sc^{3+}).

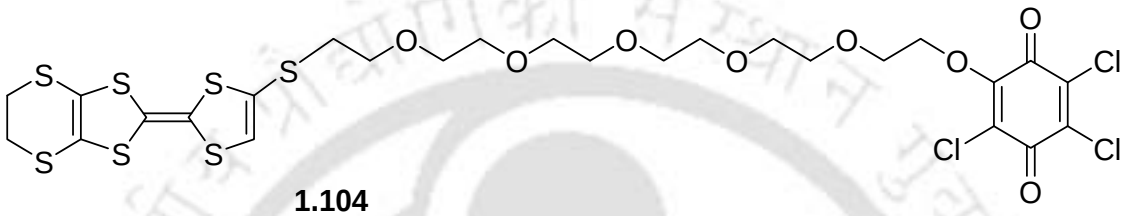

1.104

Fig. 1.24

These examples indicate the importance of amino or thiolato derivative of quinones. It is already mention that quinone undergoes C-N and C-S bond formation reaction to give various derivatives such as the one shown **fig. 1.25**.

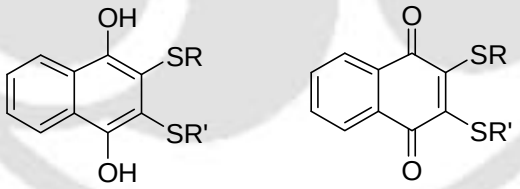

1.105 **1.106**

Fig. 1.25

With this background there is ample scope to synthesize and understand properties of a series of C-N and C-S bonded compounds such as **1.105** and **1.106** (**fig. 1.25**). The presence of substituent or substituents in the rigid quinone ring would lead to the different orientation to the form polymorph. The study on co-crystals of quinonic carboxylic acids to illustrate the guest binding of these compounds would provide the mimic of analogous substrate in biological environment.

A large number of literatures of quinonic complexes such as π-complexes[165-169] and catecholate, semiquinolate complexes are found.[185-191] There are scare of study detailing carboxylic acid tethered quinone as ligands. The systematic investigation of weak interactions in the metal directed assemblies with quinonic carboxylic acids are infancy.

Furthermore the quinones can be easily reduced to corresponding diols which can be anchored to carboxylic acid containing functional groups. This would result in ether of diol derivatives; which would serve as new class of ligands for the synthesis of metal-organic frameworks (MOFs).

Chapter 2

Carbon-sulphur and carbon-nitrogen bond formation reactions of quinone

Quinone derivatives having alkyl/aryl sulphanyl groups are useful as drugs and herbicides.[203-207] Existing literature suggests that C-S and C-N bond formation reactions on quinones[208-228] can be achieved in fairly straight forward manners. However, majority of these report lack in detail synthetic procedures and spectroscopic data[229-230] of such compounds. In this chapter we demonstrate the C-S and C-N bond formation reactions on quinones under ambient conditions with good atoms economy.

2.1 Synthesis and characterization of *bis* 2,3-arylsulfanyl naphthalenediols and *bis* 2,3-arylsulfanyl naphthoquinone

The diarylsulfanyl 1,4-naphthoquinone[106] were reported to be prepared from the reaction of 1,4-naphthoquinone with thiophenol by using potassium fluoride with celite in low yield. These reactions are believed to pass through formation of 2-arylsulphanyl-1,4-naphthoquinones. It is also known that the reaction of thiophenols with 1,4-naphthoquinone in 1:1 molar ratio leads to the formation of 2-arylsulphanyl-1,4-naphthoquinone (**equation 2.1**). However, these compounds were prepared for specific purposes and experimental details on synthesis and spectroscopic details which are not available. In the present context of the thesis, we are interested to synthesize mixed dialky/aryl sulphanyl derivatives of 1,4-naphthoquinone for studying their various structural properties and use them as precursor for ligands. This is with an objective to understand their metal binding ability of new carboxylic acid tethered naphthoquinone or naphthalenediol derivatives containing carbon-sulphur bond. So, we have taken up a systematic synthesis of 2-arylsulphanyl 1,4-naphthoquinones. We observe that the reactions of 1,4-naphthoquinone with thiophenols can be carried out in good yield without any additional reagent at room temperature yielding mono or disubstituted C-S bonded product depending on the stoichiometry. The reaction of aromatic thiols with 1,4-naphthoquinone in 1:1 molar ratio at room temperature under aerobic condition gives corresponding 2-arylsulphanyl 1,4-naphthoquinones **2.1-2.5** (**equation 2.1**).

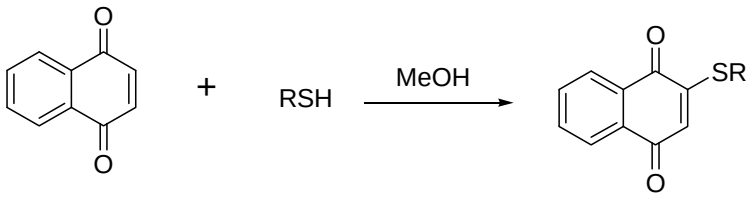

2.1-2.5

R = -C_6H_5 (**2.1**), R= 4-$CH_3C_6H_4$- (**2.2**) R= 4-$CH_3OC_6H_4$-(**2.3**), R=4-Br C_6H_4-(**2.4**) and 2-OHC_4H_4-(**2.5**)

Equation 2.1 Synthesis of 2-arylsulphanyl 1,4-naphthoquinones

These reactions are simple and applicable to varieties of aromatic thiols. A series of 2-arylsulphanyl 1,4-naphthoquinones are synthesized and they are characterized by conventional spectroscopic techniques. The reactions occur through 1,4-addition of thiols to 1,4-naphthoquinone to form unstable (highly oxidisable) mono-substituted naphthalenediol derivatives which undergoe rapid aerial oxidation. Detail of the reaction conditions and yields are shown in **table 2.1**.

Table 2.1 Products from reactions of 1,4-naphthoquinone with various thiols

Entry	Quinone	Reactants	Products	Yield, %	Time(hrs)
1	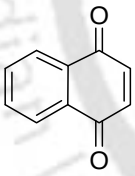	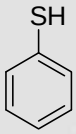	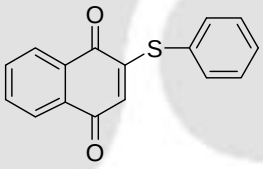 **2.1**	92	2
2	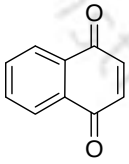	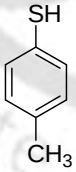	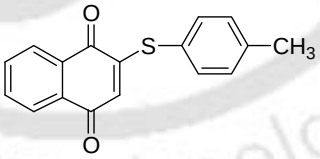 **2.2**	96	2
3	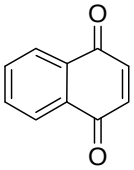	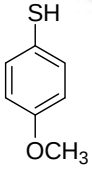	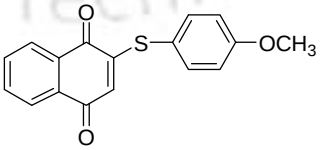 **2.3**	97	2
4	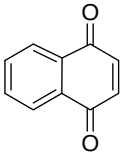	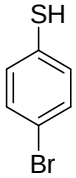	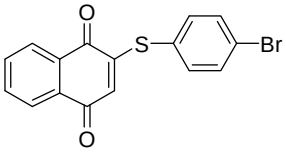 **2.4**	91	2

5	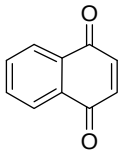	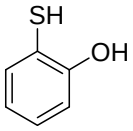	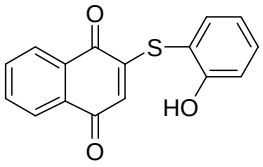 **2.5**	87	2

As a representative case for illustrating the IR spectra, the solid state FT-IR spectrum of 2-(4-methylphenyl)sulphanyl 1,4-naphthoquinone, **2.2** shows two strong C=O stretching at 1659 and 1646 cm^{-1} for two unsymmetrical carbonyl groups. It also shows sharp absorptions at 1593 and 1558 cm^{-1} for the aromatic rings. The UV-visible spectra of the 2-phenylsulphanyl 1, 4-naphthoquinone shows an absorption band at 404 nm due to n-π* transition. As a representative example the ^1H NMR spectrum of 2-(4-methylphenyl) sulphanyl 1,4-naphthoquinone, **2.2** is shown in **fig. 2.1**.

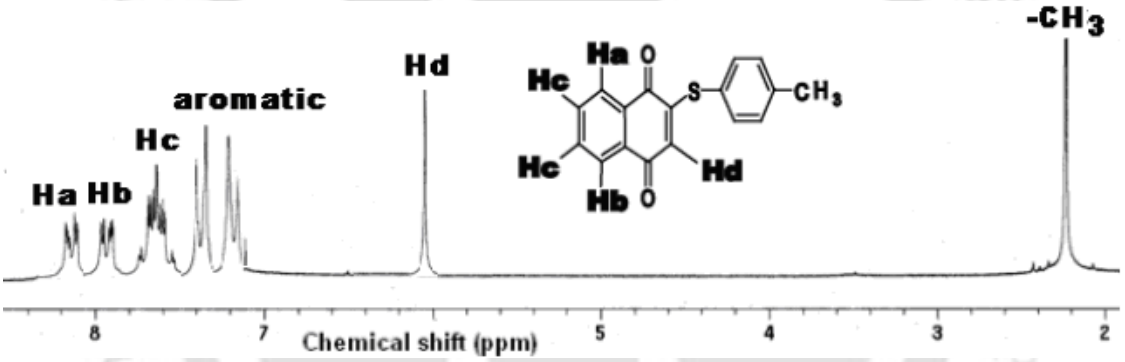

Fig. 2.1 ^1H NMR spectrum ($CDCl_3$) of 2-(4-methylphenylsulphanyl) 1,4-naphtho-quinone

The proton adjacent to the carbonyl groups of the 1,4-naphthoquinone represented as Ha in **fig. 2.1** appears as doublet at 8.14 ppm and the other aromatic proton represented as Hb appears at 8.02 ppm. The remaining two hydrogen atoms of 1,4-naphthoquinone represented as Hc appear as multiplet at 7.72 ppm and the hydrogen represented by Hd appears as singlet at 6.11 ppm. The aromatic protons of 4-methylphenyl ring appear as A_2B_2 pattern of doublet of doublet at 7.41 ppm and 7.31 ppm respectively. The methyl protons are observed as singlet at 2.23 ppm. All other compounds have satisfactory spectroscopic data and details are listed in experimental section. In these reactions when proper stoichiometry is used; no disubstituted products are formed. This makes it

easy for separation and they can be prepared in gram scale in one pot reaction making them attractive for further structural transformations.

2.1.1 Synthesis of *bis*-2,3-diarylsulfanylnaphthalene 1,4 diols

The reaction of 1,4-naphthoquinone and thiophenols in 1:2 molar ratio at room temperature in methanol gives 2,3-diarylsulfanylnaphthalene 1,4-diols **2.6-2.10** as shown in **equation 2.2**. These compounds are colorless and formed in very good yield.

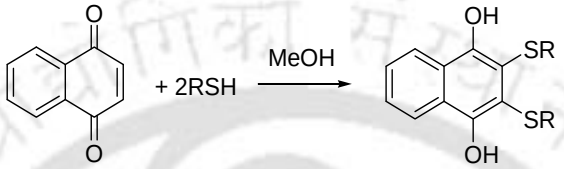

2.6-2.10

R = C_6H_5-(**2.6**), 4-$CH_3C_6H_4$-(**2.7**), 4-$CH_3OC_6H_4$-(**2.8**), 4-Br C_6H_4-(**2.9**) and 2-OHC_6H_4-(**2.10**).

Equation 2.2 Synthesis of 2,3-diarylsulfanylnaphthalene 1,4-diols

These reactions presumably pass though 2-arylsulphanyl 1,4-naphthoquinones; formation of which are completed in a short time, whereas the disubstitution reaction on the mono-substituted products require longer reaction time. The requirement of no additional reagent other than the reactant makes such reactions advantageous in terms of minimization of side products and hazard. The reactant used and yields of symmetrical 2,3-diarylsulfanylnaphthalene 1,4-diols are shown in **table 2.2**.

Table 2.2 The reactions of 1,4-naphthoquinone with various thiols

Entry	Quinone	Reactants	Products	Yield, %	Time(hrs)
1	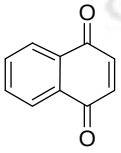	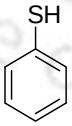	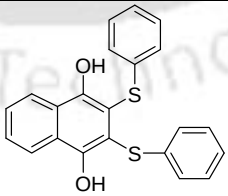 **2.6**	92	3
2	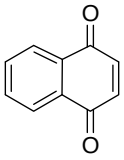	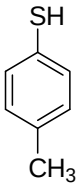	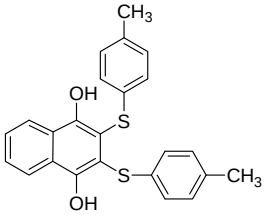 **2.7**	96	3

3	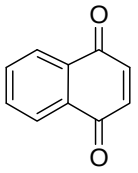	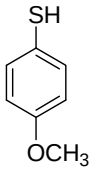	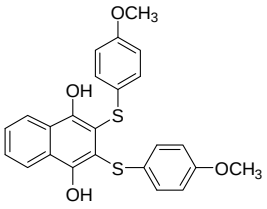 **2.8**	96	3
4	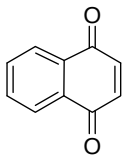	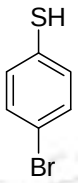	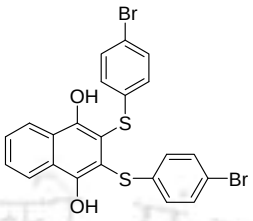 **2.9**	95	3
5	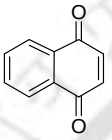	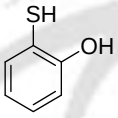	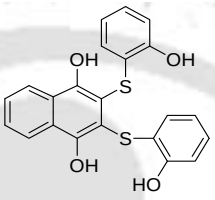 **2.10**	85	3

The formation of 2,3-diarylsulfanylnaphthalene 1,4-diols derivatives may be described by the reaction path shown in **scheme 2.1**. This mechanism is further supported by the fact that use of two different thiols in sequential manner leads to the formation of mixed aryl products of 2,3-diarylsulfanylnaphthalene 1,4-diols,

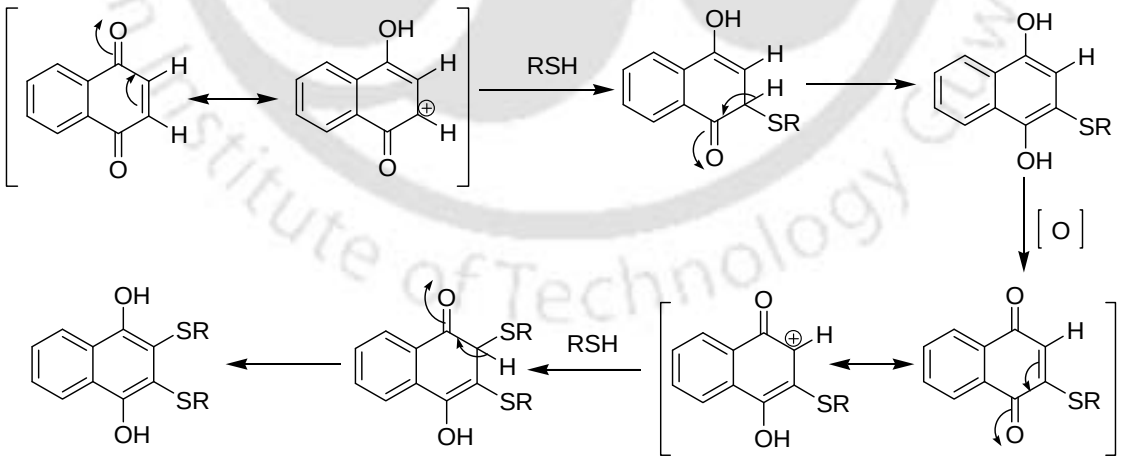

Scheme 2.1 Plausible mechanism for the synthesis of 2,3-diarylsulfanyl 1,4-naphthalenediols

however they are formed with mixture of the two other possible symmetric 2,3-diarylsulfanylnaphthalene 1,4-diols. This is possible as the formation of

monosubstituted derivative and its oxidation reaction is faster than the attack of the second thiol group. Based on this observation we proceeded further to synthesize mixed aryl 2,3-diarylsulfanylnaphthalene 1,4-diols from 2-arylsulphanyl 1,4-naphthoquinones.

The 2-phenylsulphynyl-1,4-naphthoquinones reacted with different thiophenols (**scheme 2.2**). Addition of sodium metabisulphite at the time of work up the reaction mixture gives the mixed 2,3-diarylsulfanyl 1,4-naphthalene 1,4-diols. From these reactions various unsymmetrical 2,3-diarylsulfanyl 1,4-naphthalene 1,4-diols **2.11-2.16** are synthesized and characterized. The same reaction can be carried out without sodium metabisulphite in low yield. The use of metabisulphite during the work up makes a reducing environment so that the final 1,4-naphthalendediol derivatives are not associated with 1,4-naphthoquinone derivatives in the form of charge transfer adducts and also diol derivatives do not get further oxidized.

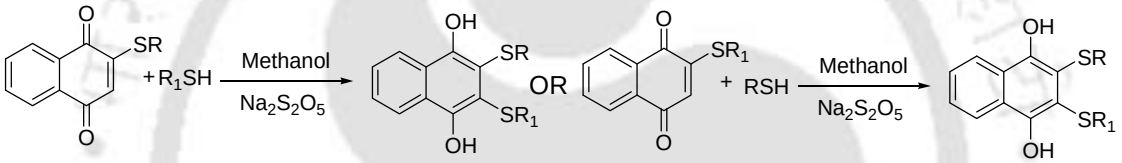

2.11-2.16

When R = C_6H_5-, R_1 = 4-$CH_3C_6H_4$-(**2.11**); 4-$CH_3OC_6H_4$-(**2.12**) and 4-BrC_6H_4-(**2.13**).
R = 4-$CH_3C_6H_4$-, R_1 = C_6H_5- (**2.11**); 4-$CH_3OC_6H_4$-(**2.14**) and 4-BrC_6H_4-(**2.15**).
R = 4-$CH_3OC_6H_4$-, R = C_6H_5-(**2.13**); 4-$CH_3C_6H_4$-(**2.14**); and 4-BrC_6H_4-(**2.16**).
R = 4-BrC_6H_4-, R_1 = C_6H_5-(**2.13**); 4-$CH_3C_6H_4$-(**2.15**); and 4-$CH_3OC_6H_4$- (**2.16**).

Scheme 2.2 Synthesis of unsymmetrical 2,3-diarylsulfanyl 1,4-naphthalene 1,4-diols

This speculative explanation is on the basis of the existence of charge transfer interactions between quinones and hydroquinones and ability of bisulphite to reduce quinones to corresponding diols.[231] The reactant used for the synthesis of unsymmetrical derivatives and product yields are shown in **table 2.3**.

Table 2.3 The synthesis of various mixed 2,3-diarylsulfanyl 1,4-naphthalene 1,4-diols

Entry	Quinones	Reactants	Products	Yield, %	Time(hrs)
1	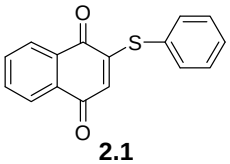 **2.1**	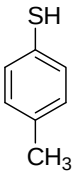	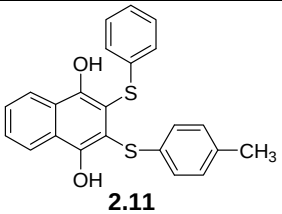 **2.11**	94	4

2	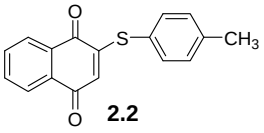 **2.2**	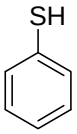	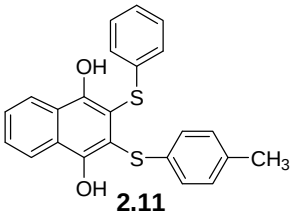 **2.11**	86	4
3	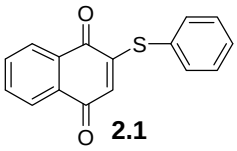 **2.1**	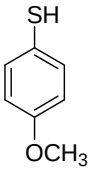	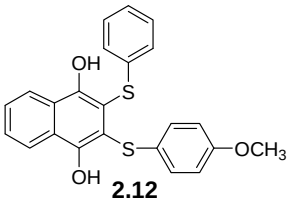 **2.12**	96	4
4	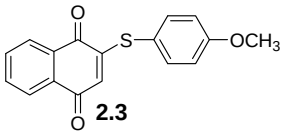 **2.3**	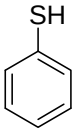	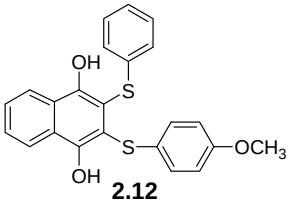 **2.12**	88	4
5	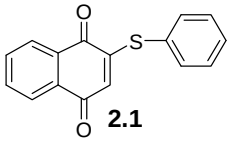 **2.1**	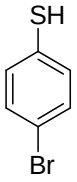	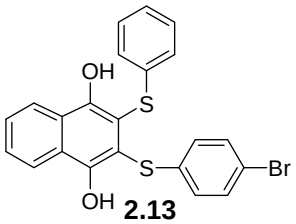 **2.13**	91	4
6	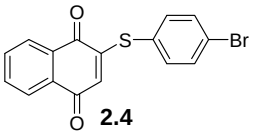 **2.4**	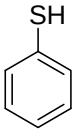	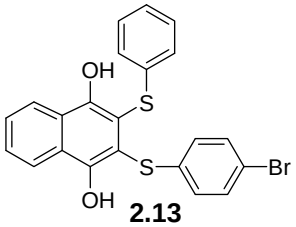 **2.13**	92	4
7	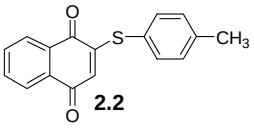 **2.2**	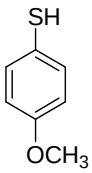	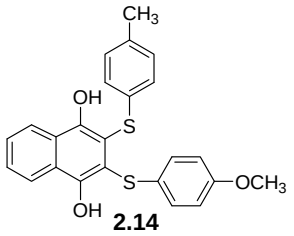 **2.14**	95	4
8	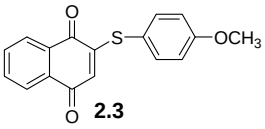 **2.3**	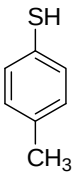	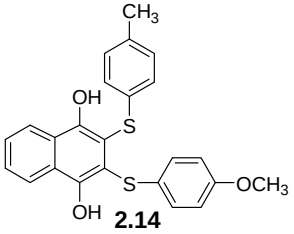 **2.14**	89	4
9	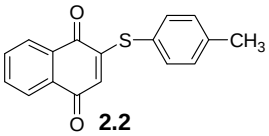 **2.2**	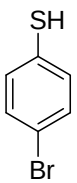	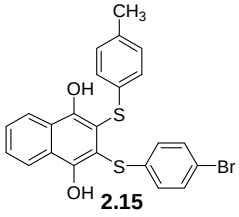 **2.15**	82	4

10	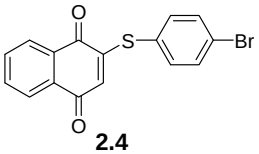 **2.4**	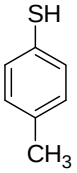	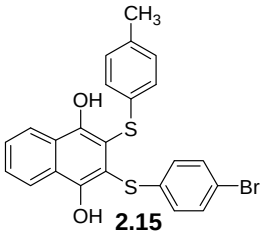 **2.15**	92	4
11	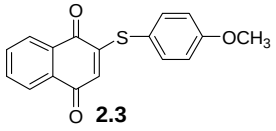 **2.3**	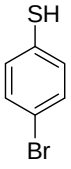	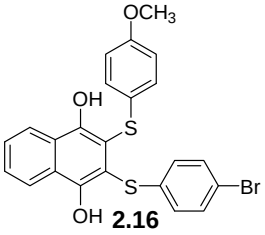 **2.16**	82	4
12	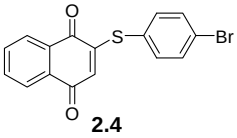 **2.4**	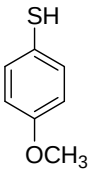	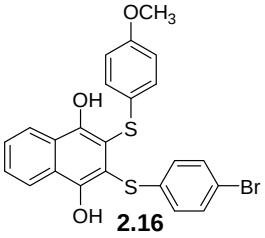 **2.16**	94	4

The above C-S bond formation reactions of 1,4-naphthoquinone is applicable to aliphatic thiols also. For example, the reaction of 1,4-naphthoquinone with thioglycolic acid in methanol in 1:2 ratio gives mixture of (3-carboxymethylsulfanyl-1,4-dihydroxy-naphthalen-2-ylsulfanyl)acetic acid, **2.17** and (3-carboxymethylsulfanyl-1,4-dioxo-1,4-dihydro-naphthalen-2-yl-sulfanyl) acetic acid **2.18**. A similar reaction of 1,4-naphthoquinone with 2-mercaptoethanol leads to 2, 3-bis-(2-hydroxy-ethylsulfanyl) naphthalene 1,4-diol, **2.19** and 2,3-bis-(2-hydroxy-ethylsulfanyl)-1,4-naphthoquinone **2.20** (**scheme 2.3**). The yield of compound **2.17** and **2.18** is 55% and 23%; while for the compound **2.19** and **2.20** yield is 38% and 52% respectively. The compound **2.18** could also be obtained by aerial oxidation of compound **2.17**.

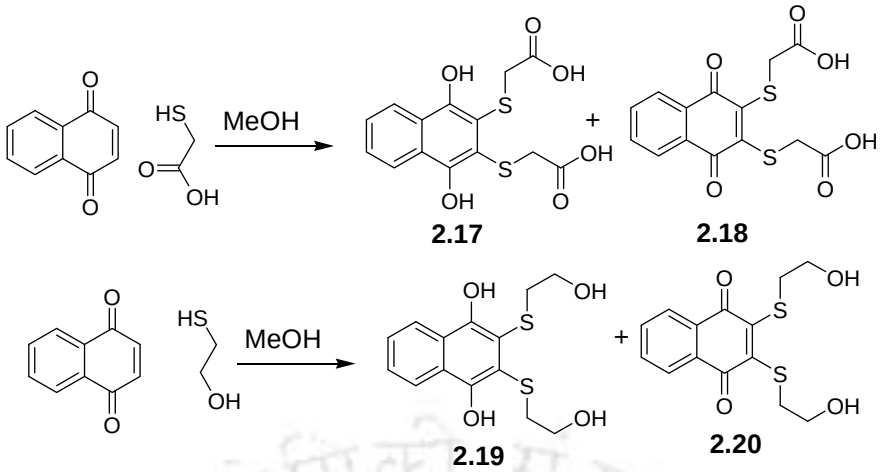

. **Scheme 2.3** Reaction of 1,4-naphthoquinone with aliphatic thiols

^{1}H NMR spectrum of 2,3-*bis*-(2-hydroxyethylthio)naphthalene 1,4-dione **2.20** in DMSO-d_6 is shown in **fig. 2.2** The proton adjacent to the carbonyl groups of the 1, 4-naphthoquinone represented as Ha appears as doublet of doublet at 8.03 ppm and other two protons of the 1,4-naphthoquinone represented as Hb is also appears as doublet of doublet at 7.69 ppm. The methylene proton adjacent to thiol group appears as triplet at 3.78 ppm and the methylene proton adjacent to hydroxyl group appears as triplet at 3.40 ppm. The protons of the hydroxyl group appear at 2.69 ppm.

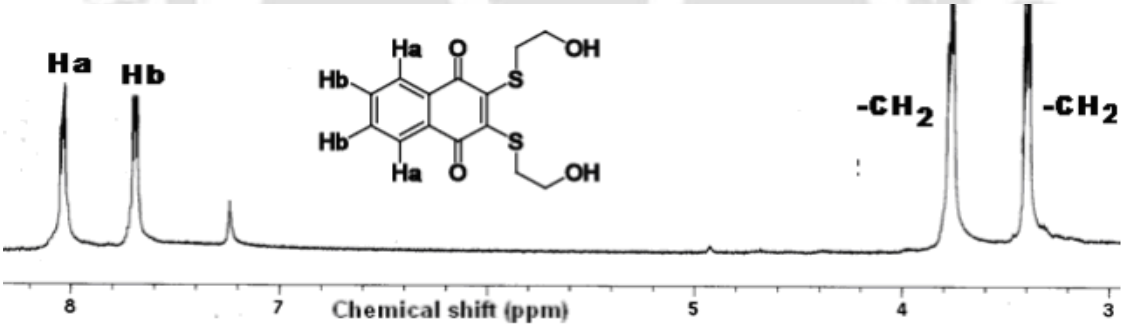

Fig. 2.2 ^{1}H NMR 2,3-*bis*(2-hydroxyethylthio)naphthalene 1,4-dione in DMSO-d_6

The reaction of 1,2-ethanedithiol and 1,3-propanedithiol with 1,4-naphthoquinone leads to cyclic products with the six and seven member ring attached to the naphthalene ring respectively (**scheme 2.4**). The cyclic products of naphthalene diols, **2.21** and **2.24** and corresponding quinone derivatives, **2.22** and **2.25** are isolated and characterized by conventional spectroscopic techniques. On repeated crystallization from methanol solution in presence of air **2.21** and **2.24** get converted to the corresponding oxidized

products **2.22** and **2.25** respectively. The crystal structure of the compound **2.22** shows the *syn*-orientation at the sulphur lone pairs (**fig. 2.3**). The three methylene groups in the molecule **2.22** are positioned in staggered manner. We could not obtain the corresponding dithiolato diquinone products **2.23** and **2.26** in these reactions**;** as such reaction leads to polymeric products easily.

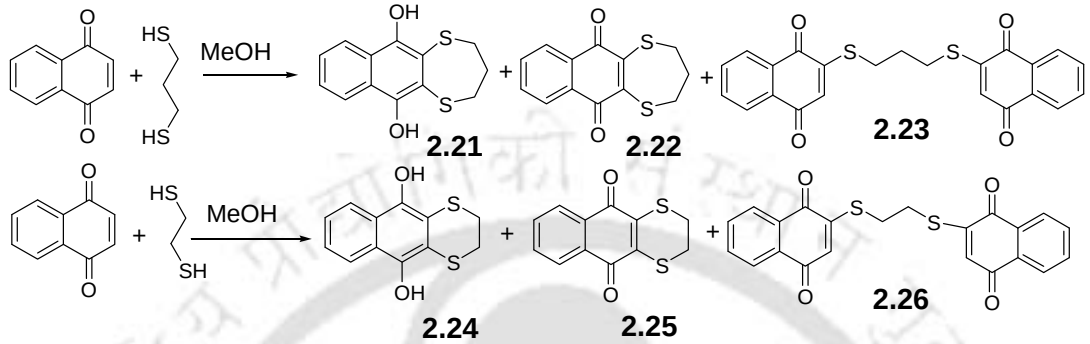

Scheme 2.4 Reactions of dithiols with 1,4-naphthoquinones

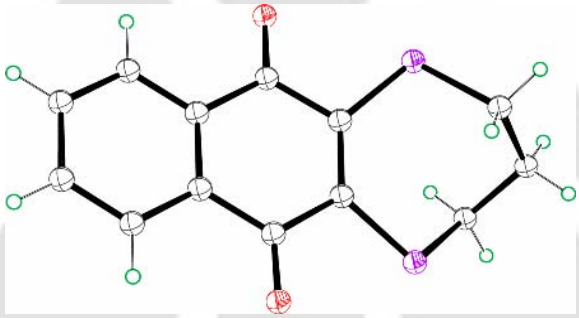

Fig. 2.3 Crystal structure of the compound **2.22** (ORTEP drawn in 30% thermal ellipsoid)

The diol derivatives **2.19**, **2.21** and **2.24** are very unstable and undergo oxidation spontaneously. It turns colorless to red indicating the formation of corresponding quinone derivatives **2.20**, **2.22** and **2.25** respectively.

Since from the reaction of 1,4-naphthoquinone with aliphatic dithiols, the 1,4-naphthoquinone derivatives bridge by two dithilato bridge of the type **2.23** and **2.26** (**scheme 2.4**) are not obtained and this is attributed to polymerization on reaction. So, we have studied the reactivity of 1,4-naphthoquinone derivative that has a methyl group at 2-position. The 2-methyl 1,4-naphthoquinone has only one site for substitution reaction to form C-S bond. It is found that the reactions of 2-methyl 1,4-naphthoquinone with various thiols gave the corresponding products **2.27-2.32** as

shown in **scheme 2.5**. In this reaction only single product was formed and the yields are near in quantitative. The reaction of 2-methyl 1,4-naphthoquinone with dithiols gave dithiolato products **2.28**-**2.31** without side reaction. The compounds **2.28** and **2.29** has flexible spacer of 1,2-ethane and 1,3-propane dithiolato groups connecting the two 2-methyl 1,4-naphthoquinones respectively. The reaction of 1,2-benzene dithiol with 2-methyl 1,4-naphthoquinone however led to a different type of product **2.31** in which there is a S-S bond. This is due to the formation of monothiolato derivative which undergoes aerial oxidation to give the compound **2.31** (**scheme 2.5**). The reaction of 2-methyl 1,4-naphthoquinone is extended to prepare C-S bonded quinone derivatives possessing heterocyclic ring such as compound **2.32** (**scheme 2.5**). The ^{1}H NMR, ^{13}C NMR spectra and elemental analysis of the compound **2.32** shows that it is in solvated form having composition $H_2L(0.5DMF)(1.5H_2O)$.

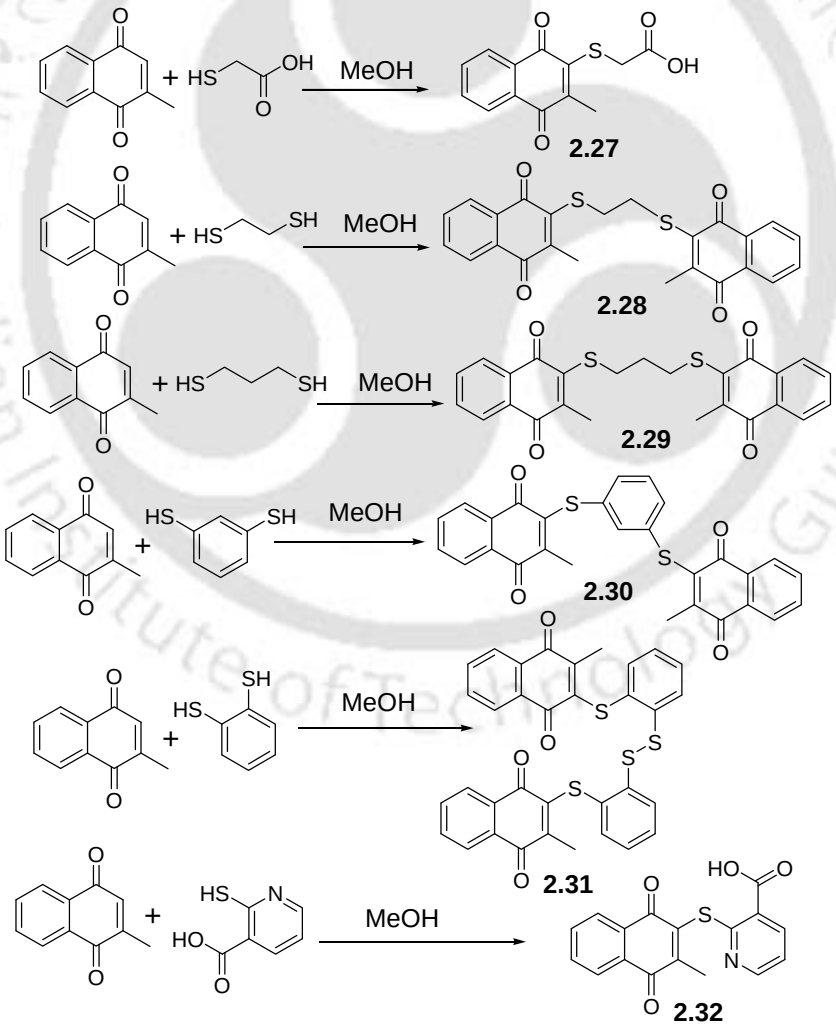

Scheme 2.5 Reactions of 2-methyl 1,4-naphthoquinone with different thiols.

2.1.2 Oxidation of *bis*-2,3-diarylsulfanyl 1,4-naphthalene-1,4-diols

Metal ions catalyzed aerobic oxidation of hydroquinone derivatives to quinone derivatives are reported in literature.[232-234] In total synthesis of targeted molecules many reaction intermediates involve the oxidation of hydroquinone to quinone derivatives that are catalyzed by metal salts.[235-247] The aerobic oxidation of hydroquinone is catalyzed by platinum nanoclusters trapped in styrene-based polymer network.[248-249] Copper(II) salts are known to oxidize hydroquinones.[233] Oxidation of various *bis*-2,3-diarylsulfanyl 1,4-naphthalene 1,4-diols to corresponding *bis*-2,3-diarylsulfanyl 1,4-naphthoquinone can be achieved in the presence of catalytic amount of copper(II) acetate under aerobic condition.

A series of *bis*-2,3-diarylsulfanyl 1,4-naphthoquinone **2.33-2.43** are synthesized from their corresponding *bis*-2,3-arylsulfanylnaphthalene 1,4-diols **2.6-2.16** respectively by catalytic reactions (**equation 2.3**). The advantage of this catalytic reaction is the ease of product purification due to single product formation.

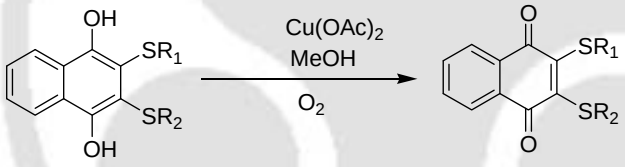

2.6-2.16 **2.33-2.43**

$R_1 = R_2 = C_6H_5$-(**2.33**); 4-$CH_3C_6H_4$-(**2.34**);4-$CH_3OC_6H_4$-(**2.35**); 4-BrC_6H_4-(**2.36**); 2-HOC_6H_4-(**2.37**);
$R_1 = C_6H_5$-; R_2 = 4-$CH_3C_6H_4$-(**2.38**); 4-$CH_3OC_6H_4$-(**2.39**); 4-BrC_6H_4-(**2.40**);
R_1 = 4-$CH_3C_6H_4$-; R_2 = 4-$CH_3OC_6H_4$-(**2.41**); 4-BrC_6H_4-(**2.42**); and
R_1 = 4-$CH_3OC_6H_4$-, R_2 = 4-BrC_6H_4-(**2.43**).

Equation 2.3 Oxidation of 1,4-naphthalenediol derivatives

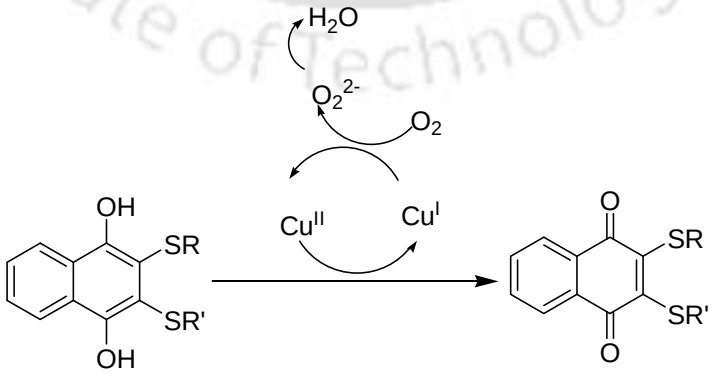

Scheme 2.6 Catalytic cycle in oxidation of 1,4-naphthalenediol derivatives

The oxidation of these stable 1,4-naphthalenediol derivatives is represented by catalytic cycle as shown in **scheme 2.6**. Firstly, the 1,4-naphthalenediol derivatives get oxidized by copper(II) ions. The copper(II) ions thus get reduced to form copper(I) ion. This reduction is followed by the reoxidation of the copper(I) ions to copper(II) ions (**scheme 2.6**). The 2,3-diarylsulfanylnaphthalene 1,4-diols and corresponding oxidation products are listed in **table 4**.

The solid state FT-IR spectrum of these 1,4-naphthalenediols (compounds **2.6-2.17**) shows one O-H stretching bands in the region 3390-3400 cm^{-1}. Apart from these O-H stretching bands, it also shows multiple bands at 2910-3000 cm^{-1} arising from C-H stretching frequency. Sharp band centered at 1570-1590 cm^{-1} due to aromatic ring.

Table 4: Catalytic oxidation of 2,3-diarylsulfanylnaphthalene 1,4-diols

Entry	Reactants	Products	Yield, %	Time(hrs)
1	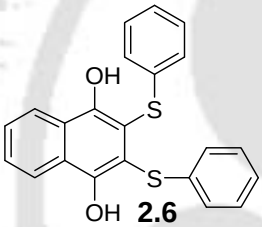 **2.6**	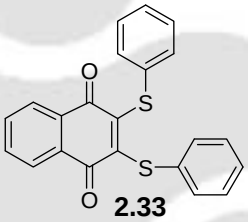 **2.33**	96	1
2	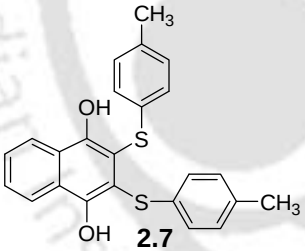 **2.7**	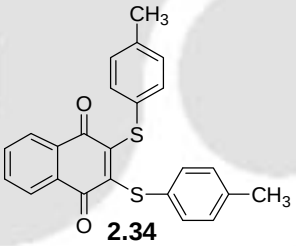 **2.34**	98	1
3	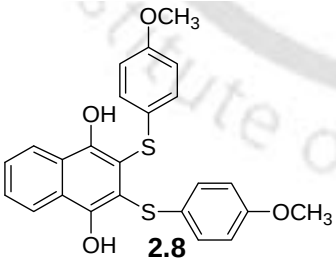 **2.8**	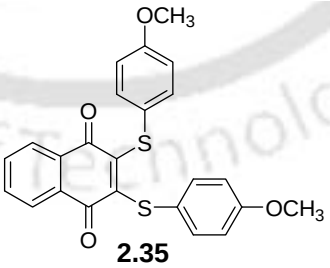 **2.35**	97	1
4	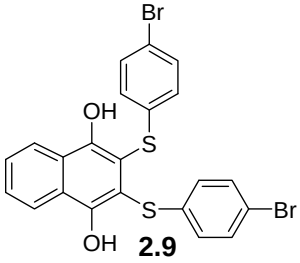 **2.9**	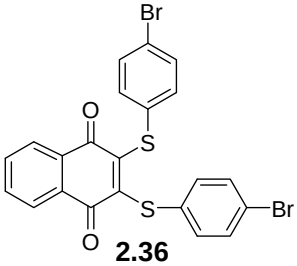 **2.36**	96	1

5	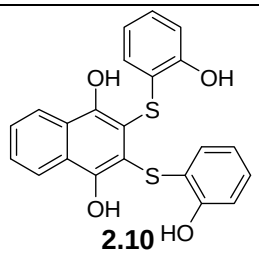 **2.10**	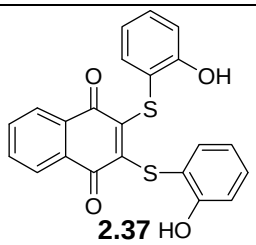 **2.37**	94	1
6	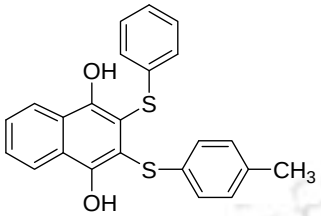 **2.11**	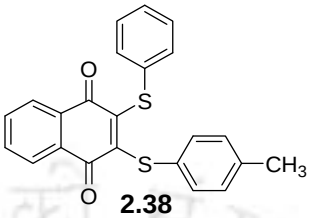 **2.38**	96	1
7	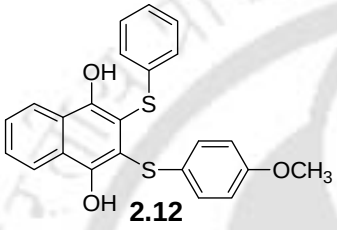 **2.12**	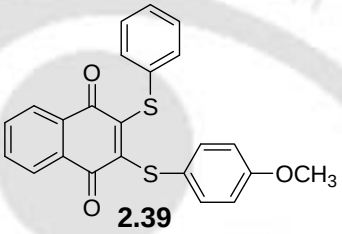 **2.39**	92	1
8	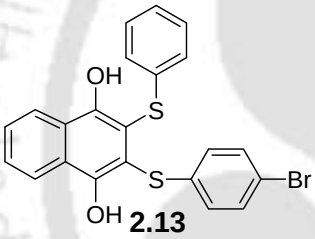 **2.13**	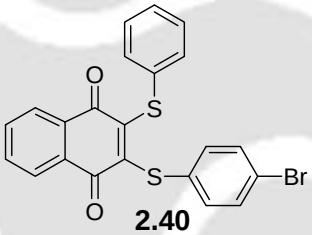 **2.40**	96	1
9	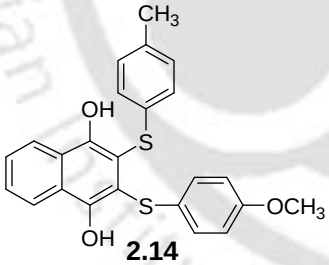 **2.14**	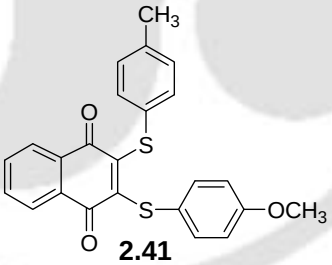 **2.41**	96	1
10	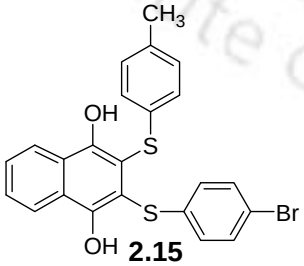 **2.15**	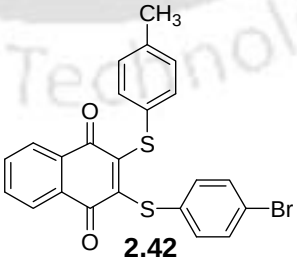 **2.42**	92	1

11	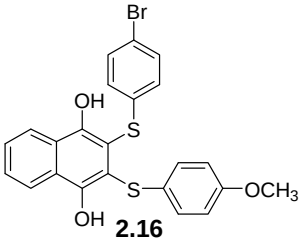 **2.16**	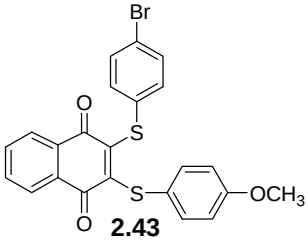 **2.43**	95	1

The FT-IR spectra of corresponding quinone counterparts (compounds **2.33-2.43**) do not have O-H stretching bands. They have one medium absorption band at 1655-1670 cm^{-1}. This shows that the two carbonyl groups are in similar environment. Similarly, the compounds have stretching bands at 2925-2935 cm^{-1} arising from C-H stretching and 1590 cm^{-1} due to C=C band of aromatic rings. For comparison the overlay FT-IR spectra of compound **2.8** (1,4-naphthalene diol, blue line) and the corresponding quinone **2.35** (black line) are shown in **fig.2.4**.

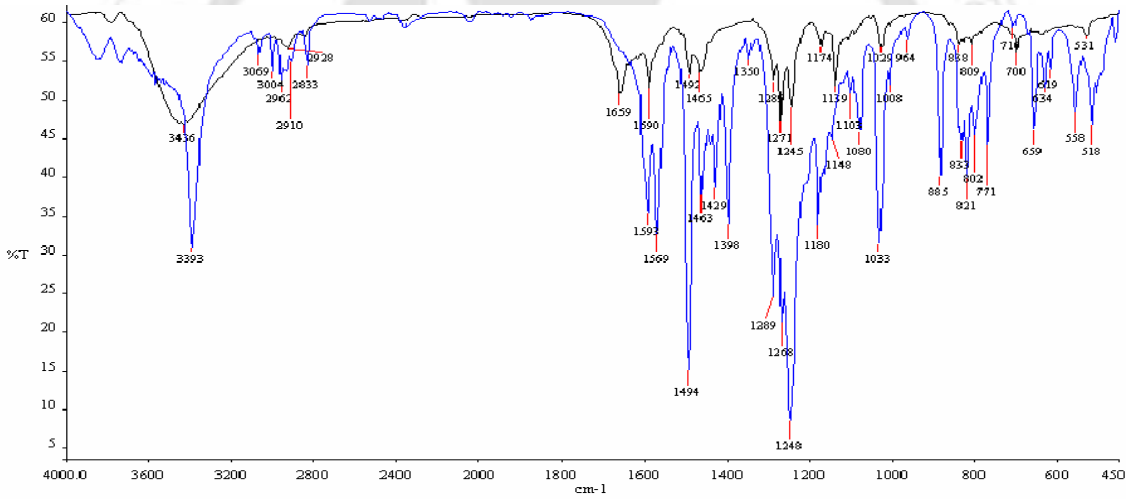

Fig. 2.4 FT-IR spectra of diol **2.8** (blue line) and quinone **2.35** (black line)

The UV-visible spectra of 1,4-naphthalenediol derivatives (compounds **2.6-2.16**) shows two absorption bands at 341 nm and 356 nm in methanol. These two absorption bands are assigned as π-π* and n-π* transition respectively. The compound **2.6** is chosen as a representative example to illustrate the UV-visible spectra of 1,4-naphthalenediol derivatives (**fig. 2.5a**). The UV-visible spectra of the corresponding quinone derivatives (compounds **2.33-2.43**) show one absorption band at 456 nm in methanol. The absorption band at 456 nm is assigned to n-π* transition. As a representative example of quinone derivatives, the UV-visible spectra of 1,4-napthoquinone derivative **2.33** is shown in **fig.2.5b**.

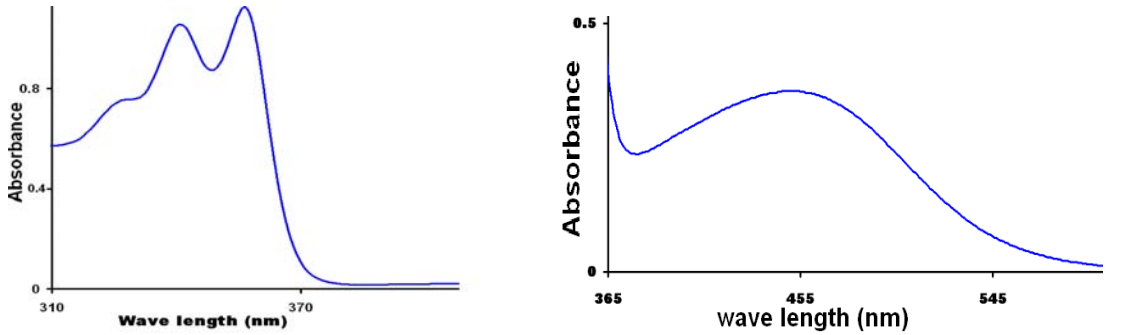

Fig. 2.5 a) UV-visible spectra of diol compound **2.6**; b) UV-visible spectra of quinone compound **2.33** (in 1×10^{-4} M solution of methanol)

The ^{1}H NMR spectrum of the 1,4-naphthalenediols (compounds **2.6-2.16**) show similar features in $CDCl_3$. The compound **2.8** is chosen as a representative example to illustrate ^{1}H NMR spectra of this class of compounds. The O-H proton appears as sharp singlet at 7.26 ppm. The protons adjacent to the hydroxyl groups of the 1,4-naphthalene diols (represented as Ha in **fig. 2.6**) appears as double of doublet at 8.28 ppm and the other protons represented as Hb appears at 7.63 ppm. The aromatic protons of 4-methoxy thiophenol appear as two doublets at 7.00 ppm and 6.65 ppm respectively. The methoxy proton appears as a singlet at 3.71 ppm.

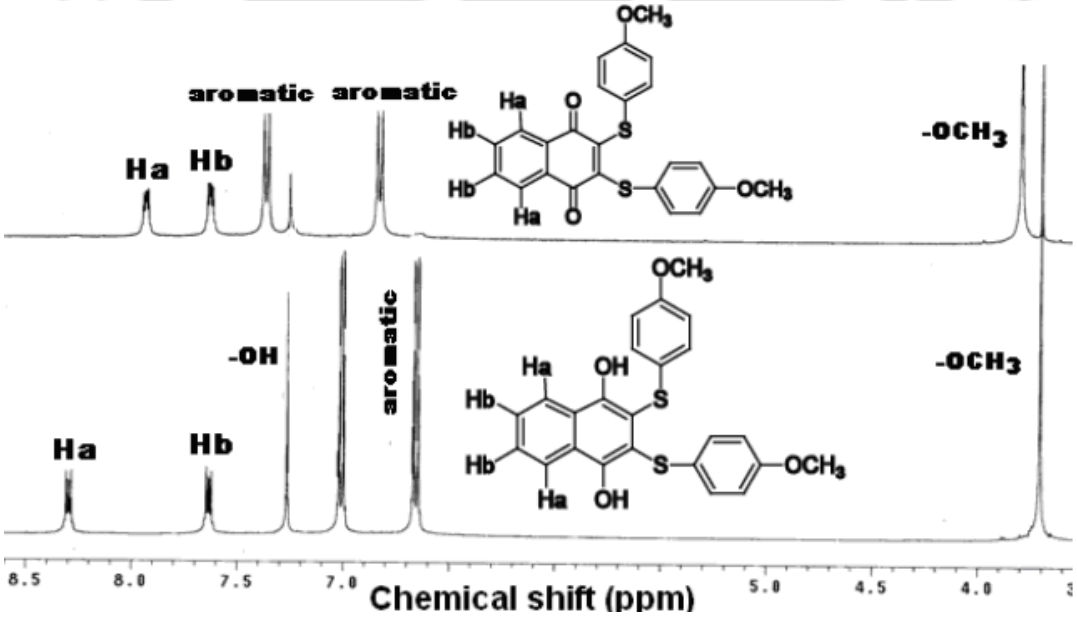

Fig. 2.6 Overlay ^{1}H NMR spectra ($CDCl_3$, 400 MHz) of diol derivative **2.8** and quinone derivative **2.35**

In the ^{1}H NMR spectra of the compound **2.35** the protons neighboring to the carbonyl groups of 1,4-naphthoquinone represented as Ha appears a peak at 7.95 ppm as doublet of doublet and the other proton represented as Hb appear at 7.64 ppm as doublet of doublet respectively. The aromatic protons of 4-methoxy thiophenol show two doublets at 7.38 ppm and 6.84 ppm respectively. The methoxy proton shows a singlet at 3.81 ppm.

From this study it is clear that the quinonic products differ in their aromatic signals in ^{1}H NMR spectra from the diol products and can be distinguished. Further to this the quinonic derivatives are intense in color than the diol derivatives to distinguish them visibly. The carbonyl stretching of the quinonic derivatives also clearly distinguishes them from the diol derivatives.

2.2.1 Reaction of quinones with primary amines and their equivalence of reactivity

Thymoquinone (**fig. 2.7**) is a bioactive benzoquinone compound derived from black seed oil of *Nigella sativa* and is a potential chemopreventive and chemotherapeutic compound.[250-252] Thymoquinone has been shown to antitumorigenic potential on cell line derived from breast, colon, ovary, larynx, lung and leukemia.[253-255] Thus there is interest in synthesis and characterization of analogous compounds for testing their biological activity.

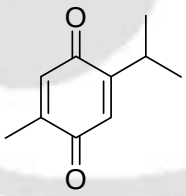

Fig. 2.7

It is well known fact that quinone reacts with different amines and amino acids to form C-N bond. We have taken advantages of such reaction to prepare series of disubstituted amino derivatives of quinone. Various 2,5-bis(alkyl/arylamino)-1,4-benzoquinones **2.44-2.49** are synthesized from the reaction of various amines with 1,4-benzoquinone in methanol in 1:2 molar (**equation 2.4**). The synthesized 2,5-bis(alkyl/arylamino)-1,4-benzoquinones **2.44-2.49** are shown in **fig 2.8**.

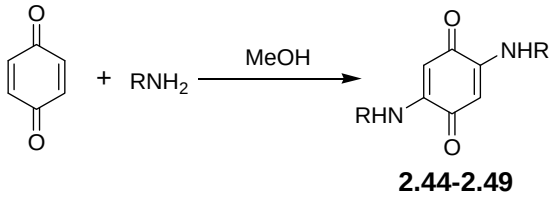

Equation 2.4 Reaction of primary amines with 1,4-benzoquinone

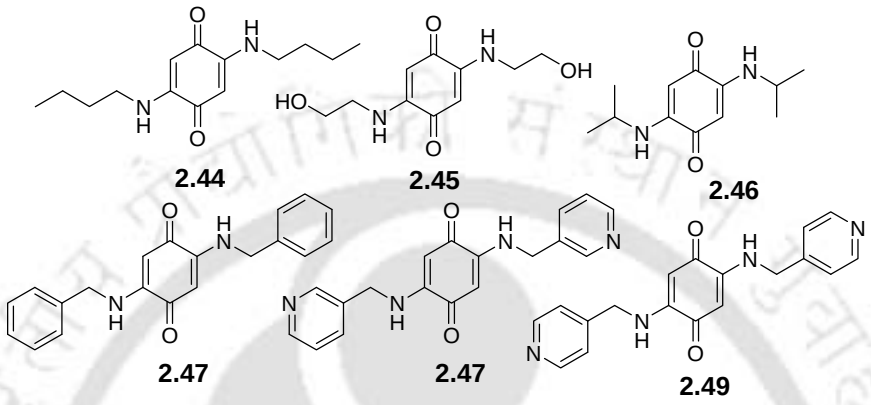

Fig. 2.8

All the compounds have satisfactory spectroscopic data and details are listed in experimental section. As an illustrative example the compound 2,5-bis(3-picolylamino) 1,4-benzoquinone **2.47** is taken up for the discussion. The solid state FT-IR spectrum of compound **2.47** shows one N-H stretching bands in the region 3305 cm^{-1}. It shows weak multiple band at 2926 cm^{-1} arising from C-H stretching and the sharp band centered at 1645 cm^{-1} due to the carbonyl groups of 1, 4-benzoquinone. It also has strong band at 1595-1557 cm^{-1} arising from C=C stretching frequency of aromatic rings. The protons of the 1, 4-benzoquinone represented as He in **fig. 2.9** appears as singlet at 8.32 ppm. The aromatic proton of 3-picolyl ring represented as Ha appears as singlet at 8.49 ppm and the protons represent as Hb shows a doublet at 8.42 ppm. The remaining two hydrogen represent as Hc and Hd shows as triplet and doublet at 7.64 and 7.33 ppm respectively. The -NH protons appears as singlet at 5.21 ppm and the methylene protons appear as doublet at 4.38 ppm.

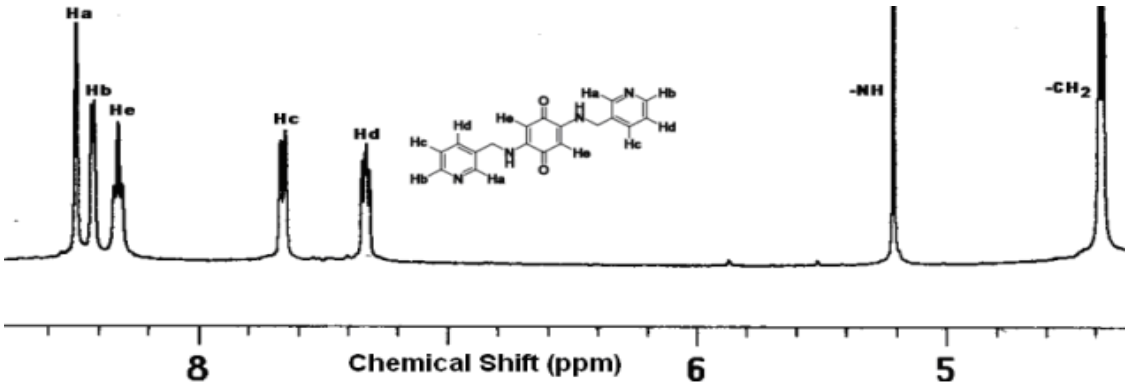

Fig. 2.9 ^{1}H NMR spectra of 2,5-*bis*(3-picolylamino)-1,4-benzoquinone **2.47**

These compounds **2.30**, **2.32** and **2.44-2.49** were tested for their cell viability against the cancerous pancreatic cancer cell lines Panc-1 (Gemcitabine-sensitive) and MiaPaCa (Gemcitabine-resistant) with thymoquinone molecule. The compounds **2.47** and **2.49** are found to be potent compared to thymoquinone molecule in both the cell line. On the other hand the analog **2.47** exhibit superior activity only against the resistant cell line MiaPaCa.

We have studied comparative reactivity of amine vs thiol towards quinone. For this purpose 1,4-naphthoquinone was reacted with 4-aminothiophenol. It is observed that the reaction exclusively leads to monosubstituted C-S bonded quinone **2.50**. The product is characterized by reading IR, NMR, and UV-visible spectra. We also have studied reaction between 1, 4-naphthoquinone with 4-aminophenol and observed that monosubstituted C-N bonded quinone **2.51** derivative is formed exclusively (**scheme 2.7**).

To understand the possible path of these reactions we performed the reaction of 4-amino thiophenol with 1,4-naphthoquinone in a NMR tube in deuterated methanol. The reaction products are compared with the isolated purified product. In this reaction the product formed through C-S bond formation is observed and no C-N bond formation was observed in the NMR tube reaction too.

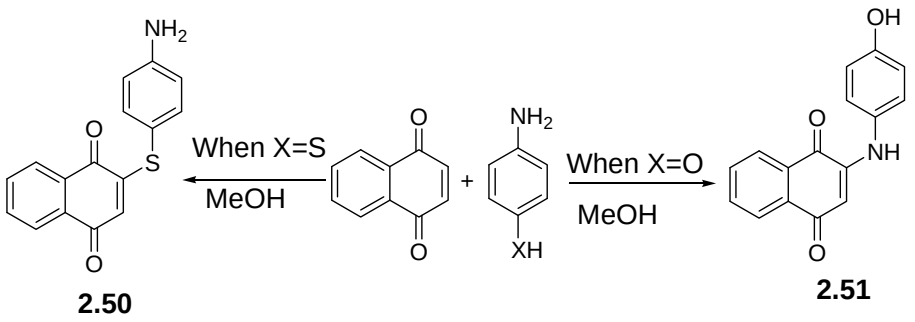

2.50 **2.51**

Scheme 2.7 Reaction of 1,4-naphthoquinone with 4-aminothiophenol and 4-aminophenol.

The ^{1}H NMR spectra were recorded at different time in a deuterated methanolic solution and two such spectra of the reaction mixture as time progresses are shown in **fig. 2.10**. The presence of few well-separated peaks of the products helps in knowing the amount of the starting materials in the NMR spectra. The formation of the one product with time is indicated by the increase in the peak intensity (designated by A in **fig. 2.10**).

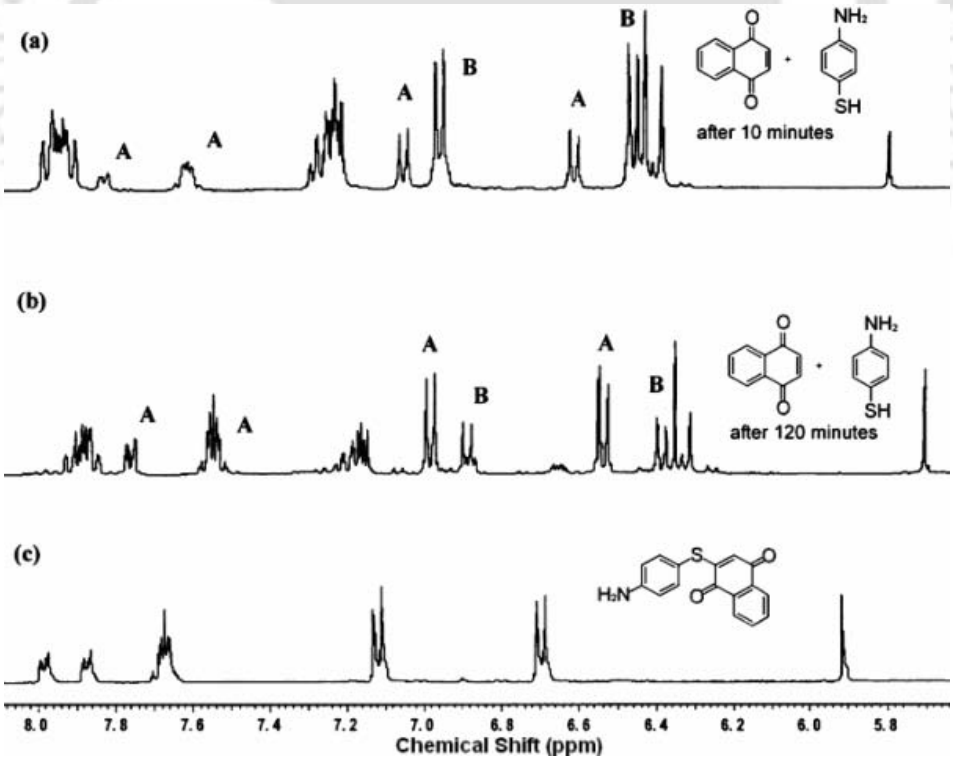

Fig. 2.10 Reaction of aminothiophenol with 1,4-naphthoquinone; monitored in NMR tube after different time intervals of a) 10 minutes, b) 120 minutes and c) complete reaction.

As time progresses the two doublets from 4-aminothiophenol (designated by B in **fig. 2.10**) decreases in intensity. In each case the proton chemical shifts are compared with the residual undeuterated methyl peak in the deuterated methanol. It is observed that ^{1}H NMR spectra of the reaction mixture comprise of only the signals from the product and the starting materials.

To further confirm about the structure of the products and to know about the self assembly formation by these compounds, the crystal structure of **2.50** and **2.51** are determined. The compound **2.50** crystallizes from methanol in non centrosymmetric space group $P2_12_12_1$. The self assembly structures of the compounds are shown in **fig. 2.11**. The compound **2.50** self-assembles in solid state and remains as repeated dimer; which further form hydrogen bonded chains. This compound is again stabilized by C−H···O (C2−H2···O1), N−H···O (N1−H1A···O2), C−H···N (C15−H15···N1), C−H···π (C12−H12···π_{C13}, C16−H16···π_{C4}) and N−H···π (N1−H1B···π_{C14}, N1−H1B···π_{C15} and N1−H1B···π_{C16}) interactions as shown in **fig. 2.11a**. Some of the important hydrogen bond parameters are shown in **table 2.5**.

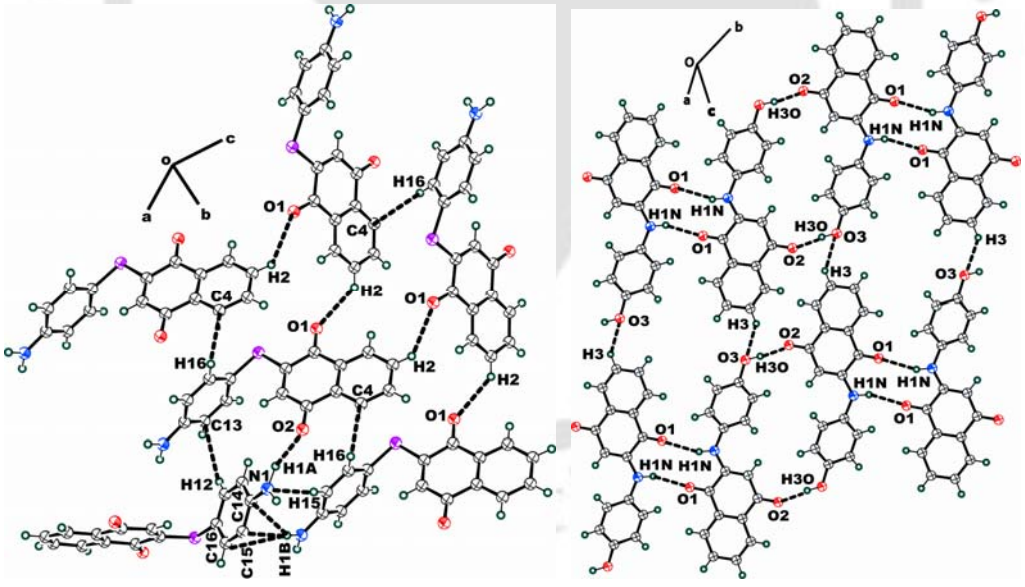

a b

Fig. 2.11 Self assembly of a) compound **2.50**; b) compound **2.51** (ORTEP drawn with 50% thermal ellipsoid)

The compound **2.51** forms self-assembly through N−H···O interactions to form dimer with basic set [$R_2^2(10)$]. The two aromatic rings are perpendicular to each other. This

compound **2.51** is also stabilized by O−H···O (O3−H3O···O2; $d_{D\cdots A}$, 2.69 Å and <D–H····A, 171.2º) and C−H···O (C3−H3···O3; $d_{D\cdots A}$, 3.32 Å and <D–H····A, 123.9º) interactions and forms two dimensional hydrogen bonded sheet like structures as shown in **fig. 2.11b**.

Table 2.5 Hydrogen bond parameters of compound **2.50**

Hydrogen bond geometry (Å, °) for compound **2.50**				
D−H···A	d (D−H)	d (H···A)	d (D···A)	<D−H···A
C2−H2··· O1	0.93	2.69	3.43	136.2
N1−H1A··· O2	1.04	1.99	2.99	161.5
N1−H1B···C π_{C14}	0.91	2.85	3.65	
N1−H1B···C π_{C15}	0.91	2.63	3.55	
N1−H1B···C π_{C16}	0.91	2.83	3.66	
C12−H12 ··· π_{C13}	0.93	2.84	3.61	
C16−H16 ··· π_{C4}	0.93	2.82	3.73	

2.2.2 Reaction of 1,2-naphthoquinone and amines

The 1,2-naphthoquinone reacts with primary amines leads to incorporation of imino group at 4-position as well as the incorporation of amine group at 2-position. For example the reaction of 1,2-naphthoquinone with *n*-butylamine gives 2-(butylamino)-naphthoquinone-1,4-butylimine, **2.52** and with 4-methoxyaniline gives 2-(4-methoxyanilino)naphthoquinone-1,4-(4-methoxyanil), **2.53** respectively. During such reactions amine functional group replaces the carbonyl group present at 2-position of 1,2-naphthoquinone. Illustrative examples of the reactions of primary amines with 1,2-naphthoquinone are shown in **equation 2.5**. The compounds **2.52** and **2.53** are characterized by determining their crystal structures and also by other spectroscopic techniques. The formations of products **2.52** and **2.53** are interesting, as in the case of 1,4-benzoquinone and 1,4-naphthoquinone we did not observe condensation reaction between either of the carbonyl group with amines under ambient conditions.

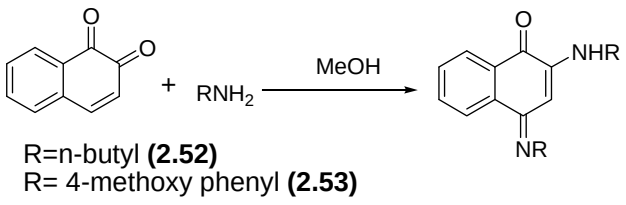

Equation 2.5 Reaction of 1,2-naphthoquinone with amines

The formation of 2-anilino-naphthoquinone-1,4-anil from the reaction of *N*-phenyliminophosphorane with 1,2-naphthoquinone is reported in literature.[256] Similar type of reaction in the presence of cerous chloride heptahydrate is also reported.[257] Further to this there are report on use of 1,2-naphthoquinone having sulfonate group at 4-position to prepare 1,4-naphthoquinone derivatives.[258] In our present investigation, we have observed that such products can be prepared just by reaction of 1,2-naphthoquinone with a primary amine without any reagent or catalyst. Thus, this method is mild and is advantageous in terms of synthetic procedure. Formation of the imine derivative at the 4-position in these reactions may be attributed to the concomitant formation of 4-amino derivative along with the imine at 2-position. Tautomerism of the imine and amine group leads to the desired product. In our reactions two moles of amines are used. There are two possible paths for formation of the products illustrated in **scheme 2.8**.

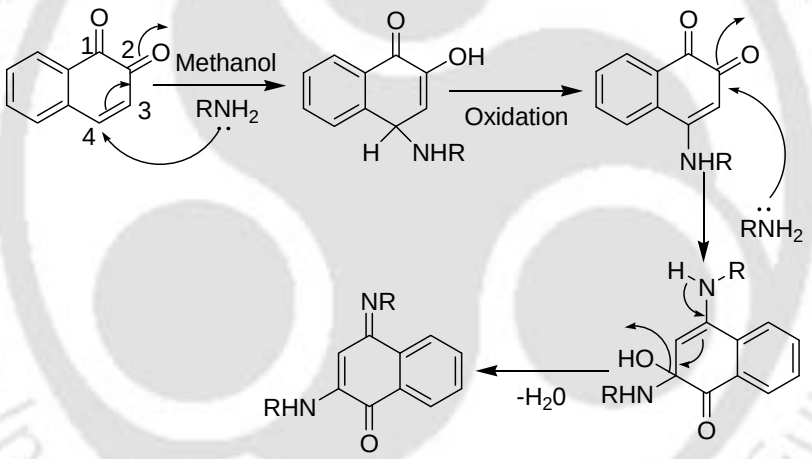

Scheme 2.8 Plausible mechanism for the synthesis of compound **2.52** and **2.53**

Firstly, amine can attack the carbon at 4-position of the ring followed by oxidation to form the 4-amino 1,2-naphthoquinone intermediate. The amine again attacks the carbon at 2-position of the quinone which is followed by rearrangement and formation of imine at 4-position as illustrated in **scheme 2.8**. The second alternative path is the formation of imine at 2-position followed by attack of the amine at 4-position to give the desired product. We could not isolate any such intermediate but based on the established fact that the presence of a carbonyl group favors γ-attack on α-β unsaturated carbonyl over formation of an imine; we would like to put forward the first path. The compounds in these reactions are characterized by recording the ^{1}H NMR and IR

spectra. The IR spectra shows a strong band in the region 3342-3434 cm^{-1} for N-H stretching.

The solid state FT-IR spectrum of compound **2.52** shows N-H stretching bands in the region 3305 cm^{-1}. Beside this N-H stretching band, it also shows weak band at 2928 cm^{-1} due to C-H stretching and strong peak centered at 1654 cm^{-1} arising from the carbonyl group. It also has strong band around 1597 cm^{-1} and 1576 cm^{-1} arising from C=C of aromatic ring and C=N of imine group respectively. In ^{1}H NMR spectra of compound **2.52**, the aromatic proton adjacent to imine group represented as Ha in **fig. 2.9** appears as doublet at 8.42 ppm and the proton adjacent to carbonyl group represented as Hb also appear as double at 8.10 ppm. The other aromatic proton represented as Hc and Hd shows two triplet at 7.61 and 7.48 ppm respectively.

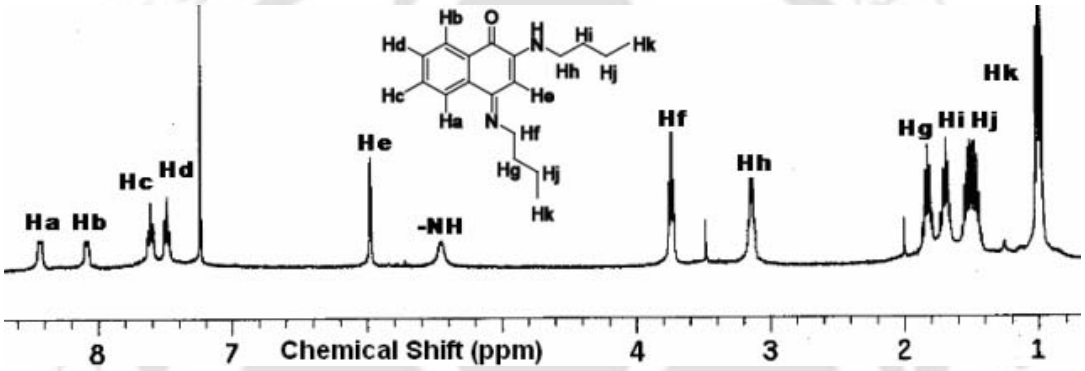

Fig. 2.12 ^{1}H NMR spectra of compound **2.52** ($CDCl_3$, 400 MHz)

The singlet at 5.97 ppm arises due to the vinyl proton (represented as He). The N-H proton shows a broad singlet at 5.45 ppm. The methylene proton neighboring to imine group represented as Hf and the methylene proton neighboring to carbonyl group represented as Hh appears two triplets at 3.74 ppm and 3.31 ppm respectively. In addition to these the methylene protons represented as Hg and Hi shows two quintets at 1.82 ppm and 1.69 ppm respectively. The remaining methylene protons represented as Hj appears as multiple centered at 1.51 ppm. The two methyl protons appear as multiple centered at 1.01 ppm.

The compounds **2.52** and **2.53** are crystallized from methanol as colorless block in P-1 and $P2_1/c$ space group respectively. The crystal structure of the compound **2.52** and **2.53** shows the molecules to self assemble through weak interactions. The solid-state structures of the compounds **2.52** and **2.53** are shown in the **fig. 2.13**.

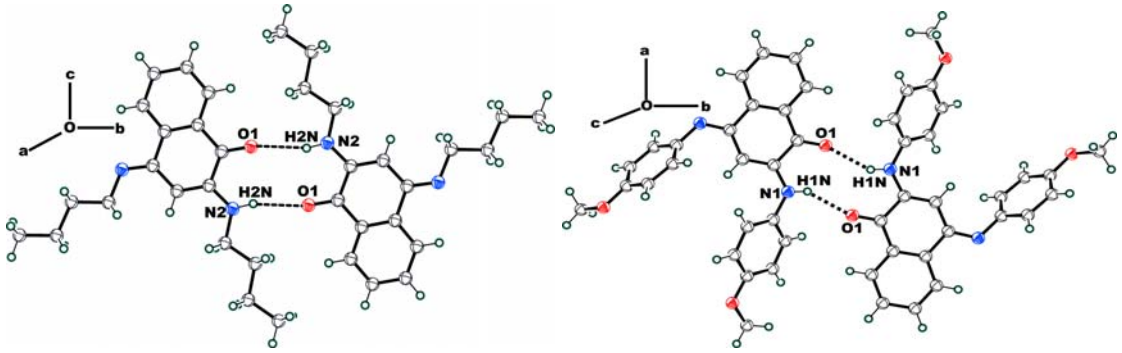

a b

Fig. 2.13 Self assembly structure of compounds a) **2.52**; b) **2.53** (ORTEP drawn with 50% thermal ellipsoid)

The compound **2.52** has carbon oxygen double bond distance C1-O1 as 2.23 Å while the compound **2.53** has the carbon oxygen double bond distance C4-O1 as 1.22 Å. In the compound **2.52** there are two carbon-nitrogen bonds, one of which corresponds to a single bond (N2-C3 as 1.35 Å) and the other to a double bond (N1-C1 as 1.28 Å). The compound **2.53** also has similar structural features as that of **2.52**. It has two different carbon-nitrogen bond distances C2-N1 as 1.36 Å and C4-N2 as 1.30 Å corresponding to a C-N and a C=N respectively. In the solid state the molecules of the compound **2.52** are held by hydrogen bonding interactions between two molecules through N−H···O interactions leading to dimeric structures having basic set [$R_2^2(10)$] with distances $d_{D\text{-}H}$, 0.89 Å, $d_{H\cdots A}$ 2.29 Å, and $d_{D\cdots A}$ 3.15 Å, with the angle <D-H···A =164.0° respectively (**fig. 2.13a**). In the crystal lattice, the compound **2.53** also forms dimeric assembly held by hydrogen bonding interaction via N−H···O and have the same basic set [$R_2^2(10)$] ($d_{D\text{-}H}$ = 0.83 Å, $d_{H\text{-}A}$ = 2.21 Å, $d_{D\cdots A}$ = 2.94 Å, <D-H···A =147.4°) as shown in **fig. 2.13b**.

We also synthesized the compounds **2.54-2.57** by the reaction of different amines with 1,4-naphthoquinone as illustrated in **scheme 2.9**. No condensation reaction to form imine derivatives between either of the carbonyl group with amines as it occurs in the case of 1, 2-naphthoquinone under ambient conditions is observed.[259] In this sense, both the reactions of 1,2-naphthoquinone and 1,4-naphthoquinone with primary amines are equivalent, as both reactions can lead to formation of 2-amino 1,4-naphthoquinone derivatives as illustrated in **scheme 2.9**. Hydrolysis of the imine group of the compound

2.52-2.53 in the presence of trifluoroacetic acid also gives the compounds **2.54** and **2.55**.

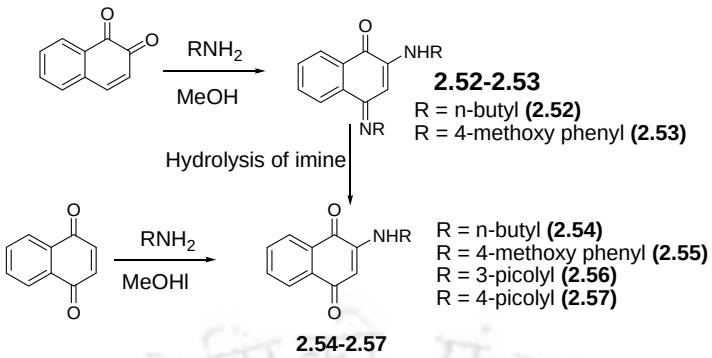

Scheme 2.9 Equivalence of reactivity between 1,2 and 1,4 naphthoquinone

The products thus formed have the structural features of 1,4-naphthoquinone which is equivalent to 1,2 to 1,4 carbonyl transposition.

2.3 Functionalisation of quinone derivatives

We extended our study to functionalize some of the quinonic compounds. We synthesized the compound **2.58** and **2.59-2.60** by functionalizing their respective parent compounds **2.18** and **2.51** respectively as shown in **scheme 2.10**. The cell viability of these compounds is also studied. The compound **2.59** is found to be active against both the cell lines as mention earlier. These compounds are also fully characterized from their spectroscopic data.

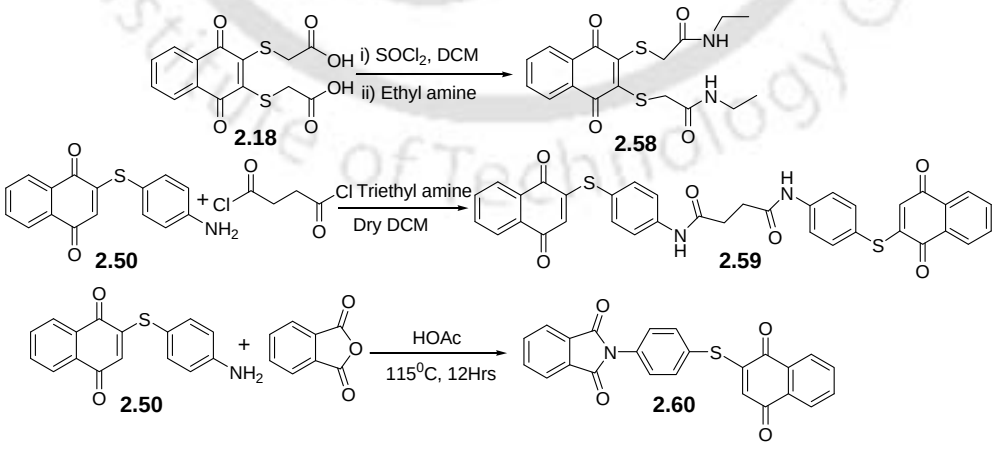

Scheme 2.10 Functionalization of quinone derivatives

The crystal data and refinement parameters of compound **2.22** and **2.50-2.53** are listed in **table 2.6**.

Table 2.6 Crystallographic table for compounds **2.22** and **2.50-2.53**

Compound No.	**2.22**	**2.50**	**2.51**	**2.52**	**2.53**
Formulae	$C_{13}H_{10}O_2S_2$	$C_{16}H_{11}NO_2S$	$C_{16}H_{11}NO_3$	$C_{18}H_{24}N_2O$	$C_{24}H_{14}N_2O_3$
Mol. wt.	262.33	281.32	265.26	284.39	378.37
Crystal system	Monoclinic	orthorhombic	Triclinic	Triclinic	Monoclinic
Space group	$P2_1/c$	$P\ 2_1\ 2_12_1$	P-1	P-1	$P2_1/C$
a /Å	10.4952(7)	5.3485(5)	3.8313(5)	5.465(1)	11.746(3)
b /Å	8.9835(6)	7.4424(7)	12.5135(18)	11.742(2)	9.579(2)
c /Å	12.9533(9)	33.559(3)	14.2512(19)	13.204(2)	17.673(4)
α/°	90.00	90.00	112.212(9)	69.478(1)	90.00
β/°	107.722(4)	90.00	93.326(11)	85.113(1)	99.284(2)
γ/°	90.00	90.00	93.864(11)	85.709(1)	90.00
V/ $Å^3$	1163.33(14)	1335.9(2)	628.52(15)	789.7(3)	1962.49(8)
Z	4	4	2	2	4
Density/Mgm^{-3}	1.498	1.399	1.402	1.196	1.281
Abs. Coeff. /mm^{-1}	0.442	0.242	0.098	0.074	0.086
F(000)	544	584	276	308	784
Total no. of reflections	14874	11033	6543	5807	10248
Max. 2θ/°	28.34	28.40	28.45	28.50	24.76
Ranges (h, k, l)	$-13 \le h \le 13$ $-12 \le k \le 12$ $-17 \le l \le 17$	$-7 \le h \le 7$ $-9 \le k \le 8$ $-37 \le l \le 44$	$-4 \le h \le 5$ $-16 \le k \le 16$ $-18 \le l \le 18$	$-7 \le h \le 7$ $-15 \le k \le 13$ $-17 \le l \le 13$	$-15 \le h \le 13$ $-12 \le k \le 7$ $-23 \le l \le 23$
Complete to 2θ (%)	97.2	99.3	95.6	86.9	89.5
Refinement method	Full-matrix least-squares on F^2	Full-matrix least-squares on F^2	Full-matrix least-squares on F^2	Full-matrix least-squares on F^2	Full-matrix least-squares on F^2
Data/ Restraints/Parameters	2815/0/154	3324/0/189	3020/0/189	3479/0/200	4361/0/272
Goof (F^2)	1.049	1.038	1.047	0.892	0.976
R indices [$I > 2\sigma(I)$]	0.0348	0.0461	0.0669	0.0785	0.0477
R indices (all data)	0.0860	0.0961	0.1295	0.1760	0.0833

2.4. Experimental

2.4.1 Materials

All chemicals are obtained from commercial sources and used without further purification. Solvents (HPLC grade) are purchased from commercial sources and used without further purification or dried according to standard procedures[260]. Organic extracts were dried with anhydrous sodium sulfate. Solvents were removed in a rotary evaporator under reduced pressure. Silica gel (60-120 mesh size) was used for column chromatography. Reactions were monitored by TLC on silica gel GF_{254} (0.25 mm).

2.4.2 Physical Measurement

X-ray diffraction data were collected on Bruker 3-circle diffractometers with CCD area detectors ProteumM APEX or SMART 6000 or Bruker Nonius Apex 2. The diffraction data for all the crystals were collected using Bruker SMART software. This software was also used for indexing and determination of the unit cell parameters. The structures were solved by direct methods and refined by full-matrix least squares against F^2 of all data, using SHELXTL software.[261-263] The IR spectra were recorded on Perkin-Elmer spectrum one spectrometer using KBr pellets. UV-visible absorption spectra were recorded using Perkin-Elmer Lambda 75 spectrophotometer equipped with double cell compartments. Melting points were recorded with a Büchi B-540 melting point apparatus. Fast atom bombardments (FAB) mass were recorded using a JEOL SX-120/DA-6000 instrument using argon (6KV, 10mA) as the FAB gas. NMR spectra were recorded in $CDCl_3$ or [D_6] DMSO with tetramethylsilane as the internal standard for ^1H (400 MHz) or $CDCl_3$ or [D_6] DMSO solvent as the internal standard for ^{13}C (100 MHz). The thermogravimetric studies were performed using a Mettler Toledo TGA/ STDA 851^e and Mettler Toledo DSC^e thermal analyser. Elemental analyses were done on a Perkin-Elmer PE 2400 II CHN analyzer 2400 (Other details of the instruments are given in Appendix).

2.4.3 General procedure for the synthesis of 2-arylsulphanyl 1,4-naphthoquinone (compounds 2.1-2.5)

To a solution of 1,4-naphthoquinone (0.632 g, 4 mmol) in methanol (20 ml), the corresponding arylthiol (4 mmol) was added. The resulting solution was stirred for 2 hrs at room temperature to give 2-arylsulphanyl 1,4-naphthoquinone (compounds **2.1-2.5**). The crystalline products of the desired compounds were obtained upon slow evaporation of the solvent.

2.4.4 Spectroscopic data for 2-arylsulphanyl 1,4-naphthoquinone (compounds 2.1-2.5)

Compound 2.1:

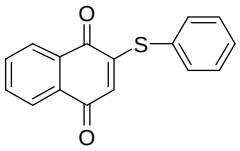

2.1

Isolated yield: 92%, Elemental anal Calcd for $C_{16}H_{10}O_2S$, C, 72.16; H, 3.79; Found C, 72.14, H, 3.79. IR (KBr,cm^{-1}): 3406 (bw), 1667 (s), 1646 (s), 1587 (s), 1557 (m), 1296 (s), 1251 (s), 1118 (m), 857 (w), 771 (m), 696 (w), 687 (w); ^{1}H NMR (400 MHz, $CDCl_3$): 8.14 (dd, J = 9.6, 2.4 Hz, 1H), 8.02 (dd, J = 9.6, 2.4 Hz, 1H), 7.73 (m, 2H), 7.53 (m, 5H), 6.12 (s,1H); Uv-vis (λ_{max}, CH_3CN) 404 nm ($\varepsilon = 5.95 \times 10^5$ $mol^{-1}dm^3cm^{-1}$).

Compound 2.2:

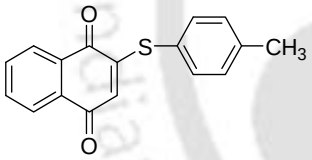

2.2

Isolated yield: 96%, Elemental anal Calcd for $C_{17}H_{12}O_2S$, C, 72.83; H, 4.31; Found C, 72.83; H, 4.30. IR (KBr, cm^{-1}): 3404 (bw), 2919 (w), 1659 (s), 1646 (s), 1593 (s), 1558 (s), 1333 (m),1298 (s), 1248 (m), 1116 (w), 1066 (m), 855 (s), 777 (m), 701 (w), 610 (w); ^{1}H NMR (400 MHz, $CDCl_3$): 8.14 (dd, J = 9.2, 2 Hz, 1H), 8.02 (dd, J = 9.2, 2 Hz, 1H), 7.73 (m, 2H), 7.42 (d, J = 8 Hz, 2H), 7.31 (d, J = 8.4 Hz, 2H), 6.11 (s, 1H), 2.43 (s, 3H); Uv-vis ($\lambda_{max,}$ CH_3CN) 402 nm ($\varepsilon = 3.35 \times 10^5$ $mol^{-1}dm^3cm^{-1}$).

Compound 2.3:

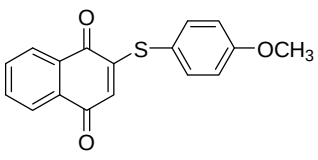

2.3

Isolated yield: 97%, Elemental anal Calcd for $C_{17}H_{12}O_3S$, C, 68.90.; H, 4.08; Found C, 68. IR (KBr, cm^{-1}): 3393 (bw), 2962 (w), 1662 (s), 1644 (s), 1591 (s), 1499 (m), 1294 (s), 1252 (s), 1178 (m), 1027 (w), 855 (s), 782 (w), 701 (w); ^1H NMR (400 MHz, $CDCl_3$): 8.07 (dd, J = 9.2, 2 Hz, 1H), 7.96 (dd, J = 9.2, 2 Hz, 1H), 7.66 (m, 2H), 7.38 (d, J = 8.8 Hz, 2H), 6.95 (d, J = 8.8 Hz, 2H), 6.04 (s, 1H), 3.81 (s, 3H); Uv-vis (λ_{max}, CH_3CN) 405 nm ($\varepsilon = 3.89 \times 10^5$ mol^{-1} dm^3cm^{-1}).

Compound 2.4:

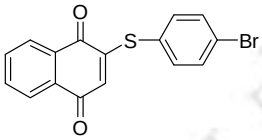

2.4

Isolated yield: 91%, Elemental anal Calcd for $C_{16}H_9BrO_2S$, C, 55.67; H, 2.63; Found C, 55.68; H, 2.61. IR (KBr, cm^{-1}): 3404 (bw), 2961 (w), 1650 (s), 1642 (s), 1588 (s), 1563 (s), 1474 (m), 1335 (m), 1294 (s), 1249 (s), 1119 (w),1068 (s), 1008 (w), 852 (m), 818 (s), 699 (w), 611 (w); ^1H NMR (400 MHz, $CDCl_3$): 8.12 (dd, J = 7.2, 2 Hz, 1H), 8.01 (dd, J = 7.2, 2 Hz; 1H), 7.714 (m, 2H), 7.62 (d, J = 9.2 Hz, 2H), 7.40 (d, J = 9.2 Hz, 2H), 6.08 (s, 1H); Uv-vis (λ_{max}, CH_3CN) 404 nm ($\varepsilon = 3.45 \times 10^5$ mol^{-1} dm^3cm^{-1}).

Compound 2.5:

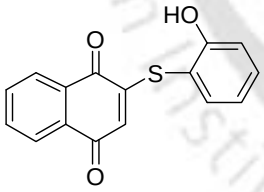

2.5

Isolated yield: 87%, IR (KBr, cm^{-1}): 3391 (s), 2962 (w), 1658 (s), 1643 (s), 1590 (s), 1489 (w), 1294 (s), 1251 (s), 1177 (m), 1119 (m), 1027 (w), 853 (s), 782 (w), 701 (w); ^1H NMR (400 MHz, $CDCl_3$): 8.07 (dd, J = 9.2, 2 Hz, 1H), 7.96 (dd, J = 9.2, 2 Hz; 1H), 7.66 (m, 2H), 7.32 (d, J = 8.8 Hz, 2H), 6.87 (d, J = 8.8 Hz, 2H), 6.04 (s, 1H); Uv-vis (λ_{max}, CH_3CN) 404 nm ($\varepsilon = 3.62 \times 10^5$ mol^{-1} dm^3cm^{-1}).

2.4.5 Procedure for the synthesis of symmetrical 2,3-diarylsulphanyl 1,4-naphthalenediol (2.6-2.10)

A solution of 1,4-naphthoquinone (0.316 g, 2 mmol) and arylthiol (4 mmol) in methanol (20 ml) on stirring at room temperature for 3 hrs gave 2,3-diarylsulphanyl 1,4-naphthalenediol. The colorless crystalline products of the desired compounds were obtained upon slow evaporation of the solvent.

2.4.6 Spectroscopic data for 2,3-diarylsulphanyl 1,4-naphthalenediol (2.6-2.10)

Compound 2.6:

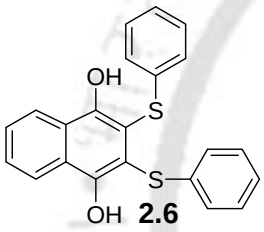

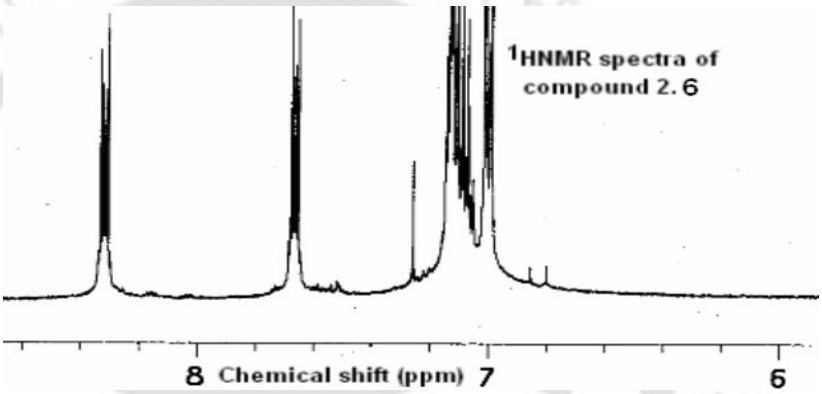

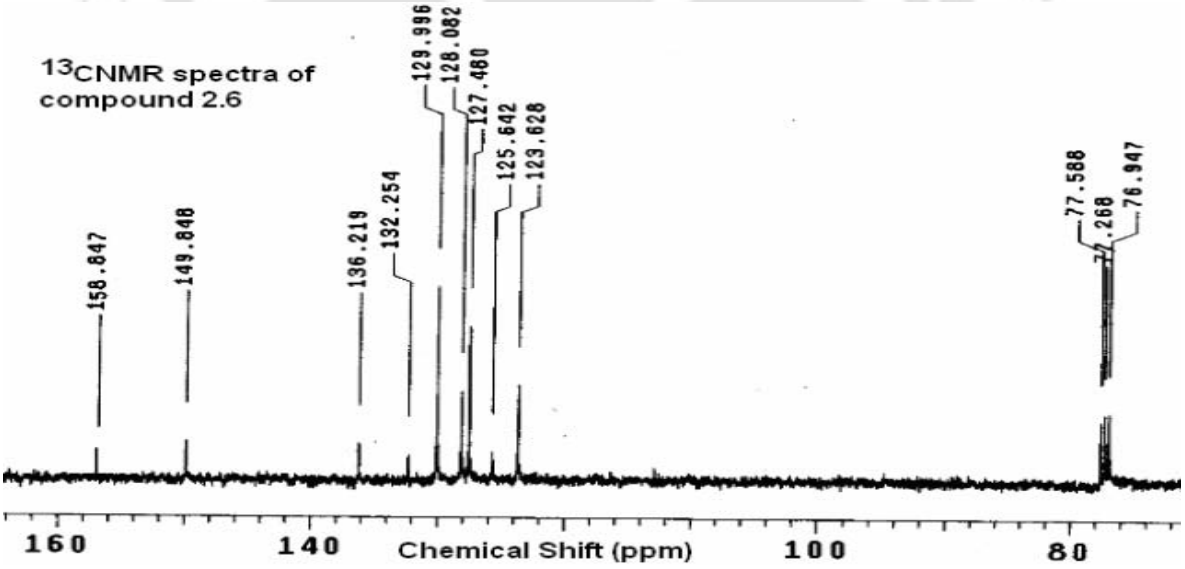

Isolated yield: 92%, m.p. 184°C, Elemental anal Calcd for $C_{22}H_{16}O_2S_2$, C, 70.18; H, 4.28; Found C, 70.20; H, 4.30. IR (KBr, cm^{-1}): 3401 (bs), 3360 (w), 3068 (w), 2366 (w), 1629 (w), 1573 (s), 1475 (m), 1431 (s), 1399 (s), 1255 (s), 1153 (m), 1081 (w), 1015 (w), 886 (s), 738 (s), 692 (w), 656 (w), 559 (w); ^1H NMR (400 MHz, $CDCl_3$):

8.32 (dd, J = 9.6 Hz, 3.2 Hz; 2H), 7.66 (dd, J = 9.6, 3.2 Hz, 2H), 7.12 (s, 2H), 7.08 (m, 6H), 7.01(m, 4H); ^{13}C NMR ($CDCl_3$, 100 MHz): 158.85, 149.65, 136.22, 132.25, 130.00, 128.08, 127.48, 125.64, 123.63; Uv-vis (λ_{max}, CH_3CN) 341, 357 nm ($\varepsilon = 1.06 \times 10^4$ and 1.12×10^4 mol^{-1} dm^3cm^{-1}).

Compound 2.7:

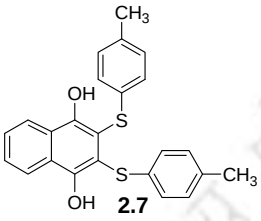

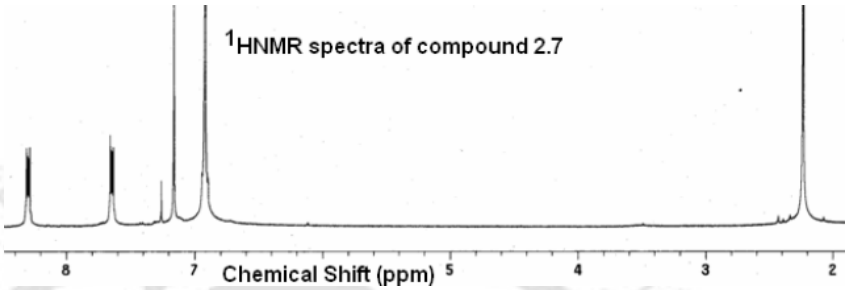

Isolated yield: 96%, m.p. 158°C, Elemental anal Calcd for $C_{24}H_{20}O_2S_2$, C, 71.25; H, 4.98; Found C, 71.21; H, 4.94. IR (KBr, cm^{-1}): 3401 (bs), 3345 (w), 2919 (w), 2858 (w), 1573 (s), 1496 (s), 1434 (m), 1399 (s), 1255 (s), 1163 (m), 1086 (m), 1020 (w), 886 (s), 799 (s), 769 (w), 661 (w), 564 (w), 477 (w); ^1H NMR (400 MHz, $CDCl_3$) 8.30 (dd, J = 9.6, 3.6 Hz, 2H), 7.64 (dd, J = 9.6, 3.6 Hz, 2H), 7.16 (s, 2H), 6.92 (s, 8H), 2.23 (s, 6H); ^{13}C NMR ($CDCl_3$, 100 MHz): 158.88, 149.85, 136.22, 132.45, 129.90, 128.88, 127.48, 125.64, 123.83, 21.15; Uv-vis (λ_{max}, CH_3CN) 341, 357 nm ($\varepsilon = 1.74 \times 10^4$ and 1.84×10^4 $mol^{-1}dm^3cm^{-1}$).

Compound 2.8:

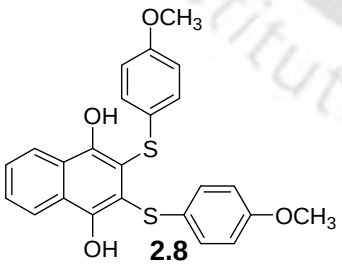

Isolated yield: 96%, m.p. 156°C, Elemental anal Calcd for $C_{24}H_{20}O_4S_2$, C, 66.03; H, 4.62; Found C, 66.04; H, 4.66. IR (KBr, cm^{-1}): 3393 (bs), 2962 (w), 2833 (w), 1593 (m), 1569 (s), 1494 (s), 1463 (m), 1398 (w), 1245 (s), 1180 (m), 1033 (s), 885 (w), 821 (w), 659 (w); ^1H NMR (400 MHz, $CDCl_3$) 8.28 (dd, J = 9.6, 3.2 Hz, 2H) 7.63 (dd, J = 9.6, 3.2 Hz, 2H), 7.26 (s, 2H), 7.00 (dd, J = 8,8, 2.4 Hz, 4H), 6.65 (dd, J = 8.8, 2.4 Hz,

4H), 3.71 (s, 6H). ^{13}C NMR ($CDCl_3$, 100 MHz): 158.70, 149.60, 129.77, 128.01, 126.23, 125.55, 123.60, 114.92, 113.78, 55.49; Uv-vis (λ_{max}, CH_3CN) 342, 358 nm (ε = 0.73 × 10^4 and 0.76 × 10^4 mol^{-1} dm^3cm^{-1}); LC-MS (m/e) (ESI m+1) 437.

Compound 2.9:

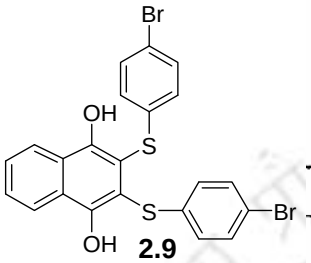

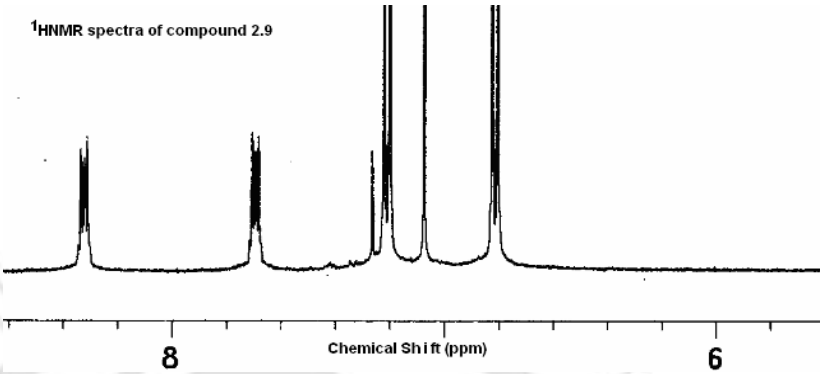

Isolated yield: 95%, m.p. 210°C, Elemental anal Calcd for $C_{22}H_{14}O_2S_2Br_2$, 49.46; H, 2.64; Found C, 49.48; H, 2.63. IR(KBr, cm^{-1}): 3398 (bs), 1569 (s), 1472 (s), 1402 (s), 1268 (m), 1251 (s), 1165 (s), 1080 (w), 1070 (w), 1008 (s), 885 (m), 806 (s), 657 (w), 557 (w); ^{1}H NMR (400 MHz, $CDCl_3$) 8.32 (dd, J = 8.8, 3.2 Hz, 2H), 7.69 (dd, J = 8.8, 3.2 Hz, 2H), 7.21(dd, J = 7.6, 2 Hz, 4H), 7.075 (s, 2H), 6.82 (dd, J = 8.4, 2 Hz, 4H); LC-MS (m/e) (ESI m+1) 533; Uv-vis (λ_{max}, CH_3CN) 341, 357 nm (ε = 1.71 × 10^4 and 1.80 × 10^4 mol^{-1} dm^3cm^{-1});

Compound 2.10:

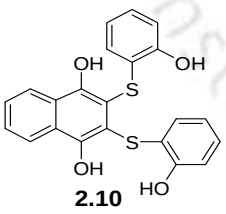

Isolated yield: 85%, m.p. 130°C; IR (KBr, cm^{-1}): 3401 (bs), 3345 (w), 2919 (w), 1591(w), 1571 (s), 1486 (s), 1434 (m), 1400 (s), 1255 (s), 1164 (w), 1084 (m), 886 (m), 798 (s), 769 (w), 661 (w), 564 (w); ^{1}H NMR (400 MHz, $CDCl_3$) 8.32 (dd, J = 8.8, 3.2 Hz, 2H), 7.67 (dd, J = 8.8, 3.2 Hz, 2H), 7.26 (s, 2H), 7.15(d, J = 7.6 Hz, 2H), 7.07 (t, J = 8.8 Hz, 2H), 6.92 (t, J = 8.2 Hz, 2H) 6.81 (d, J = 7.4 Hz, 2H), 6.28 (s, 2H); Uv-vis (λ_{max}, CH_3CN) 342, 358 nm (ε = 1.31 × 10^4 and 1.40 × 10^4 mol^{-1} dm^3cm^{-1})

2.4.7 General procedure for the synthesis of unsymmetrical 2,3-diarylsulphanyl-1,4-naphthalenediol (2.11-2.16)

A solution of arylthiol (1 mmol) and 2-arylsulphanyl 1,4-naphthoquinone (1 mmol) in methanol (20 ml) was stirred at room temperature for 4 hrs. The solution was evaporated under reduced pressure. To the crude product, a solution of sodium metabisulfite (2 mmol) in water (15 ml) was added followed by ethylacetate (15 ml). The mixture was stirred for 3 hrs. The organic layer was separated, washed several times with water (20 ml each) and the products were obtained by crystallization from the organic layer.

2.4.8 Spectroscopic data for unsymmetrical 2,3-diarylsulphanyl 1,4-naphthalene-diol

Compound 2.11:

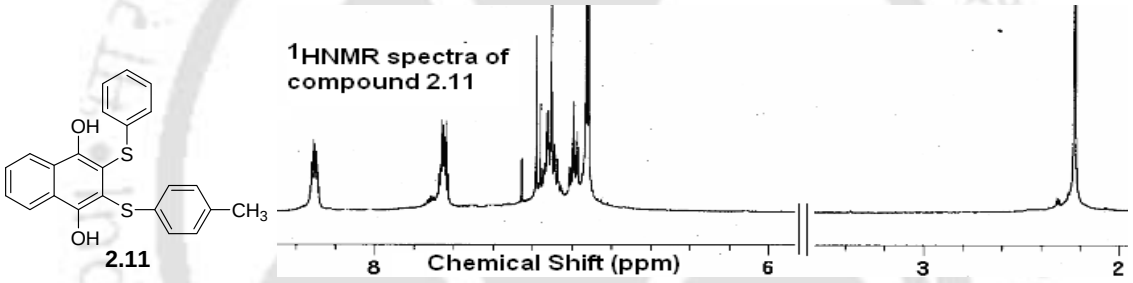

Isolated yield: 94%, m.p.149°C. Elemental anal Calcd for $C_{23}H_{18}O_2S_2$, C, 70.74; H, 4.65; Found C, 70.73; H, 4.63; IR (KBr, cm^{-1}): 3406 (bs), 3053 (w), 2919 (w), 1629 (m), 1573 (s), 1486 (m), 1434 (w), 1399 (s), 1260 (s), 1158 (m), 1081 (w), 1020 (w), 892 (s), 805 (w), 769 (w), 738 (w), 692 (w), 656 (w), 559 (w), 497 (w), 431 (s); ^1H NMR (400 MHz, $CDCl_3$): 8.31 (m, 2H), 7.65 (m, 2H), 7.19 (s, 1H), 7.17(s, 1H), 7.09 (m, 4H), 6.99 (m, 2H), 6.93 (m, 3H), 2.23 (s, 3H); Uv-vis (λ_{max}, CH_3CN) 341, 357 nm ($\varepsilon = 1.23 \times 10^4$ and 1.31×10^4 mol^{-1} dm^3cm^{-1}).

Compound 2.12:

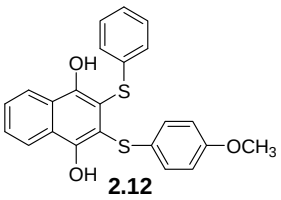

Isolated yield: 96%, m.p. 82°C, Elemental anal Calcd for $C_{23}H_{18}O_3S_2$, C, 67.96; H, 4.46; Found C, 67.95; H, 4.48. IR (KBr, cm^{-1}): 3394 (bs), 2938 (w), 1592 (m), 1568 (s),1494 (s), 1428 (m), 1398 (s), 1245 (s), 1026 (m), 885 (w), 769 (w), 659 (w); ^1H NMR (400 MHz, $CDCl_3$) : 8.30 (m, 2H), 7.64 (m, 2H), 7.30 (s, 1H), 7.26 (s, 1H), 7.10 (m, 2H), 7.05 (d, J = 8.4 Hz, 2H), 7.00 (m, 3H), 6.65 (d, J = 8.4 Hz, 2H), 3.71 (s, 3H). Uv-vis (λ_{max}, CH_3CN) 341, 357 nm ($\varepsilon = 1.33 \times 10^4$ and 1.16×10^4 mol^{-1} dm^3cm^{-1}).

Compound 2.13:

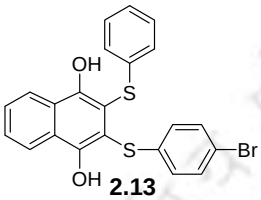

2.13

Isolated yield: 92%, m.p. 192°C. IR (KBr, cm^{-1}): 3395 (bs), 2918 (w), 1588 (s), 1492 (m), 1431 (w), 1396 (s), 1268 (s), 1246 (s), 1080 (s), 885 (s), 806 (m), 772 (w), 658 (m), 556 (w); ^1H NMR (400 MHz, $CDCl_3$): 8.32 (dd, J = 9.6, 3.2 Hz, 2H), 7.68 (dd, J = 9.6, 3.2 Hz, 2H), 7.21(d, J = 7.6 Hz, 2H), 7.09 (s,1H), 7.07 (s, 1H), 6.97 (m, 2H), 6.89 (m, 3H), 6.81 (dd, J = 8.4 Hz, 2H). Uv-vis (λ_{max}, CH_3CN) 341, 357 nm ($\varepsilon = 1.53 \times 10^4$ and 1.64×10^4 mol^{-1} dm^3cm^{-1}).

Compound 2.14:

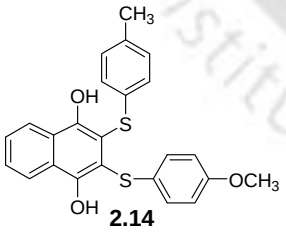

2.14

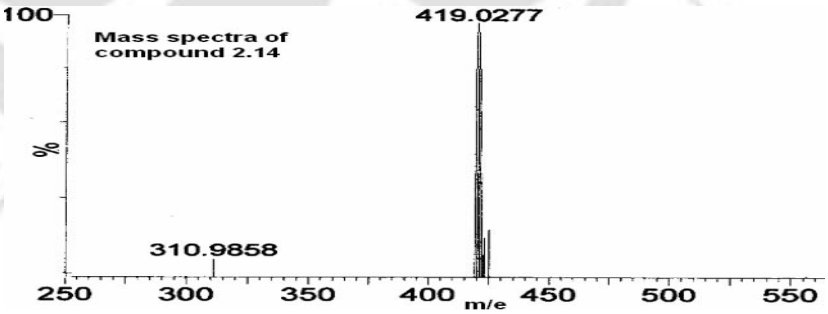

Isolated yield: 95%, m.p. 132°C, Elemental anal Calcd for $C_{24}H_{20}O_3S_2$, C, 68.54; H, 4.79; Found C, 68.56; H, 4.82. IR (KBr, cm^{-1}): 3400 (bs), 2922 (w), 2918 (w), 1578 (s), 1491 (s), 1435 (w), 1395 (w), 1247 (s), 1168 (w), 1082 (w), 1030 (w), 886 (s), 810 (w), 656 (w); ^1H NMR (400 MHz, $CDCl_3$): 8.29 (m, 2H), 7.63 (m, 2H), 7.17 (s, 1H), 7.14 (s, 1H), 7.01 (m, 2H), 6.92 (m, 4H), 6.64 (m, 2H), 3.70 (s, 3H), 2.23 (s, 3H). LC-

MS (m/e, ESI m+1) 419.Uv-vis (λ_{max}, CH_3CN) 341, 357 nm ($\varepsilon = 1.28 \times 10^4$ and 1.37×10^4 mol^{-1} dm^3cm^{-1});

Compound 2.15:

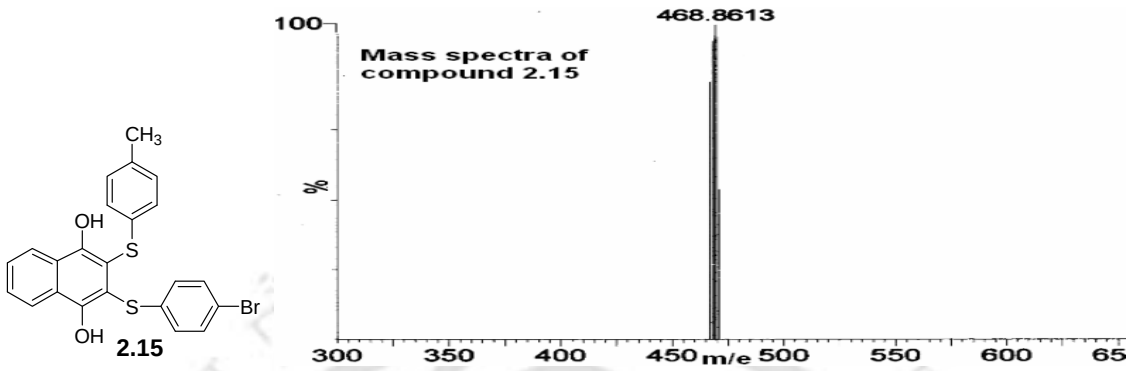

Isolated yield: 92%; mp 192^0C. Elemental anal. calcd. for $C_{23}H_{17}O_2S_2Br$: C, 58.85; H, 3.65. Found: C, 58.83; H, 3.66. IR (KBr, cm^{-1}): 3397 (bs), 2918 (w), 1568 (s), 1472 (w), 1397 (s), 1268 (s), 1246 (s), 1080 (s), 1005 (w), 885 (s), 805 (s), 772 (w), 658 (s), 556 (w); ^{1}H NMR (400 MHz, $CDCl_3$): 8.32 (dd, J = 9.6, 3.2 Hz, 2H), 7.67 (dd, = 9.6, 3.2 Hz, 2H), 7.18 (m, 2H), 7.07 (s, 1H), 7.05 (s, 1H), 6.89 (m, 4H), 6.82 (m, 2H), 2.24 (s, 3H). Uv-vis (λ_{max}, CH_3CN) 341, 357 nm ($\varepsilon = 1.76 \times 10^4$ and 1.86×10^4 mol^{-1} dm^3 cm^{-1}); LC-MS (m/e, ESI m+1) 469.

Compound 2.16:

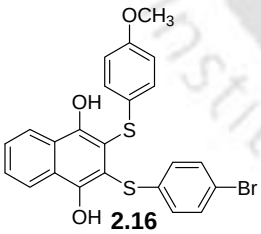

Isolated yield: 94%; mp 192^0C: IR (KBr, cm^{-1}): 3398 (bs), 2918 (w), 1578 (s), 1492 (m), 1397 (s), 1251 (s), 1246 (s), 1080 (m), 1023 (w), 883 (m), 805 (s), 777 (m), 658 (s); ^{1}H NMR (400 MHz, $CDCl_3$): 8.32 (dd, J = 9.6, 3.2 Hz, 2H), 7.66 (dd, = 9.6, 3.2 Hz, 2H), 7.22 (d, J = 7.6 Hz, 2H), 7.12 (s, 1H), 7.07 (s, 1H), 6.89 (d, J = 8.8 Hz, 2H), 6.66 (d, J = 8.8 Hz, 2H), 6.82 (d, J = 8.4 Hz, 2H), 3.71 (s, 3H). Uv-vis (λ_{max}, CH_3CN) 342, 358 nm ($\varepsilon = 1.06 \times 10^4$ and 1.14×10^4 mol^{-1} dm^3 cm^{-1}).

2.4.9 Procedure for the synthesis of compounds 2.17 and 2.18

1,4-Naphthoquinone (0.632g, 4 mmol) was dissolved in 30 ml of methanol. To this solution, thioglycolic acid (0.736 g, 8 mmol) was added slowly (drop by drop) and stirred for 6 hrs in aerial condition at room temperature. To the resulting reaction mixture 10 ml of water was added and kept undisturbed. The compound **2.17** was obtained as colorless crystal or white precipitate from this methanol: water solvent system (3:1). The compound **2.18** was obtained as red solid by decanting the solvent.

2.4.10 Spectroscopic data for compounds 2.17 and 2.18

Compound 2.17:

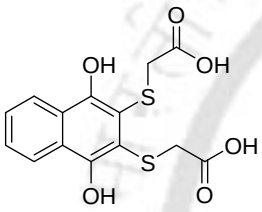

2.17

Isolated yield: 55%, FT-IR (KBr, cm^{-1}): 3390 (s), 2924 (s), 2851 (m), 1687 (s), 1568 (m), 1426 (w), 1398 (m), 1274 (s), 1200 (m), 1163 (s), 1080 (w), 1023 (w), 889 (s), 831 (w), 762 (m), 650 (w), 562 (w); ^{1}H NMR ($CDCl_3$, 400 MHz): 8.46 (2H, bs, carboxylic proton), 8.22 (dd, J = 8.6, 3.2 Hz, 2H), 7.55 (dd, J = 8.6, 3.2 Hz, 2H), 7.44 (s, 2H), 3.66 (s, 4H). ^{13}C NMR ($CDCl_3$, 100 MHz): 173.33, 150.18, 127.52, 126.14, 123.48, 113.39, 39.73.

Compound 2.18:

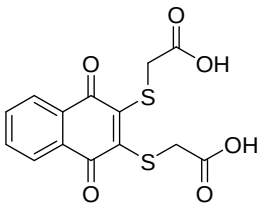

Isolated yield: 23%, (KBr, cm^{-1}): 3434 (bw), 2921 (w), 1714 (s), 1659 (s), 1590 (m), 1488 (w), 1467 (s), 1346 (m), 1281 (s), 1176 (m), 1139 (s), 869 (m), 811 (w), 702 (s). ^{1}H NMR (DMSO-d6, 400 MHz): 8.03 (dd, J= 6.0, 2.4 Hz, 2H), 7.71 (dd, J=5.6, 2.4 Hz,

2H), 4.02 (s, 4H). ^{13}C NMR (DMSO-d_6, 100 MHz): 178.97, 170.64, 145.90, 134.67, 133.05, 127.18, 36.30.

2.4.11 General procedure for the synthesis of compounds 2.19-2.26

1, 4-Napthoquinone (0. 316 g, 2 mmol) was dissolved in 20 ml of methanol. To this solution, the corresponding aliphatic thiol (4 mmol each) was added slowly and stirred for 6 hrs in aerial condition at room temperature. Subsequent removal of the solvent under reduced pressure gave the crude product. The product was purified by column chromatography (silica gel; hexane/ethyl acetate 5:1). In each case, the desired 1,4-naphthalene diols and corresponding quinone derivatives could be obtained from this purification method.

2.4.12 Spectroscopic data for compounds 2.19 and 2.26

Compound 2.19:

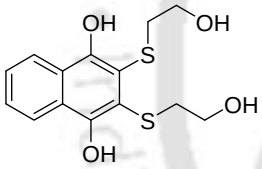

2.19

Isolated yield: 38%, FT-IR (KBr, cm^{-1}): 3392 (s), 2924 (w), 2851 (w), 1592 (s), 1426 (s), 1398 (m), 1274 (s), 1200 (w), 1173 (m), 1080 (w), 1028 (s), 889 (s), 831 (w), 762 (m), 656 (m); ^{1}H NMR ($CDCl_3$, 400 MHz): 8.22 (dd, J = 6.8, 3.2 Hz, 2H), 7.56 (dd, J = 6.8, 3.2 Hz, 2H), 7.42 (s, 2H), 3.64 (t, J = 8.0 Hz, 4H), 3.31 (t, J = 8.8 Hz, 4H), 2.69 (s, 2H); ^{13}C NMR ($CDCl_3$, 100 MHz): 149.2, 130.05, 126.41, 122.97, 114.43, 52.34, 40.7.

Compound 2.20:

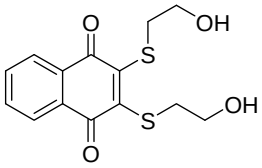

Isolated yield: 52%, (KBr, cm-1): 3434 (bw), 2921 (w), 1712 (s), 1657 (s), 1590 (m), 1488 (s), 1467 (s), 1348 (w), 1281 (s), 1227 (s), 1176 (m), 1139 (s), 869 (m), 811(w),

702 (s); ^{1}H NMR (DMSO-d6, 400 MHz): 8.03 (dd, J = 6.8, 2.4 Hz, 2H), 7.69 (dd, J = 6.8, 2.4 Hz, 2H), 3.78 (t, 4H) 3.40 (s, 4H) 2.69 (s, 2H); ^{13}C NMR (DMSO-d_6, 100 MHz): 179.87, 146.73, 130.05, 126.42, 114.42, 52.84, 39.80.

Compound 2.21:

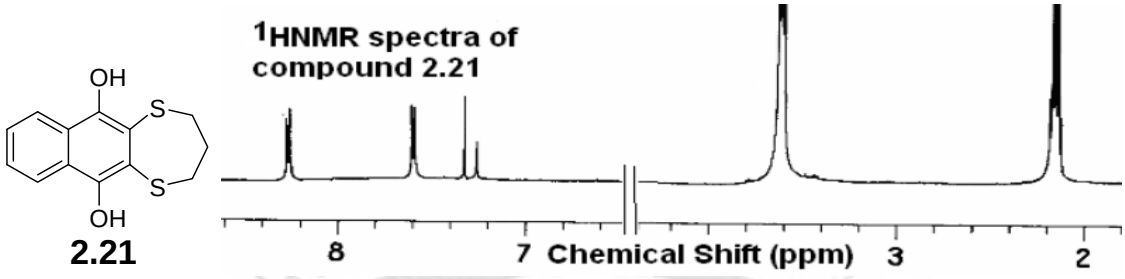

Isolated yield: 21%. IR (KBr, cm^{-1}): 3403 (s), 2924 (m), 2851 (w), 1586(s), 1499 (m), 1472 (w), 1422 (m), 1281 (s), 1127 (s), 886 (w), 792 (m), 705 (w); ^{1}H NMR (400 MHz, $CDCl_3$): 8.24 (dd, J = 7.8, 3.6 Hz, 2H), 7.62 (dd, J = 7.8, 3.6 Hz, 2H), 7.38 (s, 2H), 3.58 (t, J = 9.2 Hz, 4H), 2.15 (m, 2H).; ^{13}C NMR (100 MHz, $CDCl_3$): 142.86, 132.99, 131.39, 127.10, 122.77 30.50, 26.61.

Compound 2.22:

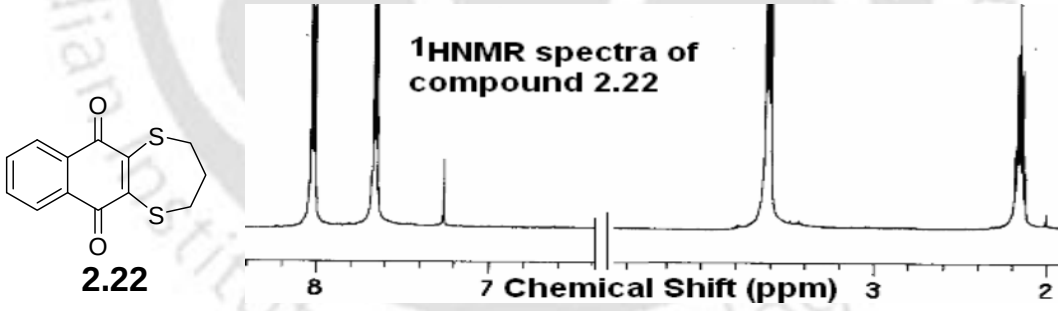

Isolated yield: 61%. IR (KBr, cm^{-1}): 3441 (bs), 2924 (m), 2851 (m), 1744 (m), 1653 (s), 1585 (m), 1499(s), 1473 (m), 1282 (s), 1126 (m), 1080 (w), 886 (w), 792 (m), 705 (w); ^{1}H NMR (400 MHz, $CDCl_3$): 8.02 (dd, J = 9.2 Hz, 3.6 Hz, 2H), 7.66 (dd, J = 9.2 Hz, 3.6 Hz, 2H), 3.61(t, J = 9.2 Hz, 4H), 2.15 (m, 2H); ^{13}C NMR (100 MHz, $CDCl_3$): 180.41, 144.60 133.92, 131.89, 127.03, 30.50, 26.62.

Compound 2.24:

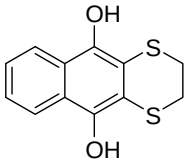

2.24

Isolated yield: 21%. IR (KBr, cm^{-1}): 3403 (s), 2925 (m), 2851 (w), 1591(s), 1498 (s), 1473 (w), 1422 (m), 1280 (s), 1127 (m), 886 (w), 792 (m), 705 (w); ^{1}H NMR (400 MHz, $CDCl_3$): 8.22 (dd, J = 8.2, 3.6 Hz, 2H), 7.63 (dd, J = 8.2, 3.6 Hz, 2H), 7.40 (s, 2H), 3.58 (s, 4H).; ^{13}C NMR (100 MHz, $CDCl_3$): 142.86, 132.96, 131.40, 127.11, 122.76, 31.98.

Compound 2.25:

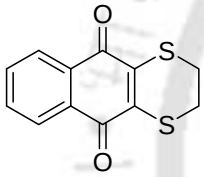

2.25

Isolated yield: 61%. IR (KBr, cm^{-1}): 3444 (bs), 2924 (s), 2851 (m), 1745 (m), 1655 (s), 1585 (m), 1499 (m), 1473 (w), 1281 (s), 1231 (w), 1126 (m), 1080 (m), 886 (w), 792 (s), 705 (w); ^{1}H NMR ($CDCl_3$, 400 MHz): 8.02 (dd, J = 9.2, 3.6 Hz, 2H), 7.66 (dd, J = 9.2, 3.6 Hz, 2H), 3.61(s, 4H); ^{13}C NMR ($CDCl_3$, 100 MHz): 180.41, 144.60 133.92, 131.89, 127.03, 32.50.

2.4.13 General procedure for the synthesis of compounds 2.27-2.31

2-Methyl 1,4-naphthoquinone (0.69 g, 4 mmol) was dissolved in 15 ml of methanol and reacted with corresponding dithiols (2 mmol) for 4 hrs at room temperature in aerobic condition. The desired products were precipitated out and further purified by crystallization. For compound **2.27** the thioglycolic acid was used in 1:1 ratio and the product was obtained as yellow crystals by direct crystallization from the mother solution. The compound **2.29** was crystallizes from methanol while the compounds **2.30** and **2.31** are crystallizes from *N, N'*-dimethylformamide.

2.4.14 Spectroscopic data for compounds 2.27 and 2.31

Compound 2.27:

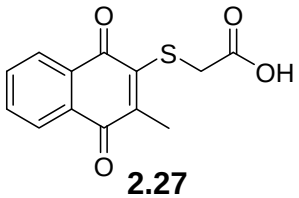

2.27

Isolated yield: 75%, (KBr, cm^{-1}): 3445 (bw), 2925 (w), 1716 (s), 1662 (s), 1589 (m), 1551 (m), 1424 (m), 1375 (w), 1318 (s), 1287 (s), 1212 (m), 1177 (m), 1113 (w), 1026 (w), 946 (m), 840 (w), 702 (s). ^{1}H NMR ($CDCl_3$, 400 MHz): 8.08 (dd, J = 7.2, 3.2 Hz, 2H), 7.54 (dd, J = 7.2, 3.2 Hz, 2H), 3.98 (s, 2H), 2.37 (s, 3H); ^{13}C NMR ($CDCl_3$, 100 MHz): 182.05, 181.09, 170.96, 146.38, 145.26, 133.78, 133.49, 132.82, 131.97, 126.75, 126.52, 35.57, 15.09.

Compound 2.28:

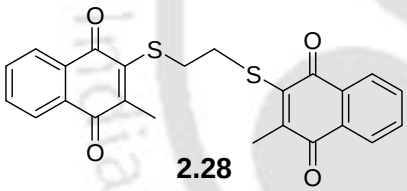

2.28

Isolated Yields 65%. FT-IR (KBr, cm^{-1}): 3302 (bw), 2917 (w), 1662 (s), 1653 (s), 1589 (m), 1563 (w), 1427 (w), 1323 (m), 1280 (s), 1181 (m), 1030 (m), 954 (w) 836 (m), 705 (m); ^{1}H NMR (400 MHz, $CDCl_3$): 8.03 (m, 4H) 7.58 (m, 4H), 3.32 (s, 4H), 2.28(s, 6H); ^{13}C NMR ($CDCl_3$, 100 MHz): 182.23, 181.40, 147.21, 146.29, 133.81, 133.54, 132.93, 132.22, 126.89, 126.75, 32.97, 15.50.

Compound 2.29:

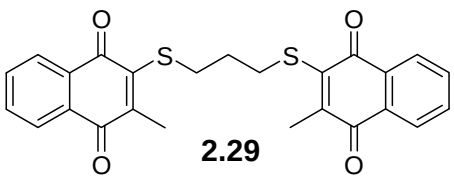

2.29

Isolated Yields 72%. FT-IR (KBr, cm^{-1}): 2917 (w), 1661 (s), 1652 (s), 1589 (m), 1564 (m), 1427 (w), 1323 (m), 1280 (s), 1030 (m), 955 (w) 837 (m), 705 (m); ^{1}H NMR (400 MHz, $CDCl_3$): 7.98 (m, 4H) 7.65 (m, 4H), 3.31 (t, J = 8.8 Hz, 4H), 2.28 (s, 6H), 1.92 (m, 2H). ^{13}C NMR ($CDCl_3$, 100 MHz): 182.22, 181.41, 147.24, 146.32, 133.87, 133.58, 132.97, 132.2, 126.93, 126.77, 32.95, 31.7, 15.50.

Compound 2.30:

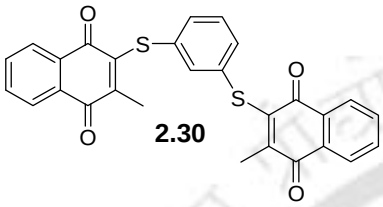

2.30

Isolated Yields 78%. IR (KBr, cm^{-1}): 2926 (w), 1666 (s), 1592 (m), 1315 (m), 1286 (s), 1184 (w), 1031 (m), 781 (m), 702 (m); ^{1}H NMR (400 MHz, DMSO-d_6): 7.97 (d, J = 6.8 Hz, 2H), 7.82 (m, 6H), 7.314 (s, 1H), 7.22 (d, J = 5.2 Hz, 2H), 2.19 (s, 6H).

Compound 2.31:

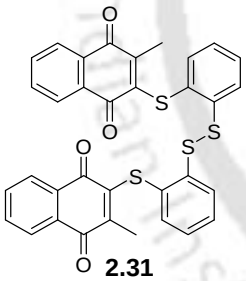

2.31

Isolated Yields 84%. IR (KBr, cm^{-1}): 3436 (bw), 2921 (w), 1655 (s), 1590 (m), 1446 (w), 1280 (s), 1030 (m), 952 (w), 752 (w), 702 (m); ^{1}H NMR (DMSO-d_6, 400 MHz,): 8.03 (d, J = 7.2 Hz, 2H), 7.91 (d, J = 7.2 Hz, 2H), 7.83 (m, 4H), 7.58 (d, J = 7.6 Hz, 2H), 7.44 (d, J = 7.6 Hz, 2H), 7.25 (t, 2H), 7.18 (t, 2H), 2.20 (s, 6H).

2.5.15 Procedure for the synthesis of 2-(3-methyl 1,4-dihydro-naphthalen-2-yl-sulfanyl) nicotinic acid 2.32

To a solution of 2-methyl 1,4-naphthoquinone (0.860 g, 5 mmol) in methanol (30 ml), a solution of 2-mercaptonicotinic acid (0.770 g, 5 mmol) in 5 ml of *N*,*N*′-dimethyl

formamide was added and stirred for 10 hrs. The resulting yellow precipitate was collected by filtration.

Compound 2.32:

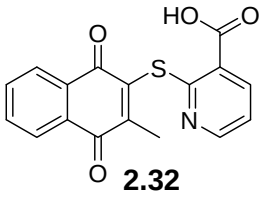

2.32

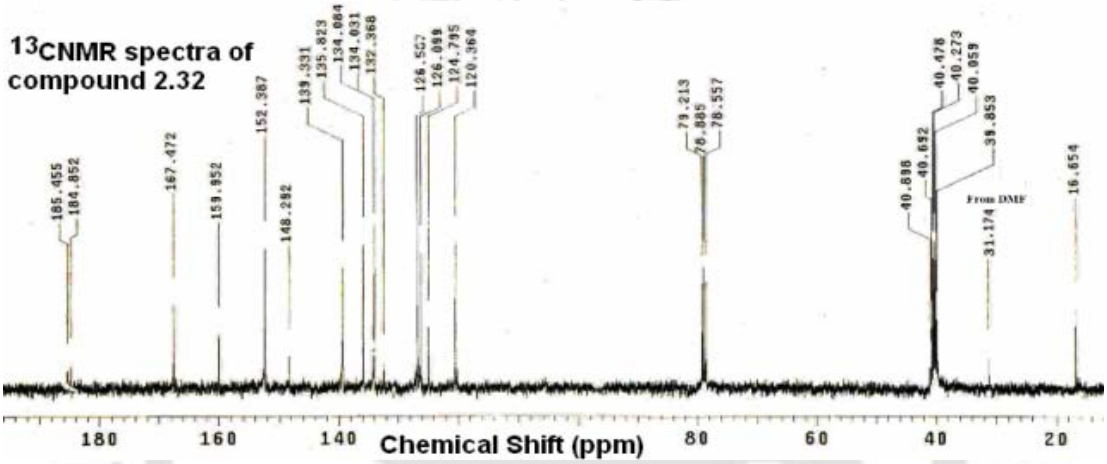

Isolated yield: 71%, Elemental anal. Calcd. for $C_{18.5}H_{17.5}N_{1.5}O_6S$; C, 57.29, H, 4.52, N, 5.42; found C, 57.99 ; H, 3.68 ; N, 5.06 ; IR (KBr, cm^{-1}): 3497 (bs), 3082 (w), 2925 (w), 1699 (s), 1666 (s), 1594 (m), 1563 (m), 1398 (s), 1354 (m), 1302 (s), 1265 (s), 1156 (w), 1139 (w), 1071 (m), 941 (w), 765 (m), 705 (m); ^{1}H NMR (DMSO-d_6, 400 MHz): 8.37 (d, J = 4.8 Hz, 1H), 8.16 (d, J = 7.6 Hz, 2H), 7.92 (d, J = 5.6 Hz 1H), 7.69 (d, J = 7.6 Hz, 2H), 7.09 (t, J = 8.4 Hz, 1H), 2.08 (s, 3H). ^{13}C NMR (DMSO-d_6, 100 MHz): 185.5, 184.9, 167.5, 159.9, 152.4, 148.3, 139.3, 135.8, 134.1, 134.0, 132.37, 132.3, 126.8, 126.1, 124.8, 120.4, 16.7. LC-MS (m/e, ESI m+1) 326.

2.4.16 General procedure for oxidation of *bis*-2,3-diarylsulphanylnaphthalenediol

To a solution of *bis*-2,3-diarylsulphanylnaphthalenediol **2.6-2.16** (2 mmol each) in 15 ml of methanol, 0.004 gm of copper(II) acetate monohydrate (0.02 mmol, 2 mol %) was added. The resulting reaction mixture was warmed for 15 minutes followed by stirring for 1 hr at room temperature. The progress of the reaction was observed from the change in color of the solution from colorless to red color and was again monitored

by TLC using ethyl acetate-hexane (1:5) as eluent. Once the reaction was completed, the solvent was removed by slow evaporation at open air and red crystals were obtained as pure products **2.33-2.43**.

2.4.17 Spectroscopic data for *bis*-2,3-diarylsulphanyl 1,4-naphthalenedione 2.33-2.43

Compound 2.33:

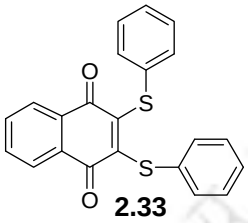

2.33

Isolated yield: 96%; m.p.140 ºC, Elemental anal calcd for $C_{22}H_{14}O_2S_2$ C, 70.56; H, 3.77; C,71.19; H, 3.75.**;** IR (KBr, cm^{-1}): 3407 (bs), 1668 (s), 1579 (w), 1498 (w), 1475 (w), 1267 (s), 1138 (w), 1081 (w), 748 (s), 706 (w), 698 (w). ^{1}H NMR (400 MHz, $CDCl_3$) 7.98 (dd, J = 6, 2.8 Hz, 2H), 7.68 (dd, J = 5.6, 2.4 Hz, 2H), 7.37 (m, 4H), 7.29 (m, 6H); UV-vis (λ_{max}, CH_3CN) 458 nm (ε = 3.85 ×10^3 mol^{-1} dm^3 cm^{-1}).

Compound 2.34:

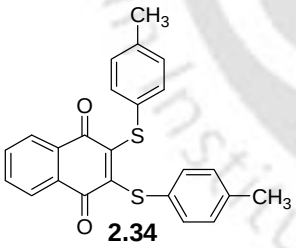

2.34

Isolated yield: 98%; m.p. 95ºC, Elemental anal calcd for $C_{24}H_{18}O_2S_2$ C, 71.61, H, 4.51; found C, 71.63, H, 4.50. IR (KBr, cm^{-1}): 3433 (bw), 2921(w), 1650 (s), 1664 (s), 1590 (w), 1492 (w), 1273 (s), 1134 (s), 1086 (w), 815 (s), 700 (w), 490 (w); ^{1}H NMR (400 MHz, $CDCl_3$) 7.98 (dd, J = 5.6, 2.4 Hz, 2H), 7.66 (dd, J = 5.6, 2.4 Hz, 2H), 7.29 (d, J = 8 Hz, 4H), 7.11 (d, J = 8 Hz, 4H), 2.34 (s, 6H); UV-vis (λ_{max}, CH_3CN) 473 nm (3.83 × 10^3 mol^{-1} dm^3 cm^{-1}).

Compound 2.35:

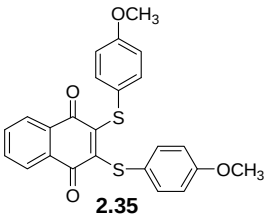

2.35

Isolated yield: 97%; m.p.91ºC, Elemental anal calcd for $C_{24}H_{18}O_4S_2$, C, 66.34; H, 4.18; found C, 66.33, H, 4.20.; IR (KBr, cm^{-1}): 3428 (bw), 2928 (w), 1659 (s), 1590 (s), 1492 (w), 1465 (w), 1289 (w), 1271 (s), 1245 (s), 1139 (s), 1029 (w), 838 (w), 700 (w) 531 (w). ^{1}H NMR (400 MHz, $CDCl_3$) 7.95 (dd, J = 5.6, 2.4 Hz, 2H), 7.64 (dd, J = 5.6, 4 Hz, 2H), 7.38 (d, J = 8.8 Hz, 4H), 6.84 (d, J = 8.8 Hz, 4H), 3.81 (s, 6H). LC-MS (m/e, ESI m+1) 435; UV-vis (λ_{max}, CH_3CN) 458 nm ($\varepsilon = 3.76 \times 10^3$ mol^{-1} dm^3 cm^{-1}).

Compound 2.36:

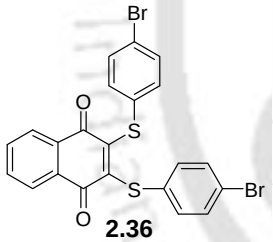

2.36

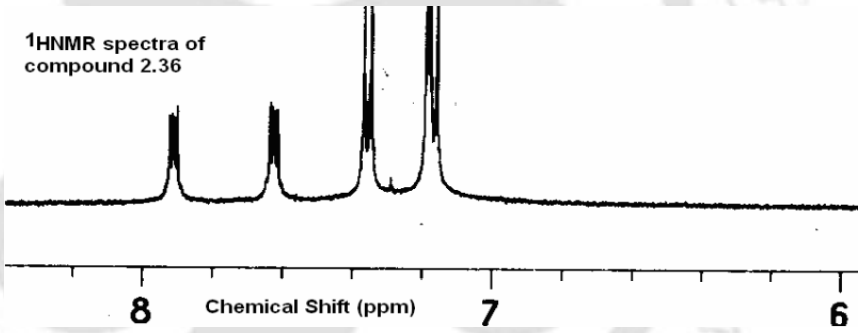

Isolated yield: 96%; mp 207^{0}C; IR (KBr, cm^{-1}): 3435 (bw), 2923 (w), 1666 (s), 1654 (s), 1590 (w), 1504 (w), 1471 (w), 1270 (s), 1135 (s), 1080 (w), 1006 (w), 816 (s), 708 (w), 478 (w); ^{1}H NMR (400 MHz, $CDCl_3$) 7.91 (dd, J = 5.6, 2.4 Hz, 2H), 7.62 (dd, J = 5.6, 2.4 Hz, 2H), 7.36 (d, J = 8.4 Hz, 4H), 7.17 (d, J = 8.4 Hz, 4H); LC-MS (m/e, ESI m+1) 533; UV-vis (λ_{max}, CH_3CN) 457 nm ($\varepsilon = 3.09 \times 10^3$ mol^{-1} dm^3 cm^{-1}).

Compound 2.37:

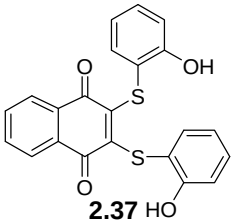

2.37

Isolated yield: 94%; IR (KBr, cm^{-1}): 3403 (bs), 2924 (w), 1665 (s), 1653 (s), 1590 (w), 1502 (w), 1472 (w), 1267 (s), 1135 (s), 1080 (w), 1006 (w), 816 (s), 708 (w); ^1H NMR ($CDCl_3$, 400 MHz) 8.11 (dd, J = 6.6, 2.4 Hz, 2H), 7.73 (dd, J = 6.6, 2.4 Hz, 2H), 7.45 (m, 4H), 7.12 (d, J = 8.8 Hz, 2H), 7.04 (t, J = 8.2 Hz, 2H), 6.28 (s, 2H).

Compound 2.38:

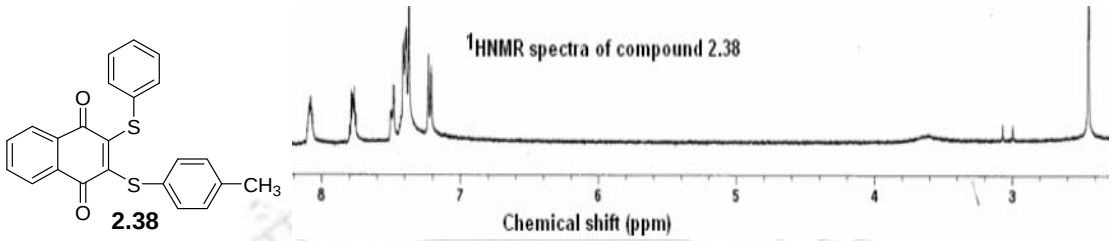

Isolated yield: 96%; m.p.121ºC, Elemental anal calcd for $C_{23}H_{16}O_2S_2$, C, 71.10, H, 4.15, found C, 71.22, H, 4.18. IR (KBr, cm^{-1}): 3436 (bs), 2924 (w), 1664 (s), 1590 (w), 1497 (w), 1475 (w), 1264 (s), 1136 (s), 1082 (w), 812 (w), 706 (s), 503 (w); ^1H NMR ($CDCl_3$, 400 MHz,) 8.08 (dd, J = 8.8, 5.6 Hz, 2H), 7.77 (dd, J = 9.2, 5.2 Hz, 2H), 7.49 (d, J = 8 Hz, 2H), 7.40 (m, 5H), 7.22 (d, J = 8 Hz, 2H), 2.45 (s, 3H); UV-vis (λ_{max}, CH_3CN) 460 nm ($\varepsilon = 4.96 \times 10^3$ mol^{-1} dm^3 cm^{-1}).

Compound 2.39:

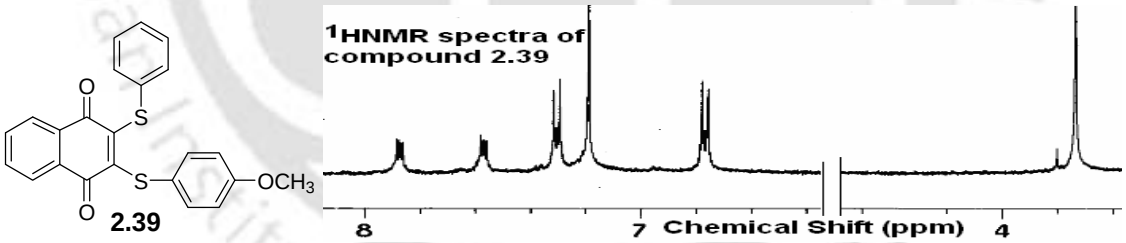

Isolated yield: 92%; m.p.93 ºC, Elemental anal calcd for $C_{23}H_{16}O_3S_2$; C, 68.29, H, 3.99; found C, 68.31, H, 4.09. IR (KBr, cm^{-1}): 3433 (bs), 2926 (w), 1659 (s), 1590 (s), 1492 (w), 1464 (w), 1270 (s), 1245 (s), 1138 (s), 1025 (w), 809 (w), 700 (w), 530 (w); ^1H NMR ($CDCl_3$, 400 MHz) 7.87 (dd, J = 5.6, 2.4 Hz, 2H), 7.57 (dd, J = 5.6, 2.4 Hz, 2H), 7.31 (d, J = 9.2 Hz, 4H), 6.77 (d, J = 8.8 Hz, 5H), 3.73 (s, 3H). UV-vis (λ_{max}, CH_3CN) 457 nm ($\varepsilon = 5.16 \times 10^3$ mol^{-1} dm^3 cm^{-1}).

Compound 2.40:

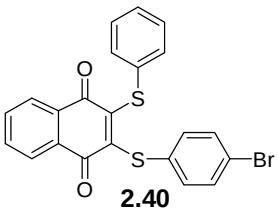

2.40

Isolated yield: 96%; IR (KBr, cm^{-1}): 3435 (bw), 2922 (w), 1667 (s), 1654 (s), 1590 (m), 1503 (w), 1471 (m), 1387(w), 1270 (s), 1135 (s), 1080 (m), 1006 (w), 816 (s), 708 (w); ^1H NMR ($CDCl_3$, 400 MHz) 8.03 (dd, J = 8.8, 5.6 Hz, 2H), 7.75 (dd, J = 9.2, 5.2 Hz, 2H), 7.47 (d, J = 8 Hz, 2H), 7.39 (m, 5H), 7.12 (d, J = 8 Hz, 2H); UV-vis (λ_{max}, CH_3CN) 457 nm ($\varepsilon = 4.16 \times 103$ mol^{-1} dm^3 cm^{-1}).

Compound 2.41:

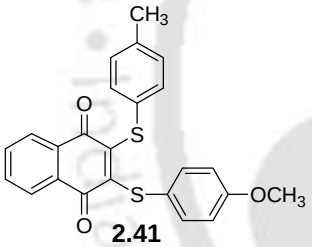

2.41

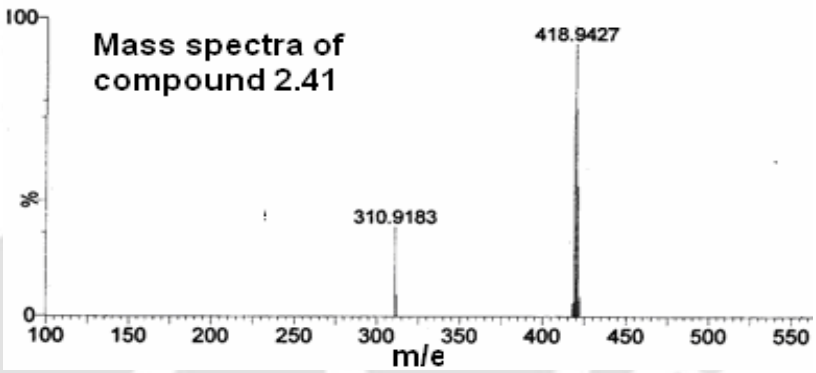

Isolated yield: 96%; mp 138^0C; IR (KBr, cm^{-1}): 3436 (bw), 2927 (w), 1664 (s), 1590 (w), 1492 (s), 1267 (s), 1138 (s), 1033 (w), 814 (w), 700 (w); ^1H NMR ($CDCl_3$, 400 MHz) 7.89 (dd, J = 5.6, 2.8 Hz, 2H), 7.58 (dd, J = 6, 3.2 Hz, 2H), 7.30 (d, J = 8.8 Hz, 2H), 7.21 (d, J = 8.4 Hz, 2H), 7.03 (d, J = 8.4 Hz, 2H), 6.77 (d, J = 7.6 Hz, 2H), 3.73 (s, 3H), 2.26 (s, 3H).; LC-MS (m/e, ESI m+1) 419. UV-vis (λ_{max}, CH_3CN) 469 nm ($\varepsilon = 5.17 \times 10^3$ mol^{-1} dm^3 cm^{-1}).

Compound 2.42:

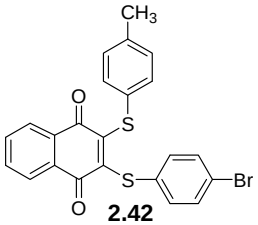

2.42

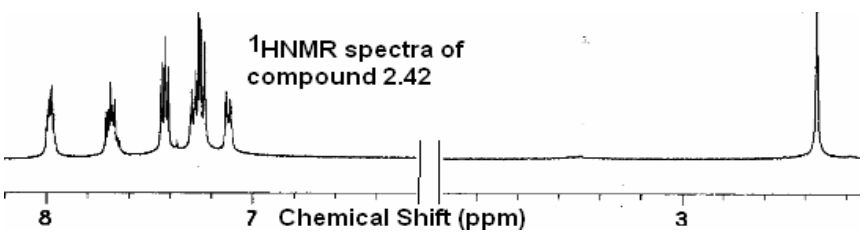

Isolated yield: 92%; mp 178^{0}C; IR (KBr, cm^{-1}): 3435 (bw), 2922 (w), 1667 (s), 1654 (s), 1590 (m), 1503 (w), 1471 (m), 1270 (s), 1135 (s), 1080 (w), 1006 (w), 813 (w), 708 (w), 479 (w); ^{1}H NMR ($CDCl_3$, 400 MHz,) 7.98 (dd, J = 5.8, 2.4 Hz, 2H), 7.69 (dd, J = 5.8, 2.4 Hz, 2H), 7.42 (d, J = 8.8 Hz, 2H), 7.26 (m, 4H), 7.12 (d, J = 8.8 Hz, 2H), 2.35 (s, 3H); LC-MS (m/e, ESI m+1) 469; UV-vis (λ_{max}, CH_3CN) 458 nm ($\varepsilon = 3.84 \times 10^3$ mol^{-1} dm^3 cm^{-1}).

Compound 2.43:

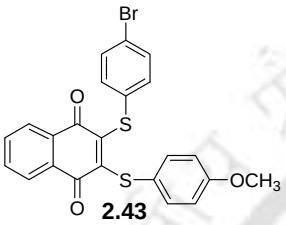

2.43

Isolated yield: 95%; IR (KBr, cm^{-1}): 3435 (bw), 2922 (w), 1667 (s), 1654 (s), 1590 (m), 1503 (w), 1471 (m), 1270 (s), 1135 (s), 1080 (s), 1006 (w), 813 (w), 708 (w), 479 (w); ^{1}H NMR ($CDCl_3$, 400MHz,) 7.98 (dd, J = 6.6, 2.8 Hz, 2H), 7.67 (dd, J = 6,8, 3.2 Hz, 2H), 7.39 (d, J = 8.8 Hz, 2H), 7.26 (d, J = 8.4 Hz, 2H), 7.13 (d, J = 8.4 Hz, 2H), 6.78 (d, J = 7.6 Hz, 2H), 3.75 (s, 3H); UV-vis (λ_{max}, CH_3CN) 469 nm ($\varepsilon = 4.31 \times 10^3$ mol^{-1} dm^3 cm^{-1}).

2.4.18 General procedure for synthesis of compounds 2.44-2.49

1,4-Benzoquinone (0.216 g, 2 mmol) was dissolved in methanol (15 ml) and corresponding amine (4 mmol) was added dropwise. The resulting solution was stirred for 8 hrs at room temperature in aerial condition. The volume of the solution was made to half under reduced pressure, the precipitate appeared was filtered and washed with methanol (5 ml) and allowed to dry at room temperature. Further recrystallization from methanol gave the 2,5-bis-(alkyl/arylamino)-1,4-benzoquinones, **2.44-2.49**.

2.4.19 Spectroscopic data for *bis*-2,3-arylsulphanyl 1,4-naphthalenedione 2.44-2.49

Compound 2.44:

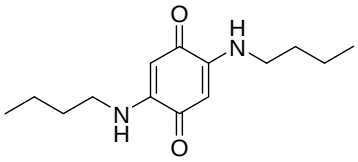

2.44

Isolated yield: 70%; Melting point: 154^{0}C. Elemental anal. calcd. For $C_{14}H_{22}N_2O_2$: C, 67.17; H, 8.86; found C, 67.34; H, 8.81; IR (KBr, cm^{-1}): 3261 (s), 2956 (w), 2862 (m), 1643 (s), 1551 (s), 1499 (s), 1458 (w), 1363 (s), 1293 (s), 1250 (s), 1207 (w), 1078 (w), 910 (w), 674 (br s); ^{1}H NMR ($CDCl_3$, 400 MHz): 6.58 (s, 2H), 5.29 (s, 2H), 3.14 (q, 4H), 1.63 (m, 4H), 1.41 (septate, 4H), 0.95 (t, J = 8.2Hz, 6H).

Compound 2.45:

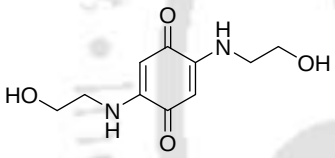

2.45

Isolated yield: 85%; Elemental anal. calcd. For $C_{10}H_{14}N_2O_4$: C, 53.09; H, 6.24; found C, 53.18; H, 6.45; IR (KBr, cm^{-1}): 3317 (br s), 3254 (w), 3215 (s), 3150 (s), 1628 (s), 1550 (s), 1491 (s), 1446 (m), 1381 (w), 1301 (s), 1262 (s), 1073 (m), 710 (w); ^{1}H NMR (DMSO-d_6, 400 MHz): 8.20 (s, 2H), 7.37 (s, 2H), 4.87 (s, 2H), 3.58 (q, J = 8.2 Hz, 4H), 3.18 (t, J = 8.0 Hz, 4H).

Compound 2.46:

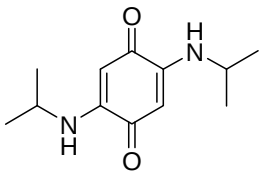

2.46

Isolated yield: 88%; Melting point: 185^{0}C. Elemental anal. calcd. For $C_{12}H_{18}N_2O_2$: C, 64.84; H, 8.16; N, 12.60; found C, 64.43; H, 8.12; N, 12.52; IR (KBr, cm^{-1}): 3210 (s), 2976 (w), 1564 (s), 1487 (s), 1314 (s), 1228 (s), 1131 (m), 835 (m), 723 (w); ^{1}H NMR ($CDCl_3$, 400 MHz): 6.70 (s, 2H), 6.50 (s, 2H), 3.65 (heptet, 2H), 1.32 (d, J= 6.8 Hz, 12H), Uv vis (λ_{max} CH_3CN) 341 nm ($\varepsilon = 1.54 \times 10^3$ mol^{-1} dm^3 cm^{-1})

Compound 2.47:

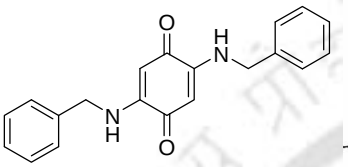

2.47

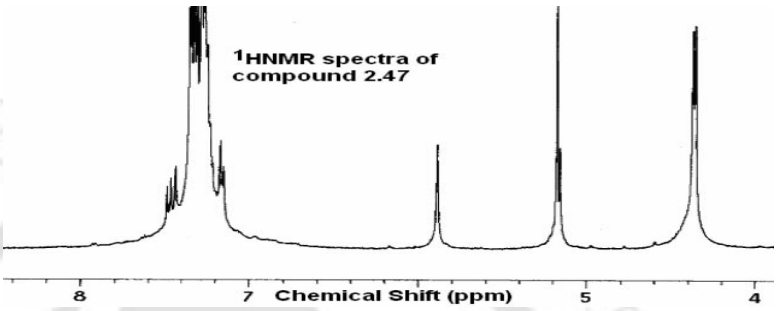

Isolated yield: 72%; Melting point: 234^{0}C. Elemental anal. calcd. For $C_{20}H_{18}N_2O_2$: C, 75.45; H, 5.70; found C, 75.13; H, 5.68; IR (KBr, cm^{-1}): 3279 (s), 3021 (s), 1643 (s), 1555 (s), 1496 (s), 1362 (s), 1253 (s), 1059 (w), 1004 (m), 856 (w), 814 (s), 697 (s); ^{1}H NMR ($CDCl_3$, 400 MHz): 7.36-7.24 (m, 10H), 5.89 (s, 2H), 5.37 (s, 2H), 4.32 (d, J = 6.0 Hz, 4H).

Compound 2.48:

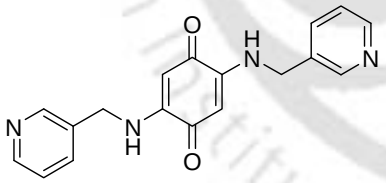

2.48

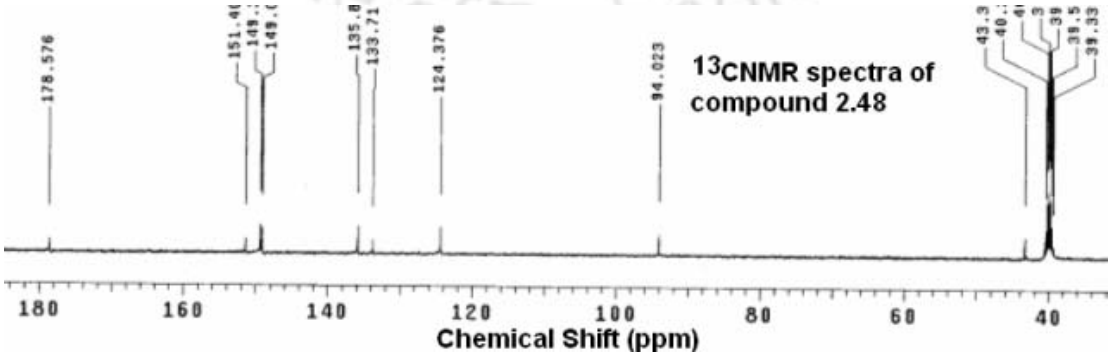

Isolated yield: 73%; IR (KBr, cm^{-1}): 3305 (b), 2926 (w), 1645 (w), 1595 (s), 1557 (s), 1496 (s), 1431 (s), 1360 (w), 1343 (m), 1257 (s), 1073 (m), 1028 (w), 1004 (m), 818 (s), 706 (s).; ^{1}H NMR (DMSO-d_6, 400 MHz): 8.49 (s, 2H), 8.42 (d, J = 4.8 Hz, 2H), 8.32 (t, J = 7.6 Hz, 2H), 7.64 (d, J = 8.0 Hz, 2H), 7.33 (t, J = 7.4, Hz, 2H), 5.21 (s, 2H), 4.38 (d, J = 6.4 Hz, 4H). ^{13}C NMR (DMSO-d_6, 100 MHz): 176.57, 151.40, 149.31, 149.01, 135.83, 133.71, 124.37, 94.02, 43.03.

Compound 2.49:

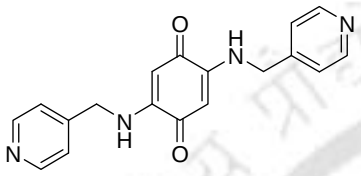

2.49

Isolated yield: 69%; IR (KBr, cm^{-1}): 3301 (s), 2923 (w), 1653 (w), 1590 (s), 1506 (s), 1475 (m), 1417 (m), 1385 (w), 1349 (m), 1241 (s), 1143 (m), 1027 (w), 794 (s), 686 (m); ^{1}H NMR (DMSO-d_6, 400 MHz): 9.66 (s, 2H), 8.43 (d, J = 5.2 Hz, 4H), 8.30 (s, 2H), 7.31 (d, J = 4.8 Hz, 2H), 5.05 (s, 2H), 4.47 (d, J = 6.0 Hz, 4H). ^{13}C NMR (DMSO-d_6, 100 MHz): 177.70, 156.29, 150.48, 132.96, 122.17, 97.7, 45.10.

2.4.20 General procedure for synthesis of compounds 2.50-2.51 and 2.54-2.57

The compounds **2.50-2.51** and **2.54-2.57** were synthesized by stirring a methanolic solution of corresponding amines (4 mmol) with 1,4-naphthoquinone (0.632g, 4 mmol) for 2 hrs at room temperature. The products were purified by crystallization.

2.4.21 Spectroscopic data for *bis*-2,3-arylsulphanyl 1,4-naphthalenedione 2.44-2.49

Compound 2.50:

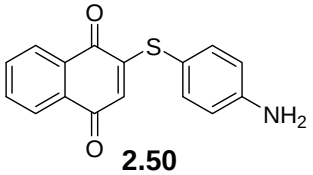

2.50

Isolated yield: 90%; IR (KBr, cm^{-1}): 3458 (s), 3364 (s), 1661 (s), 1634 (s), 1591 (s), 1556 (m), 1499 (w), 1334 (w), 1319 (w), 1301 (s), 1249 (s), 1217 (w), 1119 (w), 1065

(m), 852 (w), 781 (w), 704 (m), 531 (w); ^{1}H NMR ($CDCl_3$, 400 MHz): 8.12 (d, J = 8.8 Hz, 1H), 8.01 (d, J = 8.8 Hz, 1H), 7.71 (m, 2H), 7.17 (d, J = 8.8 Hz, 2H), 6.75 (d, J = 8.4 Hz, 2H), 5.91 (s, 1H), 3.98 (bs, 2H).

Compound 2.51:

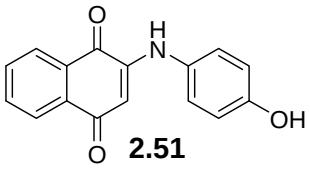

2.51

Isolated yield: 68%; IR (KBr, cm^{-1}): 3304 (s), 1670 (m), 1624 (s), 1601 (s), 1531 (m), 1519 (m), 1438 (m), 1365 (s), 1332 (w), 1268 (s), 1161 (w), 1124 (w), 991 (w), 821 (w), 775 (w), 724 (m), 672 (w); ^{1}H NMR (DMSO-d_6, 400 MHz): 9.66 (s, 1H), 9.07 (s, 1H), 8.02 (d, J = 8 Hz, 1H), 7.92 (d, J = 7.2 Hz, 1H), 7.83 (t, J = 7.2 Hz, 1H), 7.76 (t, J = 7.2 Hz , 1H), 7.14 (d, J = 8 Hz, 2H), 6.82 (d, J = 8 Hz, 2H) 5.86 (s, 1H); ^{13}C NMR (DMSO-d_6): 182.3, 181.8, 155.4, 147.2, 135.0, 132.5, 130.5, 129.0, 126.1, 125.3, 115.9, 100.8.

2.4.22 General procedure for synthesis of compounds 2.52 and 2.53

1,2-Naphthoquinone (0.158 g, 1 mmol) was dissolved in methanol (15 ml) and the corresponding amine (2 mmol) under consideration was added to obtain homogeneous solution. The solution was stirred at room temperature for 12 hrs in aerial condition at room temperature. The precipitate obtained was filtered and were recrystallized from methanol chloroform mixture (1:1 ratio) to obtain the desired product.

2.4.23 Spectroscopic data compound 2.52 and 2.53

Compound 2.52:

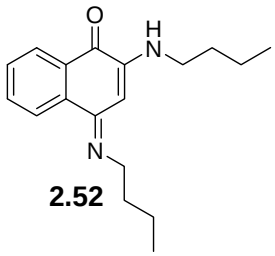

2.52

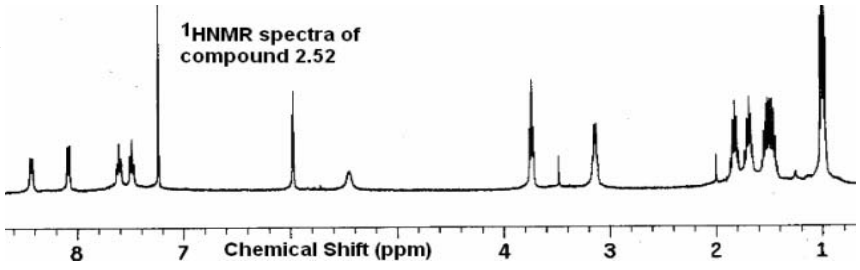

Isolated yield: 68%; IR (KBr, cm^{-1}) 3436 (s), 3342 (s), 2954 (s), 2928 (s), 2860 (s), 1654 (s), 1597 (s), 1576 (m), 1510 (m), 1476 (w), 1331 (s), 1097 (w), 765 (m), 735 (s); ^1H NMR ($CDCl_3$, 400 MHz): 8.42 (d, J = 4 Hz, 1H), 8.10 (d, J = 4 Hz, 1H), 7.61 (t, J = 8.8 Hz, 1H), 7.48 (t, J = 8.2 Hz, 1H), 5.97 (s, 1H), 5.45 (bs, 1H), 3.74 (t, J = 7.8 Hz, 2H), 3.13 (t, J = 7.8 Hz, 2H), 1.82 (q, J = 8.0 Hz, 2H), 1.69 (q, J = 7.6 Hz, 2H), 1.51 (m, 4H), 1.01 (m, 6H); UV-vis (λ_{max}, MeOH) 450 nm ($\varepsilon = 0.27 \times 10^3$ mol^{-1} dm^3 cm^{-1}).

Compound 2.53:

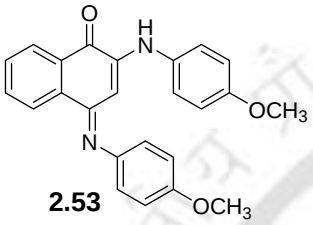

2.53

Isolated yield: 70%; IR (KBr, cm^{-1}): 3323 (br), 1654 (s), 1604 (s), 1516 (s), 1338 (m), 1292 (m), 1236 (s), 1182 (m), 1029 (s), 837 (s), 775 (m), 1097 (w), 715 (m); ^1H NMR (DMSO-d_6, 400 MHz): 8.54 (d, J = 4 Hz, 1H), 8.18 (d, J = 4 Hz, 1H), 7.74(d, J = 4 Hz, 1H), 7.65 (d, J = 4 Hz, 1H), 7.19 (m, 4H), 6.94 (d, J = 8.4 Hz, 2H), 6.88 (d, J = 8.4 Hz, 2H), 5.95 (s, 1H), 5.42 (bs, 1H), 3.82 (s, 6H). UV-vis (λ_{max}, MeOH) 486 nm ($\varepsilon = 0.43 \times 10^3$ mol^{-1} dm^3 cm^{-1}).

2.4.24 Spectroscopic data compound 2.54-2.57

Compound 2.54:

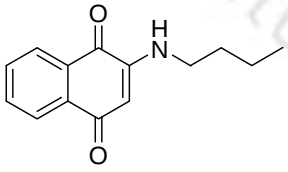

Isolated yield 73%; IR (KBr, cm^{-1}): 3432 (s), 3329 (s), 2954 (s), 1672 (s), 1610 (s), 1598 (s), 1558 (w), 1501 (m), 1358 (s), 1339 (m), 1264 (m), 1124 (s), 748 (m), 732 (w), 709 (s); ^1H NMR ($CDCl_3$, 400 MHz): 8.08 (d, J = 7.6 Hz, 2H), 7.69 (t, J = 7.6 Hz, 1H), 7.61 (t, J = 7.6 Hz, 1H), 6.24 (s, 1H), 5.63 (s, 1H), 4.41 (m, 2H), 2.28 (m, 2H), 1.64 (m, 2H), 1.55 (m, 3H).

Compound 2.55:

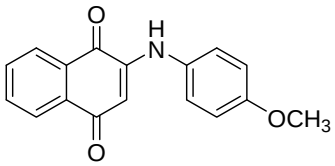

Isolated Yield: 85%; Melting point: 167^0C; IR (KBr, cm^{-1}): 3428 (br s), 3223 (s), 1676 (s), 1566 (s), 1601 (s), 1508 (s), 1355 (s), 1289 (s), 1234 (s), 1122 (s), 1039 (s), 721 (s); ^{1}H NMR ($CDCl_3$, 400 MHz): 8.1 (t, J = 5.6 Hz, 2H), 7.73 (t, J = 7.6 Hz, 1H), 7.63 (t, J = 7.6 Hz, 1H), 7.40 (br s, 1H), 7.19 (d, J = 8 Hz, 2H), 6.94 (d, J = 8 Hz, 2H), 6.20 (s, 1H), 3.82 (s, 3H).

Compound 2.56:

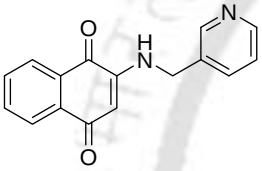

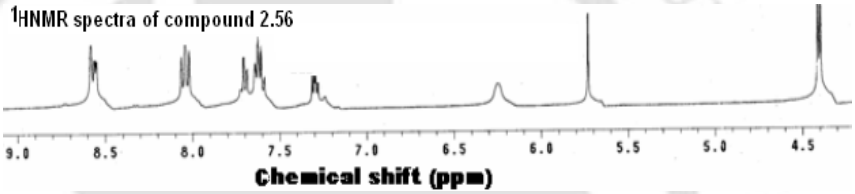

Isolated yield 72%; IR (KBr, cm^{-1}): 3430 (s), 3349 (s), 3312 (s), 1675 (s), 1610 (s), 1601 (s), 1568 (s), 1500 (s), 1358 (s), 1339 (m), 1264 (m), 1123 (s), 748 (m), 729 (s), 711 (s); ^{1}H NMR ($CDCl_3$, 400 MHz): 8.58 (m, 2H), 8.06 (t, J = 8 Hz, 2H), 7.72 (t, J = 8 Hz, 1H), 7.63-7.59 (m, 2H), 7.31-7.28 (m, 1H), 6.22 (s, 1H), 5.78 (s, 1H), 4.40 (m, 2H); UV-vis (λ_{max}, MeOH) 468 nm ($\varepsilon = 0.5 \times 10^3$ mol^{-1} dm^3 cm^{-1}).

Compound 2.57:

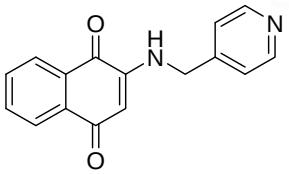

Isolated yield: 84%. IR (KBr, cm^{-1}): 3431 (s), 3332 (s), 1677 (s), 1602 (s), 1594 (s), 1568 (s), 1559 (s), 1504 (s), 1358 (m), 1340 (m), 1259 (s), 1126 (m), 733 (m); ^{1}H NMR ($CDCl_3$, 400 mHz): 8.58 (d, J = 8 Hz, 2H), 8.06 (d, J = 8 Hz, 2H), 7.72 (t, J = 8 Hz , 1H), 7.65 (t, J = 8 Hz, 1H), 7.24 (s, 1H), 7.20 (d, J = 8 Hz, 1H), 6.26 (s, 1H), 5.65 (s, 1H), 4.40 (s, 2H); UV-vis (λ_{max}, MeOH) 436 nm ($\varepsilon = 0.5 \times 10^3$ mol^{-1} dm^3 cm^{-1}).

2.4.25 Procedure for the synthesis of compound 2.58

(3-Mercapto-1,4-dioxo-1,4-dihydronaphthalen-2-ylsulfanyl) acetic acid **2.18** (0.338 g, 1 mmol) was dissolved in dichloromethane (15 ml) and stirred at ice cold condition for 10 min. To this solution thionyl chloride (0.3 ml) was added and further allowed to stir for another 45 mins. The reaction mixture was then concentrated to approximately 5 ml by heating to remove the excess thionyl chloride and allowed to cool to room temperature. The solution was diluted with dichloromethane (5 ml) and ethyl amine (0.135 g, 3 mmol) was added. The resulting solution was further stirred for 4 hrs at room temperature. The reaction mixture was washed several times with water and the organic layer was dried over anhydrous sodium sulphate (0.3 g) and the solvent was removed under reduced pressure. The product was obtained as red needle microcrystals upon crystallization from dichloromethane.

Compound 2.58:

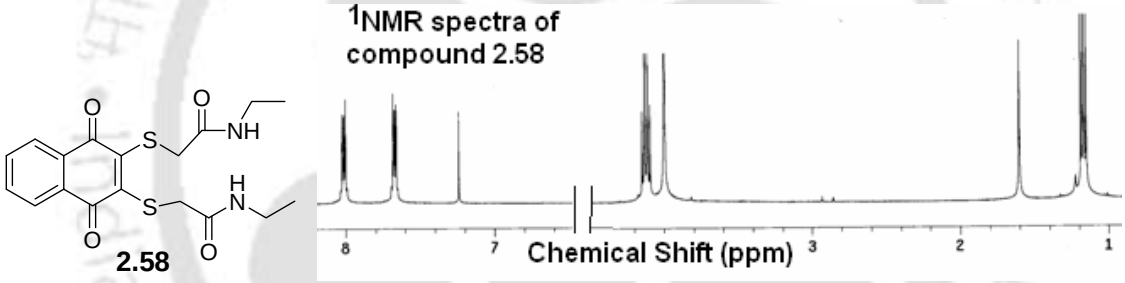

Isolated yield: 53%; IR (KBr, cm^{-1}): 3446 (bw), 2913 (m), 1732 (s), 1652 (s), 1589 (w), 1466 (m), 1385 (w), 1314 (s), 1280 (s), 1207 (m), 1143 (s), 1032 (m), 810 (w), 702 (m); ^{1}H NMR ($CDCl_3$, 400 MHz): 8.01 (dd, J = 5.6, 2.0 Hz, 2H), 7.67 (dd, J = 5.6, 2.0 Hz, 2H), 4.13 (q, J = 7.6 Hz, 4H), 4.00 (s, 4H), 2.17 (t, J = 7.4 Hz, 6H), $^{13}CNMR$ ($CDCl_3$, 100 MHz): 179.00, 169.01, 149.26, 133.90, 133.04, 127.21, 61.99, 35.93, 14.24.

2.4.26 Procedure for the synthesis of compound 2.59

2-(4-Aminophenylthio) naphthalene 1,4-dione **2.51** (0.562 g, 2 mmol) was dissolved in dry dichloromethane (25 ml) and triethylamine (0.202 g, 2 mmol) was added to it. The solution was stirred at 0ºC for 15 mins after which succinyl chloride (0.154 g, 1 mmol) was added dropwise to the stirred solution over a period of 10 min. The resulting reaction mixture was stirred for 8 hrs, after which it was washed several times with

water to remove the hydrochloride salt. The organic layer was dried over anhydrous sodium sulphate (0.3 g) and the solvent was removed under reduced pressure. The product was obtained as a light yellow solid.

Compound 2.59:

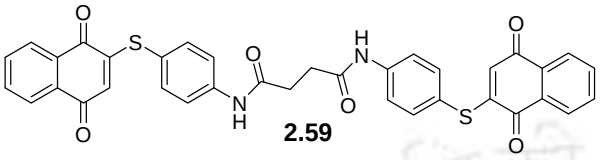

2.59

Isolated yield: 73%; IR (KBr, cm^{-1}): 3412 (bw), 3286 (w), 2922 (m), 1740 (w), 1658 (s), 1588 (s), 1561 (m), 1514 (w), 1396 (w), 1335 (m), 1296 (s), 1251 (s), 1118 (w), 1066 (w), 858 (m), 700 (m); ^{1}H NMR ($CDCl_3$, 400 MHz): 8.05 (d, J = 6.4 Hz, 2H), 7.92 (d, J = 6.0 Hz, 2H), 7.83 (m, 4H), 7.26 (d, J = 8.4 Hz, 4H), 6.83 (d, J = 7.6 Hz, 4H), 5.86 (s, 2H), 2.49 (s, 4H), ^{13}C NMR (DMSO-d_6, 100 MHz): 182.34, 182.12, 166.95, 156.24, 155.86, 136.57, 134.96, 134.67, 133.63, 131.92, 131.76, 128.60, 127.91, 127.11, 124.25, 31.48.

2.4.27 Procedure for the synthesis of compound 2.60

Phthalic anhydride (0.296 g, 2 mmol) was dissolved in glacial acetic acid (10 ml) by warming to 40^0 C. 2-(4-Aminophenylthio) naphthalene 1,4-dione **2.51** (0.562 g, 2 mmol) was added to this solution and refluxed for 12 hrs at 115^0 C. Transparent light red solution obtained was kept for crystallization and light brown crystal were obtained as pure product.

Compound 2.60:

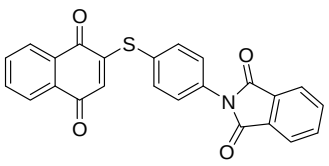

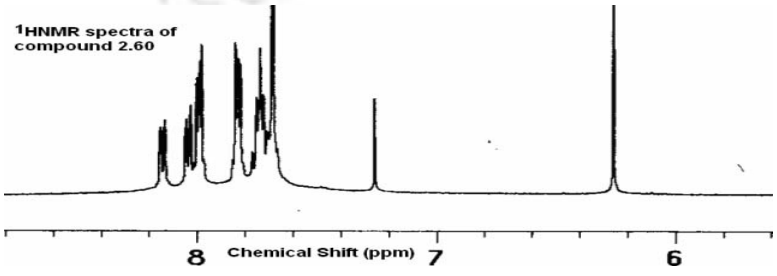

Isolated yield: 73%; IR (KBr, cm^{-1}): 3431 (bw), 3265 (w), 2922 (m), 1741 (m), 1720 (s), 1669 (s), 1593 (s), 1558 (m), 1500 (w), 1407 (w), 1374 (s), 1332 (w), 1294 (s), 1247 (s), 1118 (m), 1078 (w), 853 (m), 717 (m); ^{1}H NMR ($CDCl_3$, 400 MHz): 8.14 (d, J = 7.6 Hz, 1H), 8.02 (d, J = 7.6 Hz, 1H), 7.99 (d, J = 8.2 Hz, 2H), 7.83 (d, J = 8.2 Hz, 2H), 7.74 (m, 2H), 7.69 (s, 4H), 6.26 (s, 1H).

Chapter 3

Polymorphism in quinone derivatives

Specific drug action[264-266] and polymorphism[267-268] are generally controlled by weak interactions. Weak interactions also provide elegant means in biological molecules to build assemblies of molecules.[269] Molecular conformations, hydrogen bonding, packing arrangements, and lattice energies of the same molecule in different supramolecular environments compared in polymorphic structures.[270-274] Polymorphs may arise due to differences in intermolecular interactions and crystal packing.[275] There is increasing interest in understanding polymorphism, transformations between polymorphs, and crystallization of drugs.[276-279] Polymorphism is more widespread in pharmaceutical solids.[280] We mentioned in the **chapter 1** that the polymorphism in quinones and their derivatives may occur due to the difference in weak interactions with oxygen atom of the quinone as well as, due to the presence of the different orientations of the substituents in the rigid quinone ring.

In this chapter we describe the synthesis, structure and polymorphism behaviour of different types of quinone derivatives which have sulphur atoms separated by intervening groups.

3.1 Polymorphism and structures of few 2,3-*bis*-*p*-methylphenylsulfanyl 1,4-naphthoquinone

Sulphur containing compounds[281-283, 149] shows conformational polymorph. *Syn* and *anti* conformation across two directly bonded sulphur atoms or two sulphur atoms separated by intervening carbon atoms are well studied in literature.[149,284-289] The orientation of lone pair of electron on sulphur provides basis to make ordered metallo-organic[290-293] and biological frameworks.[294-295] A pictorial description of the *syn* and *anti* conformation of two sulphur atoms separated by intervening carbon atoms attached to the rigid unit are shown in **fig. 3.1**.

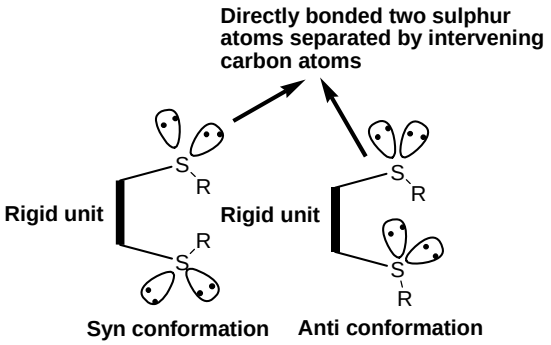

Fig. 3.1 Syn and anti conformation

.

Two conformational polymorphs of 2,3-*bis*-*p*-methylphenylsulfanyl 1,4-naphtho-quinone can be obtained from different reaction conditions. The polymorph **3.1A** was obtained by fast oxidation of 2,3-*bis*-*p*-methylphenylsulfanyl 1,4-naphthalenediol with copper(II) acetate catalyst; while the polymorph **3.1B** was obtained by slow aerial oxidation of the 2,3-*bis*-*p*-methylphenylsulfanyl 1,4-naphthalenediol in methanol. These polymorphs of 2,3-*bis*-*p*-methylphenylsulfanyl 1,4-naphthoquinone occurs due to the relative orientations of *p*-methylphenylsulfanyl groups attached to the 1,4-naphthquinone ring and their structures are shown in **fig. 3.2**. In the polymorphs **3.1A** and **3.1B**, the quinone rings are planar and the sulfanyl groups are not in the plane of the quinone plane. The sulphur atoms in these molecules are not associated with any weak interactions. These two polymorphs differ in their packing pattern **fig. 3.3**; as well as they possess different weak interactions.

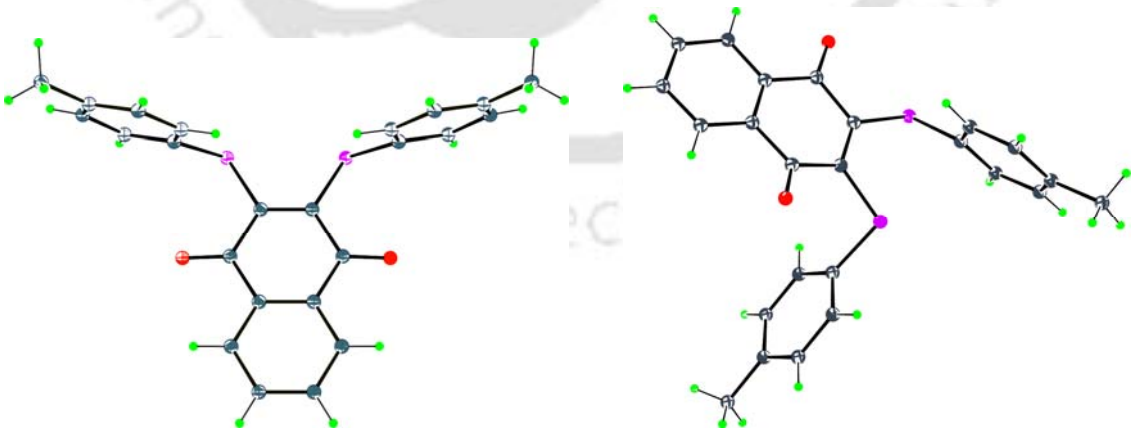

Polymorph 3.1A; *Syn* orientation **Polymorph 3.1B; *Anti* orientation**

Fig. 3.2 Crystal structure of polymorphs of **3.1** (ORTEP drawn with 30% thermal ellipsoid)

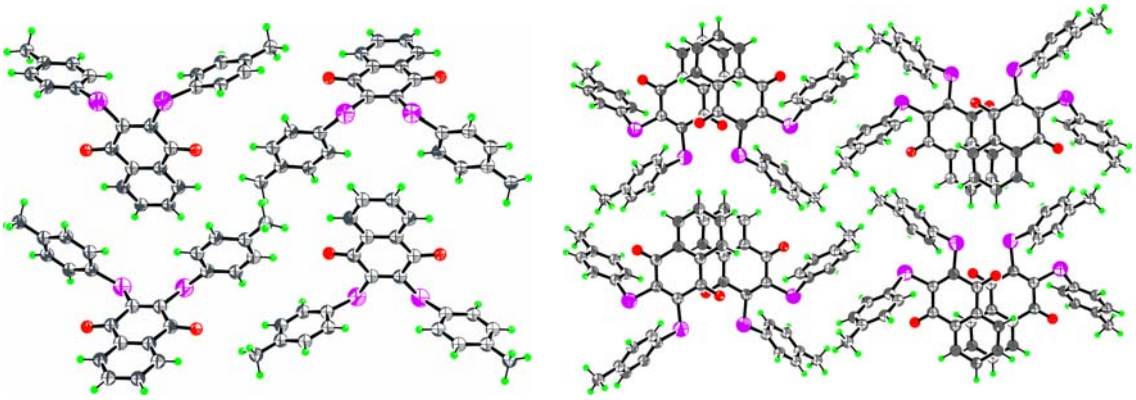

a b

Fig. 3.3 Packing pattern structure of a) polymorph **3.1A**; b) polymorph **3.1B** (ORTEP drawn with 50% thermal ellipsoid)

The polymorph **3.1A** crystallizes in the centrosymmetric Pnma space group and is highly symmetric molecule. The two *p*-methylphenylsulfanyl groups are *syn* to each other with respect to the quinone ring. Both the 4-methylphenyl groups are placed away from the quinone ring (out of the plane of the quinone ring) and are almost perpendicular. The packing pattern of the molecule are decided by the C-H···O (C10-H10···O1; $d_{D\cdots A}$, 3.39 Å, and <D-H···A 130.3º and C-H···π (C7-H7···π_{C8}; *d* = 2.866 Å) interactions as shown in **fig. 3.4**. The methyl hydrogen of the *p*-methylphenyl group are involved in C-H···O interactions. These weak interactions leads to an infinitely extended 1D hydrogen bonded network.

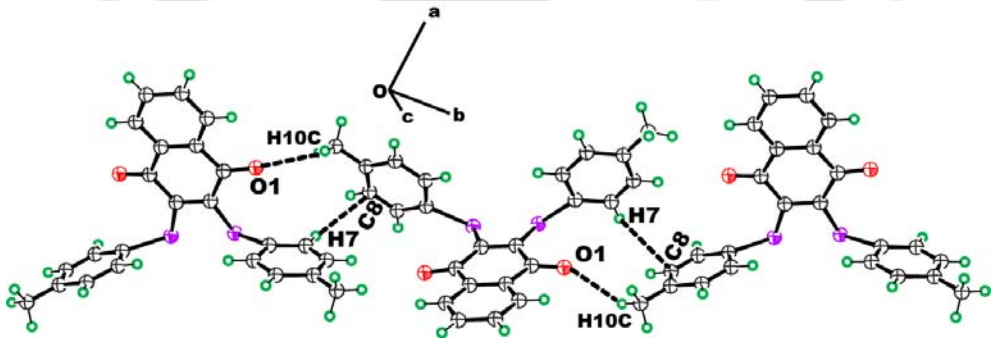

Fig. 3.4 Weak interactions of polymorph **3.1A** (ORTEP drawn with 50% thermal ellipsoid)

Polymorph **3.1B** crystallizes in non-centrosymmetric space group $C222_1$. In the case of polymorph **3.1B**; two tolylsulfanyl groups are anti to each other with respect to the rigid quinone ring. One of the *p*-methylphenyl ring is placed away from the carbonyl–

C(1)=O(1) of the quinone ring (out of the plane of the quinone ring) while the other *p*-methylphenyl ring is placed toward the carbonyl –C(8)=O(2) of the quinone ring.

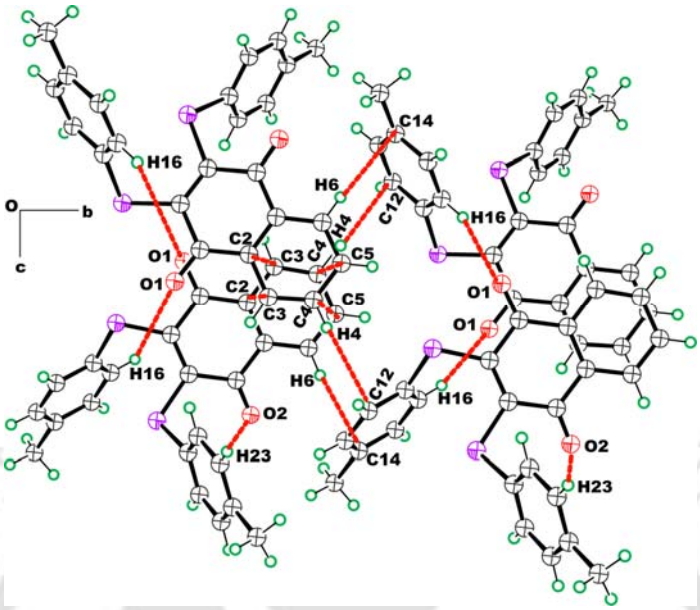

Fig. 3.5 Weak interactions of polymorph **3.1B** (ORTEP drawn with 50% thermal ellipsoid)

In the crystal lattice of polymorph **3.1B**, the methyl hydrogen atoms of the *p*-methylphenyl groups do not participate in weak interactions but in the case of polymorph **3.1A**, methyl groups participate in weak interactions. The lattice is mainly stabilized by the C−H····O (C16−H16····O1; $d_{D\cdots A}$, 3.465 Å, and <D-H····A 162.6º and C23−H23····O2; $d_{D\cdots A}$, 3.409 Å, and <D-H····A 164.3º), C7−H7···π (C4−H4···π_{C12}; *d* = 2.835 Å and C6−H6···π_{C14}; *d* = 2.803 Å) and π···π (between two aromatic benzene ring of 1,4-naphthoquinone) interactions as shown in **fig. 3.5**.

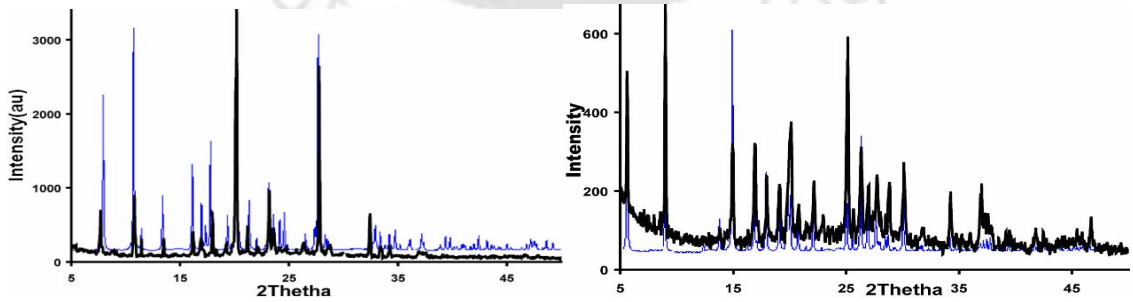

a b

Fig. 3.6 Powder diffraction pattern of polymorphs a) **3.1A**; b) **3.1B** (black line = experimental; blue line = theoretical)

The powder X-ray pattern of the samples was recorded to show the distinctions between the two polymorphs. Powder diffraction patterns of the two polymorphs have different peaks indicating their differences. When the powder X-ray diffraction patterns of the polymorphs **3.1A** and **3.1B** are compared with their theoretical patterns, there is a good agreement between them as shown in **fig. 3.6** (black line = experimental; blue line = theoretical). Both the polymorphs **3.1A** and **3.1B** have identical ^{1}H NMR, ^{13}C NMR signals, IR signals and electronic spectra in solution.

We also determined the crystal structure of 2,3-*bis*-*p*-methoxyarylsulfanyl 1,4-naphthoquinone **3.2**. The compound **3.2** was crystallized in *syn* orientation of the substituent *p*-methoxyarylsulfanyl groups with respect to quinone (**fig.3.7a**). We could not crystallize other polymorphs from different solvents such as methanol, ethanol, acetonitrile, dichloromethane, ethyl acetate, chloroform etc at varieties of crystallization conditions. The compound **3.2** is stabilized by C-H···O (C3-H3···O3, $d_{D\cdots A}$, 3.546 Å, <D-H····A 170.1º; C19-H19···O4, $d_{D\cdots A}$, 3.537 Å, <D-H····A 162.6º and C22-H22A···O2, $d_{D\cdots A}$, 3.415 Å, <D-H····A 169.0º) and C-H···π (C14-H14···π_{C4}; *d* = 2.839 Å and C15-H15···π_{C13}; *d* = 2.748 Å) interactions as shown in **fig.3.7b**.

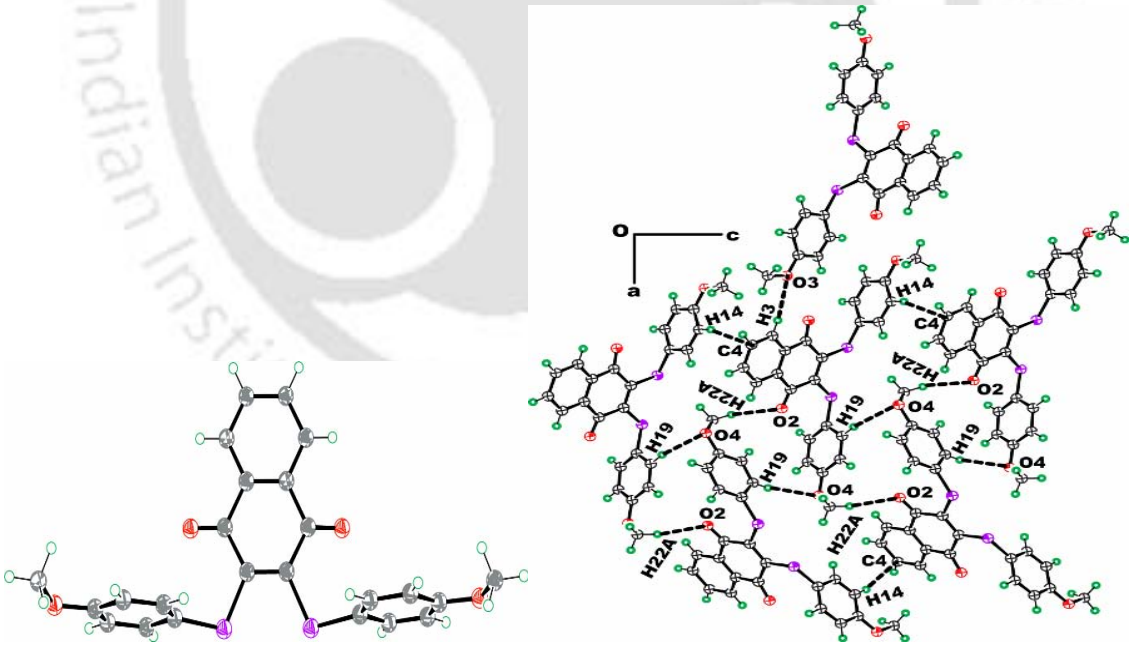

a b

Fig. 3.7 a) Crystal structure of compound **3.2**; b) Self assembly of compound **3.2** (ORTEP drawn with 50% thermal ellipsoid)

In this compound also the sulphur atoms are not involved in weak interactions. One of the oxygen atom (O1) of the two carbonyl groups of 1,4-naphthoquinone also does not participate in weak interactions.

The crystal structures of various structurally related diols derivatives (compounds **3.3-3.5**; **fig. 3.8**) are also determined. In all the cases, the two hydrogens attach to the two hydroxyl groups are oriented towards the arylsufanyl groups attach to the quinone. In the compound **3.5**, we found *anti* conformation but *syn* conformations are observed for the compounds **3.3-3.4** (**fig. 3.8**).

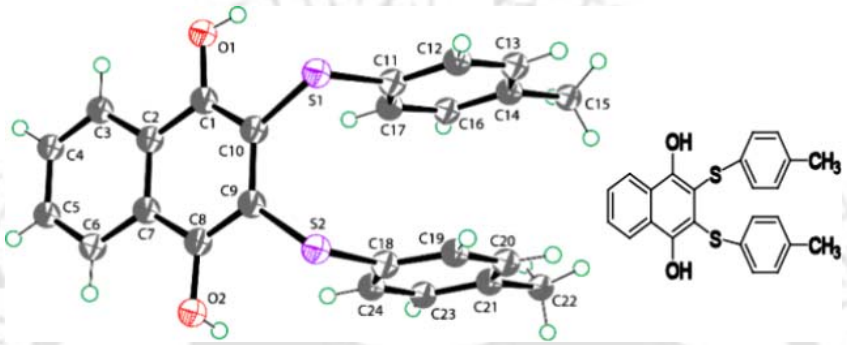

3.3

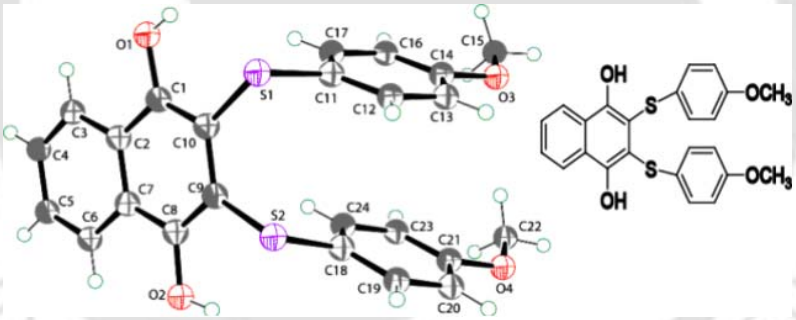

3.4

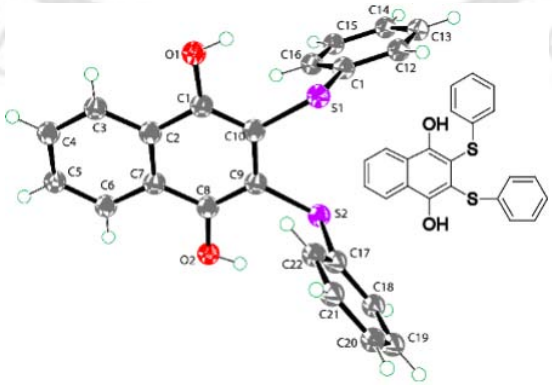

3.5

Fig. 3.8 Crystal structure of compounds **3.3-3.5** (ORTEP drawn with 50% thermal ellipsoid)

From these crystal structures it is clear that that there are two types of conformation via the orientation (compounds **3.1-3.5**) of the two arylsulfanyl groups in *anti* or *syn* with respect to the naphthalene ring. So we performed Density Functional Theory (DFT) calculations to investigate the ground state electronic structure of compounds **3.1-3.5** for both the possible conformations. Details of the optimized energy of compounds **3.1-3.5** at the B3LYP/6-31++G** level of theory are shown in **table 3.1**.

Table 3.1 Optimized energy calculation on compounds **3.1-3.5**

Compounds	Energy (E) in Hartree	Energy (E) in Kcal/mol	Energy Difference, ΔE
3.1 (*syn*)	-1872.28482210	-1174877.4487	0.7457 Kcal/mol
3.1 (*anti*)	-1872.28363520	-1174876.7030	
3.2 (*syn*)	-2022.69957850	-1269264.2125	
3.2 (*anti*)	-2022.69980860	-1269264.3569	0.1444 Kcal/mol
3.3 (*syn*)	-1873.51767500	-1175651.0762	
3.3 (*anti*)	-1873.51984260	-1175652.4364	1.3602 Kcal/mol
3.4 (*syn*)	-2023.93273270	-1270038.0318	
3.4 (*anti*)	2023.93469590	-1270039.2610	1.2292 Kcal/mol
3.5 (*syn*)	-1794.87598390	-1126302.6287	
3.5 (*anti*)	-1794.87810410	-1126303.9591	1.3304 Kcal/mol

Here ΔE = different energy between the *anti* and *syn* conformation

From this **table 3.1** we find that the optimized energies for both the conformations are comparable. The *anti* conformation has slightly lower energy *syn* conformation with difference in energy of about 0.1444 Kcal/mol to 1.3602 Kcal/mol. But the compound **3.1** has lower energy in the *syn* conformation than the *anti* conformation with difference in energy by 0.7457 Kcal/mol. We could crystallize all the *syn* conformers except in compound **3.5**. In the case of **3.5,** *anti* conformer was obtained. Since the

energy differences in each case are very small; we attribute the formation of these isomers to the crystal packing effect rather than the stability of individual isomers. Some of the selected bond distances and angles of compounds **3.1-3.5** are shown in **table 3.2**.

Table 3.2.Selected bond distances (Å) and bond angles (°) for compounds **3.1-3.5**

3.1A				**3.1B**			
Bond	Distances	Bond	Angles	Bond	Distances	Bond	Angles
S1-C5	1.71(8)	C7-C6-C12	120.1(5)	S2-C9	1.762(3)	C9-S2-C18	102.3(15)
S1-C6	1.96(7)	C7-C6-S1'	110.9(5)	S2-C18	1.786(3)	C10-S1-C11	105.0(17)
S1-S′1	2.49(12)	C12-C6-S1'	129.0(5)	S1-C10	1.742(4)	C12-C11-S1	119.4(4)
S1'-C6	1.576(9)	C7-C6-S1	123.7(5)	S1-C11	1.774(4)	C9-C10-S1	125.7(3)
S1'-C5	1.858(8)	C12-C6-S1	115.2(4)	C11-C12	1.372(5)	C1-C10-S1	114.9(2)
C6-C7	1.367(7)	O1-C4-C5	120.3(4)	C16-C11	1.393(6)	C9-C10-C1	119.4(3)
C6-C12	1.384(6)	O1-C4-C3	121.4(4)	C10-C9	1.357(4)	O2-C8-C7	120.1(3)
C4-O1	1.212(5)	C3-C3′-C4	120.5(2)	C10-C1	1.516(5)	O2-C8-C9	121.4(3)
C3-C4	1.474(6)	C4-C5-S1'	109.0(4)	C8-O2	1.209(4)	C16-C11-S1	122.0(3)
C5-C4	1.486(6)	C5-C5'-S1'	129.3(2)	C8-C7	1.469(4)	C10-C9-C8	120.5(3)
C9-C10	1.380(11)	C4-C5-S1	128.7(4)	C8-C9	1.506(4)	C10-C9-S2	122.1(3)
C5-C'5	1.330(8)	C5-C5′-S1	109.9(2)	C1-O1	1.215(4)	C8-C9-S2	117.2(2)
Bond	Angles	C5-C5'-C4	120.9(2)	C1-C2	1.474(5)	O1-C1-C2	122.8(3)
C5-S1-C6	98.6(3)	C6-S1'-C5	108.1(4)	C18-C24	1.375(5)	O1-C1-C10	118.4(4)
C5-S1-S1	70.1(2)	C6-S1-S1	144.5(2)	C18-C19	1.373(4)	C2-C1-C10	118.7(3)
				Bond	Angles	C3-C2-C1	119.3(3)
				C24-C18-S2	121.0(3)	C19-C18-S2	119.4(3)

3.2				**3.3**			
Bond	Distances	Bond	Angles	Bond	Distances	Bond	Angles
S1-C10	1.758(2)	C10-S1-C11	106.9(10)	S1-C11	1.770(4)	C11-S1-C10	105.1(15)
S1-C11	1.783(2)	C9-S2-C18	107.7(10)	S1-C10	1.771(3)	C9-S2-C18	102.7(16)
S2-C9	1.756(2)	C19-C18-S2	120.8(17)	S2-C9	1.767(3)	O1-C1-C2	114.0(3)
S2-C18	1.779(2)	C24-C18-S2	119.1(18)	S2-C18	1.770(4)	C3-C2-C1	122.5(3)
O1-C1	1.218(2)	C10-C9-C8	121.1(19)	C7-C8	1.406(4)	C7-C2-C1	118.4(3)
O2-C8	1.209(2)	C10-C9-S2	117.2(16)	C10-C1	1.353(4)	C8-C9-S2	118.8(2)
C18-C24	1.367(3)	C8-C9-S2	121.3(14)	C2-C1	1.433(4)	C10-C9-S2	122.2(2)
C18-C19	1.418(4)	O2-C8-C9	122.1(2)	C10-C9	1.446(4)	C8-C7-C2	118.4(3)
C11-C17	1.375(2)	O2-C8-C7	120.0(19)	C18-C24	1.368(5)	C1-C10-C9	119.6(3)
C11-C12	1.416(3)	C9-C8-C7	117.9(17)	C18-C19	1.384(5)	C1-C10-S1	118.9(2)

C9-C10	1.367(3)	O1-C1-C10	122.3(2)	C11-C17	1.373(5)	C9-C10-S1	121.2(3)
C9-C8	1.487(3)	O1-C1-C2	119.57(19)	C11-C12	1.378(5)	C19-C18-S2	123.7(3)
C8-C7	1.491(3)	C12-C11-S1	118.75(18)	C8-C9	1.370(4)	C24-C18-S2	117.4(3)
C2-C1	1.488(3)	C10-C1-C2	118.12(16)	C8-O2	1.380(3)	C17-C11-S1	115.5(3)
C1-C10	1.485(3)	C9-C10-C1	120.86(18)	C1-O1	1.371(3)	C12-C11-S1	124.2(3)
C7-C2	1.396(3)	C9-C10-S1	117.99(16)	C2-C7	1.427(4)	C9-C8-O2	121.2(3)
Bond	Angles	C1-C10-S1	120.41(14)	Bond	Angles	C8-C9-C10	119.0(3)
C17-C11-S1	121.1(15)	C17-C11-C12	119.8(2)	C10-C1-O1	124.1(3)	O2-C8-C7	116.2(3)
C7-C2-C1	119.9(18)			C10-C1-C2	121.9(3)		

3.4				**3.5**			
Bond	Distances	Bond	Angles	Bond	Distances	Bond	Angles
S1-C10	1.7687(19)	C10-S1-C11	104.6(8)	S2-C9	1.7695(15)	C9-S2-C17	103.6(7)
S1-C11	1.7775(18)	C9-S2-C18	102.0(9)	S2-C17	1.7804(17)	C10-S1-C11	103.2(7)
S2-C9	1.777(2)	O1-C1-C10	123.2(18)	S1-C10	1.7668(16)	C18-C17-C22	119.1(17)
S2-C18	1.7808(19)	O1-C1-C2	115.6(18)	S1-C11	1.7830(18)	C18-C17-S2	116.9(13)
C1-O1	1.363(2)	C10-C1-C2	121.1(18)	C17-C18	1.382(2)	C22-C17-S2	124.0(13)
C1-C10	1.370(3)	C1-C10-C9	119.8(18)	C17-C22	1.385(2)	C7-C2-C1	118.3(14)
C1-C2	1.423(3)	C1-C10-S1	118.4(15)	C2-C1	1.421(2)	C10-C1-O1	122.1(15)
C10-C9	1.435(3)	C9-C10-S1	121.6(15)	C1-C10	1.368(2)	C10-C1-C2	121.6(14)
C9-C8	1.368(3)	C8-C9-C10	119.8(18)	C1-O1	1.3699(18)	O1-C1-C2	116.3(14)
C11-C12	1.386(3)	C8-C9-S2	118.7(15)	C11C16	1.382(2)	C1-C10-C9	120.1(15)
C11-C17	1.387(3)	C10-C9-S2	121.5(15)	C11-C12	1.386(2)	C1-C10-S1	118.1(12)
C8-O2	1.371(2)	C12-C11-S1	125.2(14)	C7-C2	1.419(2)	C9-C10-S1	121.8(12)
C8-C7	1.423(3)	C17-C11-S1	115.7(14)	C7-C8	1.427(2)	C2-C7-C8	119.6(14)
C18-C19	1.387(3)	C7-C2-C1	119.1(18)	C8-O2	1.3622(18)	O2-C8-C9	124.2(14)
C18-C24	1.386(3)	C9-C8-O2	123.(2)	C8-C9	1.369(2)	O2-C8-C7	114.8(14)
C14-C13	1.378(3)	C24-C18-S2	119.1(15)	C9-C10	1.441(2)	C9-C8-C7	121.0(13)
Bond	Angles	C24-C18-C19	118.6(18)	Bond	Angles	C16-C11-S1	123.3(13)
C2-C7-C8	118.85(18)	C19-C18-S2	122.3(15)	C8-C9-C10	119.33(14)	C12-C11-S1	117.3(14)
C9-C8-C7	121.31(18)	C12-C11-C17	119.1(16)	C8-C9-S2	119.56(11)	C16-C11-C12	119.4(17)
O2-C8-C7	115.38(18)			C10-C9-S2	121.07(12)		

3.2 Polymorphism in (3-carboxymethylsulfanyl 1,4-dihydroxynaphthalen-2-yl-sulfanyl) acetic acid

The carboxylic acids commonly self assemble through carboxylic groups in $R_2^2(8)$ type of hydrogen bonding.[294] Polycarboxylic acids with flexible groups get self assemble in the lattice through weak interactions. These weak interactions play major role in

polymorphic properties of such compounds.[295] Strong hydrogen bonds such as O−H···O, N−H···O and O−H···N have been extensively used in the area of supramolecular chemistry and crystal engineering. But a number of interactions control molecular recognition,[296-297] self-assembly formation in complex molecules,[298-299] coordination chemistry[300-301] and biological structures.[302-304] Among the weak hydrogen bonding interactions, C−H···O, C−H···π and π···π interactions are well studied. These interactions play versatile role in polymorphism and formation of symmetry non-equivalence in crystal lattice.[305-309] Moreover, it is known that the orientation of lone pair of sulphur plays a major role in packing pattern,[310] for this purpose we have prepared a sulphur containing dicarboxylic acid in which flexible arm of carboxylic acids are attached to sulphur atoms.

The reaction of 1,4-naphthoquinone and thioglycolic acid gave (3-carboxymethyl-sulfanyl 1,4-dihydroxynaphthalen-2-ylsulfanyl) acetic acid **3.6**. Oxidation of compound **3.6** by air gives corresponding quinone compound **3.7** (**fig. 3.9**). Two polymorphs of (3-carboxymethylsulfanyl 1,4-dihydroxynaphthalen-2-ylsulfanyl) acetic acid **3.6** was obtained and characterized.

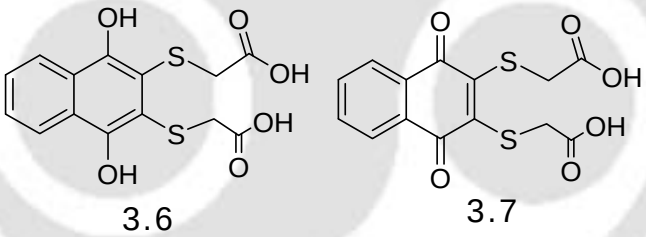

Fig. 3.9

The polymorphs of compound **3.6** were obtained by varying crystallization conditions. One form crystallizes in centrosymmetric Pbcn space group **3.6A** and other in C2/c **3.6B** respectively. Both the polymorphs crystallize as colorless block but the crystals in each case have different shape and size. The polymorph **3.6A** is obtained as the symmetry non-equivalent molecule from crystallization of **3.6** in methanol and water (1:1, v/v ratio), whereas **3.6B** was obtained from careful crystallization from methanolic solution of compound **3.7** while reducing with sodium borohydride in 3:1 molar ratio (**fig. 3.10**).

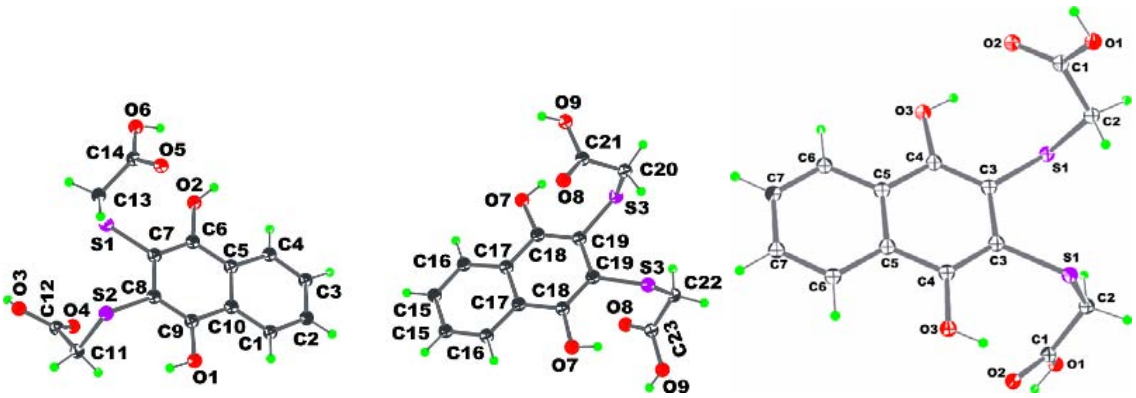

a b

Fig. 3.10 Crystal structure of a) polymorph **3.6A**; b) polymorph **3.6B** (ORTEP drawn with 50% thermal ellipsoid)

In both cases, two carboxylic acid arms are orient in *anti*-planar direction with respect to naphthalene ring for both the molecules. The two polymorphs have independent packing patterns (**fig. 3.11**) and different weak interactions.

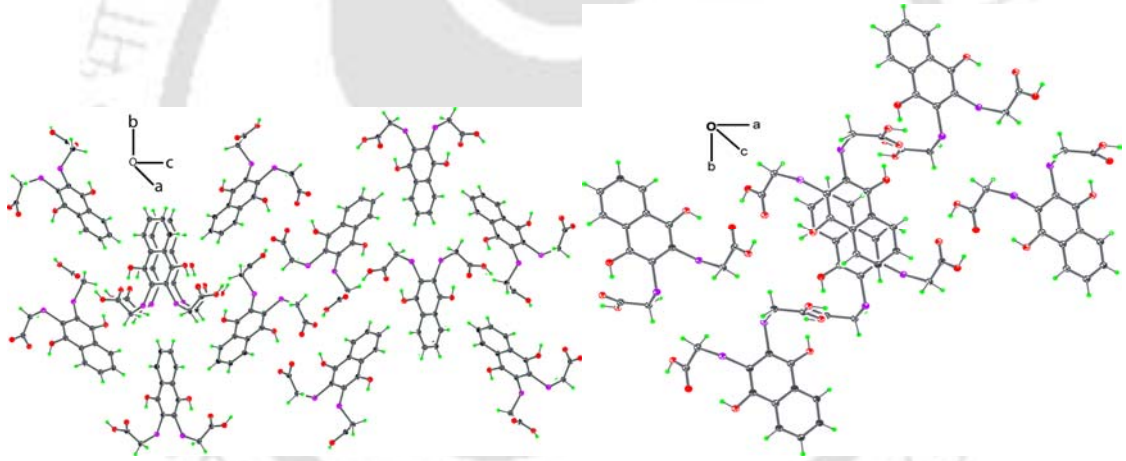

a b

Fig. 3.11 Packing pattern structure of a) polymorph **3.6A**; b) polymorph **3.6B** (ORTEP drawn with 30% thermal ellipsoid)

The polymorph **3.6A** has two symmetrically non-equivalent molecules per unit cell; the asymmetry is caused by the orientation of the lone pairs on sulphur which decides the disposition of the two carboxylic acid groups in space.

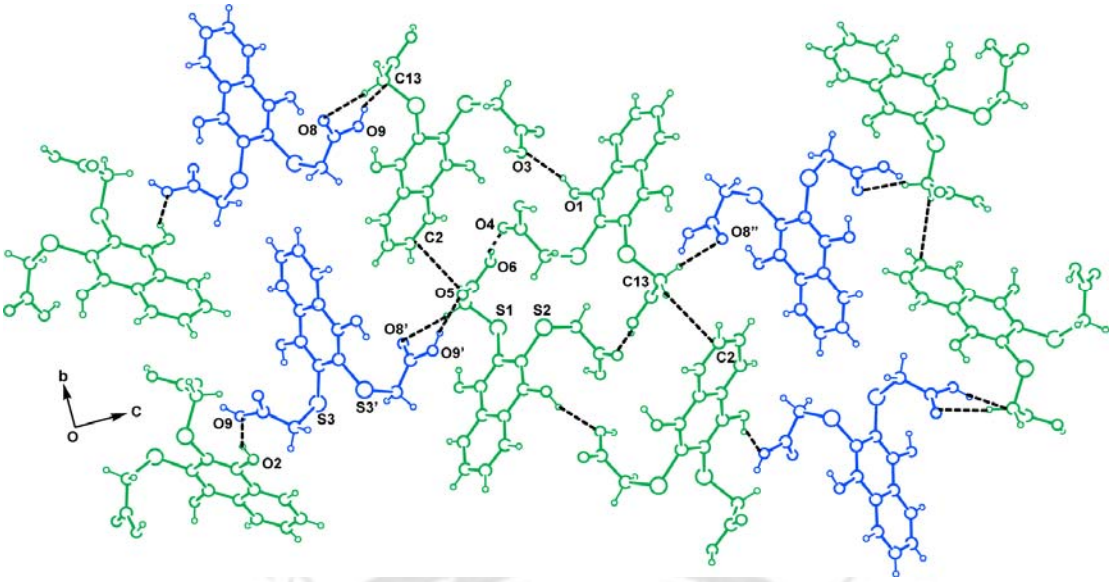

Fig 3.12: Hydrogen bond interactions between the two symmetry independent molecules in polymorph **3.6A**.

Beside this the two hydrogen atoms attached to hydroxyl groups also contributes to the formation of symmetry non-equivalent molecules. In one symmetry independent molecule both the hydrogen atoms are *cis* across the ring while *trans* in the other case (**fig. 3.10**). There is weak C-H···S interactions in this molecule. Two asymmetric units form assembly in its lattice mainly through O–H···O and C-H···O interactions.

Each of the symmetry non-equivalent molecules interacts with each other through weak interactions as illustrated in **fig. 3.12** and **fig. 3.13**. It may also be noted that the projection of the lone pairs of the sulphur atom decides the *anti* orientation of the carboxylic acid groups with respect to each other. The different orientations of carboxylic acids with respect to naphthalene ring provide the basis to make two independent molecules disposed next to each other non-symmetric. Hydroxyl groups of naphthalene ring involve in strong hydrogen bond with oxygen atom of carboxylic acid [O7−H6o···O8, O2−H2o···O9, O9−H9o···O5 interactions]. The sulphur atoms also participate in hydrogen bonding through C21−H21··· S3 (2.90 Å, 165.4°), C13−H13A··· S1 (2.88 Aº, 168.0°) contacts.

Table 3.3. Hydrogen bond geometry (Å, °) for compound **3.6A**				
D−H···A	d (D−H)	d (H···A)	d (D···A)	<D−H···A
O1−H1··· O3 [1/2+x, 1/2-y, -z]	0.82	2.05	2.83(4)	159.9
O2−H2··· O9 [1/2-x, -1/2+y, z]	0.82	2.11	2.83(4)	145.4
O3−H3···O1 [-1+x, y, z]	1.03	2.27	3.22(5)	153.3
O6−H6···O4 [1-x, -y, -z]	0.82	1.89	2.69(4)	166.5
O7−H6···O8 [-1+x, y, z]	0.82	2.18	2.84(4)	137.7
O9−H9···O5 [3/2-x, 1/2+y, z]	0.82	1.87	2.67(4)	168.1
C13−H13A···O8 [3/2-x, -1/2+y, z]	0.97	2.32	3.26(5)	163.7
C13−H13B···O5 [-1+x, y, z]	0.97	2.52	3.24(4)	131.1
O1−H1··· O4	0.82	1.89	2.69	167.8
O6−H6··· O3	0.82	2.07	2.84	156.5
C2−H2B···O2	0.97	2.51	3.24	131.2
C13−H13A···S1	0.97	2.88	3. 84	168.0
C2−H2B···π_{C8}	0.97	2.88	3.49	
O9−H9A··· O8	0.82	2.18	2.85	138.1
C21−H21···S3	0.93	2.90	3.81	165.5

One of the symmetric independent molecules shows the weak interactions through O1−H1···O4, O6−H6···O3, O6−H6···O4, C2−H2B···O2, C13−H13A···S1 and C2−H2B···π_{C8} among the same symmetric independent molecules as shown in **fig. 3.13a**. Other symmetric independent molecule also forms the weak interaction through O9−H9A···O8 and C21−H21···S3 between the same symmetric molecules as shown in **fig. 3.13b**. Hydrogen bonding parameters for polymorph **3.6A** are listed in **table 3.3**.

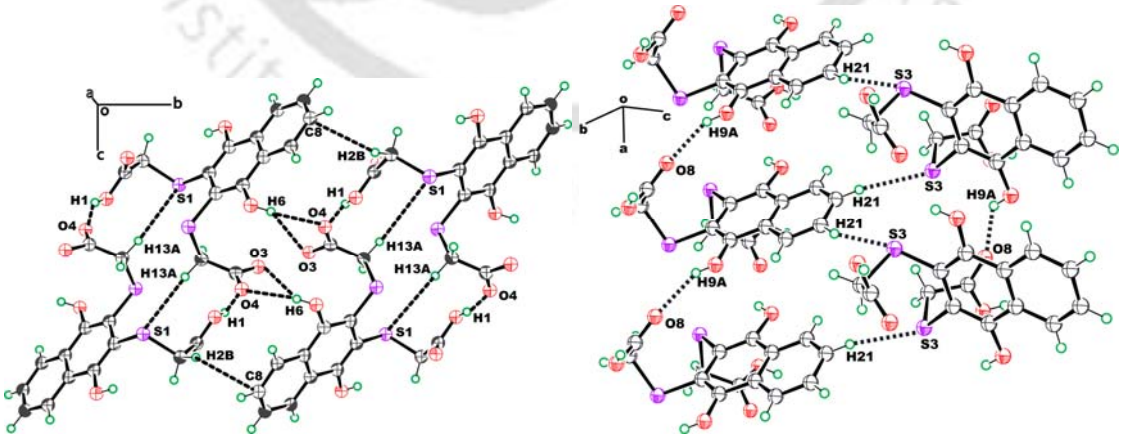

a b

Fig. 3.13 Self assembly structure of polymorph **3.6A** between same symmetric independent molecules (ORTEP drawn with 50% thermal ellipsoid)

In the polymorph **3.6B** both the hydrogen atoms of hydroxyl groups are *cis* and oriented towards the sulfanyl carboxylic acids groups (**fig. 3.10b**). The polymorph **3.6B** is stabilized by the strong hydrogen bond. The carboxylic acid units are involved in O−H···O strong hydrogen bonding with basic set $R_2^2(8)$ (**fig. 3.14a**). Such type of strong hydrogen bonding was not found in the polymorph **3.6A**. On contrary to polymorph **3.6A**, the sulphur atoms are not involved in weak interactions. The crystal packing is governed through strong O–H···O (O1−H1···O2 and O3−H3···O2) and weak C–H···O (C2−H2B····O1 and C7−H7····O1) and C−H···π (C7−H7···π_{C1}) interactions which results in an infinitely extended 3D hydrogen bonded network in the crystal lattice (**fig. 3.14b**).

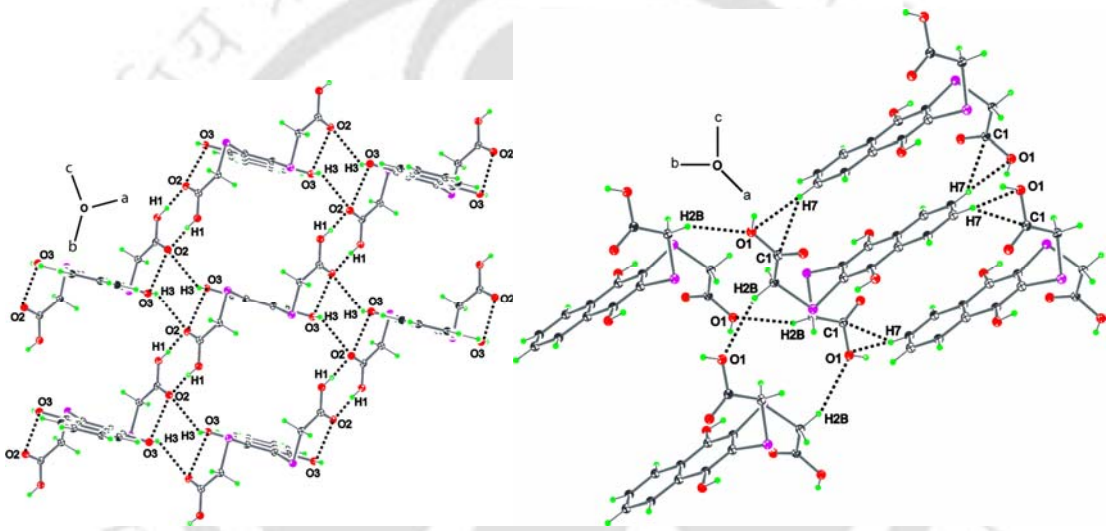

Fig. 3.14 Self assembly structure of polymorph **3.6B** (ORTEP drawn with 30% thermal ellipsoid)

Table 3.4 Hydrogen bond geometry (Å, °) for polymorph **3.6B**				
D−H····A	d(D−H)	d(H···A)	d(D···A)	<D−H···A
O1−H1··· O2	0.819	1.866	2.681	174.0
O3−H3··· O2	0.808	2.547	3.056	122.2
C2−H2B····O1	0.971	2.601	3.510	156.0
C7−H7····O1	0.930	2.719	3.627	165.7
C7−H7···π_{C1}	0.930	2.801	3.622	
O1−H1···π_{C1}	0.819	2.769	3.545	

Hydroxyl group of naphthalene ring is also involved in strong hydrogen bonding with oxygen atom of carboxylic acid (O3−H3···O2 interaction). Some of the important hydrogen bond parameters for the compound **3.6B** are given in **table 3.4**. The two polymorphs have different powder pattern (black line = experimental; blue line = theoretical) which shows the bulk purity of the two polymorphs and have different phases as shown in **fig. 3.15**.

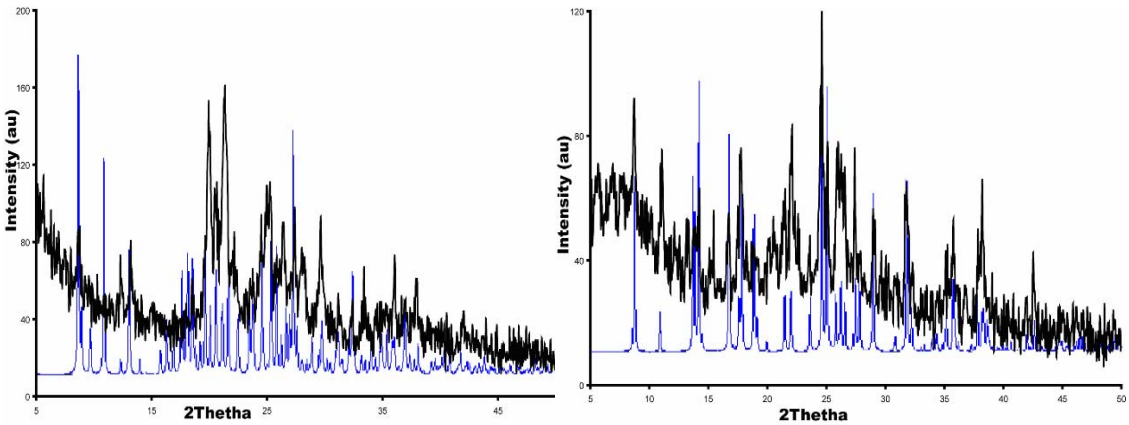

a b

Fig. 3.15 Powder diffraction pattern of polymorphs a) **3.6A**; b) **3.6B** (black line = experimental; blue line = theoretical)

From the hydrogen bonding shown in **fig. 3.12-3.14**, it is clear that these polymorphs are the result of different packing pattern having different types of weak interactions. In addition to this the different in orientations of the two hydrogen atoms attached to the hydroxyl groups are also cause the polymorphism.

3.3 Polymorphism and structure of few dithiolate bridged di-2-methyl 1,4-naphthoquinone derivatives

There are examples on structural studies on spiral V-shaped molecules[311] derived from naphthoquinone; but, the polymorphism arising from orientations of functional groups at distant sites flexible tether needs further attention. To understand the role of flexible tethers bridging naphthoquinone units, a series of compounds **3.8-3.10** were prepared and their crystal structures were determined (**fig. 3.16**; for detail of synthesis please considers the **chapter 2**). Crystallization of dithiolate bridged di-2-methyl 1,4-naphthoquinone **3.8** from varying crystallization condition, it gave two polymorphs.

One of which crystallizes in C2/c and other in P-1 space group and are designated as **3.8A** and **3.8B** respectively.

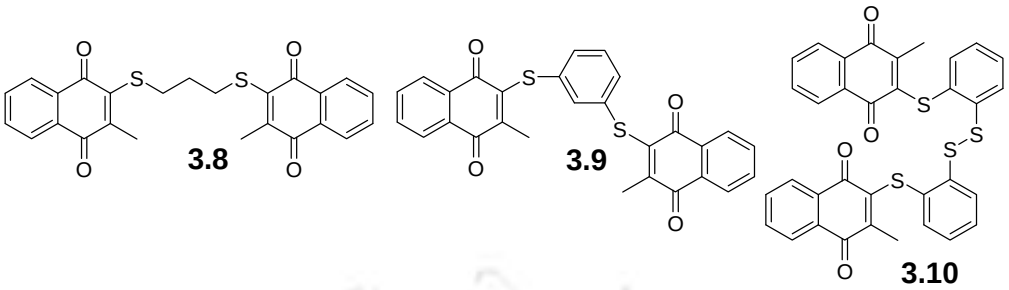

Fig. 3.16

The polymorph **3.8A** is obtained from simple crystallization of **3.8** from methanol, whereas **3.8B** is obtained from the crystallization from methanolic solution of **3.8** with 1, 4-dihydroxybenzene (1:1 molar ratio). The difference in crystallization is attributed to charge transfer interactions of quinonic part with hydroquinone. Two polymorphs are mirror image of each other (**fig.3.17**). The two polymorphs have different packing patterns with different weak interactions (**fig. 3.18**).

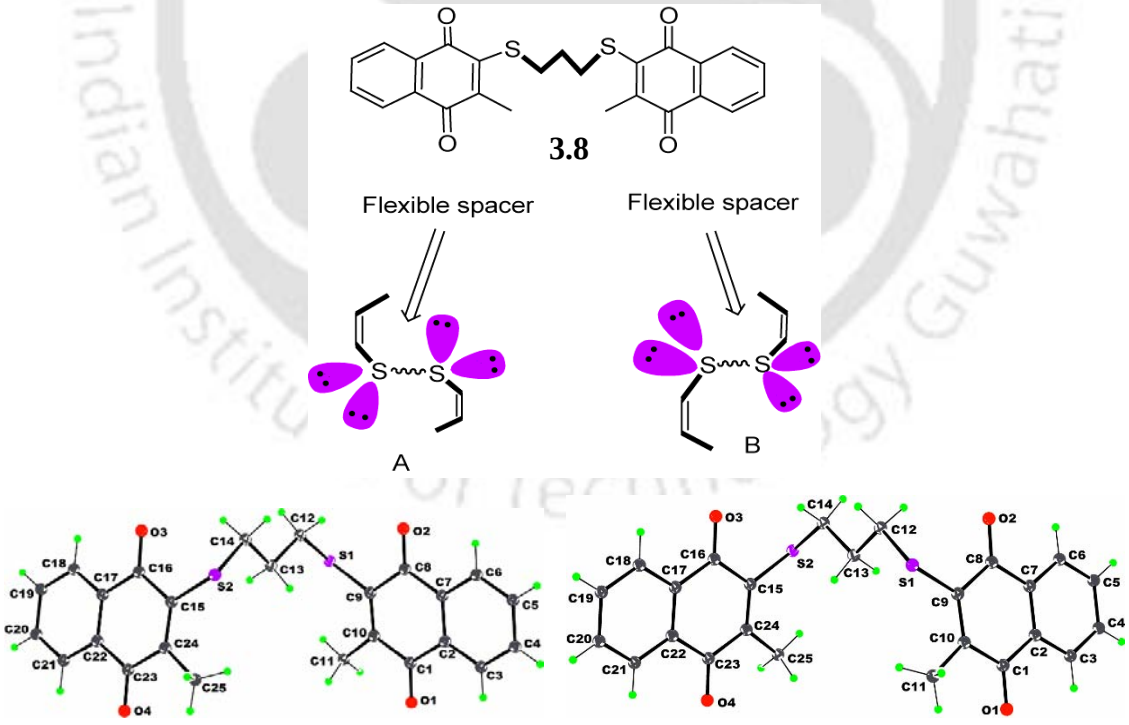

3.8A **3.8B**

Fig. 3.17 polymorphs of compound **3.8 (3.8A and 3.8B)**

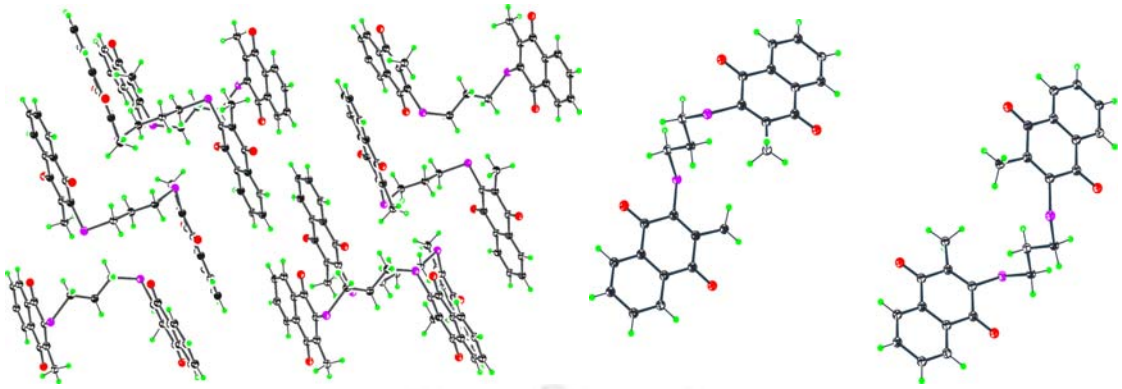

a b

Fig. 3.18 Packing patterns of two polymorphs of compound **3.8** a) **3.8A**; b) **3.8B** (ORTEP drawn with 30% thermal ellipsoid)

In both the cases, they are stabilized by very weak C-H···O interactions. In the polymorph **3.8A** it is the C11-H11A···O3 ($d_{D\cdots A}$, 3.472 Å, and <D-H····A 161.5º) and C13-H13A···O1 interactions ($d_{D\cdots A}$, 3.581 Å, and <D-H····A 151.2º) as shown in **fig. 3.19**. Whereas in the case of polymorph

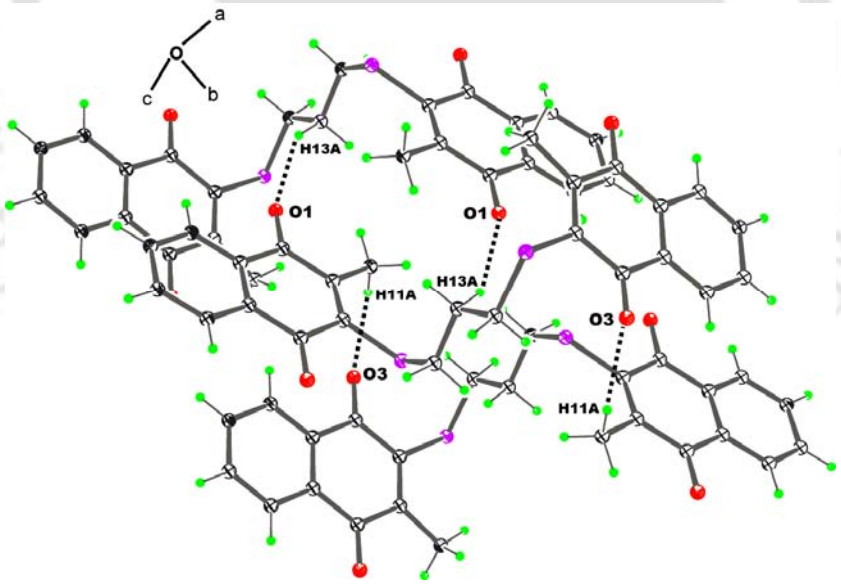

Fig. 3.19 Weak C-H···O interactions of polymorph **3.8A** (ORTEP drawn with 50% thermal ellipsoid)

3.8B it is weak C18−H18····O1, C14-H14B···O2, C25−H25C····O2, C3−H3····O3, C11−H11B····O3, and C11−H11A····O4 interactions as shown in **fig. 3.20**. Some of the prominent hydrogen bond geometry of the polymorph **3.8B** is given in **table 3.5**.

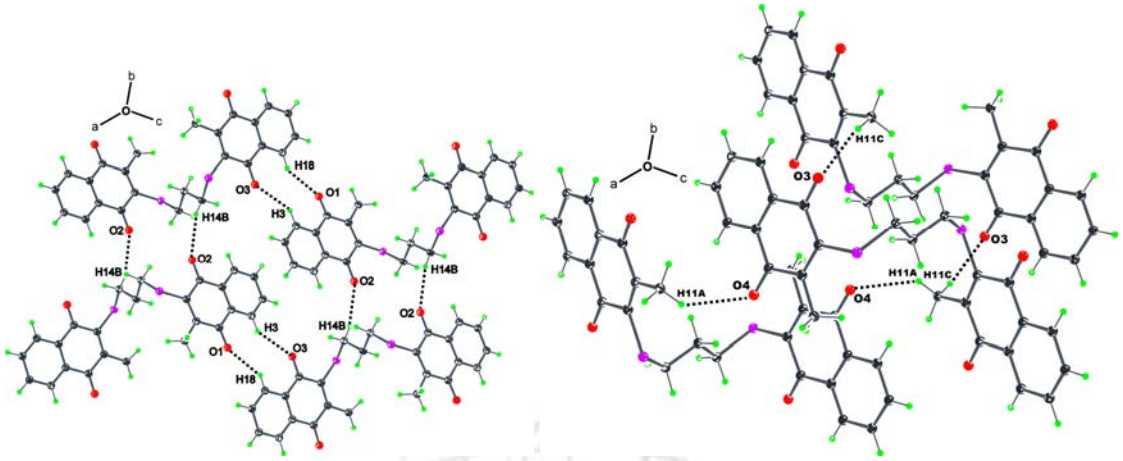

Fig. 3.20 Weak C-H···O interactions of polymorph **3.8B** (ORTEP drawn with 30% thermal ellipsoid)

In both the polymorphs the sulphur atoms are not involved in any weak interactions. The three methylene groups in the molecules have similar conformations; each of them is staggered with respect to the adjacent methylene groups.

Table 3.5 Hydrogen bond geometry (Å,°) for polymorph **3.8B**				
D−H····A	d(D−H)	d(H···A)	d(D···A)	<D−H···A
C18−H18····O1	0.930	2.497	3.306	145.5
C14−H14B····O2	0.971	2.652	3.451	139.8
C25−H25C····O2	0.960	2.704	3.654	170.4
C3−H3····O3	0.930	2.504	3.310	145.1
C11−H11B····O3	0.960	2.597	3.515	160.1
C11−H11A····O4	0.959	2.679	3.457	138.5

The torsion angles among different planes including different bonds containing the sulphur atoms are similar in two molecules. Some of the torsion angles are listed in **table 3.6**. The two polymorphs can be distinguished by their powder X-ray diffraction patterns (black line = experimental; blue line = theoretical). It shows the bulk purity of two polymorphs and they have different phases (**fig.3.21**).

Table 3.6 Torsion angles in the two molecules of compound **3.8** in polymorphs **3.8A** and **3.8B** (**fig. 3.17**)

Polymorph 3.8A		**Polymorph 3.8B**	
Bonds	Angle(º)	Bonds	Angle(º)
C12- S1-C9-C10 C12-S1-C9-C8	129.0(15) -58.5(15)	C12-S1-C9-C10 C12-S1-C9-C8	131.9(2) -57.6(2)
C8-C9-C10-C1	6.4(3)	C8-C9-C10-C1	6.5(4)
S1-C9-C10-C1	178.6(13)	S1-C9-C10-C1	176.7(2)
C8-C9-C10-C11	-174.7(16)	C8-C9-C10-C11	-174.3
S1-C9-C10-C11	-2.4(3)	S1-C9-C10-C11	-4.2(4)
O1-C1-C10-C9	178.1(18)	O1-C1-C10-C9	174.3(3)
C9-S1-C12-C13	-63.0(14)	C9-S1-C12-C13	-67.3(2)
C15-S2-C14-C13	-70.6(13)	C15-S2-C14-C13	-70.2(2)
C14-S2-C15-C24	125.2(14)	C14- S2-C15-C24	125.8(3)
C14- S2-C15-C16	-61.6(14)	C14-S2-C15-C16	-61.7(2)
C24-C15-C16-C17	-5.2(2)	C24-C15-C16-C17	-4.8(4)
S2-C15-C16-C17	-178.4(12)	S2 C15- C16 -C17	177.3(2)
S1-C12-C13-C14	-173.4(11)	S1-C12-C13-C14	169.7(19)
C12-C13-C14-S2	-176.2(11)	C12-C13-C14 -S2	178.9(19)

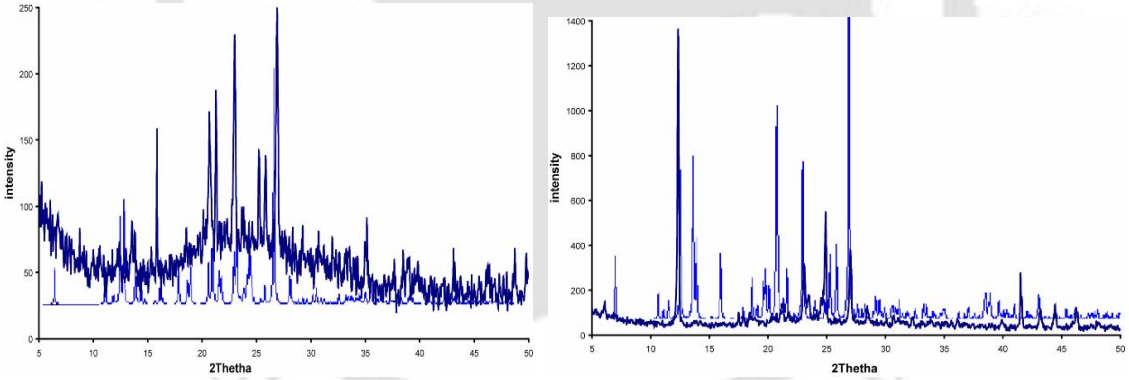

a b

Fig. 3.21 Powder pattern of polymorph a) **3.8A**; b) **3.8B** (black line = experimental; blue line = theoretical)

In the differential scanning calorimetry (DSC) we have observed that the two polymorphs transform to amorphous form at different temperatures. The polymorph **3.8A** transforms at 112º C; whereas the polymorph **3.8B** transforms at 130º C (**fig. 3.22**) when the sample were heated at a rate of 5º C increment per minute. At this heating rate we could see that the endothermic peak of **3.8B** has a shoulder which is not distinct (**fig. 3.22b**).

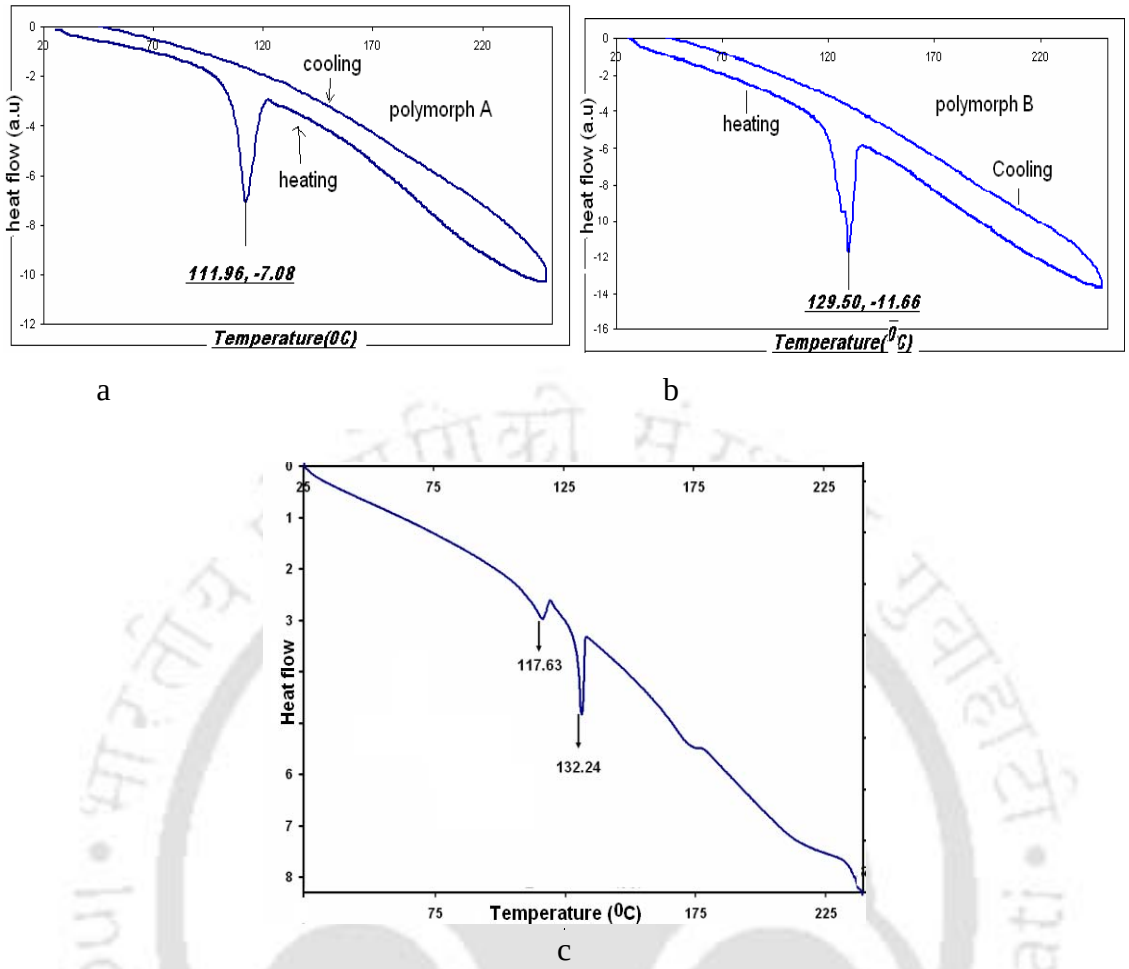

Fig. 3.22 DSC of polymorph of **3.8**, a) Polymorph **3.8A** (5º C/minute heating rate); b) Polymorph **3.8B** (5º C/minute heating rate); c) Polymorph **3.8B** (1º C/minute heating rate)

However, once the sample **3.8B** was heated at a slow heating rate namely 1º C increment per minute, we observed two distinct endothermic peaks at 117º C and 132º C (**fig. 3.22c**). This observation is indicative of solid state transformation of **3.8B** while heating, and followed by its conversion to amorphous phase. At a high heating rate such change is difficult to find out. Further to this, both the polymorphs once transforms to the amorphous state from crystalline state, the states are not reversible on cooling. Both the polymorphs have identical ^{1}H NMR and ^{13}C NMR signals in solution and are also can not be distinguished from the FT-IR spectra.

From the hydrogen bond shown in **fig. 3.19** and **fig. 3.20**, it is clear that these polymorphs are result of two different packing patterns with different weak C-H···O interactions arising from carbonyl oxygen with CH_2- group of propane unit as well as

the CH_3- groups of 2-methyl 1,4-naphthoquinone of a neighboring molecules. The structure of the 1,3-propanedithiolate bridged di-2-methyl 1,4-naphthoquinone **3.8** is compared with similar derivatives having 1,3-dithiolbenzene bridge **3.9** and di-2-methyl 1,4-naphthoquinone derivatives with two 1,2-dithiolato benzene units that are anchored by disulphide linkage **3.10**.

We have also determined the crystal structure of compound **3.9** (**fig. 3.23**). We could not obtain other polymorphic forms by crystallization from different solvents such as methanol, ethanol, acetonitrile, dimethylformamide, DMSO etc.

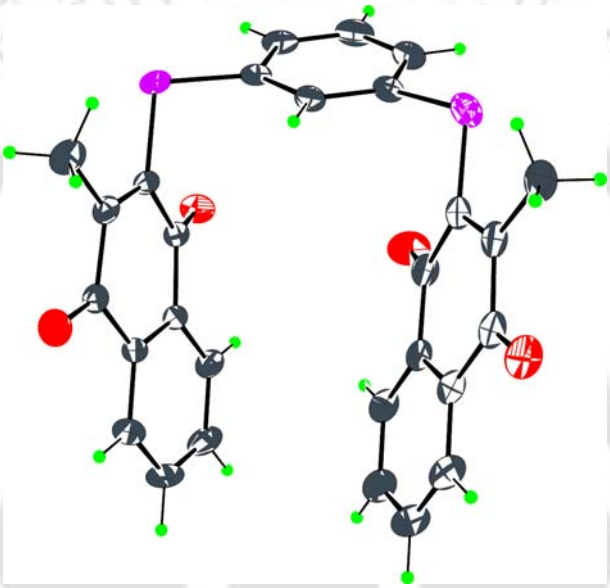

Fig. 3.23 Crystal structure of compound **3.9** (ORTEP drawn with 50% thermal ellipsoid)

The compound **3.8** and **3.9** are different in terms of spacers between the 2-methyl 1,4-naphthoquinone rings. The compound **3.8** has flexible 1,3-propanedithiolate bridged spacer (**fig. 3.17**) while the compound **3.9** has rigid 1,3-dithiolbenzene bridge spacer (**fig. 3.23**). In compound **3.9** due to rigid aromatic spacer, it adopts an arrangement such that both the substituents (namely methyl-naphthoquinone parts) attached to the sulphur are *syn* to each other. Whereas, due to flexibility of the three intervening methylene groups in the case of **3.8** the substituent groups attached to sulphur atoms are *anti* to each other. The compound **3.9** was crystallized from *N,N'*-dimethylformamide as yellow block in centrosymmetric P-1 space group. In the crystal lattice of this molecule the overall molecular structure is influenced by the weak intermolecular C–H···O

(C17−H17····O1, C28−H28B····O2, C15−H15····O3 and C21−H21····O4) interaction and relatively very weak C−H···S (C23−H23····S2) interaction (**fig. 3.24**). In this molecule **3.9** all the four oxygen atoms are involved in weak C−H···O interactions. Some of the hydrogen bond parameters are listed in **table 3.7**.

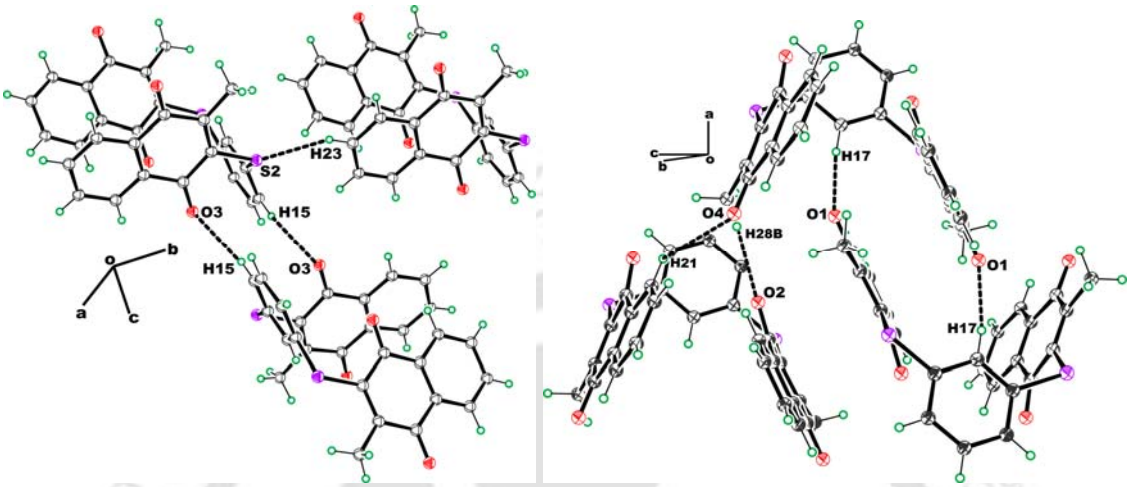

Fig. 3.24 Self assembly of compound **3.9** (ORTEP drawn with 30% thermal ellipsoid)

Table 3.7 Hydrogen bond geometry (Å,°) for compound **3.9**

D−H····A	d(D−H)	d(H···A)	d(D···A)	<D−H···A
C17−H17····O1	0.930	2.685	3.573	159.9
C28−H28B····O2	0.960	2.511	3.693	128.3
C15−H15····O3	0.930	2.561	3.438	157.4
C21−H21····O4	0.930	2.552	3.314	139.4
C23−H23····S2	0.931	2.842	3.712	156.1

Another crystal structure of structurally related molecule **3.10** is also studied. In this case we could obtain only one form by crystallization from different solvents such as methanol, ethanol, acetonitrile, dimethylformamide, DMSO etc.

The compound **3.10** has a self-assembled structure through weak interactions (**fig. 3.25a**). The compound is highly symmetric; and two halves of the molecules bisected at the center of S-S bond; such halves are related by a C_2 axis of symmetry.

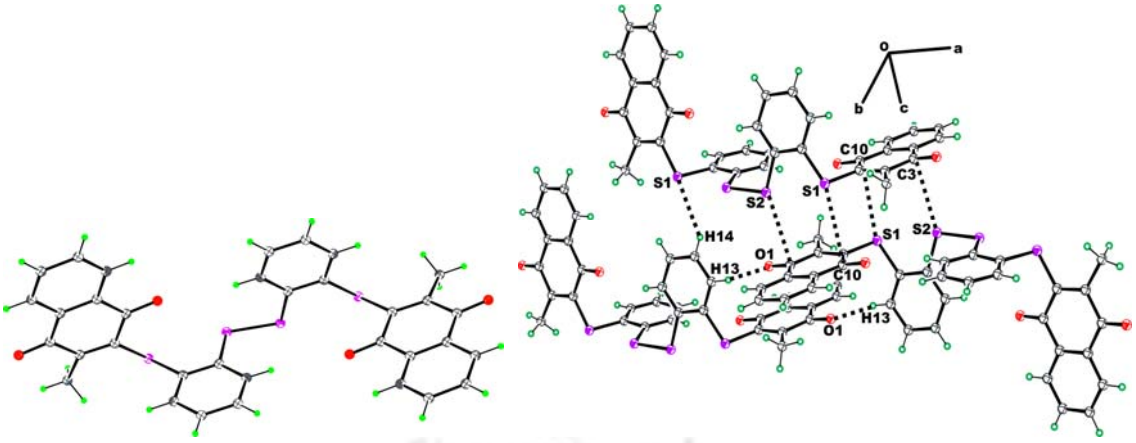

a b

Fig. 3.25 a) Crystal structure of compound **3.10**; b) Self assembly of compound **3.10** (ORTEP drawn with 30% thermal ellipsoid)

The crystal packing is governed mainly through weak S···π (S2····C3, 3.316 Å and S1····C10, 3.498 Å) interactions. In addition to these, the C13-H13····O1 ($d_{D\cdots A}$, 3.283 Å, and <D-H····A 170.1º) and C14−H14···S1 ($d_{D\cdots A}$, 3.667 Å, and <D-H····A 137.5º) weak interactions are also found in crystal lattice as illustrated in **fig. 3.25b**.

The crystal data and refinement parameters of compound **3.1-2.10** are listed in **table 3.8**.

Table 3.8 Crystallographic parameter of compounds **3.1-3.6** and **3.8-3.10**

Compound No.	**3.1A**	**3.1B**	**3.2**	**3.3**
Formulae	$C_{24}H_{18}O_2S_2$	$C_{24}H_{18}O_2S_2$	$C_{24}H_{18}O_4S_2$	$C_{24}H_{20}O_2S_2$
Mol. wt.	402.50	402.50	434.50	404.52
Crystal system	Orthorhombic	Orthorhombic	Orthorhombic	Monoclinic
Space group	Pnma	$C222_1$	$P2_12_12_1$	$P2_1/n$
a (Å)	16.3268(5)	6.7587(2)	42.0988(8)	7.8946(4)
b (Å)	22.0140(8)	19.4871(8)	5.15740(10)	11.2286(6)
c (Å)	5.34810(10)	31.0120(11)	9.3726(2)	21.6646(12)
α/°	90.00	90.00	90.00	90.00
β/°	90.00	90.00	90.00	96.669
γ/°	90.00	90.00	90.00	90.00
V ($Å^3$)	1922.20(10)	4084.5(3)	2034.98(7)	1907.47(18)
Z	4	8	4	4
Density/Mgm^{-3}	1.391	1.309	1.418	1.409
Abs. Coeff. /mm^{-1}	0.295	0.277	0.291	0.297
Abs. correction	none	none	none	none
F (000)	840	1680	904	848
Total no. of reflections	24597	20811	17321	22666
Reflections,I 2σ(I)	2424	5044	4934	4678

Max. 2θ/°	56.56	56.58	56.54	56.70
Ranges (h, k, l)	-21 ≤ h ≤ 19 -29 ≤ k ≤ 26 -7 ≤ l ≤ 7	-6 ≤ h ≤ 8 -25 ≤ k ≤ 25 -41 ≤ l ≤ 41	-56 ≤ h ≤ 53 -6 ≤ k ≤ 6 -12 ≤ l ≤ 12	-10 ≤ h ≤ 10 -14 ≤ k ≤ 14 -28 ≤ l ≤ 28
Completeness to 2θ (%)	99.4	99.7	97.9	98.2
Data/Restraints/Parameters	2424 / 7 /138	5044 / 0 /255	4934 / 0 / 273	4678 / 0 / 257
Goof (F2)	1.025	1.051	1.044	0.897
R indices [I > 2σ(I)]	0.0807	0.0553	0.0406	0.0638
R indices (all data)	0.1780	0.0942	0.0520	0.1671
wR indices	0.2911	0.1758	0.0857	0.2051

Compound No.	**3.4**	**3.5**	**3.6A**	**3.6B**
Formulae	$C_{24}H_{20}O_4S_2$	$C_{22}H_{16}O_2S_2$	$C_{14}H_{12}O_6S_2$	$C_{14}H_{12}O_6S_2$
Mol. wt.	436.52	376.47	340.36	340.36
Crystal system	Monoclinic	Monoclinic	Orthorhombic	Monoclinic
Space group	$P2_1/c$	$P2_1/c$	Pbcn	C2/c
a (Å)	12.3823(4)	13.2090(9)	5.5518(4)	16.7893(7)
b (Å)	29.0900(10)	7.7573(5)	19.8748(14)	12.8194(7)
c (Å)	5.6918(2)	18.7942(12)	39.870(3)	7.1792(3)
α/°	90.00	90.00	90.00	90.00
β/°	92.7910(10)	107.931(4)	90.00	106.152(4)
γ/°	90.00	90.00	90.00	90.00
V (Å^3)	2047.76(12)	1832.2(2)	4399.3(5)	1484.18(12)
Z	4	4	12	4
Density/Mgm^{-3}	1.416	1.365	1.542	1.523
Abs. Coeff. /mm^{-1}	0.290	0.304	0.389	0.385
Abs. correction	none	none	none	none
F(000)	912	784	2112	704
Total no. of reflections	22815	21543	56827	7516
Reflections,I 2σ(I)	5096	4456	5325	1845
Max. 2θ/°	56.66	56.96	56.58	56.58
Ranges (h, k, l)	-16 ≤ h ≤ 16 -38 ≤ k ≤ 38 -7 <= l <= 7	-17 ≤ h ≤ 15 -10 ≤ k ≤ 10 -22 ≤ l ≤ 25	-7 ≤ h ≤ 7 -24 ≤ k ≤ 26 -50 ≤ l ≤ 51	-22 ≤ h ≤ 22 -17 ≤ k ≤ 17 -9 ≤ l ≤ 6
Completeness to 2θ (%)	99.6	96.0	96.9	99.9
Data/Restraints/Parameters	5096 / 0 / 275	4456 / 0 /237	5325 / 0 / 307	1845 / 0 / 100
Goof (F2)	1.019	1.030	1.042	1.044
R indices [I > 2σ(I)]	0.0457	0.0373	0.0587	0.0465
R indices (all data)	0.0769	0.0572	0.1158	0.0613
wR indices	0.1139	0.0968	0.1728	0.1465

Compound No.	**3.8A**	**3.8B**	**3.9**	**3.10**
Formulae	$C_{25}H_{20}O_4S_2$	$C_{25}H_{20}O_4S_2$	$C_{28}H_{18}O_4S_2$	$C_{34}H_{22}O_4S_4$
Mol. wt.	448.53	448.53	482.54	622.76
Crystal system	Monoclinic	Triclinic	Triclinic	Monoclinic
Space group	C2/c	P-1	P-1	C2/c
a (Å)	30.571(6)	9.5248(4)	7.9045(12)	15.6021(16)
b (Å)	8.4467(11)	9.5755(5)	10.4851(17)	10.9530(13)
c (Å)	17.204(4)	13.2177(6)	14.197(2)	18.760(3)

α/°	90.00	93.095(3)	99.744(5)	90.00
β/°	110.393(13)	102.025(3)	93.063(5)	111.225(9)
γ/°	90.00	115.095(3)	99.967(5)	90.00
V (Å^3)	4164.1(14)	1053.89(9)	1138.0(3)	2988.4(7)
Z	8	2	2	4
Density/Mgm^{-3}	1.431	1.413	1.408	1.384
Abs. Coeff. /mm^{-1}	0.287	0.284	0.268	0.356
Abs. correction	none	none	none	none
F(000)	1872	468	500	1288
Total no. of reflections	12964	9647	11964	11977
Reflections,I2σ(I)	3799	5114	5671	2778
Max. 2θ/°	51.00	56.56	57.08	57.06
Ranges (h, k, l)	-36 ≤ h ≤ 36 -9 ≤ k ≤ 10 -20 ≤ l ≤ 20	-12 ≤ h ≤ 10 -12 ≤ k ≤ 12 -17 ≤ l ≤ 17	-10 ≤ h ≤ 10 -13 ≤ k ≤ 14 -18 ≤ l ≤ 19	-18 ≤ h ≤ 17 -13 ≤ k ≤ 13 -22 ≤ l ≤ 22
Completeness to 2θ (%)	98.1	97.7	97.8	99.3
Data/Restraints/Parameters	3799 / 0 /282	5114 / 0 /282	5671 / 0 / 309	2778 / 0 / 191
Goof (F2)	1.013	1.061	1.040	1.036
R indices [I > 2σ(I)]	0.0497	0.0431	0.0490	0.0450
R indices (all data)	0.0995	0.0663	0.0821	0.0625
wR indices	0.1234	0.1258	0.1340	0.1304

3.4 Experimental:

Matrials and physical measurement as described in **Chapter 2**, **Section 2.42** and **Section 2.41**.

3.4.1 Computational Details

We have considered quinone derivatives having syn and anti conformation as model system for calculation of energy. The geometries of the models have been calculated with DFT[312-313] using the combined Becke's three-parameter exchange functional and the gradient-corrected functional of Lee, Yang and Parr (B3-LYP functional)[314-315] at 6-31++G** levels.[316-317] Single point calculations at 6-31++G** is performed on the fully optimized geometries using B3-LYP/6-31++G**.[318] All calculations are performed using the Gaussian03 program.[319-320] The choice of this basis set is based on the consideration to obtain reliable properties for hydrogen-bonded systems, and it is essential to employ basis sets that possess sufficient diffuseness and angular flexibility.[321] This basis set 6-31++G** is sufficient to predict reliable properties for *syn* and *anti* conformations. All calculations are carried out in the gas phase.

3.4.2 Procedure for the synthesis of polymorph 3.1-3.10

The synthesis and spectroscopic data of compounds **3.1-3.10** are available in chapter 2 however; we renumbered the compounds as **3.1-3.2** = **2.34-2.35, 3.3-3.4** = **2.7-2.8**, **3.5** = **2.6**, **3.6-3.7** = **2.17-2.18** and **3.8- 3.10** = **2.29-2.31** respectively.

3.4.3 Procedure for the synthesis of polymorph 3.1A

To a solution of *bis*-2,3-(*p*-methylphenylsulphanyl) naphthalenediol (0.402 g, 1 mmol) in 15 ml of methanol, 0.002g of copper (II) acetate monohydrate (0.02 mmol, 2 mol %) was added. The resulting reaction mixture was warmed for 10 minutes followed by stirring for 15 minute at room temperature. The solvent was removed by slow evaporation at open air; red micro crystals were obtained within 2 hrs and collected by filtration.

3.4.4 Procedure for the synthesis of polymorph 3.1B

Bis-2,3-(*p*-methylphenylsulphanyl) naphthalenediol (0.201 g, 0.5 mmol) was dissolved in methanol (15 ml) in a 50 ml conical flask. The resulting solution was kept for crystallization. After complete evaporation of solvent at open air, the crystallization process is repeated till the change in color of the crystal form is observed from colorless to red color. After 3-4 days, red block crystals of polymorph **3.1B** were collected.

3.4.5 Procedure for the crystallization of polymorph 3.6B

(3-Carboxymethylsulfanyl 1,4-dihydroxynaphthalen-2-ylsulfanyl) acetic acid **3.6** (0.34 g, 1 mmol) was dissolved in methanol (20 ml) in a 100 ml beaker and added the 20 ml of milli Q water (1:1 molar ratio) and kept it for crystallization. After 12 hrs the colorless crystals were formed on the wall of the beaker and were collected by filtration.

3.4.6 Procedure for the crystallization of polymorph 3.6B

(3-Carboxymethylsulfanyl 1,4-dioxo-1,4-dihydronaphthalen-2-ylsulfanyl) acetic acid **3.7** (0.338 g, 1 mmol) was dissolved in methanol (15 ml) and added a solution of

sodium borohydride (0.0115 g, 0.33 mmol) dissolved in 5 ml methanol (3:1 molar ratio). The resulting solution was kept undisturbed for crystallization. After 1 day the polymorph **3.6B** are obtained as colorless block crystals and collected by filtration.

3.4.7 Procedure for the crystallization of polymorph 3.8A

Dithiolate bridged di-2-methyl 1,4-naphthoquinone **3.8** (0.209 g, 0.5 mmol) was dissolved in methanol (20 ml) and kept it for crystallization. After 1 day the polymorph **3.8A** is obtained as yellow block crystal and collected by filtration.

3.4.8 Procedure for the crystallization of polymorph 3.8B

Dithiolate bridged di-2-methyl 1,4-naphthoquinone **3.8** (0.209 g, 0.5 mmol) and 1,4-dihydroxybenzene (0.055 g, 0.5 mmol) were dissolved in methanol (20 ml) and kept it for crystallization. After 1 day the polymorph **3.8B** is obtained as yellow block crystal and collected by filtration.

Chapter 4

Structural studies on co-crystals and salt of quinonic carboxylic acids

Organized molecular assemblies in solids have potential for design and development of new functional materials.[322] Weak intermolecular interactions play crucial role in the design of such materials.[323] The supramolecular features of quinones are governed by molecular charge-transfer π-complexes and weak interactions (such as C-H···O, N-H···O etc). Introducing a carboxylic acid group on the quinone ring will increase complexity in weak interactions. This is due to the fact that a strong tendency of the carboxylic acid group to adopt different hydrogen bonded structures. Such structures are (a) cyclic hydrogen bonded dimers of type $R_2^2(8)$,[324] (b) hydrogen bonded catemers and (c) bridged dimers[325] (**fig. 4.1**).

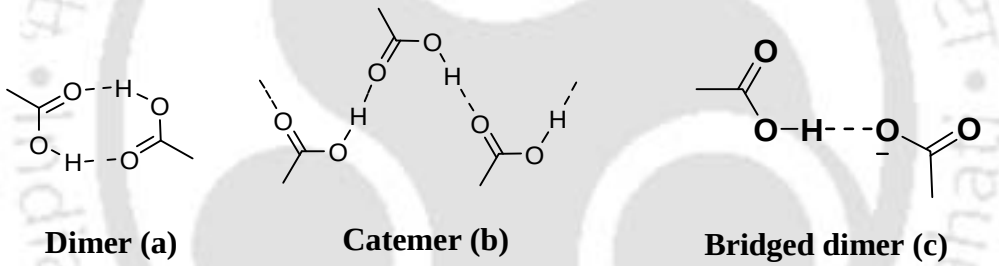

Fig. 4.1 Different hydrogen bonded structures of carboxylic acid

Thus to understand the influence of carboxylic acid groups on weak interactions of quinones, quinonic carboxylic acids **4.1** and **4.2** are prepared and their structures are studied. Further to this, carboxylic acids form co-crystals or salts with amines. Cyclic aromatic amines such as 4,4′-bipyridine and 1,10-phenanthroline form different types of self assembled structures with carboxylic acids. Some possible hydrogen bonded motifs arising from interactions of carboxylic acid with 4,4′-bipyridine and 1,10-phenanthroline are shown in **fig. 4.2**.

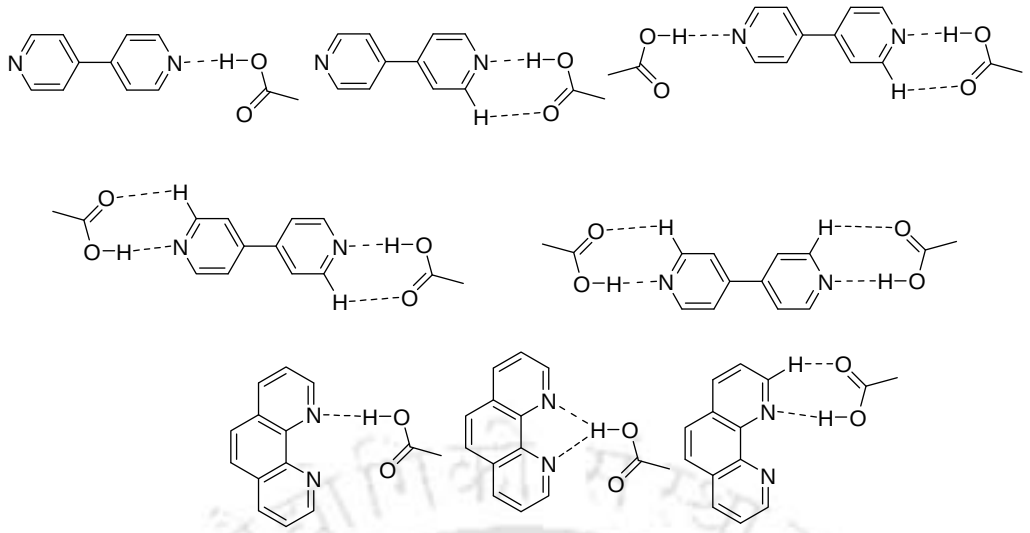

Fig. 4.2 Different hydrogen bonded motifs of carboxylic acids with aromatic amines

The compound (3-methyl-1,4-dioxo-1,4-dihydronaphthalen-2-yl-sulfanyl) acetic acid **4.1** was prepared by reacting 2-methyl-1,4-naphthoquinone with thioglycolic acid. It crystallized from methanol as yellow block. The crystals belong to centrosymmetric triclinic P-1 space group (**fig. 4.3**). In the crystal structure, the carboxylic acid group is non planar with respect to the quinone ring. The molecules of **4.1** self-assemble through O1−H1···O2 interactions to form dimeric structures having [$R_2^2(8)$] type hydrogen bonds[324] (**fig. 4.4**). The carboxylic oxygen atom O2 is involved in hydrogen bonds such as intermolecular C−H···O interactions between hydrogen atoms of C8. Thus, relatively strong O−H···O interactions and weak C−H···O interactions among the carboxylic acids assemble the molecules to form an infinite one dimensional dimeric chain running parallel to the c-axis, as shown in **fig. 4.4**. The hydrogen atoms of methyl groups of 2-methyl 1,4-naphthoquinone, and methylene groups does not involve in weak interactions. The sulphur atom of sulfanyl carboxylic acid also donot participate in any weak interactions. There are no C−H··· π and π···π interactions are present in this lattice. The important hydrogen bond parameters of compound **4.1** are shown in **table 4.1**.

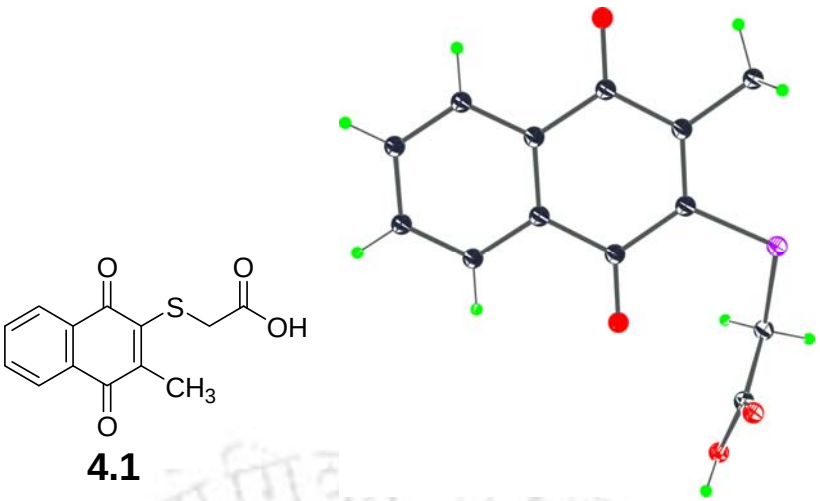

4.1

Fig. 4.3 Crystal structure of compound **4.1** (ORTEP drawn with 30% thermal ellipsoid)

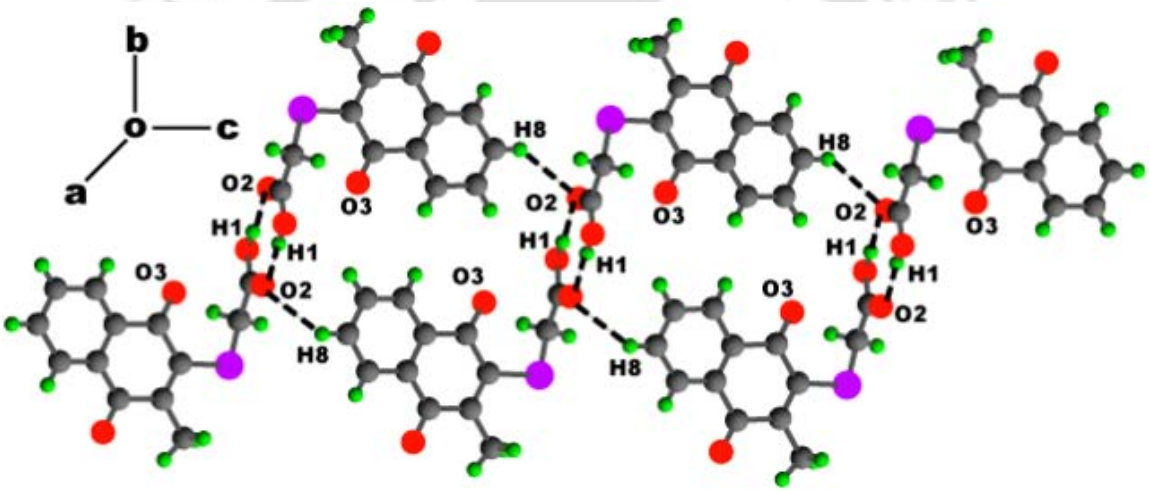

Fig. 4.4: One dimensional dimeric chain of compound **4.1** through O−H···O and C−H···O hydrogen bond

Table 4.1. The hydrogen bond parameters for compound **4.1**				
D−H···A	D−H (Å)	H···A (Å)	D···A (Å)	<D−H···A(°)
O1−H1··· O2 (-x+2, -y+1, -z)	0.820	1.815	2.633	175.6
C8−H8···O2	0.930	2.552	3.239	131.0

The (3-methyl-1,4-dioxo-1,4-dihydronaphthalen-2-ylsulfanyl) acetic acid **4.1** forms 1:2 co-crystal **4.2** with 4,4′-bipyridine (**equation 4.1**); the co-crystals crystallize as red blocks from methanol-chloroform solvent (1:1 molar ratio) in centrosymmetric

monoclinic $P2_1/n$ space group (**fig. 4.5**). The co-crystal has two molecules of (3-methyl-1,4-dioxo-1,4-dihydronaphthalen-2-ylsulfanyl) acetic acid **4.1** anchored to one molecule of 4,4′-bipyridine. The co-crystal is stabilized by O2···H14−C14 and O1−H1···N1 interactions which has $[R_2^2(7)]$ type hydrogen bond pattern. It forms two dimensional hydrogen bonded networks through weak C−H···O interactions (C2−H2B···O3, C14−H14···O2, C15−H15···O2 and C8−H8···O4). Some important donor acceptor bond distances and bond angles contributing to the H-bond interactions are O1···N1, 2.64 Å and H14···O2, 2.58 Å; <O1−H1···N1, 175.8º and <C14−H14···O2, 128.5º respectively (**fig. 4.6**). Similar to quinonic acid **4.1**, the hydrogen atoms of methyl groups of 2-methyl 1,4-naphthoquinone and the sulphur atom of sulfanyl carboxylic acid are not participating in any weak interactions. There are no π···π interactions present in this lattice. Some important hydrogen bond geometries of co-crystal **4.2** are shown in **table 4.2**.

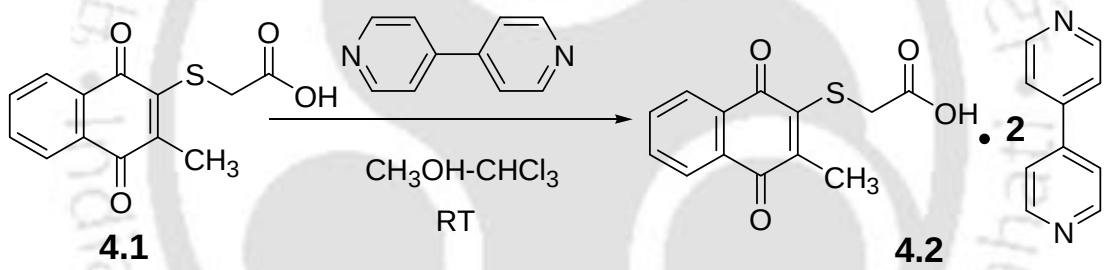

Equation 4.1 Synthesis of co-crystal **4.2**

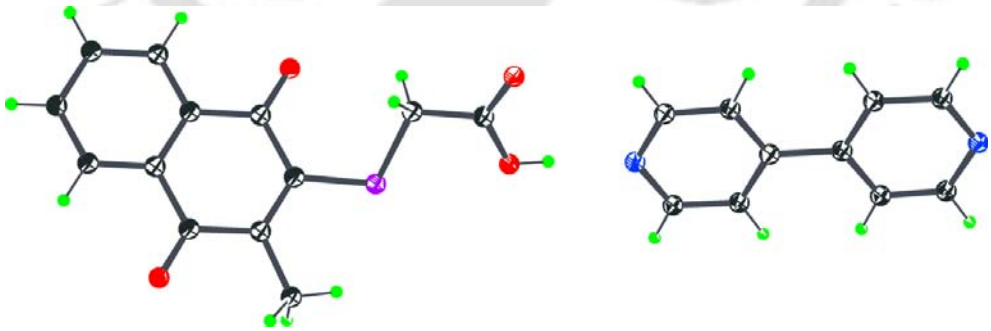

Fig. 4.5 Crystal structure of co-crystal **4.2** (ORTEP drawn with 30% thermal ellipsoid)

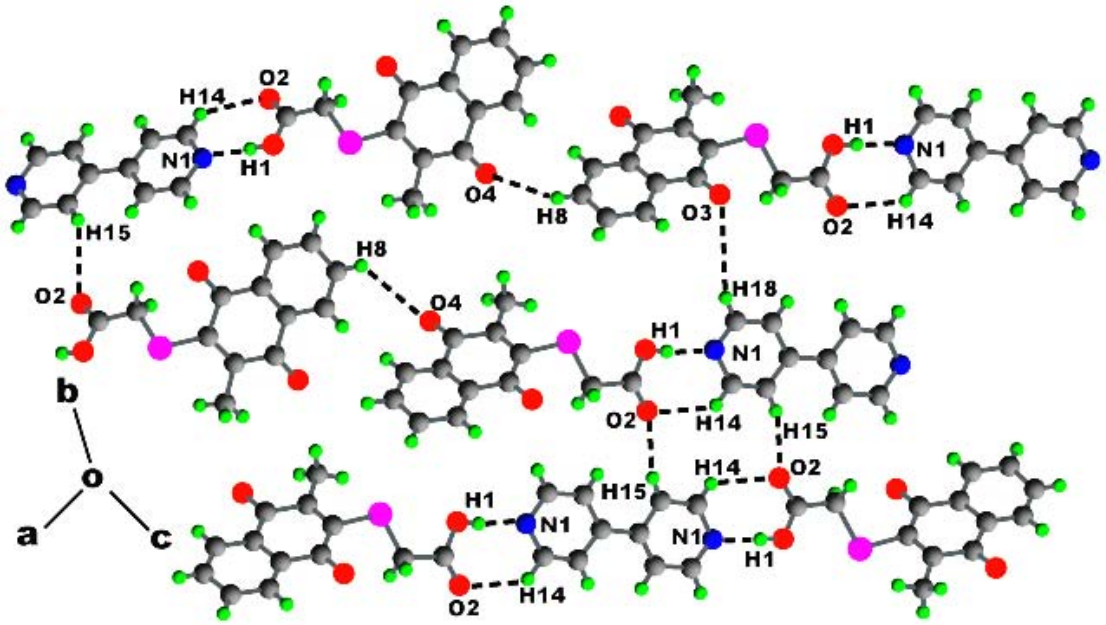

Fig. 4.6 Hydrogen bonded two dimensional network of co-crystal **4.2**

Table 4.2. The hydrogen bond parameters for co-crystal **4.2**

D−H···A	D−H (Å)	H···A (Å)	D···A (Å)	<D−H···A(°)
O1−H1···N1	0.819	1.821	2.639	175.8
C14−H14···O2	0.930	2.581	3.243	124.5
C15−H15···O2	0.929	2.419	3.313	161.6
C8−H8···O4	0.930	2.713	3.630	169.5
C2−H2B···O3	0.970	2.423	3.371	165.3

The (3-methyl-1,4-dioxo-1,4-dihydronaphthalen-2-ylsulfanyl) acetic acid **4.1** also forms 1:1 co-crystal **4.3** with 1,10-phenanthroline (**equation 4.2**). The co-crystals crystallize as yellow block from methanol-chloroform solvent mixture in (2:1 v/v). The unit cell of co-crystals **4.3** is symmetry non equivalent molecules (**fig. 4.7**).

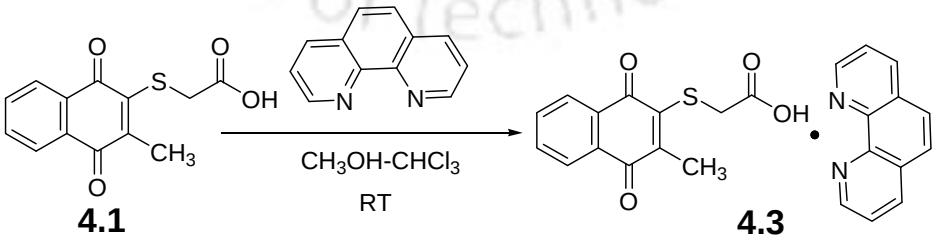

Equation 4.2 Synthesis of co-crystal **4.3**

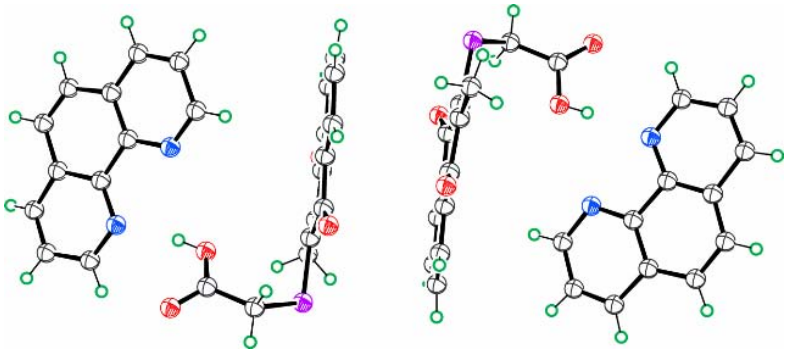

Fig. 4.7 Crystal structure of co-crystal **4.3** (ORTEP drawn with 50% thermal ellipsoid)

In this co-crystal **4.3**, one molecule of (3-methyl-1,4-dioxo-1,4-dihydronaphthalen-2-ylsulfanyl) acetic acid **4.1** is attached to one 1,10-phenanthroline molecule. The co-crystal **4.3** is stabilized by O−H···N interactions (O3−H3A···N3, O3−H3A···N4, O5−H5···N1 and O5−H5···N2) which leads to five member cyclic structure with $R_1^2(5)$ type hydrogen bond. The H3A atom of the carboxylic acid is involved in a bifurcated type of hydrogen bonding with N3 and N4 atoms of 1,10-phenanthroline. Similarly the H5 atoms of carboxylic acid is also involved in a bifurcated type of hydrogen bonding with N1 and N2 atoms of 1,10-phenanthroline as shown in **fig. 4.8**.

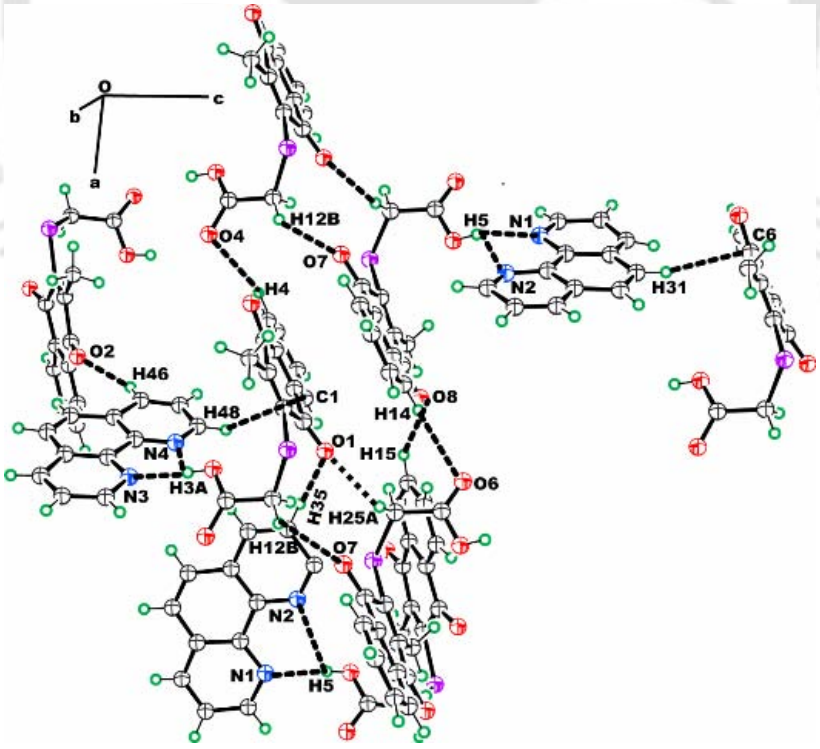

Fig. 4.8 Self assembly structure of co-crystal **4.3** (ORTEP drawn with 50% thermal ellipsoid)

The sulphur atom does not involve in any weak interactions. On contrary to co-crystal **4.2**, co-crystal **4.3** does not have O···H−O interactions. Beside this the O1 atoms of one of the carbonyl group of 2-methyl 1,4-naphthaquinone (act as acceptor) forms a bifurcated type of hydrogen bonding with H35 atoms of 1,10-phenanthroline molecule and H25A atoms of methylene groups (which act as donors).

The assembly of co-crystals **4.3** is also stabilized by the C−H···O (C46−H46···O2, C4−H4···O4, C14−H14···O6, C12−H12B···O7 and C15−H15···O8) and C−H···π (C31−H31···π_{C6} and C48−H48···π_{C1}) interactions (**fig. 4.8**). The methyl groups and sulphur atoms do not participating in any interactions. There is no interaction between the carboxylic acid groups to form the conventional $R_2^2(8)$ type hydrogen bond. Some of the important hydrogen bond distances and bond angles of co-crystal **4.3** are shown in **table 4.3**.

Table 4.3. The hydrogen bond parameters for co-crystal **4.3**

D−H···A	D−H (Å)	H···A (Å)	D···A (Å)	<D−H···A(°)
O3−H3A···N3	0.819	1.912	2.730	175.3
O3−H3A···N4	0.819	2.670	3.023	107.8
O5−H5···N1	0.819	2.005	2.760	152.9
O5−H5···N2	0.819	2.582	3.048	117.5
C35−H35···O1	0.933	2.473	3.329	152.6
C25−H25A···O1	0.969	2.583	3.390	140.8
C46−H46···O2	0.930	2.499	3.373	156.6
C4−H4···O4	0.926	2.654	3.442	143.4
C14−H14···O6	0.932	2.631	3.522	160.1
C12−H12B···O7	0.971	2.696	3.525	143.7
C15−H15···O8	0.931	2.594	3.309	133.9
C31−H31··· π_{C6}	0.930	2.786	3.695	
C48−H48··· π_{C1}	0.931	2.812	3.631	

In the IR spectra of co-crystal **4.2** and **4.3**, the relatively strong absorption at 1716 cm^{-1} of carboxylic acid groups of the compound **4.1** shift to around 1698 cm^{-1} which indicates that the carbonyl groups of carboxylic acid participates in hydrogen bond. The broad and strong absorption at 3444 cm^{-1} is attributed to the hydrogen bonded carboxylic acid group of the co-crystal. The ^{1}H NMR spectra of the co-crystal **4.2** and **4.3** show all the signals of the parent components with the desired proton integration without significant shift in the chemical shift position as compared to the parent

compound but only noticeable change can be observed in the methylene hydrogen signals. The signal of carboxylic acid group is not observed in the ^{1}H NMR spectra of the compound **4.1**, its co-crystal **4.2** and **4.3** in DMSO-d_6 at room temperature**.** This occurs probably due to exchange with water present in the solvent.

Spectroscopic characterization shows that the two components are present in the co-crystal **4.2** in 1:2 ratio while the co-crystal **4.3** in 1:1 host guest ratio. The overlay ^{1}H NMR spectra of compound **4.1** and its co-crystals **4.2** and **4.3** in DMSO-d_6 are shown in **fig. 4.9**.

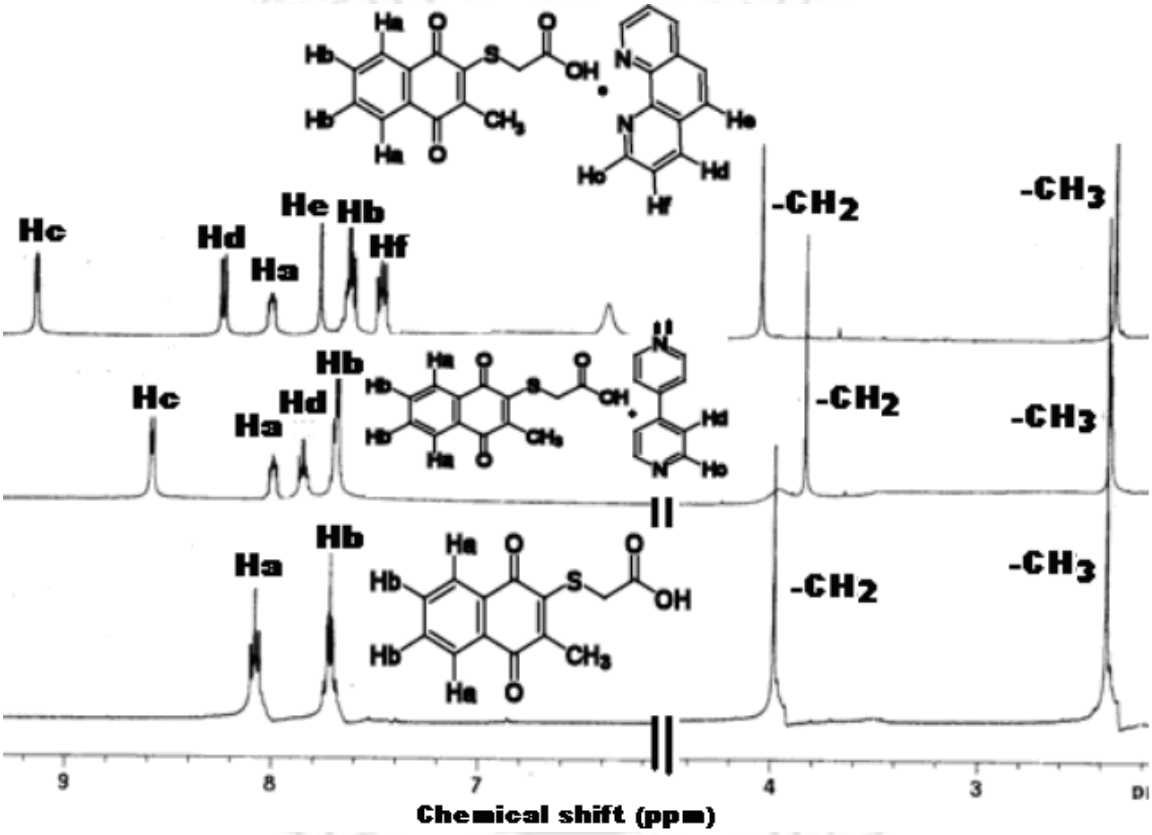

Fig. 4.9 ^{1}H NMR spectra of compound **4.1** and its co-crystal with 4,4'-bipyridine **4.2** and 1,10-phenanthroline **4.3** in DMSO-d_6

The (3-carboxymethylsufanyl-1,4-dioxo-1,4-dihydronaphthalen-2-ylsulfanyl) acetic acid **4.4** (**fig. 4.10**) was prepared from reaction of 1,4-naphthoquinone with thioglycolic acid (**equation 4.3**). The (3-carboxymethylsulfanyl-1,4-dioxo-1,4-dihydronaphthalen-2-yl-sulfanyl) acetic acid **4.4** forms 1:1 co-crystal, **4.5** with triphenylphosphine oxide. It crystallises as red block from methanol in centrosymmetric monoclinic C2/c space group.

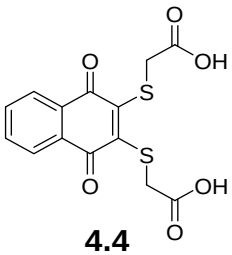

4.4

Fig. 4.10

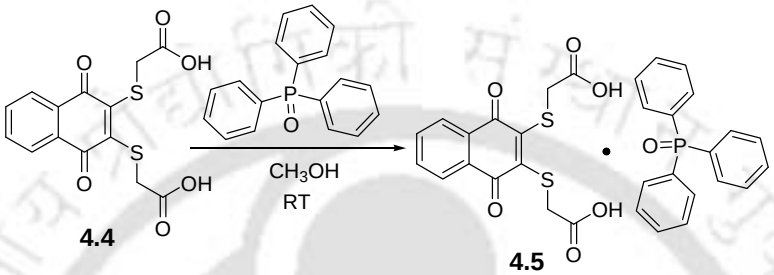

Equation 4.3 Synthesis of co-crystal **4.5**

In the crystal structure it is seen that the two carboxylic acid groups are disposed in same plane with respect to the naphthoquinone ring and these molecules adopt planar geometry as shown in **fig. 4.11**. In this co-crystal two molecules of triphenylphosphine interact at the distal end of two carboxylic acid units and are stabilized by O1···H3A−O3 ($d_{D\cdots A}$, 2.53 Å and <D-H···A 169.5º) interaction and the O3···O4 has distance 4.47 Å. The crystal packing of the co-crystal **4.5** is governed by weak C−H···O (C19−H19···O4, $d_{D\cdots A}$, 3.35 Å and <D-H···A 143.2º; C24−H24B···O2, $d_{D\cdots A}$, 3.36 Å and <D-H···A 153.5º and C24−H24A···O1 $d_{D\cdots A}$, 3.14 Å and <D-H···A 123.4º) interactions. It has two dimensional infinitely extended hydrogen bonded networks in the crystal lattice as shown in **fig 4.12**. The hydrogen atoms of the quinone unit and methylene groups are involved in C−H···O interactions but the hydrogen atoms of the triphenylphosphine oxide are not involved in weak interactions. In its crystal lattice there are no C−H···π and π ···π interactions.

In the IR spectra of co-crystal **4.5** in solid state, a relatively broad and strong absorption at 3431 cm^{-1} is observed and it is attributed to O-H stretching frequency of the hydrogen bonded carboxylic acid groups. It also shows the strong absorption at 1732 cm^{-1} and 1651 cm^{-1} are attributed to the C=O stretching frequency of 1,4-naphthoquinone and carboxylic acid groups respectively.

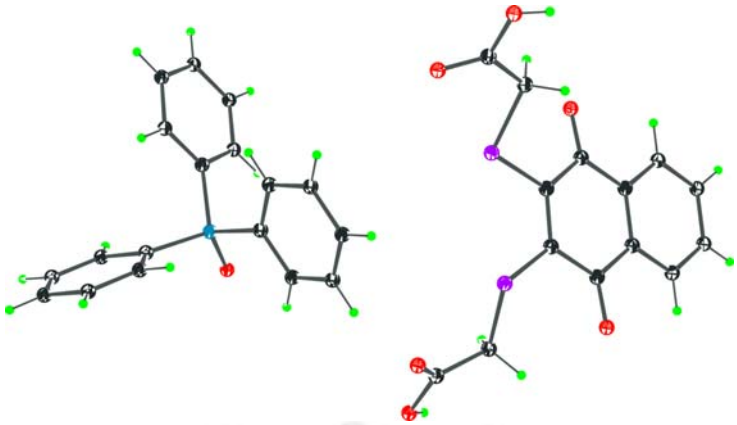

Fig. 4.11 Crystal structure of co-crystal **4.5** (ORTEP drawn with 30% thermal ellipsoid)

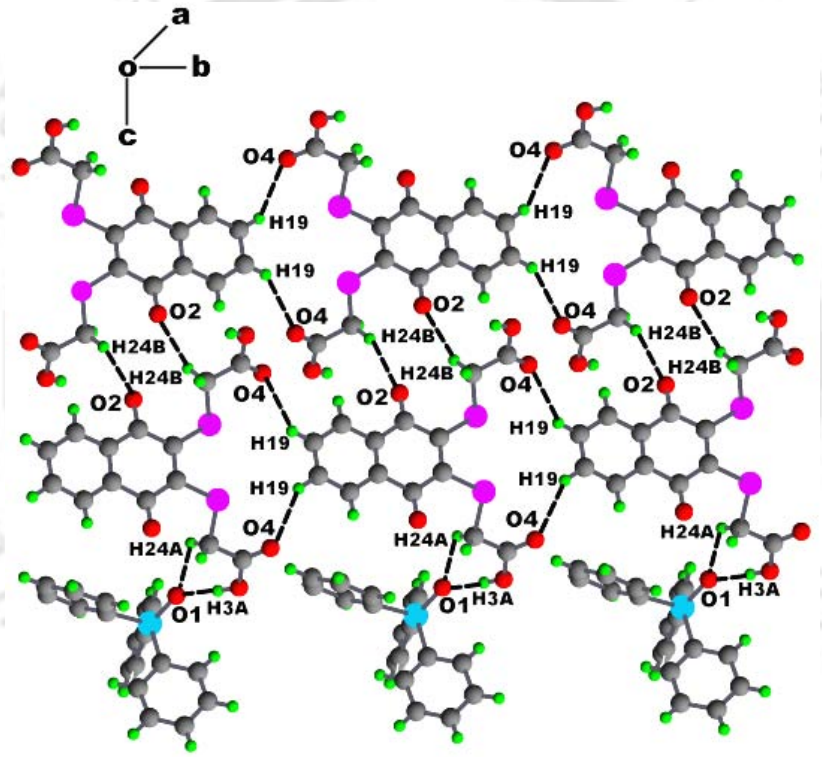

Fig. 4.12 Two dimensional hydrogen bond network of co-crystal **4.5**

Beside this the P=O stretching frequency of triphenylphosphine oxide is observed as a strong absorption at 1120 cm^{-1}. The ^{1}H NMR spectra of the co-crystal **4.5** shows all the signals of the parent components with the desired proton integration without significant shift in the chemical shift position as compared to the parent compound **4.4**. The signal of carboxylic acid group is not observed in the ^{1}H NMR spectra of the parent compound **4.4** and co-crystal **4.5**. The ^{31}P NMR spectrum of the **4.5** shows one singlet at -25.69 ppm in DMSO-d_6.

We extended our study to incorporate a pyridine containing tether to quinone with a view to make a new series of compounds that may have anion binding ability. We prepared two picolyl derivatives of 1,4-naphthoquinone from independent reactions of 3-picolylamine **4.6** and 4-picolylamine **4.7** with 1,4-naphthoquinone respectively (**fig. 4.14**).

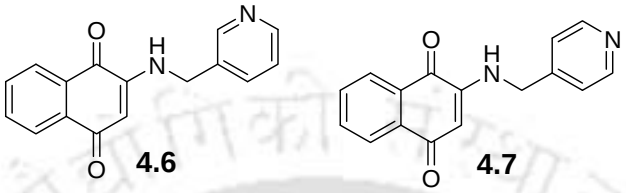

Fig. 4.14

The compound 2-[(pyridin-3-ylmethyl)-amino]-1,4-naphthoquinone **4.6** is crystallized from methanol in chiral space group $P2_12_12_1$ and its structure is shown in **fig. 4.15**.

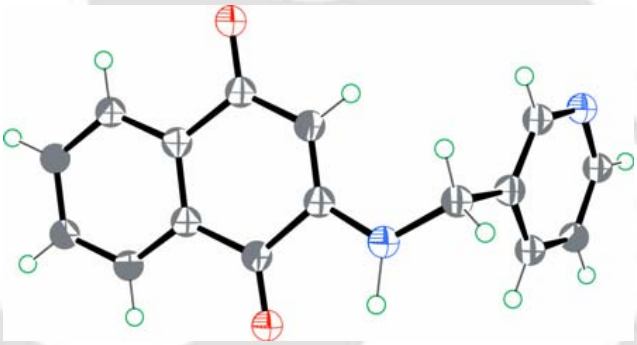

Fig. 4.15 Crystal structure of compound **4.6** (ORTEP drawn with 50% thermal ellipsoid)

In solid state the molecule **4.6** self assemble through weak interactions. Prominent weak interactions are N−H···O (N2−H2N···O2; $d_{D\cdots A}$, 3.01 Å and <D-H···A 126.8º) and C−H···O (C3−H3···O1, $d_{D\cdots A}$, 3.47 Å and <D-H···A 163.5º; C16−H16···O1, $d_{D\cdots A}$, 3.49 Å and <D-H···A 159.6º and C13−H13···O2, $d_{D\cdots A}$, 3.35 Å and <D-H···A 143.7º) interactions (**fig. 4.16**). In addition to these the crystal lattice is stabilized by the C−H···π (C11−H11A···π_{12}, $d_{D\cdots\pi}$, 3.92 Å and C11−H11A···π_{13}, $d_{D\cdots\pi}$, 3.63 Å) interactions.

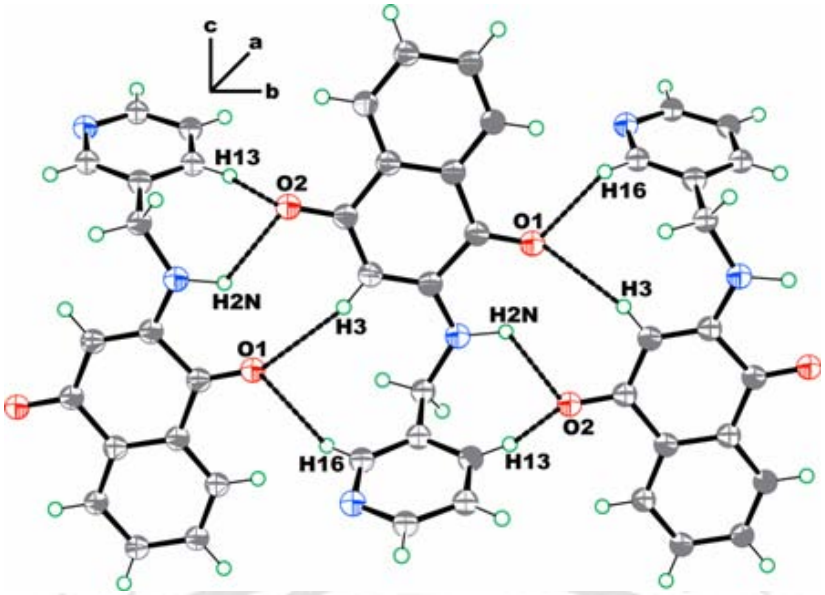

Fig. 4.16 Self assembly of compound **4.6** (ORTEP drawn with 50% thermal ellipsoid)

The crystal obtained for compound **4.7** from methanol are in centrosymmetric orthorhombic $Pca2_1$ space group (**fig. 4.17**). Some of the important weak interactions responsible for hydrogen bonding assemblies in **4.7** are N2−H2N···O2 ($d_{D\cdots A}$, 2.88 Å and <D-H···A 140.2º), C6−H6···O1 ($d_{D\cdots A}$, 3.30 Å and <D-H···A 153.1º) and C11−H11B···O1 ($d_{D\cdots A}$, 3.54 Å and <D-H···A 143.4º) interactions. In addition to this the C5 and C13 carbon centers are involved in C−H···π (C13−H13···π_5, $d_{D\cdots\pi}$, 3.75 Å and C11−H11A···π_{13}, $d_{D\cdots\pi}$, 3.81 Å) interaction with H13 and H11A atoms of another neighboring molecule respectively. Beside this the crystal packing of the compound **4.7** is also stabilized by $\pi_4\cdots\pi_8$ ($d_{\pi\cdots\pi}$, 3.39 Å) interactions as shown in **fig. 4.18**.

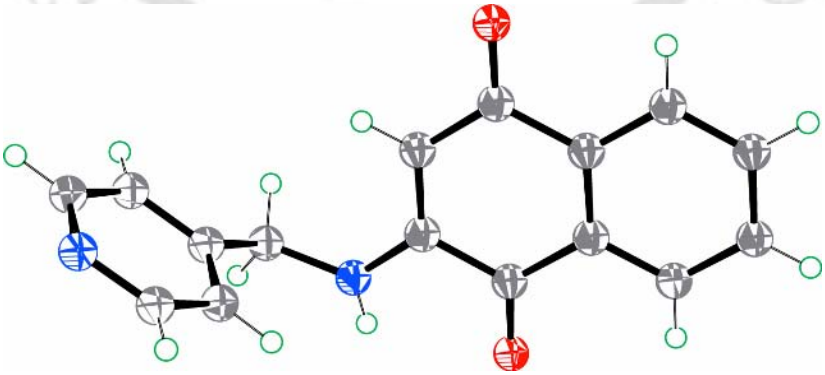

Fig. 4.17 Crystal structure of compound **4.7** (ORTEP drawn with 50% thermal ellipsoid)

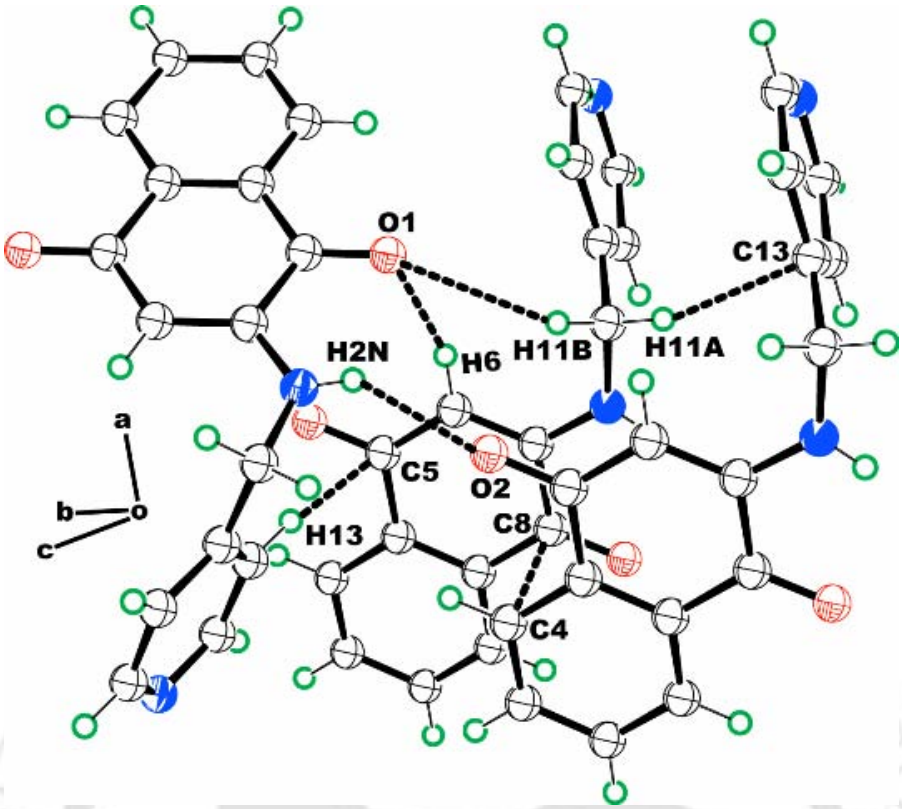

Fig. 4.18 Self assembly of compound **4.7** (ORTEP drawn with 50% thermal ellipsoid)

The perchlorate salt **4.8** of 2-[(pyridin-3-ylmethyl)-amino]-1,4-naphthoquinone **4.6** is formed as a monohydrate from the reaction as shown in **equation 4.4**. The perchlorate salt crystallizes as red block, having P-1 space group. It is obtained as hydrated molecule as shown in **fig. 4.19**.

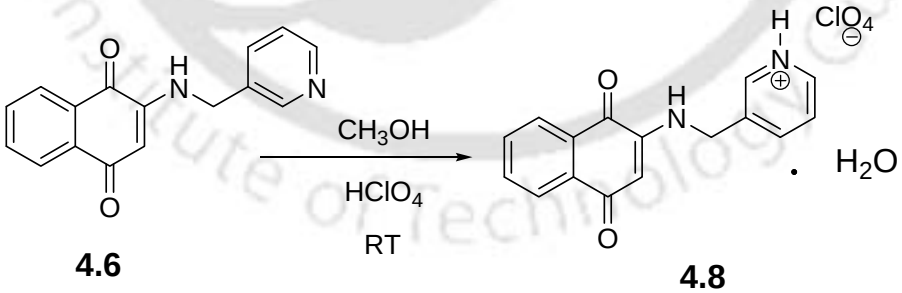

Equation 4.4 Reaction of perchloric acid and with compound 4.6

Compound **4.8** gets protonated at the picoline-N atom to result a cation and this hydrogen involves in N−H···O hydrogen bonding with perchlorate anion. Crystal structure shows that the self assembly of the salt through weak C−H···O (C4−H4···O2, C6−H6···O4, C14−H14···O7, C14−H14···O6, and C15−H15···O7), N−H···O

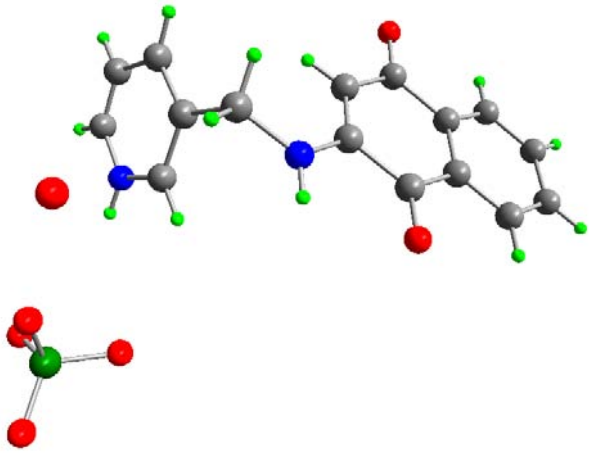

Fig. 4.19 Crystal structure of salt **4.8** (oxygen atoms of water is not located)

(N1−H1N···O1) and N2−H2···O6) and C−H···π (C11−H1A···π_5; $d_{H\cdots\pi}$ =2.87 Å) interactions as shown in **fig. 4.20**. These weak interactions provide extra stabilities to the lattice. Beside this the hydrated water molecule is also involved in weak interactions making a bridge between the two 2-[(pyridin-3-ylmethyl)-amino]-1,4-naphthoquinone cations. It also makes a bridge between 2-[(pyridin-3-ylmethyl)-amino]-1,4-naphthoquinone cation and perchlorate anion. Some important donor acceptor bond distances and bond angles contributing to the hydrogen bonding interactions are H1N···O1, 2.45 Å and H4···O2, 2.43 Å; <N1−H1N···O1, 137.2º and <C4−H4···O2, 140.9º respectively as shown in **fig. 4.20a**. The lattice is also stabilized by intermolecular C−H···π (C11−H1A···π_5) interactions between the methylene hydrogen H1A of 2-[(pyridin-3-ylmethyl)-amino]-1,4-naphthoquinone **4.6** and the C5 of 1,4-naphthoquinone ring as shown in **fig. 4.20b**. Due to the electron deficient nature of the quinone the unsaturated hydrogen of 1,4-naphthoquinone is not involved in any weak interactions. Some of the important bond distances and bond angles of the compound **4.6-4.8** are given in **table 4.5**.

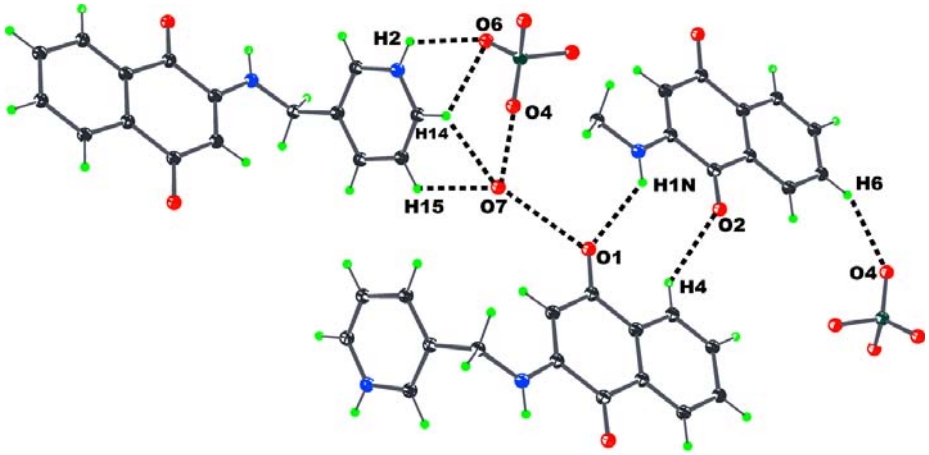

a

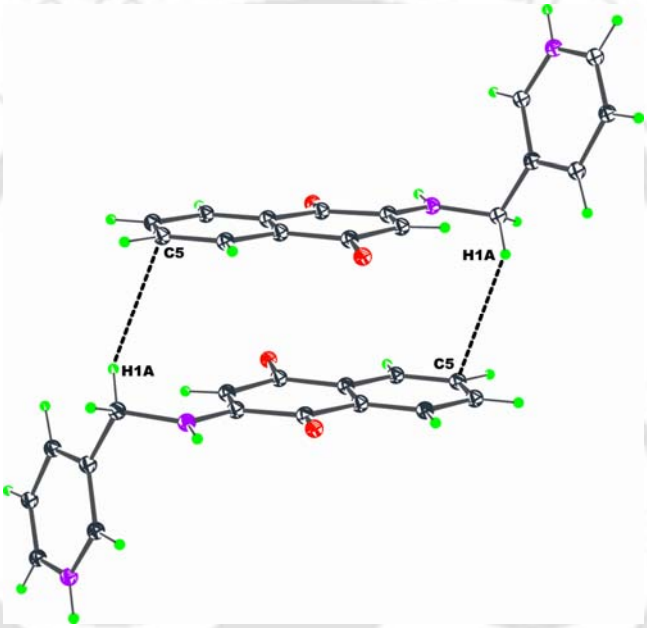

b

Fig. 4.20 a**)** Self assembly of compound **4.8** (One pyridyl group is not shown for clarity); b) Self assembly through C−H···π interactions (ORTEP drawn with 30% thermal ellipsoid)

Table 4.5 Selected bond distances (Å) and bond angles (°) for compounds **4.6-4.8**

4.6				**4.7**			
Bond	Distances	Bond	Angles	Bond	Distances	Bond	Angles
N2-C2	1.368(4)	C2-N2-C11	122.2(3)	O1-C8	1.226(3)	C7-N2-C11	124.6(3)
N2-C11	1.473(5)	N1-C15-C14	123.6(4)	O2-C5	1.235(3)	C7-N2-H2N	112.3(16)
C15-N1	1.324(5)	O1-C1-C9	121.7(4)	N2-C7	1.345(3)	C11-N2-H2N	123.1(16)
C2-C3	1.316(5)	O1-C1-C2	121.1(4)	N2-C11	1.434(3)	C14-N1-C15	115.9(3)
O1-C1	1.220(4)	C9-C1-C2	117.2(3)	C11-C12	1.505(3)	O1-C8-C7	119.1(2)
O2-C4	1.243(4)	N2-C11-C12	112.9(3)	N1-C14	1.306(4)	C13-C12-C11	123.2(3)
C2-C1	1.517(5)	O1-C1-C9	121.7(4)	N1-C15	1.323(4)	C9-C8-C7	118.2(3)

C10-C9	1.400(5)	O1-C1-C2	121.1(4)	C9-C10	1.378(3)	C7-C6-C5	122.3(3)
C10-C4	1.492(5)	O2-C4-C3	122.7(4)	C12-C13	1.368(4)	O2-C5-C6	121.5(3)
N1-C16	1.335(5)	O2-C4-C10	118.2(4)	C9-C8	1.466(3)	O2-C5-C10	119.9(3)
C9-C1	1.464(5)	C3-C4-C10	119.1(3)	C6-C7	1.360(3)	C6-C5-C10	118.6(3)
C4-C3	1.407(5)	C13-C12-C16	116.3(4)	C6-C5	1.419(3)	N2-C7-C6	124.5(3)
1C12-C13	1.371(5)	C13-C12-C11	121.9(3)	C5-C10	1.495(4)	N2-C7-C8	115.2(3)
C12-C16	1.380(5)	C16-C12-C11	121.8(4)	C7-C8	1.494(3)	C16-C12-C13	116.1(3)
C12-C11	1.505(5)	C15-N1-C16	115.9(4)	C12-C16	1.367(3)	N1-C15-C16	123.8(3)
Bond	Angles	N1-C16-C12	125.2(4)	Bond	Angles	N2-C11-C12	115.7(2)
C3-C2-C1	121.3(3)	C3-C2-N2	127.0(4)	O1-C8-C9	122.7(3)	C16-C12-C11	120.7(3)
N2-C2-C1	111.6(3)			C6-C7-C8	120.3(2)		

4.8							
Bond	Distances	Bond	Angles	Bond	Distances	Bond	Angles
C3-C2	1.492(7)	C8-C3-C2	120.5(4)	C10-N1	1.345(5)	C12-C13-N2	118.3(6)
C2-O1	1.241(5)	O1-C2-C1	121.5(5)	C10-C1	1.357(6)	C13-C12-C11	120.6(5)
C2-C1	1.427(6)	O1-C2-C3	120.2(4)	C12-C13	1.381(7)	N1-C10-C9	113.7(4)
C8-C3	1.401(6)	C14-N2-C13	121.0(6)	C12-C16	1.385(7)	C1-C10-C9	120.7(4)
C9-O2	1.216(5)	O2-C9-C10	120.2(4)	C13-N2	1.404(8)	C10-C1-C2	122.8(4)
C9-C8	1.478(6)	C8-C9-C10	117.8(4)	C11-N1	1.438(6)	C15-C14-N2	122.3(6)
C9-C10	1.497(6)	O2-C9-C8	122.0(4)	Bond	Angles	N1-C11-C12	113.3(4)
C14-N2	1.292(9)	C3-C8-C9	119.8(4)	C1-C2-C3	118.3(4)	C10-N1-C11	123.4(4)
C11-C12	1.505(7)	C13-C12-C16	118.2(5)	N1-C10-C1	125.7(4)		

The solid state FT-IR spectra of salt **4.8** has a relatively strong absorption peak at 1704 cm^{-1}, due to C=O group of 1, 4-naphthoquinone and it gets shifted from 1681 cm^{-1} of parent compound **4.6**. There is also a strong absorption peak at 1100 cm^{-1} due to perchlorate group. The sharp and strong N-H stretching vibrations of the 3-picolylamine of parent compound **4.6** (absorption at 3357 cm^{-1}) is shifted at 3174 cm^{-1} which indicates that the N-H participates in hydrogen bond.

The ^{1}H NMR spectra of the salt **4.8** show all the signals of the parent components with the desired proton integration. It occur noticeable change in significant chemical shift position as compared to the parent compound. The signal of N-H hydrogen is observed to shift from 6.25 to 8.93 ppm in the ^{1}H NMR spectra of the salt **4.8** in DMSO-d_6 at

room temperature, suggesting its participation in strong intermolecular hydrogen bonding.

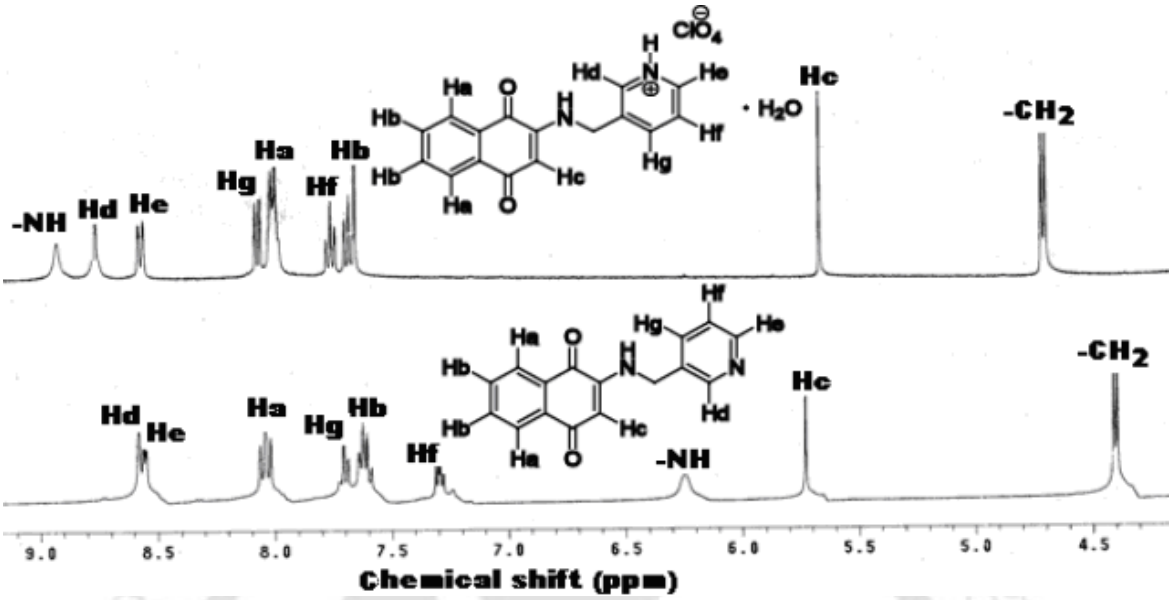

Fig. 4.21 ^{1}H NMR spectra of compound **4.6** and its perchlorate salt **4.8** in DMSO-d_6

If we compare the ^{1}H NMR spectra of **4.6** and **4.8**, it is observed that after protonation the aromatic protons are shifted towards the downfield. The overlay ^{1}H NMR spectra of compound **4.1** and its co-crystals **4.2** and **4.3** in DMSO-d_6 are shown in **fig. 4.21**.

The crystal data and refinement parameters of compound **4.1-4.8** are listed in **table 4.6**.

Table 4.6: The crystallographic parameters of **4.1-4.3** and **4.5**

Compound No.	**4.1**	**4.2**	**4.3**	**4.5**
Formulae	$C_{13}H_{10}O_4$ S	$C_{18}H_{14}NOS$	$C_{25}H_{18}N_2O_4S$	$C_{25}H_{20}O_4PS$
Mol. wt.	262.27	340.36	442.47	447.44
Crystal system	Triclinic	Monoclinic	Monoclinic	Monoclinic
Space group	P-1	$P2_1/n$	$P2_1$	C2/c
a (Å)	7.5378(6)	9.3383(7)	10.364(5)	26.0494(13)
b (Å)	7.6413(7)	3.9700(3)	13.436(6)	10.5402(5)
c (Å)	10.3101(9)	42.130(3)	15.491(7)	17.1023(8)
α/°	89.779(7)	90.00	90.00	90.00
β/°	81.041(5)	91.056(5)	99.577(17)	108.719(5)
γ/°	89.101(7)	90.00	90.00	90.00
V (Å ^{3})	586.53(9)	1561.6(2)	2127.1(17)	4447.3(4)
Z	2	4	4	8
Density/Mgm^{-3}	1.485	1.448	1.382	1.321
Abs. Coeff. /mm^{-1}	0.279	0.230	0.188	0.246
Abs. correction	none	none	none	none
F(000)	272	708	920	1824

Total no. of reflections	3559	13891	20071	15860
Reflections, I 2σ(I)	1635	3549	7584	3277
Max. 2θ/°	47.00	54.94	51.00	46.98
Ranges (h, k, l)	$-5 \le h \le 8$ $-8 \le k \le 8$ $-11 \le l \le 11$	$-11 \le h \le 12$ $-5 \le k \le 3$ $-54 \le l \le 53$	$-12 \le h \le 12$ $-16 \le k \le 14$ $-18 \le l \le 18$	$-28 \le h \le 29$ $-11 \le k \le 11$ $-19 \le l \le 19$
Completeness to 2θ (%)	94.1	99.7	99.6	99.6
Data/Restraints/Parameters	1635 / 0 /164	3549 / 0 /219	7584 / 1 / 581	3277 / 0 / 281
Goof (F2)	1.047	1.124	0.935	1.048
R indices [I > 2σ(I)]	0.0304	0.0819	0.1180	0.0468
R indices (all data)	0.0337	0.1495	0.3110	0.0700
wR indices	0.0855	0.2186	0.4378	0.1203

Compound No.	**4.6**	**4.7**	**4.8**
Formulae	$C_{16}H_{12}N_2O_2$	$C_{16}H_{12}N_2O_2$	$C_{16}H_{13}ClN_2O_7$
Mol. wt.	264.28	264.28	380.73
Crystal system	Orthorhombic	Orthorhombic	Triclinic
Space group	$P2_12_12_1$	$Pca2_1$	P-1
a (Å)	4.3029(8)	24.503(4)	7.8032(3)
b (Å)	12.249(2)	5.0679(8)	10.8468(3)
c (Å)	23.927(6)	10.750(2)	14.372(5)
α/°	90.00	90.00	83.079(2)
β/°	90.00	90.00	87.557(2)
γ/°	90.00	90.00	70.765(2)
V ($Å^3$)	1261.0(5)	1335.0(4)	824.81(5)
Z	4	4	2
Density/Mgm^{-3}	1.392	1.315	1.533
Abs. Coeff. /mm^{-1}	0.094	0.089	0.276
Abs. correction	none	none	none
F(000)	552	552	392
Total no. of reflections	10374	12332	8688
Reflections, I 2σ(I)	3052	3055	2987
Max. 2θ/°	56.90	58.42	50.98
Ranges (h, k, l)	$-5 \le h \le 5$ $-15 \le k \le 5$ $-31 \le l \le 1$	$-33 \le h \le 33$ $-6 \le k \le 6$ $-12 \le l \le 14$	$-9 \le h \le 9$ $-9 \le k \le 9$ $-17 \le l \le 17$
Completeness to 2θ (%)	95.5	98.5	97.4
Data/Restraints/Parameters	3052 / 0 / 185	3055 / 1 / 186	2987 / 0 / 236
Goof (F2)	0.885	0.986	1.007
R indices [I > 2σ(I)]	0.0681	0.0538	0.1010
R indices (all data)	0.1538	0.1630	0.1102
wR indices	0.1795	0.0818	0.2279

4.1 Experimental

Materials and physical measurement as described in **Chapter 2**, **Section 2.41** and **Section 2.42**.

The synthesis and details of spectroscopic data of compounds **4.1**, **4.4** and **4.6-4.7** are given in the **chapter 2**. The compound numbers in this chapter **4.1** = **2.27**, **4.4** = **2.18** and **4.6- 4.7** = **2.56-2.57** are renumberd respectively.

4.1.1 Procedure for the synthesis of co-crystal 4.2

(3-Methyl-1,4 dioxo-1,4-dihydronaphthalen-2-yl-sulfanyl) acetic acid **4.1** (0.131 g, 0.5 mmol) and 4,4′-bipyridine was dissolved in 10 ml of methanol-chloroform solvent system (1:1 v/v) and kept undisturbed for 24 hrs. The resulting red block crystals were collected by filtration.

Isolated yield: 84%, IR (KBr, cm^{-1}): 3444 (bs), 2922 (w), 1698 (s), 1661 (s), 1588 (s), 1564 (m), 1508 (m), 1422 (m), 1384 (w), 1325 (w), 1283 (s), 1265 (m), 1180 (w), 1140 (w), 1035 (w), 956 (w), 840 (s), 730 (m), 710 (s); ^{1}H NMR (DMSO-d_6, 400 MHz): 8.63 (d, J = 4.4 Hz, 4H), 7.93 (dd, J = 7.2, 3.4 Hz, 2H), 7.65 (dd, J = 5.6, 2.4 Hz, 2H). 7.54 (d, J = 4.4 Hz, 4H), 3.86 (s, 2H), 2.24 (s, 3H); ^{13}C NMR (DMSO-d_6, 100 MHz): 178.9, 170.6, 146.2, 133.9, 132.9, 132.2, 132.1, 128.9, 128.8, 127.0, 36.4, 16.8.

4.1.2 Procedure for the synthesis of co-crystal 4.3

(3-Methyl-1,4 dioxo-1,4-dihydronaphthalen-2-yl-sulfanyl) acetic acid **4.1** (0.131 g, 0.5 mmol) and 1,10-phenanthroline was dissolved in 5 ml of methanol. To this solution 5ml of chloroform was put slowly from the wall of the test tube to make a layer between the methanol and chloroform solvent mixture and kept undisturbed for 48 hrs. The resulting yellow block crystals were collected by filtration.

Isolated yield: 84%, IR (KBr, cm^{-1}): 3434 (bs), 2924 (w), 1694 (s), 1662 (s), 1588 (s), 1558 (m), 1507 (s), 1422 (m), 1381 (w), 1275 (s), 1265 (m), 1180 (w), 1140 (w), 1035 (w), 958 (m), 852 (s), 710 (s); ^{1}H NMR (DMSO-d_6, 400 MHz): 9.15 (d, J = 4.4 Hz, 2H), 8.25 (d, J = 6.4 Hz, 2H), 8.01(dd, J = 5.6, 2.4 Hz, 2H). 7.77 (s, 2H), 7.62 (m, 4H),

4.05 (s, 2H), 2.17 (s, 3H); ^{13}C NMR (DMSO-d_6, 100 MHz): 179.9, 171.6, 150.2, 145.2, 136.5, 133.9, 133.8, 132.9, 132.2, 128.9, 127.0, 126.8, 123.5, 35.8, 15.3.

4.1.3 Procedure for the synthesis of co-crystal 4.5

Synthesis of (3-Carboxymethylsufanyl-1,4-dioxo-1,4-dihydronaphthalen-2-ylsulfanyl) acidic acid **4.4** (0.1041 g, 0.3 mmol) and triphenylphosphine oxide (0.0831 g, 3 mmol) was dissolved in 15 ml of methanol and heated it for 30 min at boiling temperature. The resulting solution was left undisturbed for 24 hrs. The red plate crystals were collected by filtration.

Isolated yield: 61%, IR (KBr, cm^{-1}): 3431 (bs), 2923 (w), 1732 (s), 1651 (s), 1588 (w), 1495 (w), 1436 (m), 1384 (s), 1315 (m), 1274 (m), 1149 (s), 1138 (s), 1120 (s), 1089 (m), 801 (w), 752 (m), 725 (s), 690 (s),542 (s); ^{1}H NMR (DMSO-d_6, 400 MHz): 8.04 (d, J = 3.2 Hz, 2H), 7.86 (d, J = 6.8Hz, 2H), 7.65 (m, 6H), 7.56 (m, 3H), 7.48 (m, 6H), 4.06 (s, 4H); ^{13}C NMR (DMSO-d_6, 100 MHz): 170.9, 150.8, 144.3, 134.1, 133.8, 132.7, 126.9, 121.7, 35.7; ^{31}P NMR (DMSO-d_6): -25.69.

4.1.4 Procedure for the synthesis of salt 4.8

2-[(Pyridine-3-yl-methyl)-[1,4]-naphthoquinone **4.6** (0.132 g, 0.5 mmol) was dissolved in 15 ml of methanol in a conical flask and 5 ml of 15% perchloric acid (0.75 ml by volume of concentrated perchloric acid) was added slowly from the wall of the conical flask. The resulting solution was kept undisturbed and it gave reddish yellow crystals within 2 hrs on the wall of the conical flask. This desired hydrated salt **4.8** was collected by filtration.

Isolated yield: 62%, IR (KBr, cm^{-1}): 3439 (bw), 3174 (w), 2923 (w), 1709 (s), 1679 (m), 1642 (s), 1591 (m), 1437 (m), 1387 (s), 1353 (s), 1295 (s), 1231 (m), 1202 (s), 1130 (m), 1100 (s), 982 (w), 875 (w), 784 (s); ^{1}H NMR (DMSO-d_6, 400 MHz): 8.92 (s, 1H), 8.76 (s, 1H), 7.56 (d, J = 8.4, 1H). 8.06 (d, J = 7.6 Hz, 1H), 8.01 (d, J = 7.6Hz, 4H), 7.58 (t, J = 7.6, 1H), 7.74 (d, J = 7.6, 1H), 5.66 (s, 1H), 4.70 (d, J = 6.8Hz, 2H); ^{13}C NMR (DMSO-d_6, 100 MHz): 183.0, 148.3, 145.1, 141.4, 134.9, 132.6, 127.6, 126.5, 126.1, 102.0, 42.9.

Chapter 5

Carbon-sulphur bond breaking reaction of carboxylic acids attached to quinone to form the metal complexes

Carbon-sulphur bond cleavage via transition-metal complexation is useful in organic synthesis[326-345] but less numbers of such reactions are studied to synthesize metal complexes.[346-347] Advantages of chelate effect can be taken in synthesis of metal-sulphide containing complexes.[346-347] The thiolato ether containing sulphur compounds are interesting biological models of galactose oxidase for selective oxidation reactions.[348-350] From this context, the carbon-sulphur bond cleavage reaction of sulphanyl carboxylic acids attached to quinone via transition-metal complexation and their utility in oxidation reactions are described. We have selected (3-carboxymethylsulfanyl 1,4-dioxo-1,4-dihydronaphthalen-2-yl-sulfanyl) acetic acid **5.1** and 2-(3-methyl 1,4-dihydronaphthalen-2-yl-sulfanyl) nicotinic acid **5.2** for such study (**fig. 5.1**).

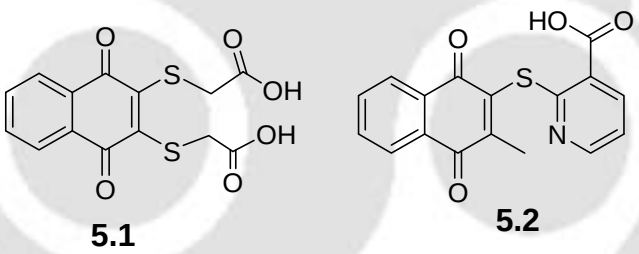

Fig. 5.1

5.1 Copper(II) complexes of 2-(1,4-dihydro-2-mercapto 1,4-dioxonaphthalen-3-ylthio) acetic acid

The (3-carboxymethylsulfanyl 1,4-dioxo-1,4-dihydronaphthalen-2-yl-sulfanyl) acetic acid **5.1** have several possible paths for carbon-sulphur bond cleavage as shown in **fig. 5.2**. However, the reaction of (3-carboxymethylsulfanyl 1,4-dioxo-1,4-dihydro-naphthalen-2-ylsulfanyl) acetic acid **5.1** with copper(II) nitrate tetrahydrate found to selectively cleavage of one of the carbon-sulphur bond of **5.1** to form

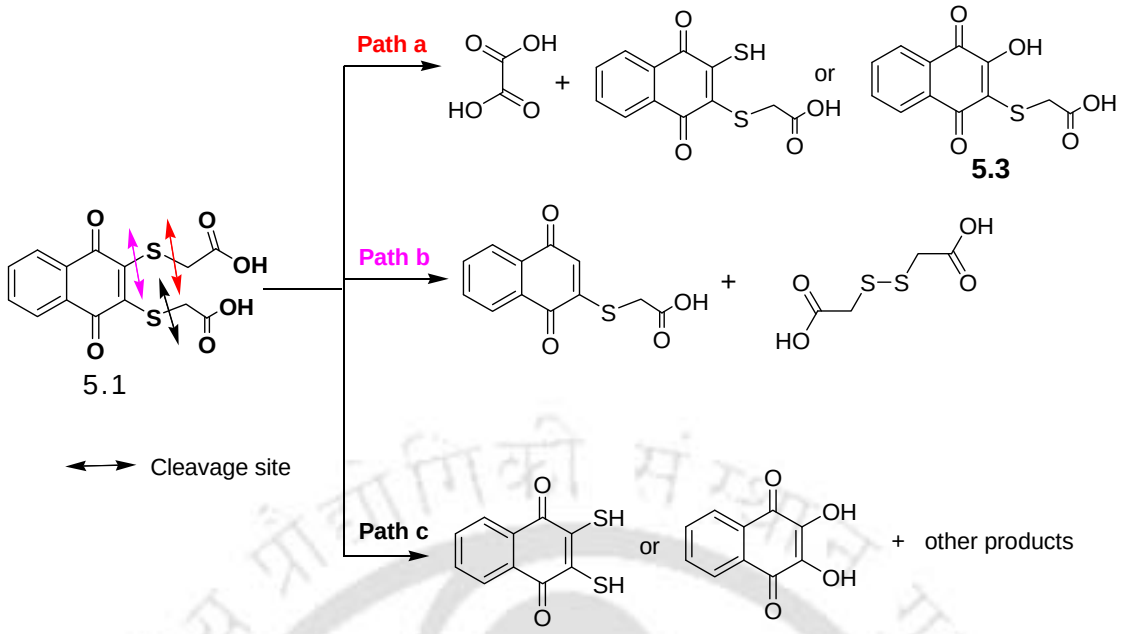

Scheme 5.1 Different possibilities for C-S bond cleavage in compound **5.1**

copper(II) complexes $[Cu_2(L_1)_2(bipy)_2]$, **5.4** and $[Cu_2(L_1)_2(phen)_2][Cu(L_1)(phen)].5H_2O$ **5.5** of 2-(1,4-dihydro-2-hydroxy 1,4-dioxonaphthalen-3-ylthio) acetic acid **5.3** (**scheme 5.1**). Such reactions of copper(II) nitrate tetrahydrate with (3-carboxymethylsulfanyl 1,4-dioxo-1,4-dihydronaphthalen-2-ylsulfanyl) acetic acid **5.1** were used to synthesize two different metal complexes of **5.3** by further reaction with 2,2'-bipyridine or 1,10-phenanthroline such as compounds **5.3** and **5.4**, respectively (**scheme 5.2**).

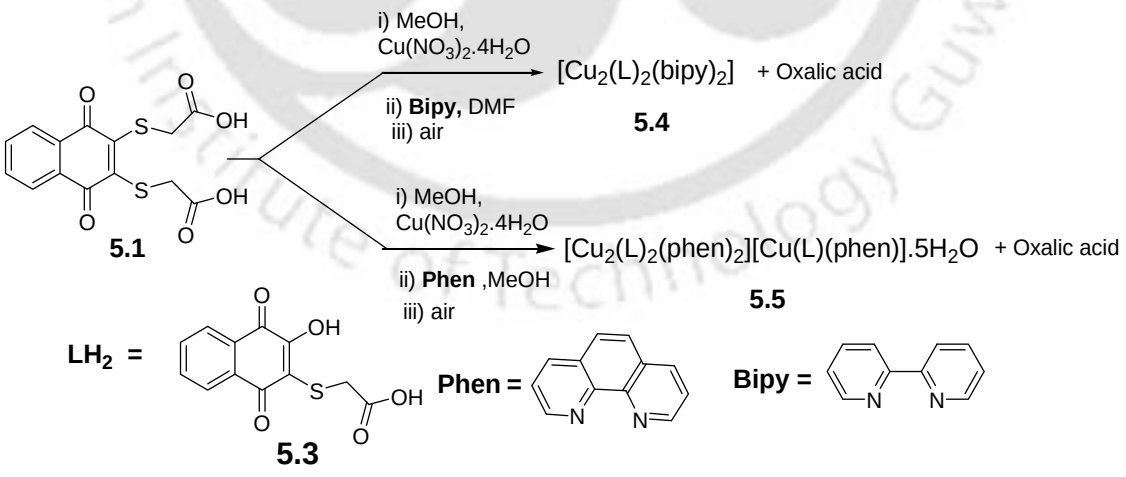

Scheme 5.2 Synthesis of copper(II) complexes through C-S bond cleavage

The complex **5.3** was obtained as greenish solid and it crystallizes in centrosymmetric monoclinic $P2_1/n$ space group. This binuclear copper(II) complex **5.3**, has copper(II) ions in six coordinated distorted octahedron environment.

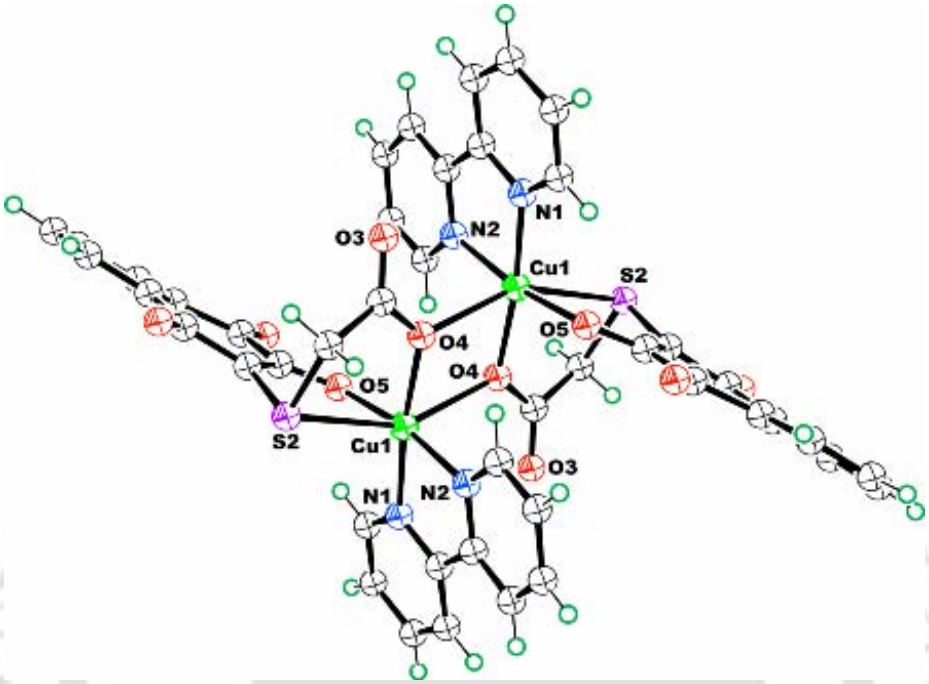

Fig. 5.1 Crystal structure of complex **5.4** (ORTEP drawn with 50% thermal ellipsoids)

Each copper (II) ion is coordinated to two oxygen atoms of two carboxylates from two ligands **5.3** in bridging mode. There is also one sulphur atom coordinating to copper(II) one each from thioether part. One oxy group derived from the hydroxyl part of **5.3** and two nitrogen atoms from 2,2′-bipyridine (**fig. 5.1**) are attached to copper ion. The Cu–N distances 1.99 Å and 2.01 Å are similar to those found in other copper(II) complexes.[351-353] The Cu1–O4 bond (1.99 Å) and Cu1–O5 bond distances (1.95 Å) are comparable. The Cu1–S2 bond distance is 2.75(8) Å which is usual; however there are examples in the literature of short copper–sulphur distances.[354-355] The bridging mode of carboxylate in the complex to hold two copper(II) ions resembles the diamond core Cu_2O_2.[356-357] The molecule has a center of inversion located at the center of diamond core of Cu_2O_2. The dinuclear copper(II) acetate has Cu···Cu distance of separation 2.61 Å,[358] whereas in generally observed Cu_2O_2 cores, such distances are in the range of 2.79–2.99 Å.[346-348] In the case of complex **5.4** the Cu···Cu distance of separation is 3.473 Å, this supports much weaker interactions to form such core. This observation is reflected in the ESI mass spectra record of the sample dissolved in DMF and

acetonitrile mixed solvent, which shows a mass ion peak at 439.96 (m/e) due to formation of $[Cu(L_1)(DMF)(CH_3CN)]$ in such solution. The ligand **5.1** has an absorption maximum at 440 nm which on addition of copper(II) nitrate tetrahydrate decreases and a new absorption peak at 780 nm develops as shown in **fig. 5.2**.

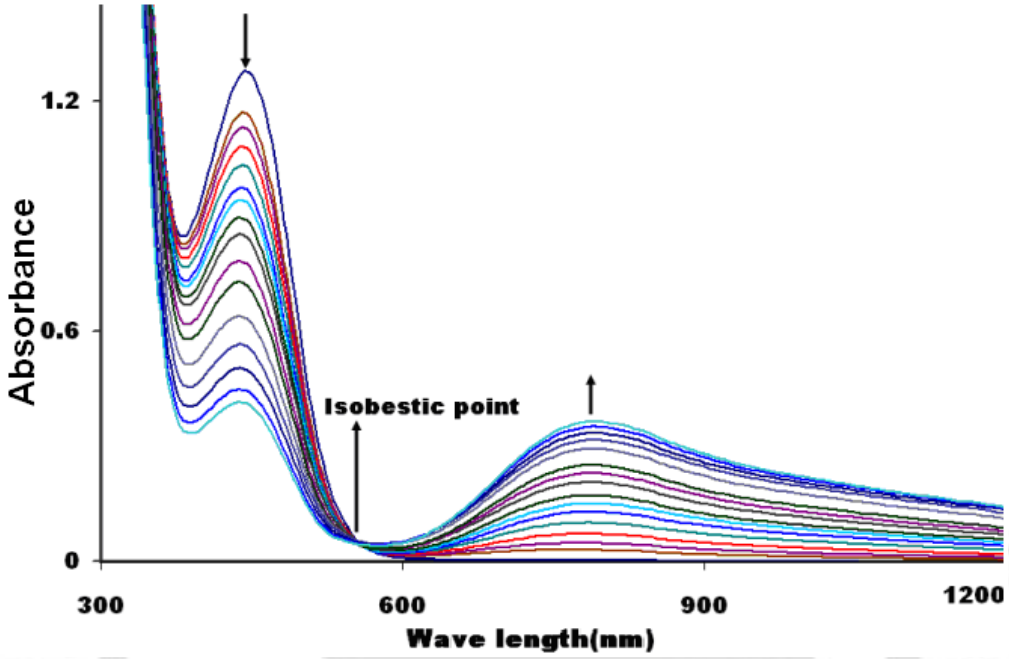

Fig. 5.2 UV-visible spectra of **5.1** upon addition of copper nitrate tetrahydrate in methanol (1×10^{-3} M)

This presumably occurs due to formation copper(II) complex through C–S bond cleavage. The process passes through an isosbestic point at 560 nm. Further addition of 2,2′-bipyridine to this solution results in shift of the absorption maximum towards the lower wavelength. Both the copper(II) complexes **5.4** and **5.5** shows absorption maximum at 630 nm due to the d-d electronic transitions as shown in **fig. 5.3b**. This suggests the formation of the complex **5.4**, (**fig. 5.3**). When we compared the absorption spectra of different compositions of mixture of copper nitrate tetrahydrate and 2,2′-bipyridine in methanol (1:3 molar ratios); we have found that an absorption maximum at 750 nm as shown in **fig. 5.3a** in the presence of bipyridine ligand. From this also it is clear that the shifting of the absorption maximum is due to formation of the desired copper complex. This also suggests the hydrolytic C–S cleavage of **5.1** ligand by copper(II) nitrate to form the copper(II) complexes of **5.3**.

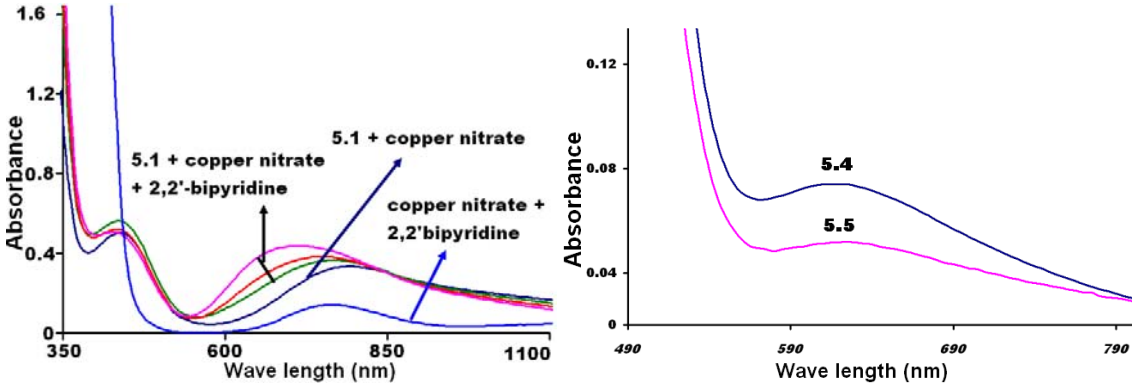

a b

Fig. 5.3 UV-visible spectra of a) compound **5.1** upon addition of copper nitrate tetrahydrate and 2,2′-bipyridine in methanol (1×10^{-3} M); b) complexes **5.4** and **5.5** in DMF **(**1×10^{-3} M)

Based on this a reaction mechanism is proposed as illustrated in **scheme 5.3**. In this proposed reaction path, in the first step the ligand **5.1** reacts with copper(II) nitrate tetrahydrate to form a polymeric complex and it gets hydrolytically cleaved. In the presence of 2,2'-bipyridine, the bond rearrangement occurs to form the complex **5.4** as shown in **scheme 5.3**.

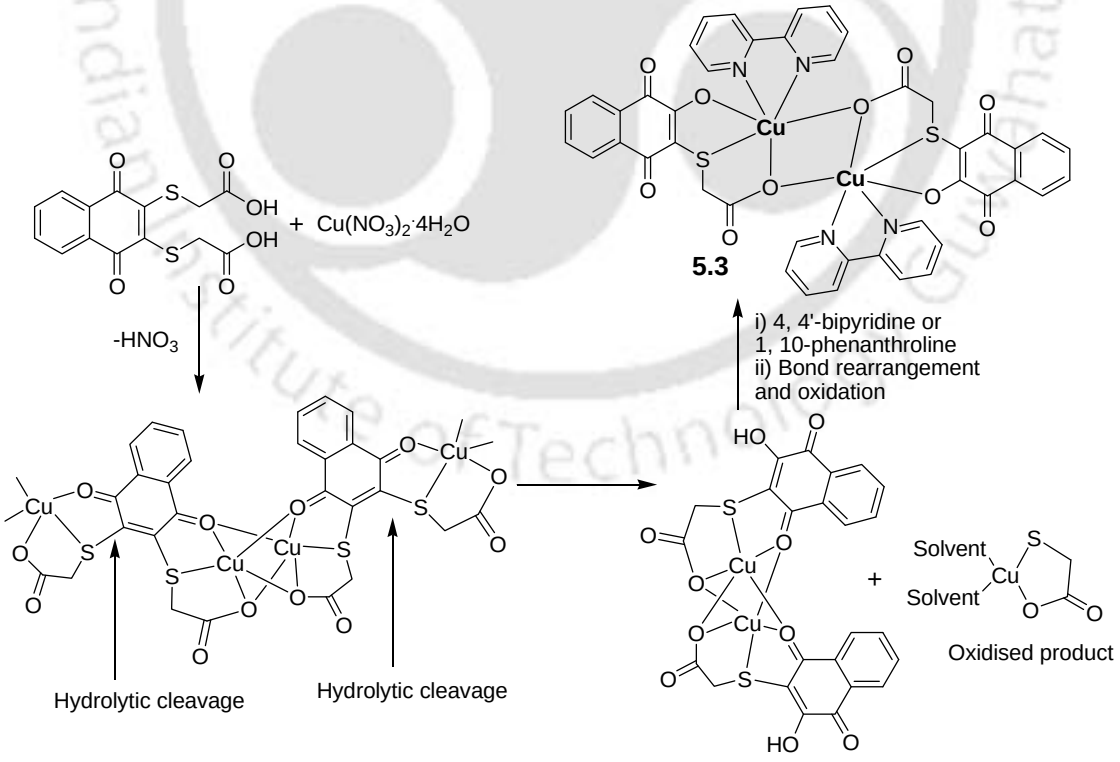

Scheme 5.3 Plausible mechanism for the synthesis of copper(II) complexes **5.3** and **5.4**

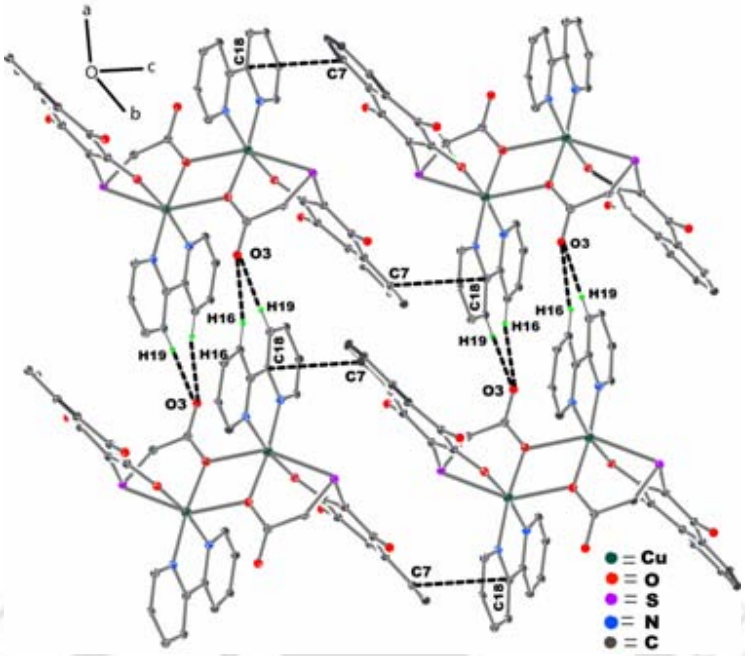

Fig. 5.4 Self assembly of complex **5.4** (Hydrogen atoms are removed for clarity; ORTEP drawn with 30% thermal ellipsoids)

The complex **5.4** is stabilized by C−H···O (C4−H4···O3, C14−H14···O2, C16−H16···O3 and C19−H19···O3), C−H···π (C4−H4···π_{12} $d_{D\cdots\pi}$, 3.49 Å) and π···π ($\pi_7\cdots\pi_{18}$ $d_{\pi\cdots\pi}$, 3.38 Å) interactions as shown in **fig. 5.4**. Some of the important hydrogen bond distances and bond angles of complex **5.4** are shown **table 5.1**.

Table 5.1. The hydrogen bond parameters for compound **5.4**

D−H···A	D−H (Å)	H···A (Å)	D···A (Å)	<D−H···A(°)
C4−H4···O3	0.930	2.429	3.313	158.9
C14−H14···O2	0.930	2.645	3.342	132.3
C16−H16···O3	0.931	2.573	3.471	162.4
C19−H19···O3	0.930	2.266	3.193	175.8

The complex **5.5** is a self-assembly of a neutral mononuclear copper(II) and a binuclear copper(II) complexes having five water molecules of crystallization and we could not locate the hydrogen of these water molecules. The complex **5.5** crystallizes in centrosymmetric triclinic P-1 space group. The mononuclear part of the assembly has five coordination environments by one oxygen from carboxylate ion; one oxygen from oxy group derived from hydroxyl group, one sulphur from thioether of ligand **5.3** and two nitrogen atoms from chelating 1,10-phenanthroline.

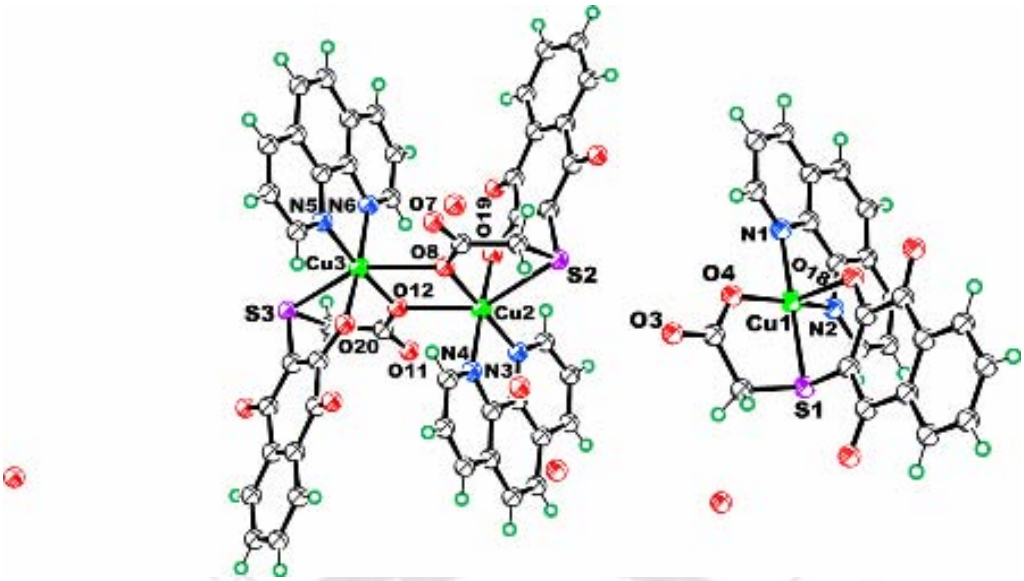

Fig. 5.5: The crystal structure of molecular complex **5.5** (ORTEP drawn with 50% thermal ellipsoids).

Table 5.2 Some of the metal ligand bond distances (Å) and the bond angles (°) for copper(II) complexes **5.4** and **5.5**

5.4		**5.5**					
Bond	Distances	Bond	Distances	Bond	Angles	Bond	Angles
Cu1-O5	1.95(17)	Cu2-O8	1.964(5)	O8-Cu2-O19	93.8(2)	O20-Cu3-N5	91.0(2)
Cu1-O4	1.99(16)	Cu2-O19	1.963(5)	O8-Cu2-N3	175.6(3)	O12-Cu3-N5	175.0(2)
Cu1-N1	1.99(2)	Cu2-N3	1.980(7)	O19-Cu2-N3,	90.2(3)	O20-Cu3-N6	172.0(3)
Cu1-N2,	2.01(2)	Cu2-N4	2.016(6)	O8-Cu2-N4	94.4(3)	O12-Cu3-N6	94.4(2)
Cu1-S2	2.75(8)	Cu2-O12	2.423(5)	O19-Cu2-N4	171.3(3)	N5-Cu3-N6	81.1(3)
Bond	Angles	Cu2-S2	2.755(2)	N3-Cu2-N4	81.7(3)	O20-Cu3-S3	80.5(16)
O5-Cu1-O4	93.7 (7)	Cu3-O20	1.970(5)	O8-Cu2-O12	74.8 (2)	O12-Cu3-S3	79.5(16)
O5-Cu1-N1	170.5(8)	Cu3-O12	1.978(5)	O19-Cu2-O12	86.8(19)	N5-Cu3-S3	103.6(17)
O4-Cu1-N1	95.4 (8)	Cu3-N5	1.986(6)	N3-Cu2-O12	107.4(2)	N6-Cu3-S3	101.7(18)
O5-Cu1-N2	90.5 (8)	Cu3-N6	2.042(6)	N4-Cu2-O12	92.5(2)	N3-Cu2-S2	100.5(18)
O4-Cu1-N2	172.9(7)	Cu3-S3	2.665(2)	O8-Cu2-S2	78.5(16)	N4-Cu2-S2	105.6(18)
N1-Cu1-N2	80.9(8)	Cu1-O4	1.904(6)	O19-Cu2-S2,	79.0(16)		
O5-Cu1-S2	79.6(5)	Cu1-N2	2.006(7)	O12-Cu2-S2	148.7(13)		
O4-Cu1-S2	78.3(5)	Cu1-N1	2.013(6)	O20-Cu3-O12	93.5(2)		
N1-Cu1-S2	99.2(6)	Cu1-O18	2.133(5)				
N2-Cu1-S2	108.2(6)	Cu1-S1	2.345(2)				

These bonds form trigonal pyramidal geometry around each copper ion with O4, O18, N2 making a triangular plane with N1 and S1 occupying epical positions as shown in **fig. 5.5**. The dinuclear part of complex **5.5** has similar structural feature of the complex **5.4**. The dimeric part of the complex **5.4** may arise from a combination of two mononuclear five coordinated species that combined together through expansion of coordination number of copper to six. Some of the metal ligand bond distances (Å) and

the bond angles (°) for copper(II) complexes **5.4** and **5.5** are listed in **table 5.2**. The formation of the mononuclear and dinuclear molecular assembly in **5.4** and **5.5**, is due to the weak interactions among the mononuclear part to associate to form dinuclear molecules as evident from the Cu···Cu separation of 3.54 Å in the complex **5.5**, which is slightly higher than the observed separation for **5.4**. This complex also degrades in solution of dimethylformamide and acetonitrile and shows identical mass spectra as that of **5.4**.

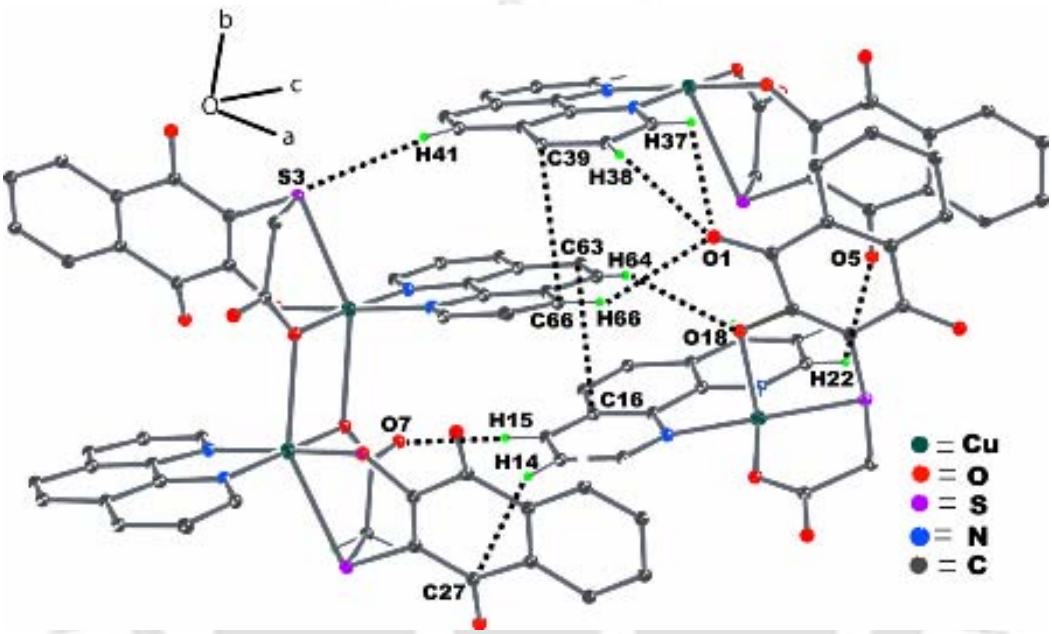

Fig. 5.6 Weak interactions in the formation of self-assembled structure of complex **5.5** (Hydrogen atoms are removed for clarity; ORTEP drawn with 30% thermal ellipsoids)

Table 5.3 The hydrogen bond parameters for compound **5.5**

D−H···A	D−H (Å)	H···A (Å)	D···A (Å)	<D−H···A(°)
C15−H15···O7	0.930	2.289	3.170	157.8
C22−H22···O5	0.930	2.449	2.899	109.8
C37−H37···O1	0.930	2.501	2.862	102.2
C38−H38···O1	0.930	2.708	2.952	95.9
C64−H64···O18	0.930	2.554	3.391	150.0
C66−H66···O1	0.930	2.708	3.534	148.3
C41−H41···S3	0.930	2.941	3.635	132.6
C14-H14···π_{C27}	0.930	2.873	3.718	

The solid state assembly of mononuclear and dinuclear part of **5.5** is stabilized by C–H···O, C–H···π, and C–H···S, interactions among the ligands **5.3** and 1,10-

phenanthroline rings (**fig. 5.6**). The crystal structure is also stabilized by π···π ($\pi_{16}\cdots\pi_{63}$, $d_{\pi\cdots\pi}$, 3.354 Å; $\pi_{39}\cdots\pi_{66}$, $d_{\pi\cdots\pi}$, 3.274 Å) interactions between the 1,10-phenanthroline molecules. Some of the selective hydrogen bond parameters of complex **5.5** are listed in **table 5.3**.

The powder X-ray diffraction of both the complexes **5.4** and **5.5** were recorded and compared with theoretical patterns. A very good agreement with the theoretical powder X-ray diffraction from the determined crystal structure was observed. This shows bulk purity of the samples and also confirms the determined structures. The powder patterns are shown in **fig. 5.7** (black line = experimental; blue line = theoretical). The molar conductance of complexes **5.4** and **5.5** in *N,N′*-dimethylformamide gives 4 and 0.5 S cm^2 mol^{-1} respectively.

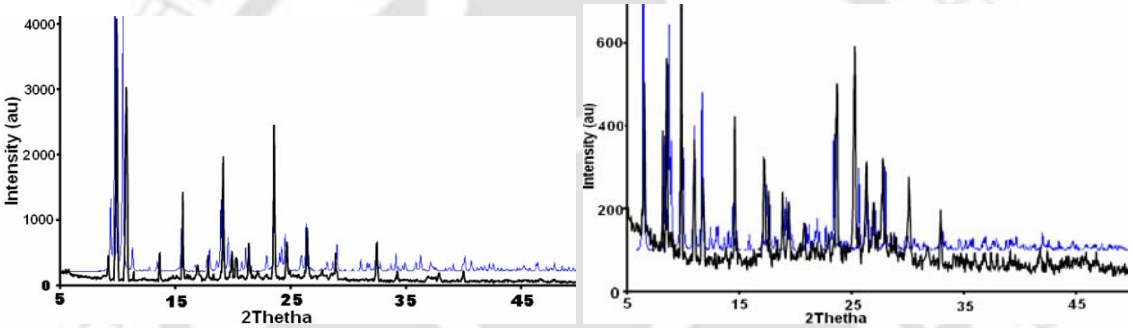

Fig. 5.7 Powder diffraction pattern of complex a) **5.4**; b) **5.5** (black line = experimental; blue line = theoretical)

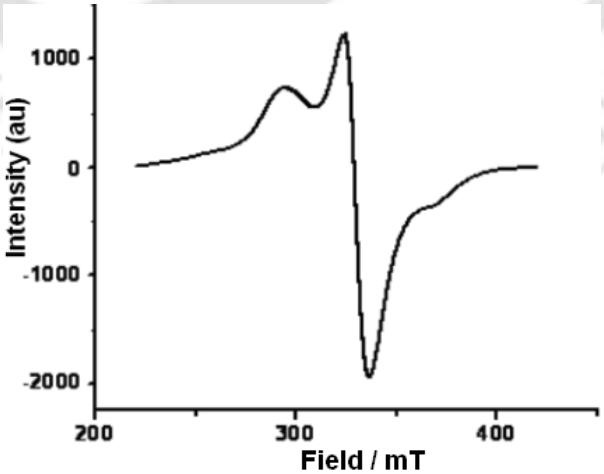

Fig. 5.8 Solid state EPR spectra of copper(II) complex **5.5** at room temperature (center field = 350.0G, power = 998000 mw, frequency = 9447.059, sweep time = 30s)

The solid state electron paramagnetic resonance spectra of the complexes **5.4** and **5.5** were recorded on crystalline samples at room temperature. The EPR spectra of these complexes closely resemble to those obtained for binuclear complexes. We have assigned pair of bands at 297.3053 G (g_{II} = 2.26) and 324.0635 G ($g_{\perp}$ = 2.08) as due to $\Delta M_s = \pm 1$ transitions. The EPR spectra of copper(II) complex **5.5** is shown in **fig. 5.8** as an illustrative example.

Oxalic acid is formed in each of these reactions and a copper(II) oxalato complex $[Cu_2(oxalato)(py)_2(NO_3)_2(H_2O)_2]$, **5.6** could be isolated from the reaction of **5.1** with copper(II) nitrate tetrahydrate followed by treatment with pyridine (py). Even though it has poor quality crystals, based on X-ray data the crystal structure of the complex **5.6** is shown in **fig. 5.9**. This complex **5.6** has characteristic strong absorption at 1667 cm^{-1}, due to oxalate group and strong absorption at 1384 cm^{-1} due to coordinated nitrate anion. The coordinated water appears at 3420 cm^{-1}. The compound has two unsymmetric copper sites; one is anchored by two nitrate anions and two pyridine molecules, whereas the other is anchored by two pyridines, two water molecules and two anionic oxygen atoms of oxalate. These two units are held together by the two carbonyl groups of the oxalate that act as a bridge to make both the copper sites six coordinated.

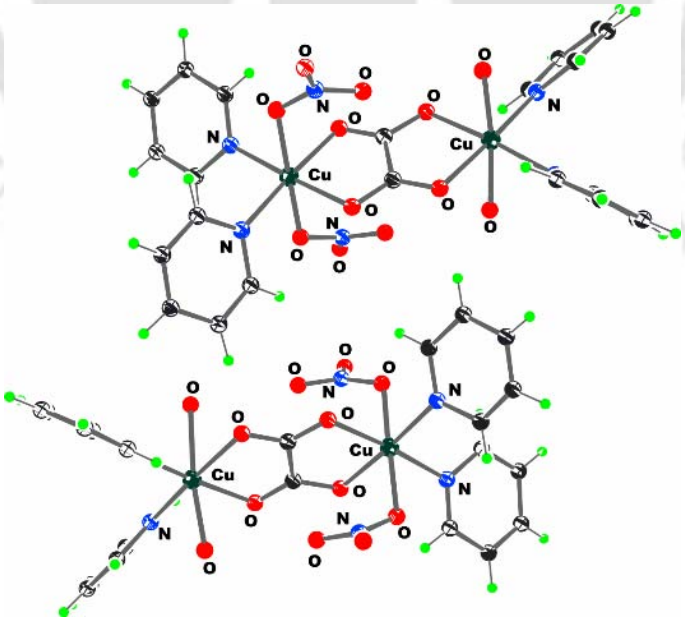

Fig. 5.9 Crystal structure of complex **5.6** (ORTEP drawn with 50% thermal ellipsoids)

Thus, isolation of such oxalate complex also suggests an oxidative cleavage of the carbon-sulphur bond. Coordination chemistry of quinone complexes[177-181, 165-169] is extensively studied. They are important due to their electron-transfer rates and redox potentials is often linked to their biological action. However, despite this wide interest of quinone derivatives in coordination chemistry, the metal complexes of quinonic carboxylic acid ligands are not available. Due to multiple possibilities of coordination of carboxylic acid group on the quinone ring, the increased complication in binding of ligand to metal ions make it interesting to take up such study. Thus the above study provides a general and simple synthetic procedure to prepare metal complexes of sulfur containing quinonic carboxylic acid ligand.

5.2 Carbon-Sulphur bond cleavage by iron(II) and manganese(II): utilities of such reactions

The cleavage of benzylic C-S bond to prepare copper(I) clusters from thioether ligands is reported.[359] So, we have chosen this compound 2-(3-methyl-1,4-dihydronaphthalen-2-yl-sulfanyl) nicotinic acid **5.2** that has a carboxylic acid group and also a nitrogen atom adjacent to sulphur atom. The compound 2-(3-methyl-1,4-dihydronaphthalen-2-yl-sulfanyl) nicotinic acid **5.2** also occurs C-S bond cleavage reaction in the presence of metal ions such as Fe^{+2} and Mn^{+2} and lead to the formation of S-S bond containing compounds as illustrate in **scheme 5.4**. We report here reactions of **5.2** with iron(II) and manganese(II) salts to prepare new complexes through C-S bond cleavage. An iron complex containing 1,10-phenanthroline ligand formed during such C-S bond cleavage reaction is a useful catalyst for epoxidation and oxidation reactions.

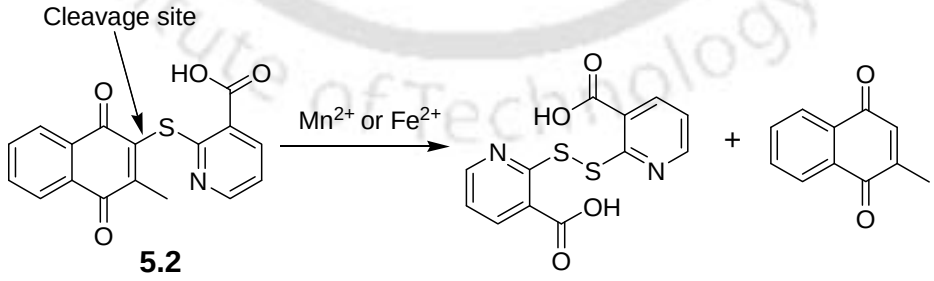

Scheme 5.4 C-S bond cleavage leading to S-S bond formation

The 2-(3-methyl-1,4-dioxo-1,4-dihydronaphthalene-2-yl-sulfanyl) nicotinic acid **5.2** was synthesized by reaction of 2-methyl 1,4-naphthoquinone with 2-mercaptonicotinic

acid. The elemental analysis shows that ligand is obtained in solvated form having composition $H_2L(0.5DMF)(1.5H_2O)$, **5.2**. This is further supported by the ^1H NMR and ^{13}C NMR spectra, in which signals of the DMF can be clearly seen. The high resolution mass spectrum shows highest mass corresponding to the ligand at 326.0512 (m/z, m +1). The ligand **5.2** reacts with iron(II) sulphate tetrahydrate and 1,10-phenanthroline, resulted in the formation of a mononuclear iron(II) complex **5.7**. Whereas, a polymeric manganese(II) complex **5.8** was formed from the reaction of **5.2** with manganese(II)

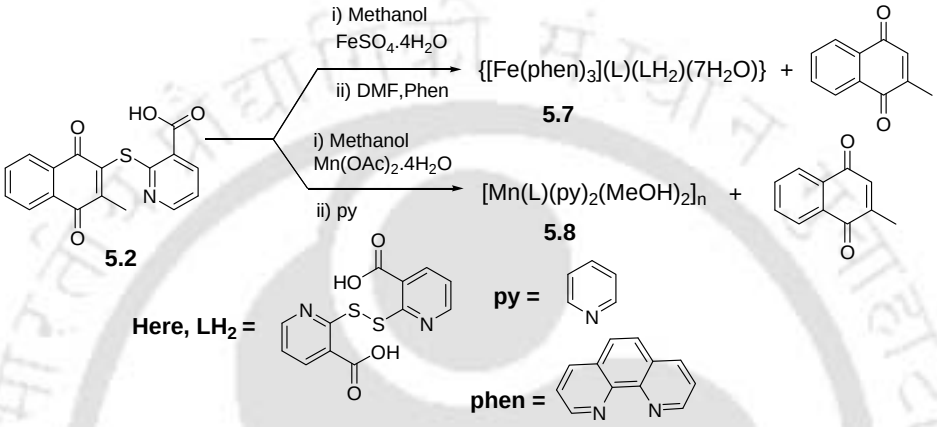

Scheme 5.5 Synthesis of complexes **5.7** and **5.8**

acetate tetrahydrate in the presence of pyridine as shown in **scheme 5.5**. In both the reactions, after the C-S bond cleavage 2-methyl 1,4-naphthoquinone is formed. There are good numbers of examples on C-S bond cleavage reactions that are believed to pass through radical mechanism leading to hydrodesulfurised products.[360-362] Thus, these reactions are also believed to pass through radical mechanism via cleavage of C-S bond, leading to formation of S-S bond. The complex **5.7** was obtained as crystalline red blocks in centrosymmetric monoclinic $P2_1/c$ space group; it has a crystal structure that is shown in **fig. 5.10**. The elemental analysis of the bulk sample of complex was not consistent, repeated crystallization of product showed a composition of the complex with **$[Fe(HL)_2]$**, which corresponds to the loss of 1,10-phenanthroline ligands. However, the crystalline compound **5.7** is stable under ordinary condition. It is a hexa-coordinated mononuclear octahedral iron(II) complex; having three chelating 1,10-phenanthroline ligands. The complex has one deprotonated and one neutral dicarboxylic acid (**LH_2**) outside the coordination sphere.

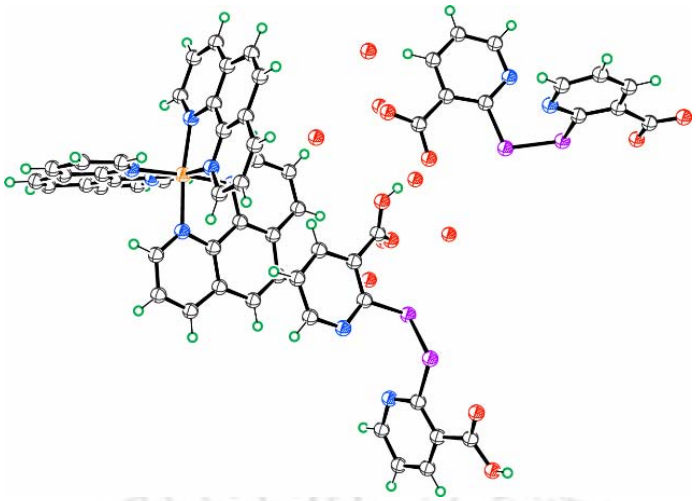

Fig. 5.10 Crystal structure of the iron(II) complex **5.7** (ORTEP drawn with 50% thermal ellipsoids)

These act as wrapper for the complex *tris*-(1, 10-pheanthroline) iron(II) cation as illustrated in fig. **5.11d**. The two carboxylic acid/carboxylate groups across the S-S bond are *anti* to each other. The complex has seven molecules of water of crystallization. The complex **5.7** is highly soluble in common solvents including water, makes it easy to handle in solution.

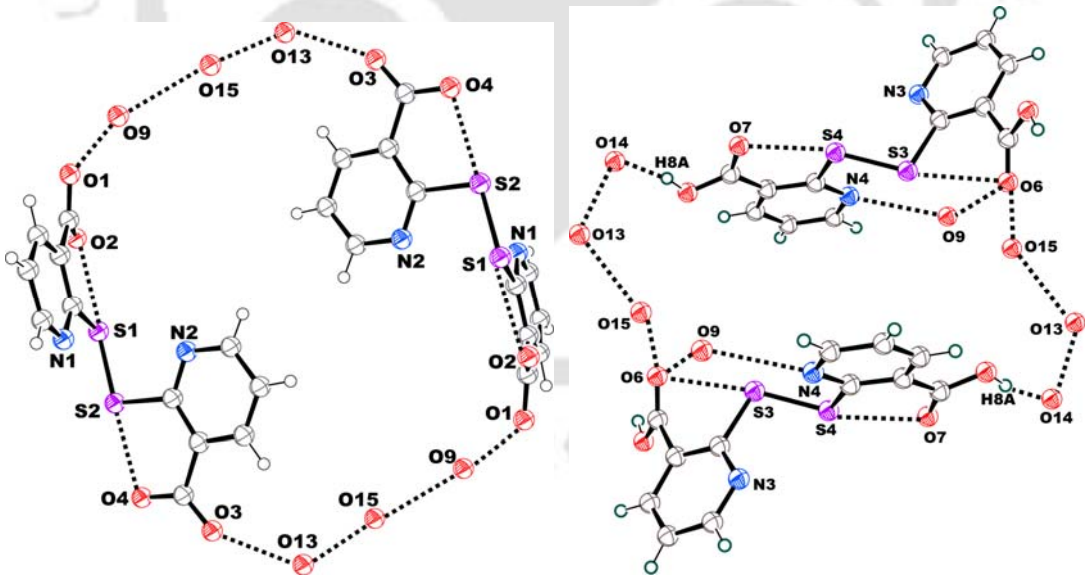

a b

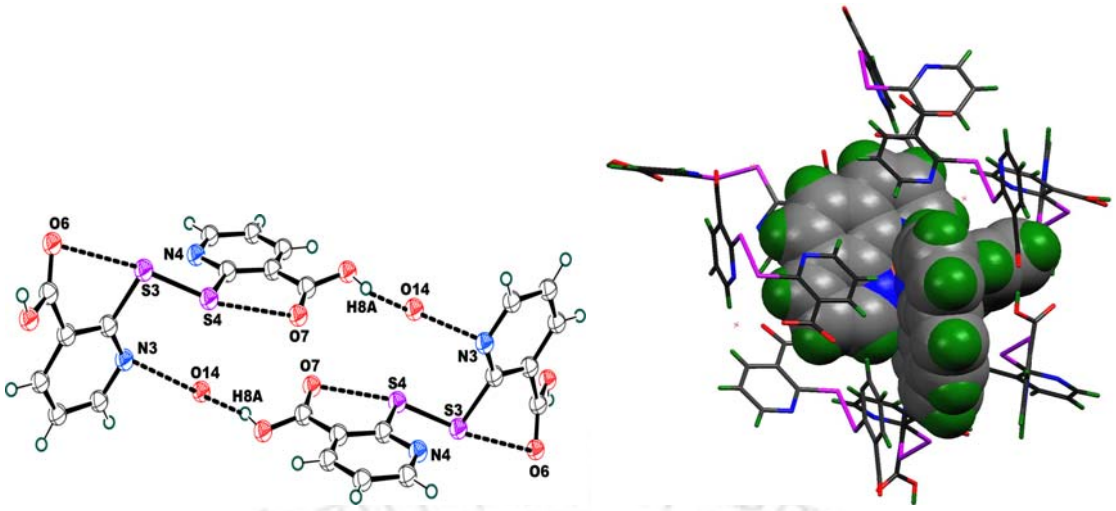

c d

Fig. 5.11 The position of oxygen atoms of water molecules in cyclic structures formed by a) **L** with water; b) **H_2L** with water molecules; c) between another **H_2L** with water molecules (The hydrogen atoms attached to oxygen of water could not be located; ORTEP drawn with 50% thermal ellipsoids); d) The encapsulation of $[Fe(Phen)_3]^{2+}$ by the carboxylates and carboxylic acids.

The iron-nitrogen bond distances of the complex are in the range of 1.97-1.98 Å, which are typical of high spin iron(II) complexes.[363] The complex is stabilized by O−H···O, C−H···N, C−H···O, C−H···S, C−H···π and π···π interactions. It also forms hydrogen bonded macrocyclic structure between the carboxylate ions **L** or carboxylic acids **LH_2** with water molecules as shown in **fig. 5.11**.

The solid state X-band (9.44GHz) EPR pattern complex **5.7** is analyzed at room temperature. Complex **5.7** does not show any line spectrum indicating the complex is iron(II) complex as it has the even number of unpaired electrons. The complex **5.7** shows visible absorption at 507 nm in methanol. The cyclic voltamogram of a 10^{-4} M solution of complex **2** in acetonitrile with tetrabutyl ammonium perchlorate as supporting electrolyte at scan rate of 50 mV per second shows reversible redox couple of Fe(II)/Fe(III) at $E_{1/2}$ = 1.08 V (i_p/i_c = 1.0 and ΔEp = 0.062V) as shown in **fig. 5.12**. This value is comparable to similar complex cation namely *tris*-(3-bromo-1,10-phenanthroline) iron(II) ($E_{1/2}$=1.26V).[364]

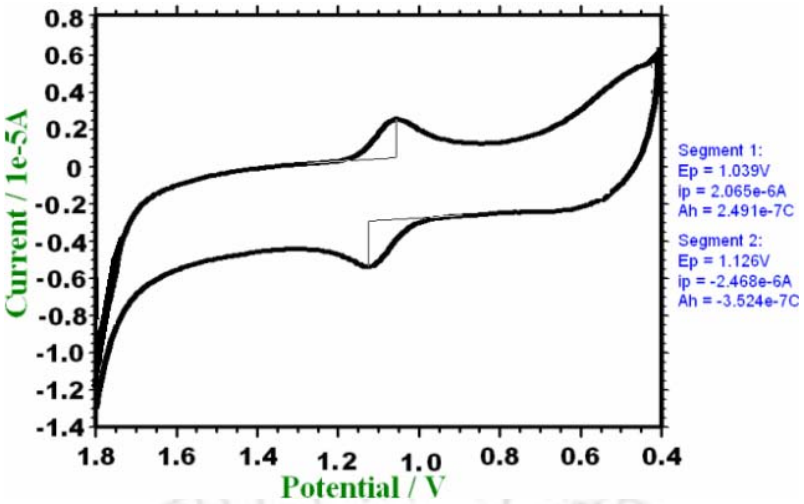

Fig. 5.12 Cyclic voltametry of iron(II) complex **5.7** in 10^{-4} M solution acetonitrile

The reaction of **5.2** with manganese(II) acetate followed by treatment with pyridine gave a one dimensional coordination polymer **5.8** (**fig. 5.13**). The formation of **5.8** occurs through C-S bond cleavage and concomitant S-S bond formation. The coordination polymer has six coordination environments around the manganese centers. The carboxylate groups of the ligand (**LH_2**) bridges two manganese ions and each manganese ion has two pyridine ligands and two methanol ligands. The polymer has manganese ions that have octahedral geometry (**fig. 5.14**). There are two pyridine ligands as well as the two methanol ligands both the pairs are *trans* to each other. The two aromatic rings attached to the sulphur atoms are also *trans* to each other across a S-S bond. The polymer is stabilized by the strong O−H···O (O3−H3O···O2, $d_{D\cdots A}$, 2.64 Å, and <D-H···A 164.0º) interactions and weak C−H···π (C3−H3···π_{10}, $d_{D\cdots\pi}$, 3.55 Å) and C5−H5···π_{11}, $d_{D\cdots\pi}$, 3.63 Å) interactions and has a chain like structure going along the c axis as shown in **figure 5.14**. The coordination polymer has magnetic moment 5.42 B.M. per manganese ion at room temperature; which is slightly less than the expected spin only value for a d^5-system. Molar susceptibility, effective magnetic moment and spin only magnetic moment (μ_M, μ_{eff} and μ_{so}) of complex **5.8** are list in **table 5.4**. In complex **5.8** $\mu_{eff} < \mu_{so}$ reveals the existence of antiferromagnetic interactions.

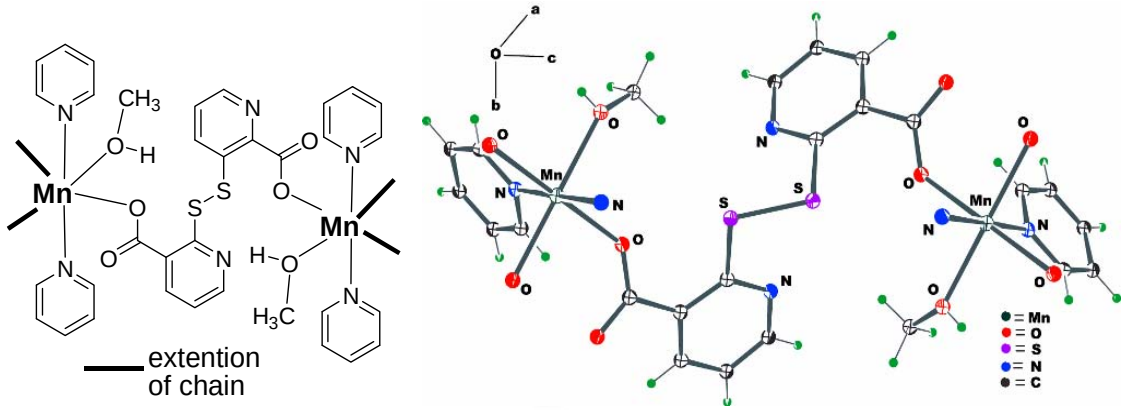

a b

Fig. 5.13 (a) The repeated units of manganese(II) coordination polymer **5.8**, (b) Crystal structure of the repeated unit in the **5.8** (ORTEP drawn with 30% thermal ellipsoids)

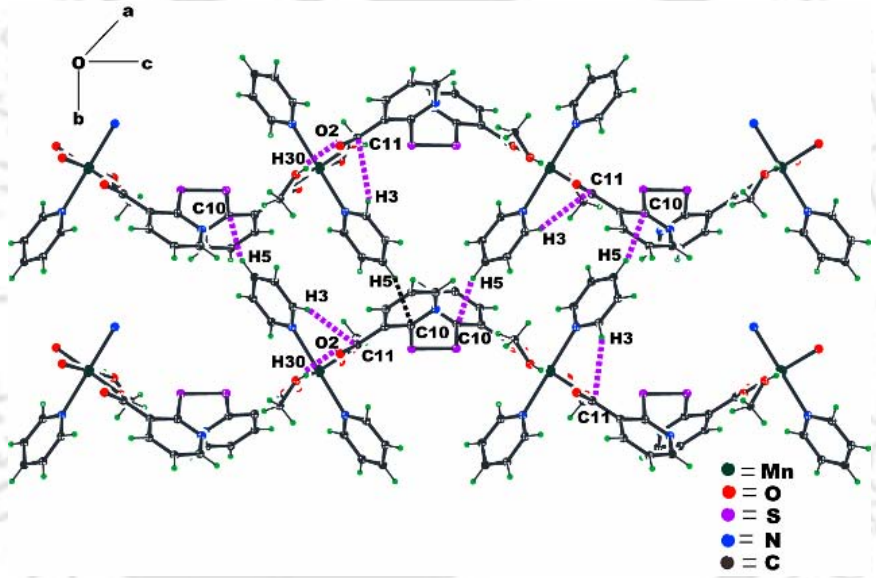

Fig. 5.14 Structure of complex **5.8** showing the chain like structure (ORTEP drawn with 30% thermal ellipsoids)

Table 5.4 Molar susceptibility (μ_M), Effective magnetic moment (μ_{eff}) and Spin only magnetic moment (μ_{so}) value of complex **5.8**

Compound	**5.8**
$\mu_M \times 10^3$ (emumol^{-1})	12.31
μ_{eff} (BM)	5.42
μ_{so}	5.92

The solid state X-band (9.44GHz) EPR spectra of **5.8** at room temperature shows a broad single-line spectrum around 349.5 G and it has the g_{iso} = 1.995 (**fig. 5.15**). To ascertained this reaction, the reaction was performs by using already synthesized disulphide of 2-mercapto-nicotinic acid at same reaction condition.[365] In the case of iron we could not find the good quality crystal for crystallography but in case of manganese it forms already reported two dimensional coordination polymer.[366] However we obtained a crystal with one water molecule of crystallization but earlier they found two water molecules of crystallizations. Thus, the polymer formed through C-S bond cleavage has a different structure than the in situ generated polymer.

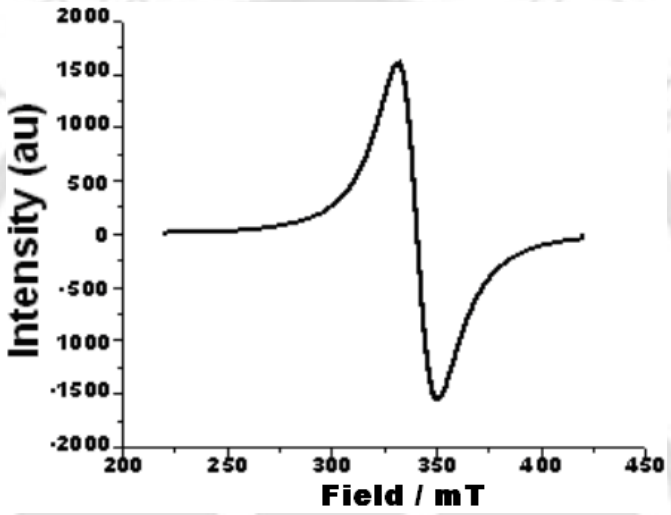

Fig. 5.15 Solid state EPR spectra of manganese(II) coordination polymer **5.8** at room temperature (center field = 350.0G, power = 998000 mw, frequency = 9442.829, sweep time = 30s)

In the above study, we have shown some novel C-S bond cleavage reactions leading to inorganic complexes which are conventionally difficult to prepare.

The iron(II) complex **5.7** is also a catalyst for epoxidation of alkenes in presence of hydrogen peroxide (**scheme 5.6**). Iron catalyzed epoxidation reactions are synthetically and mechanistically useful.[367-370] There are many iron containing enzyme catalysts[371-375] for epoxidation reactions of olefins. Biocompatible non-heme iron complexes[376-378] are also important catalysts for epoxidation reaction. The activity and selectivity of iron(II)[378-379] catalysed epoxidation reactions are controlled by carboxylic acids. Several epoxidation reaction catalysed by iron complexes are carried out in the presence of acid additives.[380-382]

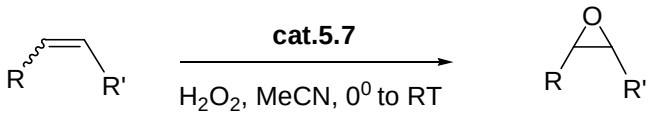

Scheme 5.5 Epoxidation reaction of olefins catalysed by **5.7**

Since the compound **5.7** has carboxylate anion as well as carboxylic acid outside the coordination sphere; these are expected to serve the purpose of the additives, in fact for this reason we did not require addition of any acid additive to carry out the epoxidation reactions. Various olefinic compounds were converted to corresponding epoxides by catalytic amount of complex **5.7** in the presence of hydrogen peroxide, which are listed in **table 5.5**.

Table 5.5 Epoxidation of olefins catalyzed by **5.7** (1 mole %) with hydrogen peroxide

Entry No.	Olefin	Product	Isolated yield [%]
1	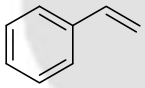	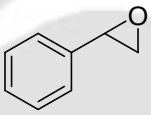	91%
2	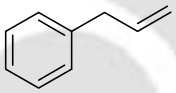	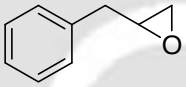	88%
3	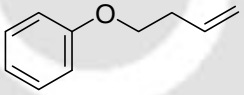	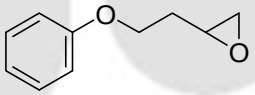	89%
4	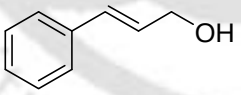	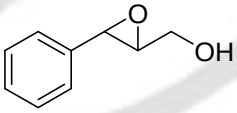	85%
5	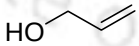	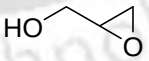	83%
6	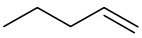	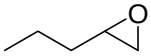	32%
7	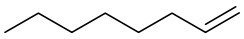	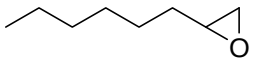	84%
8		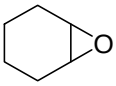	83%

The reaction proceeds under neutral condition. We did not observe any side product that were observed in the case of iron(III) catalysed epoxidation reactions.[381-382] The various epoxides formed in these reactions do not get converted to any other product such as *cis*-diols with the catalyst and showing selective product formation. It was reported earlier that the hydrogen bonding helps in epoxidation reactions of hydrogen peroxide,[383] thus we studied the catalytic activity of complex **5.7** (1 mole %) on epoxidation of styrene in different solvents such as dichloromethane, tetrahydrofuran, acetonitrile and in dimethylformamide respectively. From this study, we found comparable conversion more than 90% in the solvents tetrahydraofuran, acetonitrile and dimethylformamide. But the catalytic activity of complex **5.7** in dichloromethane was found to be lower with about 75% conversion of styrene to epoxide under identical conditions. To understand the ability of **5.7** to undergo solvation with different solvents, visible spectra of the complex was recorded in different solvents. It is found that the absorption peaks of the complex slightly changes with solvents (**fig 5.16a**). Strongly coordinating solvent DMSO takes the absorption to higher wavelength than the relatively less coordinating solvent acetonitrile (**fig. 5.16a**). The coordination polymer **5.8** was tested for catalytic activity in epoxidation reactions, but found to be inactive for such reactions.

The iron(II) complex **5.7** is also a catalyst for the oxidation of dihydroxy aromatic compounds. For example, the catalytic oxidation of hydroquinone and catechol led to corresponding quinones in quantitative yield (**scheme 5.6**) under ambient condition. We also have monitored the reaction of catechol by following the growth of absorption maximum at 356 nm while reacting with the catalytic amount of iron complex **5.7**.

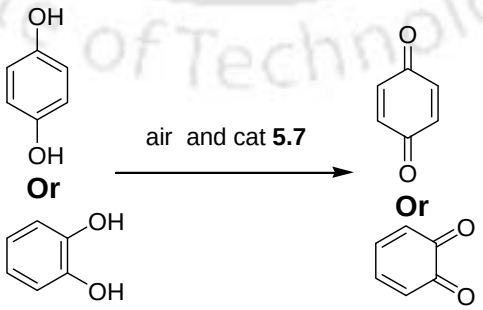

Scheme 5.6 Aerial oxidation of dihydroxy aromatic compounds catalysed by **5.7**

It is found that there is an induction period prior to the oxidation reaction (**fig. 5.16b**). This induction period is attributed to the transformation of the complex **5.7** to a suitable catalytic species.

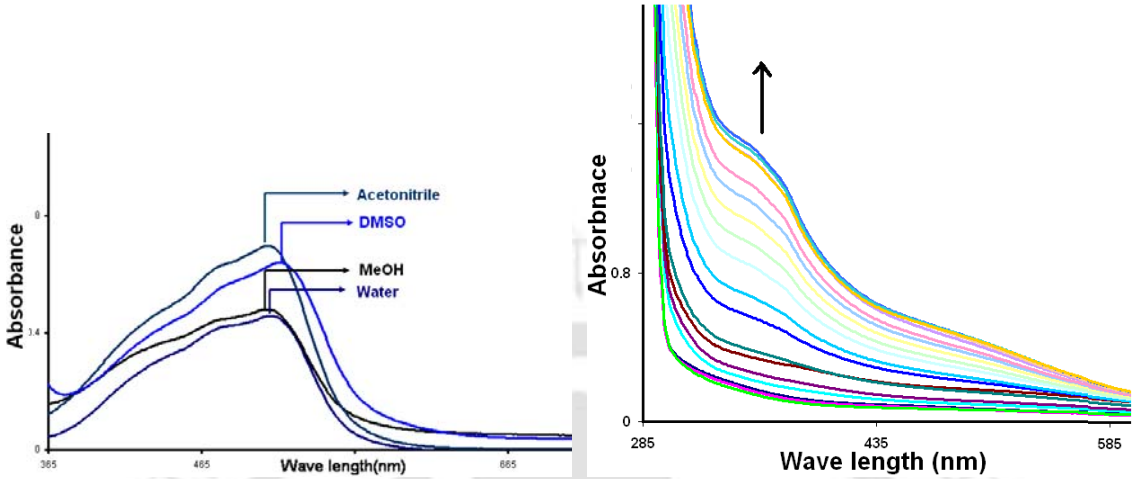

a b

Fig. 5.16 a) The Visible spectra of complex **5.7** (10^{-3} molar) in different solvents; b) Changes in visible spectra of catechol (10^{-3} molar) with complex **2** (1 mole %) with time (recorded at every six minutes intervals).

The complex $[Fe^{II}(phen)_3]^{2+}$ (phen = 1,10-phenanthroline) is stable[384-386] and is not a catalyst for epoxidation reactions. But the reaction of $[Fe^{II}(phen)_3]^{2+}$ with chlorine(I) species in acid solution is a auto catalyst.[387] The templated *bis*-(phenanthroline) site in porous silica is also a catalyst for the epoxidation reactions.[388] Thus in our reaction also the observed induction period in this catalyst presumably corresponds to dissociation of at least one of the three 1,10-phenanthroline ligands under reaction mixture to form the catalytic species. Furthermore, several iron catalysed epoxidation reactions are carried out in acetic acid.[377-378] The complex **5.7** has a dicarboxylate ion and a dicarboxylic acid outside the coordination sphere. These dicarboxylate ion or dicarboxylic acid, serve the purpose of additives to increase the relative activity of catalytic process. Oxo-bridged iron(III) complexes containing 1,10-phenanthroline ligand are used in catalytic epoxidation reactions of olefins.[389-391] In our case also the iron(II) may be getting transformed to form oxo-iron complex which is causing the catalytic oxidation and epoxidation reactions.

The crystal data and refinement parameters of compound **5.4-5.8** are listed in **table 5.6**.

Table 5.6 Crystallographic parameters of compound **5.4-5.6**

Compound No.	**5.4**	**5.5**	**5.6**
Molecular formulea	$C_{44}H_{28}N_4O_{10}S_2Cu_2$	$C_{72}H_{42}Cu_3N_6O_{20}S_3$	$C_{22}H_{20}N_6O_{12}\ Cu_2$
Molecular weight	963.90	1597.92	687.54
Crystal system	Monoclinic	Triclinic	Triclinic
Space group	$P2_1/n$	P-1	P-1
Temperature	296K	296K	296K
a (Å)	10.4646(6)	11.6289(17)	11.515(5)
b (Å)	16.6275(10)	14.666(2)	13.252(6)
c (Å)	11.0738(7)	21.214(3)	20.637(10)
α/°	90.00	77.895(10)	80.01(3)
β/°	91.428(2)	78.345(9)	89.33(3)
γ/°	90.00	72.717(9)	69.79(4)
V ($Å^3$)	1926.2(2)	3339.9(9)	2907(2)
Z	2	2	4
Density/Mgm-3	1.662	1.589	1.571
Abs. Coeff. /mm^{-1}	1.282	1.123	1.532
Abs. correction	none	none	none
F(000)	980	1622	1392
Total no. of reflections	15784	32803	25558
Reflections, I > 2σ(I)	2701	10634	12577
Max. 2θ/°	47.00	49.00	56.80
Ranges (h, k, l)	$-11 \le h \le 11$ $-18 \le k \le 18$ $-11 \le l \le 11$	$-13 \le h \le 13$ $-17 \le k \le 16$ $-24 \le l \le 24$	$-15 \le h \le 15$ $-16 \le k \le 17$ $-27 \le l \le 27$
Complete to 2θ (%)	94.7	95.5	95.5
Data/Restraints/Parameters	2701 / 0 / 280	10634 / 24 /937	12577 / 0 /758
Goof (F2)	1.047	1.069	0.916
R indices [I > 2σ(I)]	0.0273	0.0664	0.1541
R indices (all data)	0.0351	0.1506	0.3974
wR indices	0.0749	0.2250	0.5243

Compound No.	**5.7**	**5.8**
Molecular formulae	$C_{60}H_{37}N_{10}O_{15}S_4Fe$	$C_{24}H_{24}N_4O_6S_2Mn$
Mol. wt.	1322.09	583.53
Crystal system	Monoclinic	Monoclinic
Space group	$P2_1/c$	C2/c
a (Å)	11.575(7)	14.7154(11)
b (Å)	21.530(12)	9.0292(11)
c (Å)	23.212(13)	20.568(2)
α/°	90.00	90.00
β/°	90.13(2)	93.032(9)
γ/°	90.00	90.00
V ($Å^3$)	5785(6)	2729.0(5)
Z	4	4
Density/Mgm^{-3}	1.519	1.420
Abs. Coeff. /mm-1	0.485	0.681
Abs. correction	none	none
F(000)	2712	1204
Total no. of reflections	48211	18701
Reflections, I > 2σ(I)	9195	3430

Max. 2θ/°	49.00	56.96
Ranges (h, k, l)	-13 ≤ h ≤13 -22 ≤ k ≤ 25 -26 ≤ l ≤ 25	-19 ≤ h ≤19 -11 ≤ k ≤12 -27 ≤ l ≤ 27
Complete to 2θ (%)	95.5	99.0
Data/ Restraints/Parameters	9195 / 0 / 813	3430 / 0 / 174
Goof (F2)	0.931	1.038
R indices [I > 2σ(I)]	0.0787	0.0529
R indices (all data)	0.2626	0.0920
wR indices	0.2048	0.1443

5.3 Experimental section:

Materials and physical method as described in **Chapter 2**, **Section 2.41** and **Section 2.42** .

The synthesis and spectroscopic data of compounds **5.1** and **5.2** are available in chapter 2 however; we renumbered the compounds as **5.1** = **2.18** and **5.2** = **2.32** respectively.

5.3.1 Cyclic voltametry, GC-MS and EPR

The cyclic-voltametric experiments were performed on a CHI660A electrochemical work-station with three electrodes system. Platinum electrode, glassy carbon electrode were used as auxiliary and working electrode respectively, with Ag/AgCl electrode as reference electrode. The cyclic voltametry are recorded by dissolving adequate amounts of complex **5.7** (10^{-4}M) in dry acetonitrile. The experiments were performed with tetra butyl ammonium perchlorate as supporting electrolyte under nitrogen atmosphere.

GC-MS experiments were recorded on a Hewlett-Packard HP6890 series instrument equipped with an HP-5 column. GC analyses were carried out on a Hewlett-Packard HP6890 series instrument equipped with an FID detector and HP7683 series autosampler and injector and analyzed using HP Chemstation software. The column was a 30 m HP-5 (cross-linked 5% PH ME siloxane) capillary column with 0.32 mm inner diameter and 0.25 μm film thickness (inlet pressure = 13.9 psig; column flow = 1.2 mL/min; temperature program for all analyses, initial temp = 50^0 C, initial time = 0 min, rate = 5^0 C/min, final temp) 250^0 C, final time = 15 mins.

X-Band EPR spectra were recorded with a Jeol JES-FA series spectrometer. The spectra were calibrated with DPPH (g = 2.0037).

5.3.2 General procedure for the synthesis of Copper(II) complexes 5.4 and 5.5

(3-Carboxymethylsufanyl-1,4-dioxo-1,4-dihydronaphthalen-2-ylsulfanyl) acetic acid (0.2082 g, 0.6 mmol) was dissolved in methanol (20 ml). To this solution $Cu(NO_3)_2.4H_2O$ (0.156 g, 0.6mmol) was added and kept it stirring for 30 mins at room temperature. The resulting precipitate was collected by filtration and dried. In the case of complex **5.4**, the precipitate was dissolved in 15 ml of methanolic solution of 2,2′-bipyridine (0.138 g, 1 mmol) while in the case of complex **5.5**, the precipitate was dissolved in 10 ml of 1,10-phenanthroline (0.180 g, 1 mmol) solutions in dimethyl formamide. The resulting solution was left undisturbed. The blackish green block crystals were collected by filtration.

5.3.3 Spectroscopy data of complex 5.4 and 5.5

Complex 5.4

Yield 37%: IR (KBr, cm^{-1}): 3418 (bw), 3036 (w), 2924 (w), 1676 (m), 1622 (s), 1519 (s), 1474 (w), 1360 (m), 1327 (s), 1270 (s), 1222 (m), 1155 (w), 1000 (m), 766 (m).

Complex 5.5

Yield 29%: IR (KBr, cm^{-1}): 3435 (bs), 3059 (w), 2924 (w), 1680 (m), 1599 (s), 1520 (s), 1428 (m), 1365 (w), 1334 (m), 1269 (s), 1222 (m), 1149 (w), 999 (m), 854 (m), 723 (s).

5.3.4 General procedure for the synthesis of iron(II) complex 5.7

A solution of 2-(3-methyl-1,4-dihydronaphthalen-2-ylsulfanyl) nicotinic acid **5.2** (0.163 g, 0.5 mmol) and ferrous sulphate tetrahydrate (0.057 g, 0.25 mmol) in 15 ml of methanol was stirred for 20 mins. The precipitate formed was filtered. The residue was dissolved in a solution containing 1,10-phenanthroline (0.179 g, 1 mmol) in *N*,*N*′-dimethylformamide (10 ml). Red crystals of complex **5.7** were obtained after one week.

Isolated yield 68%: IR (KBr, cm^{-1}): 3391 (bs), 2923 (w), 1699 (s), 1629 (m), 1574 (m), 1561 (w), 1422 (s), 1309 (w), 1188 (s), 1053 (w), 844 (s), 723 (m), 601 (s).

5.3.5 General procedure for the synthesis of manganese(II) coordination polymer 5.8

2-(3-methyl-1,4-dihydronaphthalen-2-ylsulfanyl) nicotinic acid **5.2** (0.163g, 0.5 mmol) and manganese(II) acetate tetrahydrate (0.123 g, 0.5 mmol) were mixed together methanol (15 ml) and stirred for 20 mins. To the resulting solution pyridine (1 ml) was added and the solution was kept undisturbed. After 3 hrs colorless crystals were obtained.

Isolated yield 65%: IR (KBr, cm^{-1}): 3584 (bw), 3176 (bw), 2925 (w), 1586 (s), 1574 (s), 1557 (s), 1445 (m), 1398 (s), 1384 (s), 1166 (m), 1076 (s), 841 (m), 781 (s), 723 (m).

5.3.6 General procedure for the iron(II) catalyzed epoxidation reactions

To an ice-cold solution of the complex **5.7** (0.264 g, 0.02 mmol) and olefin (2 mmol) in acetonitrile (2 ml) a solution of 30% hydrogen peroxide (320 μL, 4 mmol) in 2ml of acetonitrile was added over a period of 2 mins. After stirring the solution at ice cold condition for 30 mins, further stirring continued for 60 mins at room temp. The reaction mixture was extracted with 40 ml of dichloromethane and organic layer was dried over anhydrous sodium sulphate (0.5 g) and analyzed by GC-MS for characterization and yield. The dichloromethane solution was evaporated to dryness and further purification was done by column chromatography using hexane/ethyl acetate and products were further confirmed by comparing their NMR and IR with authentic sample.

GC-MS of 2-phenyloxirane:

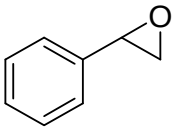

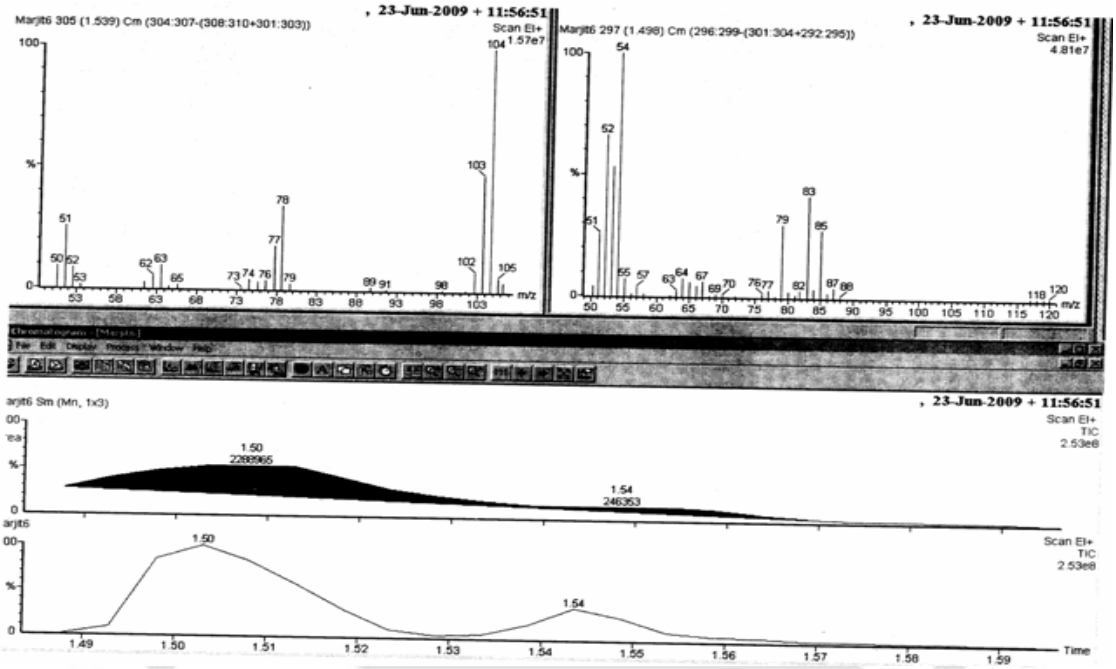

GC-MS of 2-hexyloxirane:

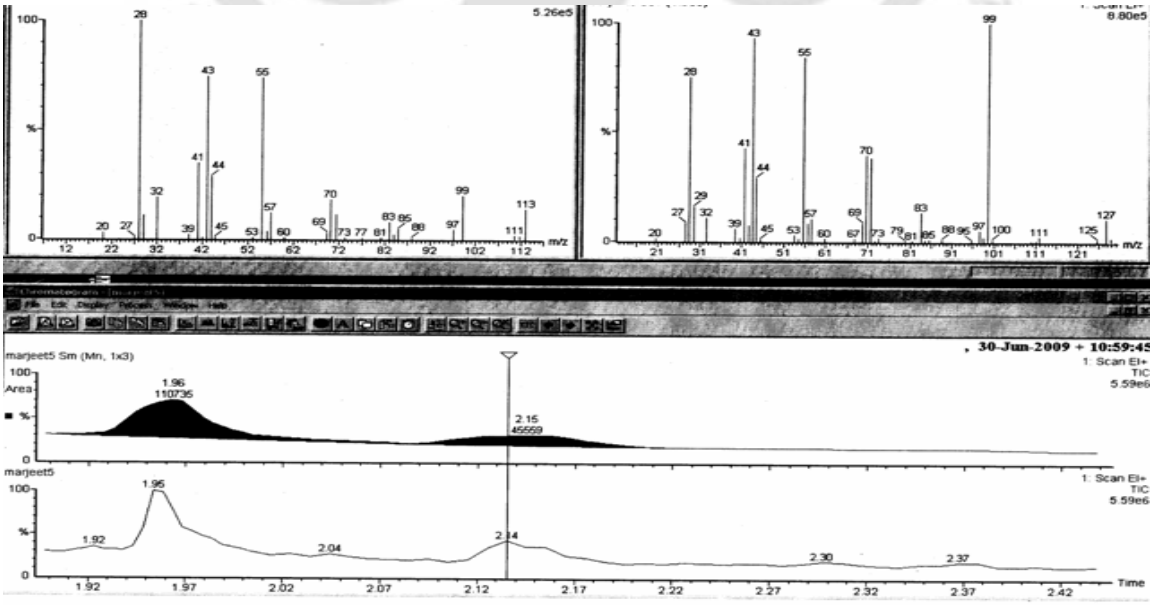

GC-MS of 2-benzyloxirane:

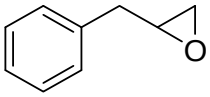

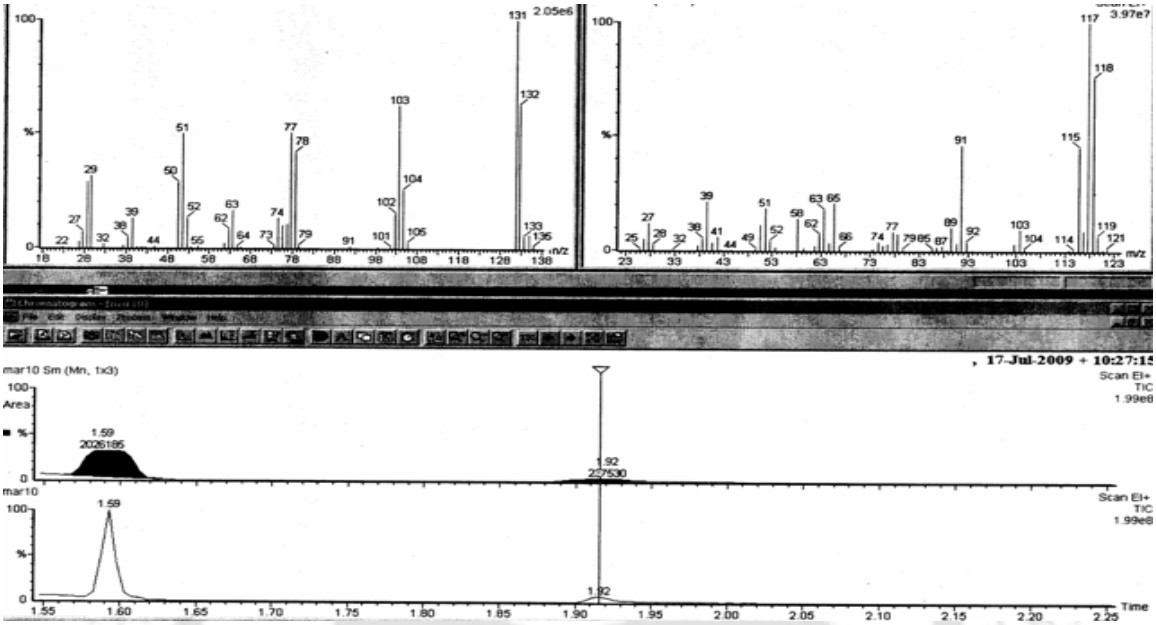

GC-MS of (3-phenyloxiran-2-yl) methanol:

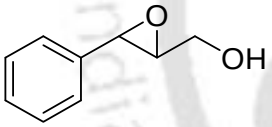

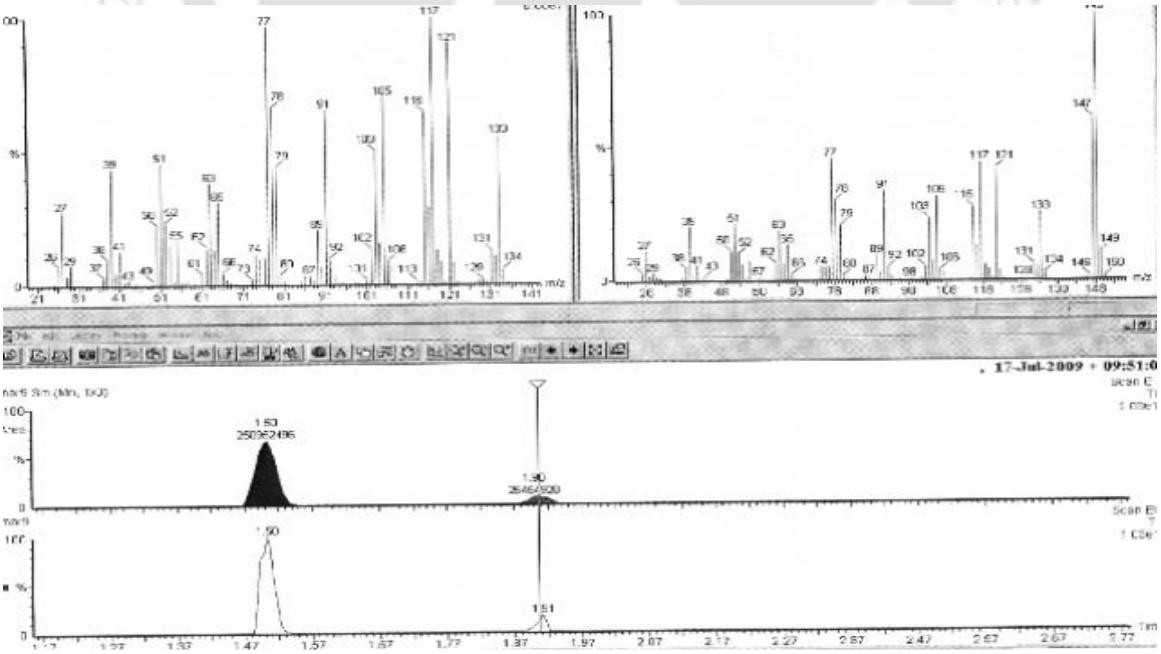

GC-MS of 7-oxa-bicyclo[4.1.0] heptane:

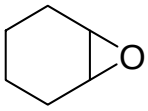

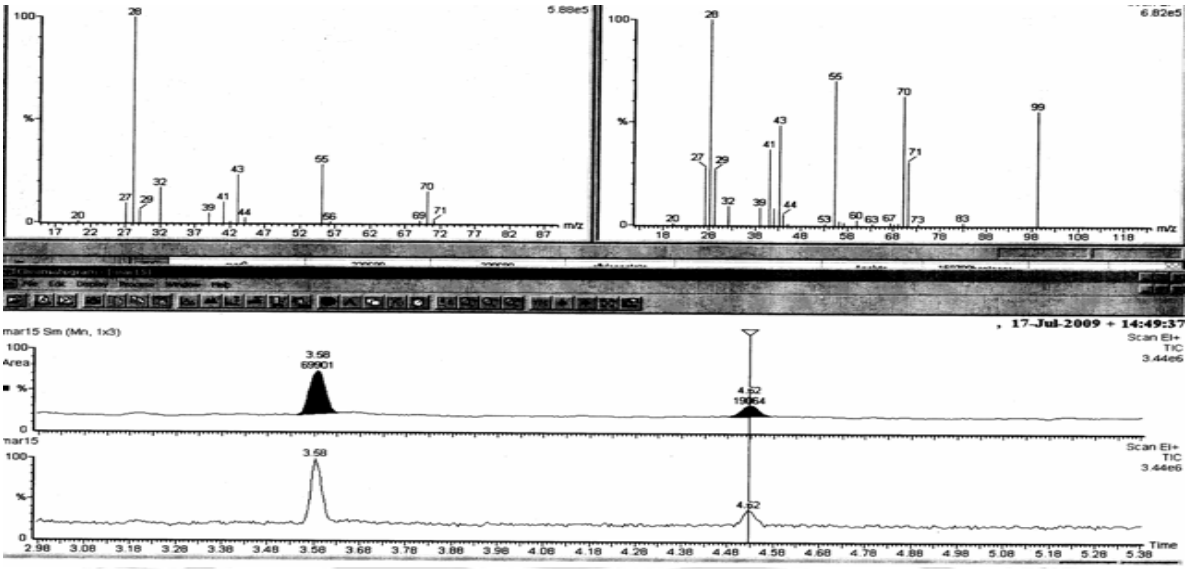

5.3.7 General procedure for the Oxidation of hydroquinone and catechol

To a solution of hydroquinone or catechol (0.316 g, 2 mmol) in acetonitrile (10 ml), the complex **5.7** (0.264 g, 0.02 mmol) was added and stirred at room temperature. After 30 mins the solution was analyzed by GC-MS and found quantitative formation of the corresponding quinones. The quinones formations are further confirmed by isolating them and comparing their spectra with authentic samples. Further to this the reaction was monitored by taking 2 ml of acetonitrile solution of **5.7** (0.01 mmol) with catechol (1mmol) in a quartz cuvette and monitoring the growth of absorption at 356 nm in UV-visible spectra.

Chapter 6

Coordination polymers of flexible dicarboxylic acids

Metal Organic Frameworks (MOFs), also known as metallorganic coordination networks or coordination polymers have infinite frameworks constructed from metal ions and organic ligands via coordination bonds and other weak interactions.[392-395] Molecular architectures in MOFs consist of metal ions that functions as nodes and organic ligands act as spacer to forms different dimensionalities such as one-, two- or three-dimensional architectures.[396] The framework structures are primarily dependent on the coordination preferences of the metal-unit and the functionality of the ligands.[397] The structural variety of the coordination polymers constructed from poly-carboxylato ligands are due to the following factors: a) the number of the carboxylate groups, b) the spatial orientation of the carboxylato groups, c) the coordination modes of carboxylate groups and d) ancillary ligands in the coordination sphere of the metal ions. So, depending on these factors, coordination polymers may adopt different structures.

Beside these the carboxylate ligand binds to metal ions in various binding modes viz. monodentate, bridging bidentate, symmetric chelating, bidentate chelate bridging etc. The different binding modes of carboxylate anion with metal ions are illustrated in **fig. 6.1**.

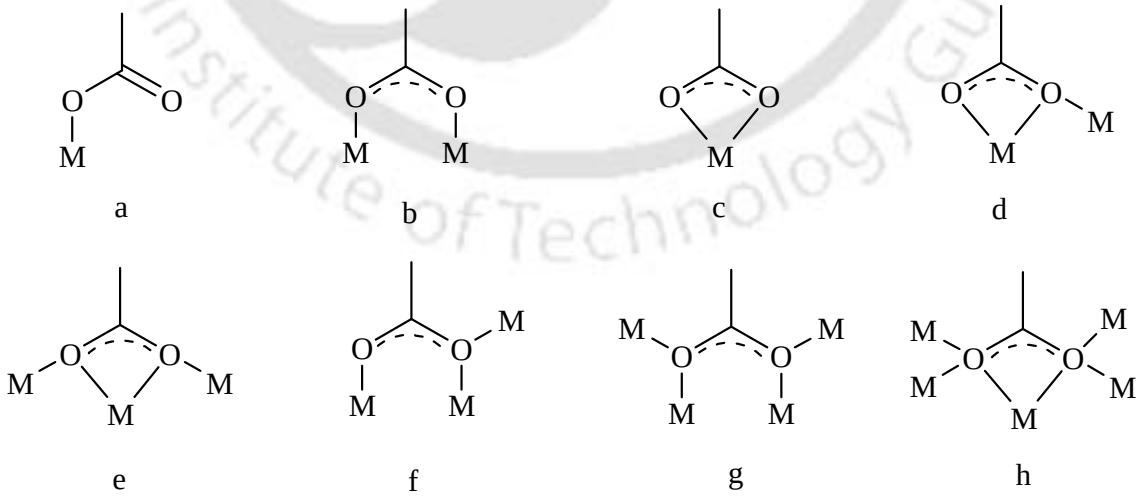

Fig. 6.1 Different binding modes of carboxylate anion

It is a challenge to make different metal carboxylate motifs in a predictable manner.[398-399] Several structural motifs based on carboxylates are employed to design new open framework structures.[400-402] In this context we have chosen flexible dicarboxylic acids (4-carboxymethoxy-2,3-*bis*-aryllsulfanylnaphthalene-1-yloxy) acetic acids **6.5-6.8** (**scheme 6.1**) having arylsulfanyl groups and studied their metal complexation properties. The (4-carboxymethoxy-2,3-bis-aryllsulfanylnaphthalene-1-yloxy) acetic acids (**6.5-6.8)** abbreviated as $\mathbf{LH_2}$, have two carboxylic acid groups attached to flexible arms. So, they are suitable for the synthesis of cyclic or open chain polymeric structures with metal ions and capable to change the dimension of coordination polymers with change in ancillary ligands. Moreover, the naphthalene ring and the arylsulfanyl groups of the ligand $\mathbf{LH_2}$ have contribution to give rise to π-interactions.

Earlier in chapter 2, we have described synthesis of a series of 1,4-naphthalenediols from the reaction of 1,4-naphtoquinone with thiols. These 1,4-naphthalenediols were used to synthesize their corresponding flexible dicarboxylic acids **6.5-6.8**. The sulphur containing dicarboxylic acids namely (4-carboxymethoxy-2,3-bis-arylsulfanyl-naphthalene-1-yloxy) acetic acid **6.5-6.8** were prepared by three steps procedure starting from 1,4-naphthoquinone as illustrated in **scheme 6.1**. For this purpose diol precursors 2,3-bis-(arylsulfanyl)-1,4-naphthalenediol was synthesized by reacting 1,4-naphthoquinone with corresponding thiols, which was further reacted with bromomethylacetate to obtain (4-methoxycarbonylmethoxy-2,3-*bis*-arylsulfanylnaptha-lene-1-yloxy) acetic acid methyl ester **6.1-6.4**. The methyl ester **6.1-6.4** on acid hydrolysis gave the corresponding acids **6.5-6.8** (**scheme 6.1**). These flexible dicarboxylic acids derived from the quinone were used to make the different motifs of coordination polymers. The compounds **6.1-6.8** are fully characterized by spectroscopic technique. In FT-IR spectra of the compounds **6.1-6.4** shows the asymmetric stretching frequency for C=O group of carboxylate appears at 1759 cm^{-1} and two strong band around 1216 and 1101 cm^{-1} appear due to the C-O stretching of ether groups. In the ^1H NMR spectra in $CDCl_3$, three sets of aromatic protons are appeared for arylsulfanyl groups at 7.14, 7.01 and 7.00 ppm. Beside these the aromatic protons of naphthalene ring appears two peaks at 8.40 and 7.70 ppm. The methoxy and the methylene protons appear at 3.78 and 4.77 ppm, respectively. Due to the less solubility the ^1H NMR spectra of the compounds **6.5-6.8** are performed from their

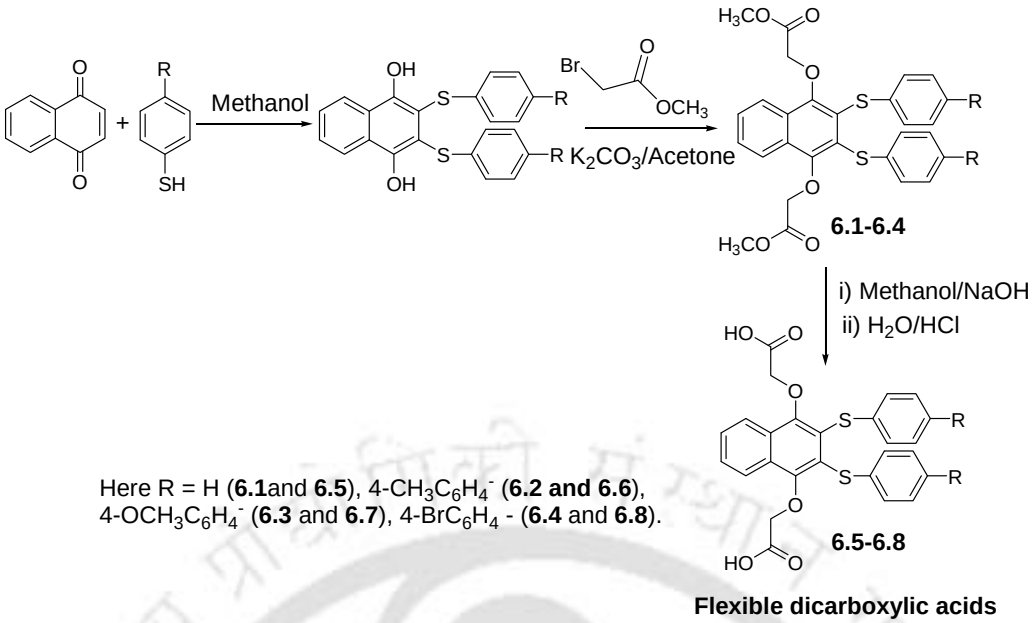

Scheme 6.1 Synthesis of flexible dicarboxylic acids

sodium salts in D_2O. The aromatic protons of naphthalene ring appear two peaks at 8.06 and 7.53 ppm. The arylsulfanyl aromatic protons and -CH_2- protons appear at 7.03, 6.95, 6.87 and 4.24 ppm respectively. The present methodology involves a high yield reaction scheme as direct reaction of naphthalene diols with chloroacetic acid results such products in very low yield under drastic reaction conditions.

6.1 One-dimensional coordination polymer of aqua-bridged binuclear manganese(II) carboxylate

Aqua-bridged metal carboxylate complexes are found in some active sites of binuclear metallo-enzymes.[403-405] Study of aqua-bridged binuclear transition metal complexes[406-408] are expected to increase understanding on the catalytic activity of metallo-enzymes.[409-414] The binuclear aqua-bridged manganese compounds[415] are also studied as precursor of biological model compounds. There are large numbers of multinuclear manganese complexes[416-422] as well as other coordination polymers having binuclear paddlewheel type carboxylate units,[423] but polymeric complexes with aqua-bridge manganese complexes are rare and only one grid like structure with rigid dicarboxylic acid[424] is reported. However, in biological system flexible one dimensional coordination polymers would be more relevant and they are not explored. We could prepare a manganese(II) carboxylate complexes, in the form of one dimensional coordination polymer that contains repeated units of aqua-bridged binuclear manganese

carboxylates and the core has close structurally analogy to biological aqua-bridged metal carboxylates.

The sodium salt of (4-carboxymethoxy-2,3-bis-*p*-methylphenylsulfanylnaphthalene-1-yloxy) acetic acid **6.6** react with manganese chloride in methanol-water solvent mixture (2:1 ratio) in the presence of pyridine to give a polymeric manganese complex **6.9** (**scheme 6.2**).

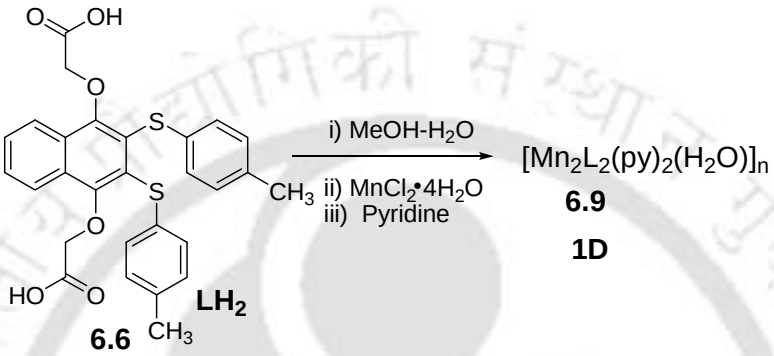

Scheme 6.2

The coordination polymer **6.9** was obtained as colorless block and it crystallizes in centrosymmetric triclinic P-1 space group. The coordination polymer consists of repeated units of binuclear aqua-bridged manganese.

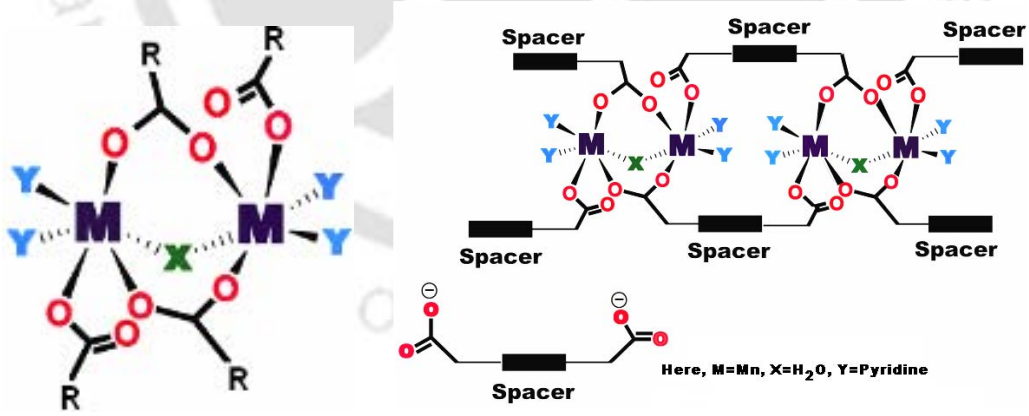

a b

Fig. 6.2 Pictorial representation of coordination polymer **6.9** a) repeated unit and the coordination environment around two manganese(II) centers; b) chain like structure along the crystallographic b-axis

The binuclear units have also two carboxylate bridges. Each of these binuclear units is attached to one another by mono-dentate carboxylate groups. In addition to carboxylate

ligands, the six co-ordination around the manganese is completed by two additional pyridine ligands. The pictorial representation of the repeated unit of coordination polymer in the unit cell and the chain like structure present along the crystallographic b-axis is shown in the **fig. 6.2**. Both the manganese centers have distorted octahedral geometry and in each binuclear unit the Mn1-Mn2 distance are 3.703 Å, which is slightly longer than the isolated binuclear aqua-bridged complexes.[415] The crystal structures of repeated units in the coordination polymer in the unit cell are shown in **fig. 6.3a** and the chain like structure present along the crystallographic b-axis is shown in the **fig. 6.3b**.

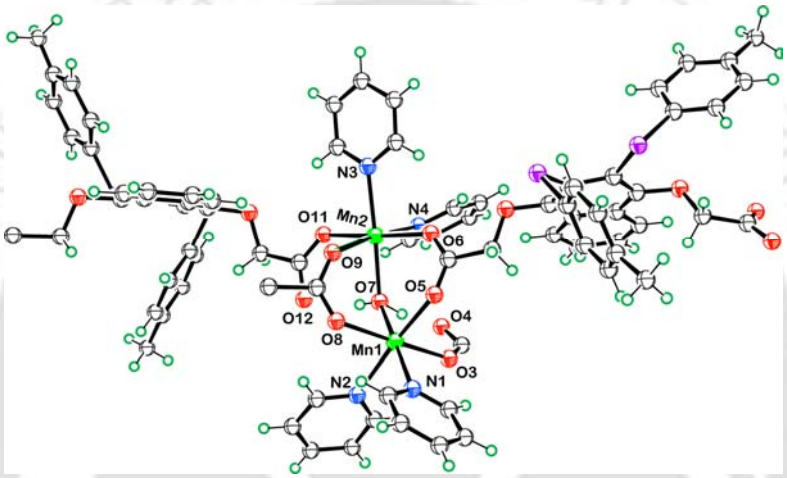

a

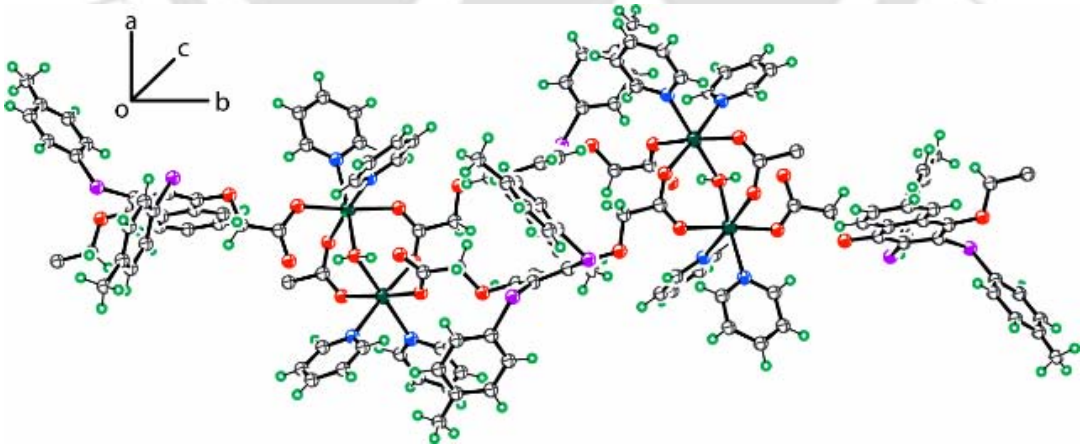

b

Fig. 6.3 Crystal structure of coordination polymer **6.9** a) repeated unit; b) chain like structure along the crystallographic b-axis

Some of the important bond distances and bond angles are listed in **table 6.1**. It may be mentioned that Mn1-N1 and Mn1-N2 distances in the complex are unequal; same is

happen for Mn2-N3 and Mn2-N4 bond distances; it suggests that in each cases out of two pyridines, one of the pyridine is weakly bonded to the manganese than the other.

Table 6.1 Selected metal-ligand bond distances (Å) and angles (º) of coordination polymer **6.9**

Bonds	Bond distances(Å)	Bonds	Bond angles (º)	Bonds	Bond angles (º)
Mn1-O8	2.137(4)	O3-Mn1-O8	174.8(16)	O7-Mn1-N2	86.9(19)
Mn1-O3	2.159(4)	O5-Mn1-O8	96.0(17)	N1-Mn1-N2	88.2(2)
Mn1-O5	2.163(4)	O3-Mn1-O5	88.7(16)	O6-Mn2-O9	96.1(17)
Mn1-O7	2.220(4)	O7-Mn1-O8	95.5(17)	O6-Mn2-O7	87.1(17)
Mn1-N1	2.264(5)	O3-Mn1-O7	86.6(17)	O9-Mn2-O7	94.7(17)
Mn1-N2	2.338(5)	O5-Mn1-O7	86.6(16)	O6-Mn2-N4	96.5(18)
Mn2-O6	2.149(4)	O3-Mn1-N1	86.4(19)	O9-Mn2-N4	89.1(17)
Mn2-O6	2.131(4)	O5-Mn1-N1	98.1(18)	O7-Mn2-N4	174.5(18)
Mn2-O7	2.229(5)	O7-Mn1-N1	171.5(2)	N3-Mn2-O6	87.2(16)
Mn2-O9	2.157(4)	O8-Mn1-N2	85.7(18)	O9-Mn2-N3	175.9(18)
Mn2-N3	2.331(5)	O3-Mn1-N2	89.6(19)	N3-Mn2-O7	88.0(18)
Mn2-N4	2.238(5)	O5-Mn1-N2	173.4(18)	N3-Mn2-N4	88.1(18)

Such binuclear cores in active enzymes generally possess terminal nitrogen donor ligands, thus they can be considered to have structural resemblance to biological enzymes. The earlier reported structure on a three dimensional grid having aqua-bridged manganese units has a very rigid structure and includes solvent,[424] however in the present case we are being able to make polymer that is linear and the aqua sites are exposed. The coordination polymer has characteristic carboxylate absorptions at 1633 cm^{-1}, whereas the disodium salt of the ligand shows absorption at 1606 cm^{-1} suggesting the carboxylate coordination to manganese. The solid state X-band (9.44GHz) EPR spectra of polymer **6.9** at room temperature shows a broad single-line spectrum around 346.5 G and it has the g_{iso} = 2.026 (center field = 350.0G, power = 998000 mw, frequency = 9447.829, sweep time = 30s).

At room temperature, the coordination polymer **6.9** shows effective magnetic moment of 5.32 BM, which is slightly lower than the calculated spin only value for a d^5 system. We also measure the low temperature gram susceptibility value of the polymer **6.10**.

The plot of susceptibility inverse (1/χ′ g/amu) vs. temperature (º K) passes through a maxima showing magnetic phase transition suggesting antiferromagnetic behaviour of the polymers. To this plot we fit a straight line (**fig. 6.4**) and found out the Curie

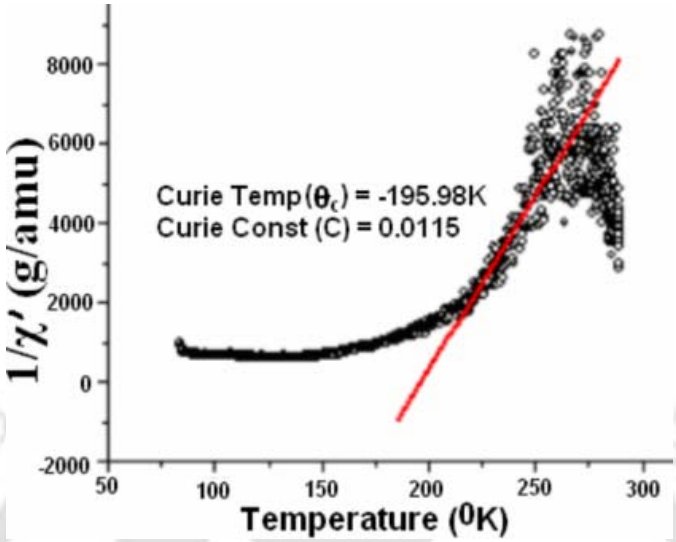

Fig. 6.4 The plot of susceptibility inverse (1/χ′ g/amu) vs temperature (º K) of polymer **6.9**

temperature, Θ_C = -195.98º K and Curie constant, C = 0.12. The negative value of Curie temperature, Θ_C = -195.98º K also suggest the antiferromagnetic properties of the polymers. From the above investigation, in conclusion we have developed a simple route for novel sulphur containing dicarboxylic acid ligand and one dimensional aqua-bridged carboxylate coordination polymer that have structural similarities to aqua-bridged manganese-active sites in biological systems.

6.2 Copper (II) one dimensional coordination polymers with alternating five and six coordination geometry

The synthesis of multicentered coordination polymer with same metal but with variation of co-ordination number in systematic manner is a challenge; as such synthesis requires control of steric or geometric factors of the ligand[425-426] and choice of metal.[427] This is particularly the case for a linear coordination polymer. The control of geometry by steric effect sulphur is being achieved in complexes containing disulphide bond.[428] Another way may be through control of orientation of mono-dentate carboxylic acid across a metal by changing the orientation.

The reaction of disodium salt of (4-carboxymethoxy-2, 3-*bis*-*p*-methylphenylsulfanyl naphthalene-1-yloxy) acetic acid **6.6** with cupric chloride dihydrate in aqueous methanol in the presence of pyridine gives a one dimensional coordination polymer **6.10** as shown in equation **6.3**. In similar manners a series of complexes with R = -OCH_3 (**6.11**), -Br (**6.12**) groups are also prepared. The structures of the polymers are determined by the X-ray crystallography. The complexes **6.10-6.12** have characteristic IR frequencies at 1633, 1599 and 1603 cm^{-1}, respectively, due to the coordinated carboxylate group. The coordination polymers **6.10-6.12** are isostructural and they crystallize in same centrosymmetric orthorhombic Pnaa space group.

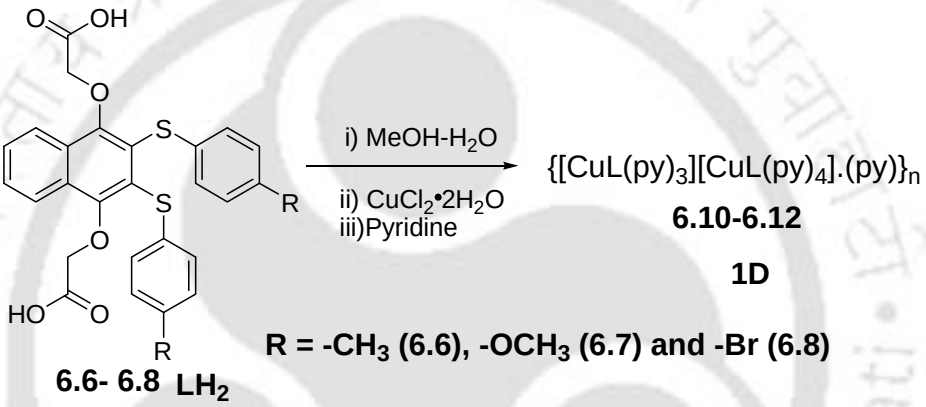

Scheme 6.3

The bond geometry in each case is also similar. Thus, only one representative structure of the polymer **6.10** is shown in **fig. 6.5**. The formation of similar structures in the three cases depicts general synthetic methodology to these coordination polymers from the sulphur containing dicarboxylic acid ligands. The pictorial representation of the coordination polymers of copper(II) carboxylate complexes **6.10-6.12** is shown in **fig. 6.5a**. The segments of the five and six co-ordination environment in the polymer and the bond geometry of the aromatic part connected to sulphur atoms is illustrated in **fig. 6.5b**.

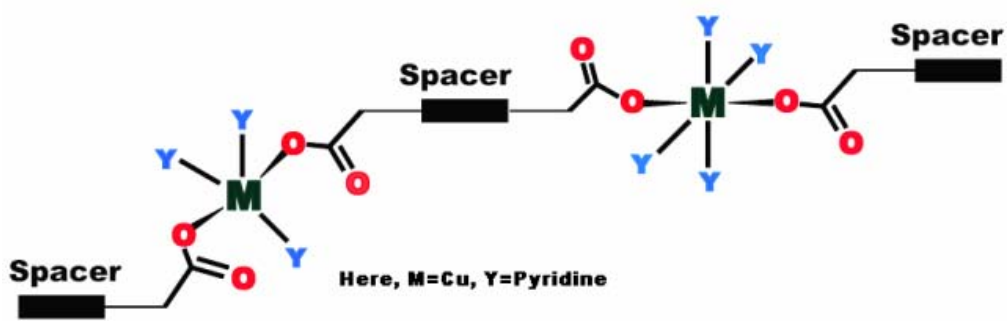

a

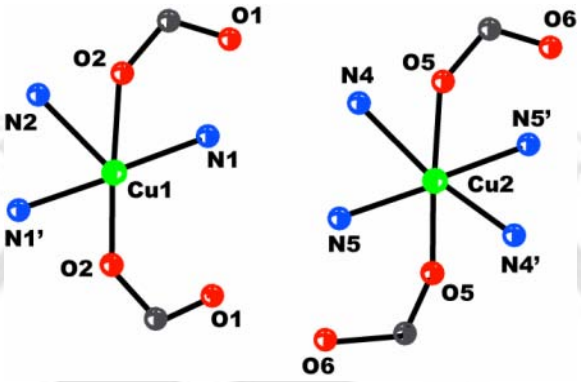

b

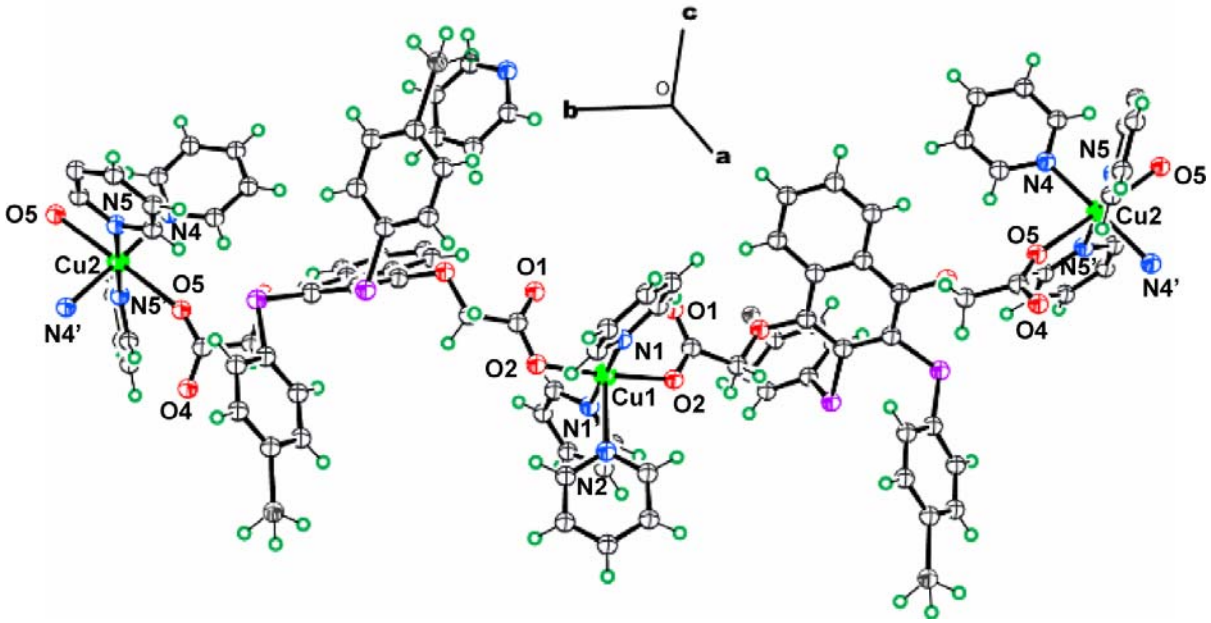

c

Fig. 6.5 a) The pictorial representation of the coordination polymers **6.10**-**6.12**; b) The segments of the five co-ordination and six co-ordination environment in the polymer and c) Crystal structure of the repeated unit of coordination polymer **6.10**

The crystal structure of the repeated unit of polymer **6.10** containing the alternative five and six co-ordination geometry is shown in **fig. 6.5c**. The five coordinated copper

centers have square pyramidal geometry with two nitrogen and two oxygen atoms on the basal plane and a nitrogen ligand in the axial position. The Cu2-N bond lengths in the basal plane are comparable where the axial bond is about 0.25 Å longer than the other two Cu2-N bonds. The six coordinated copper centers have four Cu1-N bonds in one plane and the other two co-ordination sites are occupied by Cu1-O bond that are *trans* to each other and overall it has a distorted octahedral geometry. The metal-ligand bond distances and bond angles as of the coordination polymer **6.10** is listed in **table 6.2**.

Table 6.2 Selected metal-ligand bond distances (Å) and angles (°) of coordination polymer **6.10**

Bonds	Bond distances(Å)	Bonds	Bond angles (°)
Cu2-N3	2.05(5)	N3-Cu2-N4	88.7(11)
Cu2-N5	2.08(5)	N5-Cu2-N4	91.3(11)
Cu2-N4	2.08(3)	N3-Cu2-O5	90.9(9)
Cu2-O5	2.35(3)	N5-Cu2-O5	89.2(9)
Cu1-O2	1.97(3)	N4-Cu2-O5	92.1(12)
Cu1-N1	2.02(4)	O2-Cu1-N1	88.4(14)
Cu1-N2	2.37(6)	O2-Cu1-N2	92.5(10)
		N1-Cu1-N2	91.4(12)

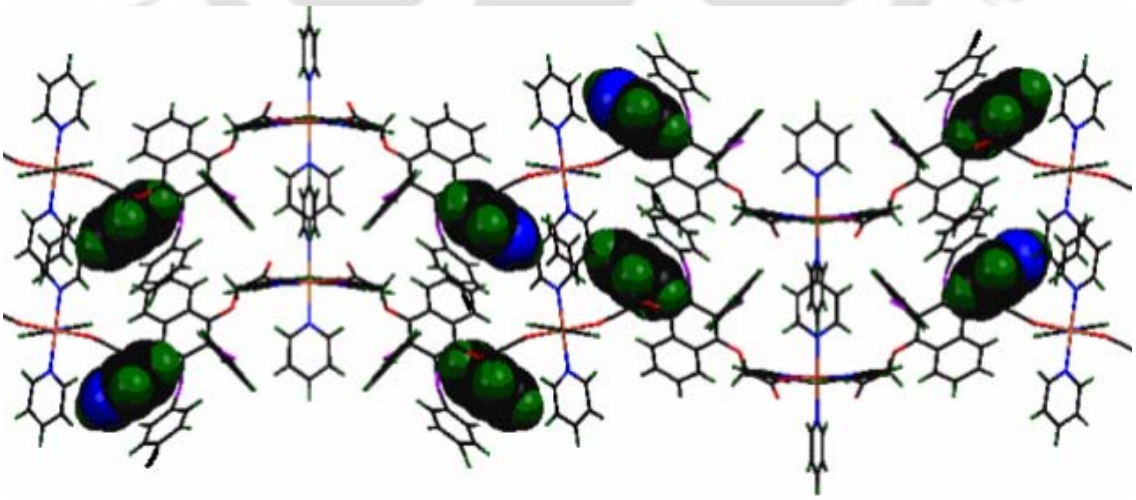

Fig. 6.6 Encapsulation of pyridine molecules in the interstices of polymer **6.10**

Crystallography confirms that the polymers have five and six co-ordination numbers and one pyridine molecule occupies the interstitial position between the two polymeric helical structures as shown in **fig. 6.6**. Despite of five and six being the coordination numbers in the polymers, the stoichiometry of the polymers corresponds to six coordination numbers for the two repeating copper(II) centers. The spatial arrangements of the two carbonyl groups of mono-dentate carboxylates differ across the two carbons, and in the six coordinated case the carbonyls are *trans* to each other and makes the approach of four pyridine favorable, whereas in the case of the five coordinated copper they project towards same side and prevents a sixth pyridine to penetrate to the coordination sphere thereby making the copper center to have five coordinated geometry. The origin of such alternate change in coordination is from the preferential spatial arrangement of lone pair on sulphur which may be compared to geometry changes in palladium complexes with disulphide ligands caused by orientation of the substituent on sulphur.[427] In the complexes the orientation of these aromatic carboxylic rings are totally different and they project away from each other. Thus, they provide space for accommodation of pyridine molecule in the lattice. The coordination polymers have helical structures. The helicity occurs due to the disposition of naphthalene rings in different planes to minimize electrostatic repulsions. All the carboxylate groups in the coordination polymers are mono-dentate. Generally copper carboxylate complexes prefer to have paddlewheel structure and the paddle wheel structure with nitrogen donor linkers are studied as hybrid materials.[429] In our case we have obtained mono-dentate carboxylates as we have incorporated bulky thiophenol groups in the aromatic ring which prefers to keep themselves apart and do not provide the required twist on the carboxylate group to form bridging coordination compounds. In the hexa-coordinated geometry two axial Cu2-O5 bonds are exceptionally long 2.35 Å in comparison to the 1.97 Å observed for Cu1-O2 bond. Julve et al.[430] have demonstrated in copper 1-D polymers with malonate network polymer the penta coordinated species with different orientation of copper leading to interesting properties, however these polymers are held together by intermolecular hydrogen bonding and they show interesting magnetic properties.

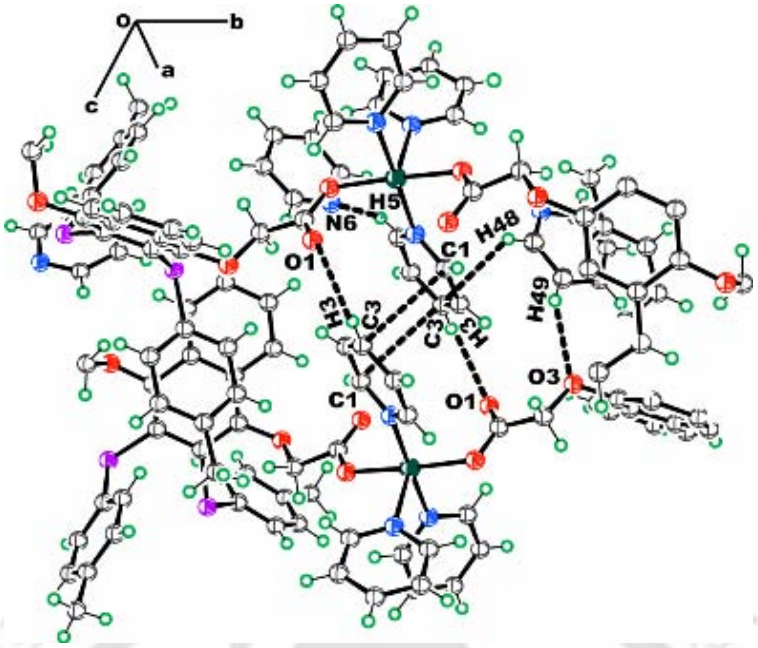

Fig. 6.7 A part of polymer **6.10** showing the self assembly in the molecule

Our system is also self assembled but the self-assemblies are formed through weak C–H···O, C–H···N, C–H···π and π···π type of interactions. The location of the pyridine molecule in the unit cell of **6.10** is shown in **fig. 6.6**. It is clear from **fig. 6.7** that the aromatic rings occur in pairs. There is π···π interactions between the pyridine pairs and each of the individual pyridine molecules are also held by C–H···O and C–H···N and C–H···π interactions as shown in **fig. 6.7**.

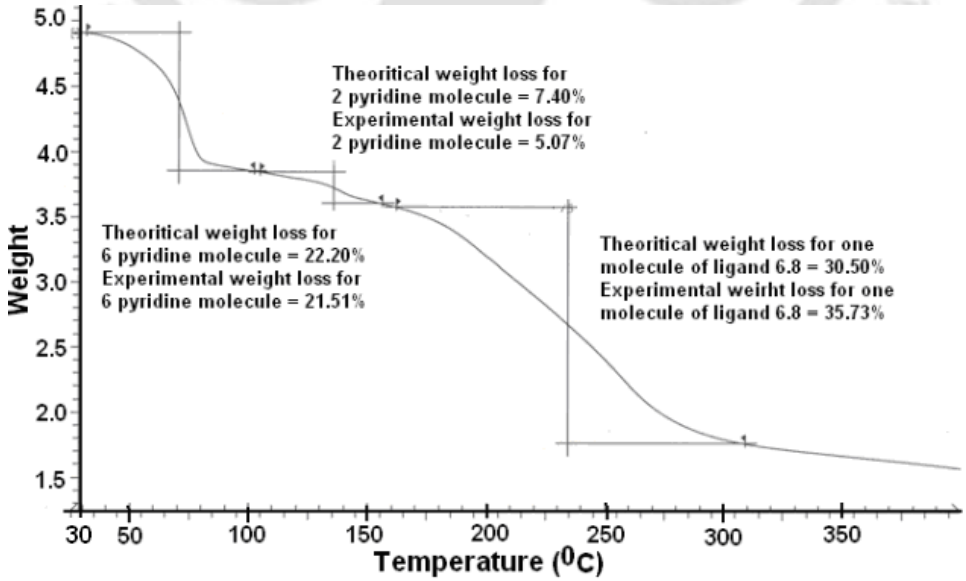

Fig. 6.8 Thermogram for complex **6.12** (heating rate 5°C/minute)

The thermo gravimetric analysis shows loss of six pyridine molecules at relatively low temperature 113º C and the other two pyridine ligands are lost at around 150º C. Thus, from the thermogravimetry it is not possible to distinguish the interstitial pyridine molecules from the pyridine ligands bonded to metal. The one molecule of dicarboxylic acid ligand **6.8** is lost at around 260º C as shown in **fig. 6.8**.

At room temperature, the coordination polymer **6.10** shows effective magnetic moment of 1.78 BM, which is slightly higher than the calculated spin only value for a d^9 system. We also measure the low temperature gram susceptibility value of the polymer **6.9**.

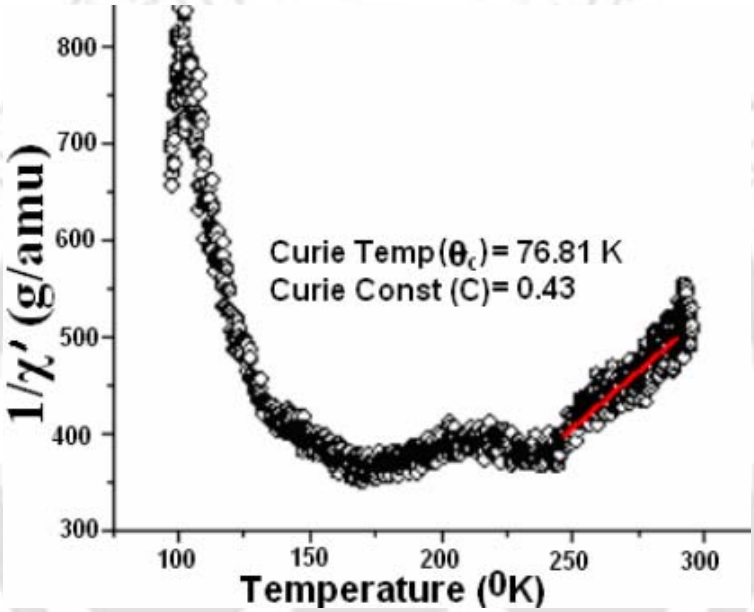

Fig. 6.9 The plot of susceptibility inverse (1/χ′ g/amu) vs temperature (° K) of polymer **6.10**

The plot of susceptibility inverse (1/χ′ g/amu) vs. temperature (º K) passes through a maxima showing magnetic phase transition suggesting ferromagnetic behaviour of the polymers. To this plot we fit a straight line (**fig. 6.9**) and found out the Curie temperature, Θ_C = 76.81º K and Curie constant, C = 0.43. The positive value of Curie temperature, Θ_C = 76.81º K also suggest the ferromagnetic properties of the polymers.

6.3 Coordination polymers of zinc (II) carboxylate

Depending on the orientations of multiple binding sites of carboxylate ligands, coordination polymers can adopt different dimensionality.[431-438] Weak interactions such

as C-H···π interactions[392-395] play a major role in deciding the packing pattern and also provide extra stability to carboxylate polymers.[439-443]

The reactions of zinc(II) acetate dihydrate with disodium salt of 2,2′- (2,3-bis-arylsulfanylnaphthalene-1,4-yloxy) acetic acid leads to polymeric complexes **6.13-6.16**. These coordination polymers can bind to different ancillary ligands and depending on them they adopt different structures. For example, complexes having pyridine ancillary ligands, **6.13** and **6.16** are one dimension coordination polymers while the complex having *N*,*N*′-dimethylformamide is two dimensional coordination polymers.

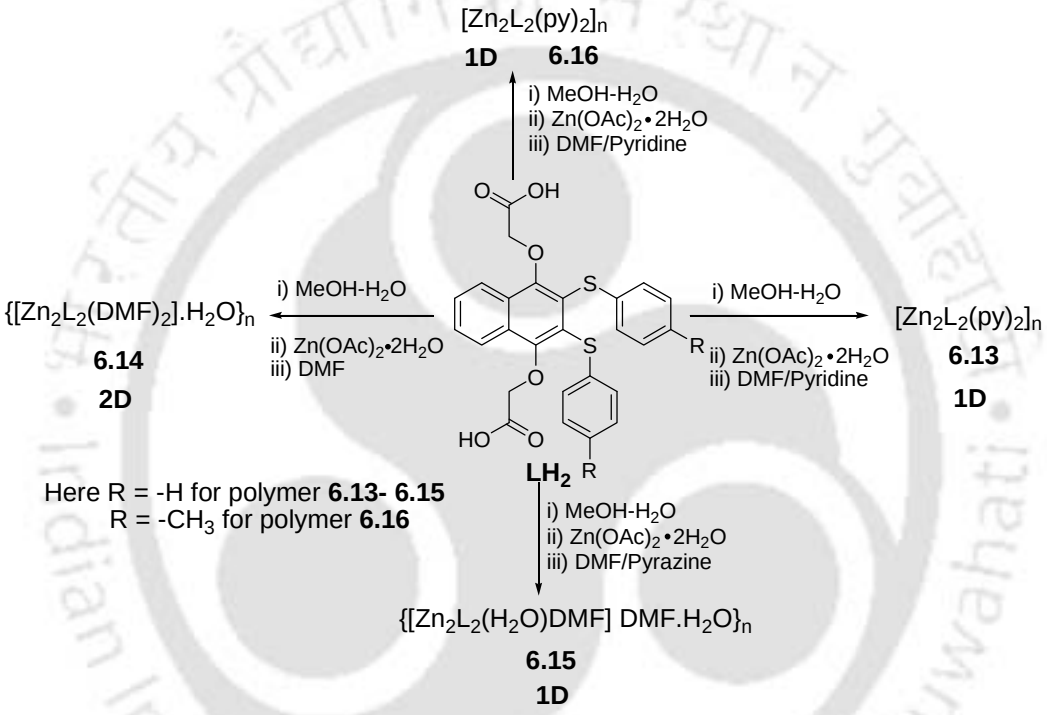

Scheme 6.4 Synthesis of coordination polymers of zinc(II) carboxylate

The crystal structures of each of these coordination polymers are determined. The coordination polymers have conventional paddle wheel type structures, which are commonly found in related zinc carboxylate complexes.[444-446] The crystal structure of the coordination polymer **6.13** is shown in **fig. 6.10**. In both the complexes **6.13** and **6.14**, the zinc atoms have square pyramidal geometry. Oxygen atoms occupy the equatorial positions of the square pyramid, whereas the axial positions are by the auxiliary ligands

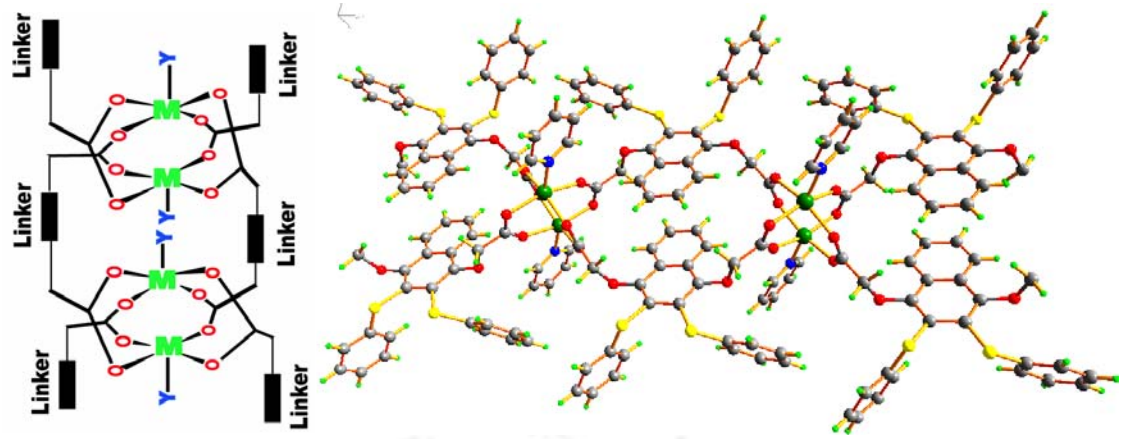

Here **M = Zn; Y = pyridine**

a b

Fig. 6.10 a) Pictorial presentation of polymer **6.13**; b) Crystal structure of repeated unit of polymer **6.13**

such as pyridine or dimethylformamide. In the case of one dimension coordination polymers the polymeric arrays are constructed by two interconnecting ligands, which coordinate two pairs of zinc atoms and form a cyclic structure. The complex **6.14** (**fig. 6.11**) is a two dimensional coordination polymer; it has two dimethylformamide (DMF) ancillary ligands.

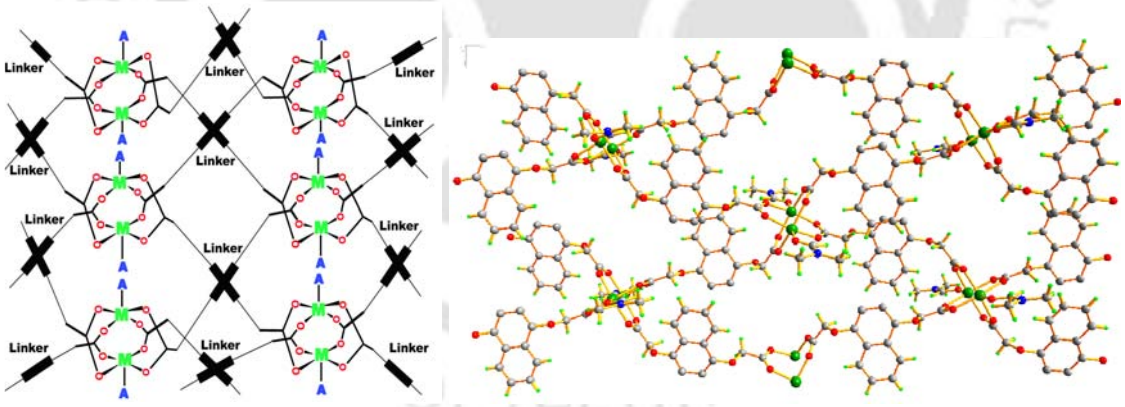

Here **M = Zn; A = DMF**

a b

Fig. 6.11 a) The pictorial presentation of the polymer **6.14**; b) Crystal structure of the repeated unit of polymer **6.14** (arylsulphenyl groups are remove for clarity)

In the case of this two dimensional coordination polymer each ligand binds two pairs of zinc atoms so that no two ligands coordinate to two common pairs of zinc atoms. Thus, in the latter case, the cyclic structures comprise of four paddle wheel units. Thus, the

1-D polymer has resemblance with **fig. 6.10a** whereas the 2-D has resemblance with **fig. 6.11a**. The bond distances and bond angles involving the coordination sphere around zinc for complex **6.13** and **6.14** are given in **table 6.3**. In the zinc complexes **6.13** and **6.14**, the lone pairs project away from each other to minimize repulsion and they are placed in a nonparallel manner, however, the arrangement is *syn* with respect to each other.

Table 6.2 Selected metal-ligand bond distances (Å) and angles (º) of coordination polymers **6.13** and **6.14**

6.13				**6.14**			
Bond	Distances	Bond	Angles	Bond	Distances	Bond	Angles
Zn1-N1	2.02(6)	N1-Zn1-O5	107.3(2)	Zn1-O3	2.04(2)	O4-Zn1-O6	89.6(9)
Zn1-O3	2.10(4)	N1-Zn1-O6	100.2(2)	Zn1-O4	2.02(2)	O4-Zn1-O7	86.9(1)
Zn1-O4	2.02(4)	O4-Zn1-O3	86.8(1)	Zn1-O5	1.99(1)	O5-Zn1-O3	99.5(8)
Zn1-O5	2.06(4)	O4-Zn-O5	89.5(1)	Zn1-O6	2.08(2)	O5-Zn1-O4	102.4(8)
Zn1-O6	2.03(4)	O4-Zn1-O6	157.4(1)	Zn1-O7	2.04(2)	O5-Zn1-O6	97.9(9)
Zn1-Zn1	3.03(1)	O5-Zn1-O3	157.4(1)	Zn1-Zn1	3.01(6)	O5-Zn1-O7	104.0(9)
		O6-Zn1-O3	86.0(1)			O7-Zn1-O3	90.2(1)
		O6-Zn1-O5	88.9(1)			O7-Zn1-O6	158.1(1)
		N1-Zn1-O3	95.3(2)			O3-Zn1-O6	85.0(1)
		N1-Zn1-O4	101.7(1)			O4-Zn1-O3	157.9(9)

The presence of dimethylformamide and pyridine auxiliary ligand makes totally different types of weak interactions in the packing pattern of the crystal structures of the two coordination polymers, namely **6.13** and **6.14**. The important weak interactions present among the different moieties are shown in **fig. 6.12**. The pyridine containing 1-D coordination polymer **6.13** (**fig. 6.12a**) has C–H···π interactions ($d_{H30\cdots\pi C21}$, 2.76 Å, $d_{H27\cdots\pi C18}$, 2.88 Å). The one dimensional coordination polymer has weak C-H···O interaction between aromatic C22–H22 with O6 of carboxylate group ($d_{D\text{-}A}$, 3.47 Å; $d_{D\text{-}H}$ 0.93 Å; <D-H-A, 140.4º). The two dimensional coordination polymer **6.14** (**fig. 6.12b**) is anchored by C13–H13B···S1 ($d_{D\text{-}A}$ 3.65 Å, $d_{D\text{-}H}$ 0.970 Å; <D-H-A 134.8º) whereas the one dimensional coordination polymer has no C–H···S interactions. The C–H···S interactions are important in organic sulfur containing compounds to make intercrossing between layers,[447] polymorphs[448] and also deciding conformation.[449] The

dimethylformamide containing two dimensional coordination polymer **6.14** has C–H···π interactions ($d_{H13A\cdots\pi C10}$, 2.82 Å).

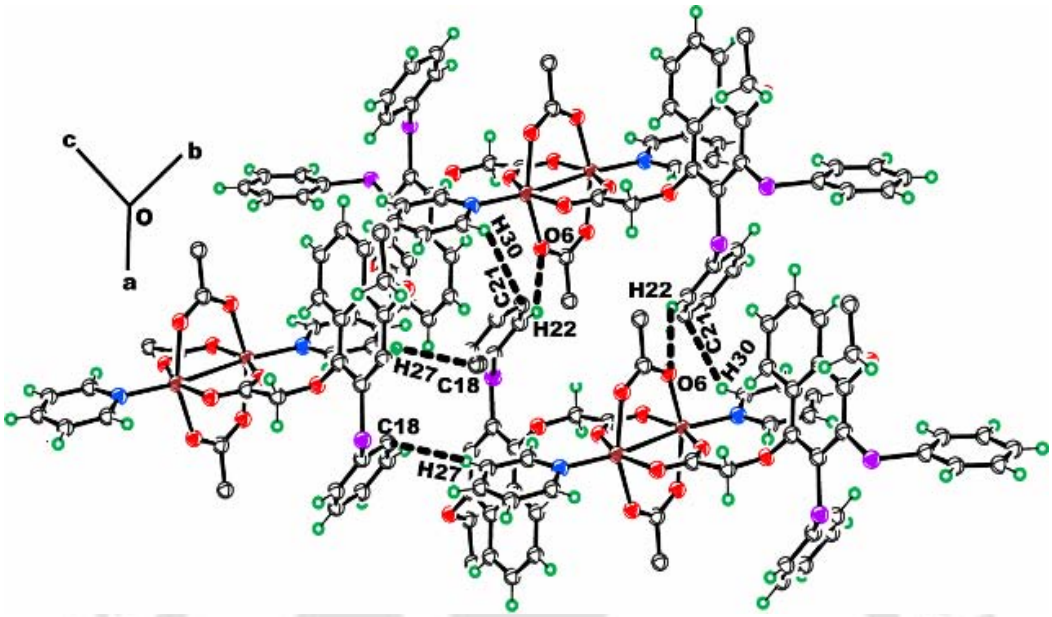

a

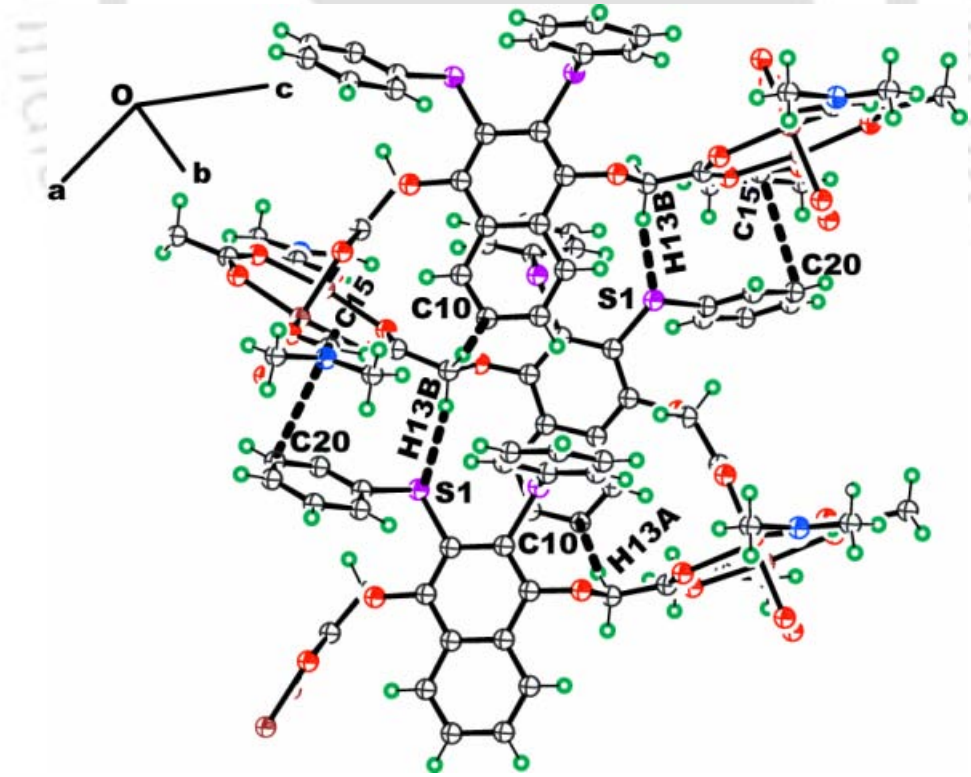

b

Fig. 6.12 a) Self assembly structure of polymer **6.13**; b) Self assembly structure of polymer **6.14** (ORTEP drawn with 50% thermal ellipsoid)

There is also a π···π interaction between the dimethylformamide and benzene ring attached to the sulfur (**fig. 6.12b**). The centroid to centroid separation for the carbonyl carbon and the aromatic carbon atom of the ring $d_{C15\cdots C20}$ is 3.38 Å. In addition to this very weak C17–H···O4 interaction ($d_{D\text{-}A}$ 3.36 Å, $d_{D\text{-}H}$ 0.96 Å, <D-H-A 124.9º) between the methyl groups of dimethyl formamide with one oxygen atom of the carboxylate is also present. Some of the important hydrogen bond distances and bond angles of polymers **6.13** and **6.14** are listed in **table 6.4** and **6.5** respectively.

Table 6.4. The hydrogen bond parameters for polymer **6.13**

D−H···A	D−H (Å)	H···A (Å)	D···A (Å)	<D−H···A(°)
C22−H22···O6	0.930	2.703	3.471	140.4
C27−H27··· π_{C18}	0.930	2.879	3.780	
C30−H30··· π_{C21}	0.931	2.760	3.449	

Table 6.5. The hydrogen bond parameters for polymer **6.14**

D−H···A	D−H (Å)	H···A (Å)	D···A (Å)	<D−H···A(°)
C17−H17C···O4	0.959	2.718	3.360	124.9
C13−H13A··· π_{C10}	0.970	2.817	3.758	
C13−H13B··· S1	0.970	2.753	3.654	154.8
$\pi_{15}\cdots\pi_{C20}$			3.379	

It is reported in the literature that the weak interactions can change the dimensionality of coordination polymers.[449] In our case also similar observations are observed but in this case the spatial arrangement of the naphthalene rings plays a major role in doing so. The differences in these directional C–H···π and π···π interactions[450] in the two cases makes the disposition of the naphthalene rings different, although they are placed parallel manner in both cases. In the case of the one dimensional polymer the aromatic ring attached to the sulfur atoms of each parallel pair is oriented towards the opposite sides with respect to each other, whereas such rings of parallel pairs of naphthalene rings are on the same side in the case of the two dimensional coordination polymers. This disposition of the naphthalene rings force the carboxylate to bind to the metal ions in different orientations and changes the dimensionality of the two polymers.

The ligand has infra-red absorption at 1634 cm^{-1} due to the carboxylate carbonyl C=O frequency and in complex **6.13** this absorption appears at 1619 cm^{-1}. In the complex

6.14 the C=O of dimethylformamide and of the ligand appears together as a broad signal at 1660 cm^{-1}. Thermogravimetry of two complexes **6.13** and **6.14** are different. In the case of **6.13** one pyridine is lost below 250º C whereas the other one pyridine loses along with arylsulfanyl groups which are lost as disulfide at about 250-500º C. The complex **6.14** loses the dimethylformamide groups at 80-100º C and it loses the two arylsulfanyl groups at 270-400º C as shown in **fig. 6.13**.

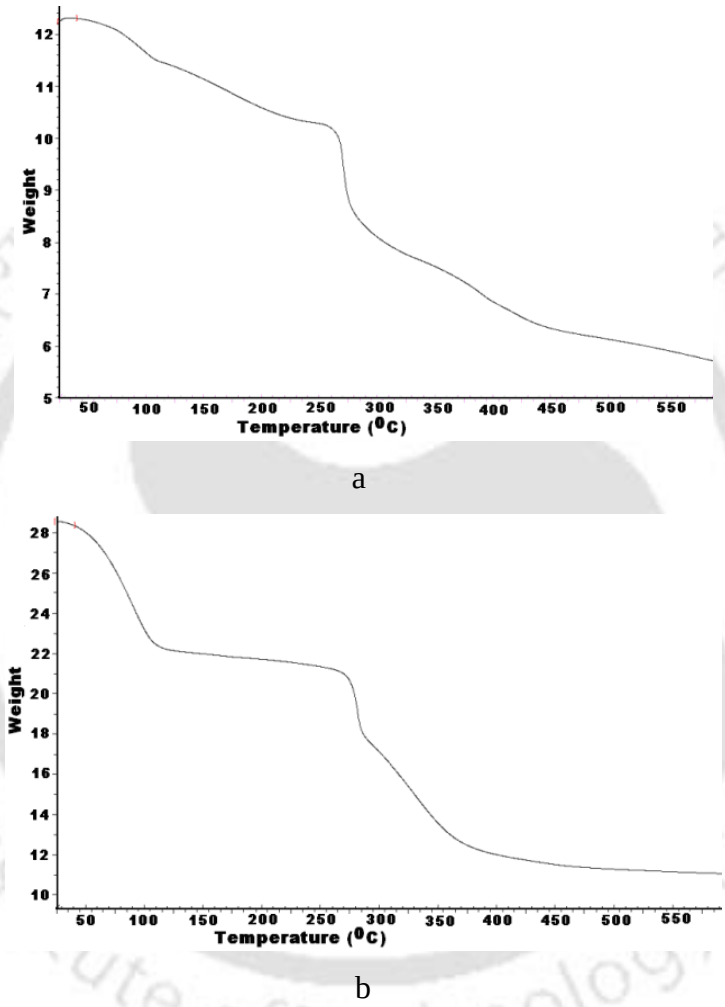

Fig. 6.13 Thermogram for the complexes a) **6.13**; b) **6.14** (heating rate 5° C/minute)

A coordination polymer of zinc with **LH2** (where Ar is a phenyl group) having water and dimethylformamide ancillary ligands having a composition {[$Zn_2L_2(H_2O)$DMF] DMF.H_2O}n **6.15** is also prepared. In the crystal structure of this coordination polymer **6.15**, we could not locate the hydrogen atoms of the water molecules lying outside the co-ordination sphere. The structural backbone (**fig. 6.14**) is a one dimensional polymer of interconnected zinc paddle wheel structures. The bond distances and bond angles

involving zinc ions are given in **table 6.6**. A careful look at the structure suggests that the phenylsulfanyl groups on the parallel naphthalene rings project exactly in opposite directions. This type of arrangement is observed in structure **6.13**.

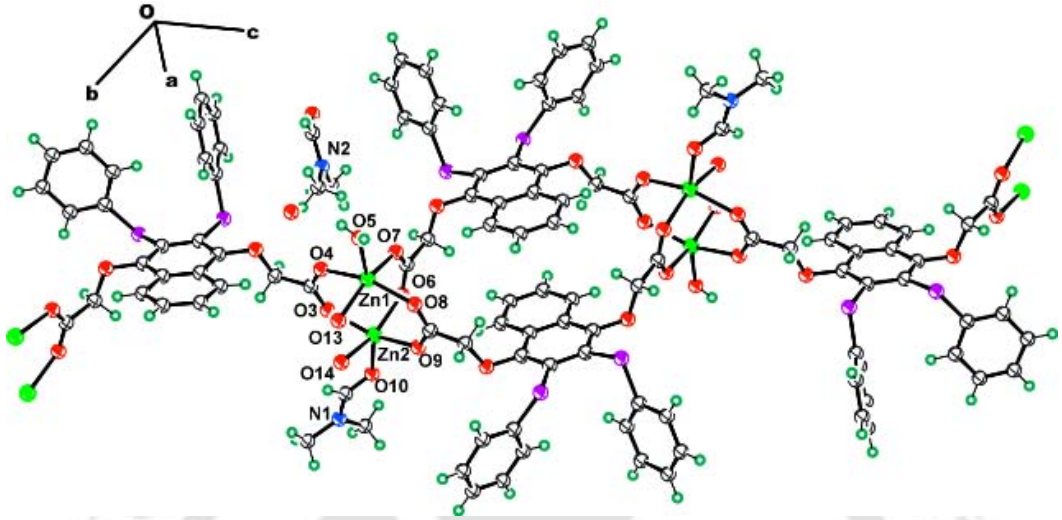

Fig. 6.14 Crystal structure of repeated unit of coordination polymer **6.15** (ORTEP drawn with 30% thermal ellipsoid)

Table 6.6 Selected metal-ligand bond distances (Å) and angles (º) of coordination polymers **6.15**

Bonds	Bond distances (Å)	Bonds	Bond angles (º)	Bonds	Bond angles (º)
Zn1-O4	2.06(5)	O8-Zn1-O7	88.3(2)	O10-Zn2-O3	96.9(2)
Zn1-O5	1.98(6)	O8-Zn1- O13	88.9(2)	O5-Zn1-O4	95.2(3)
Zn1-O7	2.05(5)	O7-Zn1-O4	88.3(2)	O10-Zn2-O9	105.3(2)
Zn1-O8	2.03(5)	O13-Zn1-O4	86.0(2)	O5-Zn1-O7	100.7(2)
Zn1-O13	2.05(5)	O13-Zn1-O7	158.0(2)	O10-Zn2-O6	104.9(2)
Zn2-O3	2.06(5)	O3-Zn2-O14	85.2(2)	O5-Zn1-O8	107.5(3)
Zn2-O6	2.04(5)	O6-Zn2-O3	88.4(2)	O10-Zn2-O14	96.9(1)
Zn2-O9	2.03(5)	O6-Zn2-O14	157.9(2)	O5-Zn1-O13	100.9(2)
Zn2-O10	1.99(5)	O9-Zn2-O3	157.6(2)	O8-Zn1-O4	157.3(2)
Zn2-O14	2.10(5)	O9-Zn2-O6	88.7(2)	O9-Zn2-O14	89.2(2)

This similarity suggests the role of orientation of the naphthalene ring in the change of dimensionality of the coordination polymers. It may be mentioned that the coordination polymer **6.15** adopts a three dimensional supramolecular network structure, built by weak interactions in the lattice. The interstitial water, coordinated water,

dimethylformamide along with an oxygen atom of carboxylate contributes to the formation of cyclic hydrogen bonded arrays that hold the layers in three dimensions. The dimension increases in supramolecular coordination polymers through interlayer interactions is well known.[449] However we clearly demonstrate the effect of variation of the backbone of the coordination polymer by changing ancillary ligands and changing the directional weak interactions. The crystal lattice is mainly stabilized by the C−H··· O and C−H··· π interactions (**fig. 6.15**). Some of the important hydrogen bond distances and bond angles of polymers **6.15** are listed in **table 6.7**.

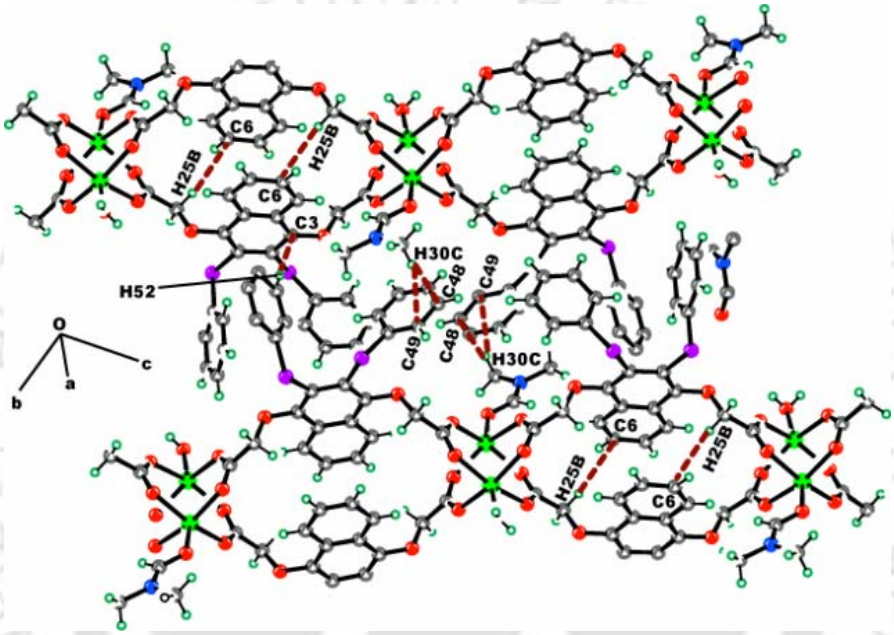

Fig. 6.15 Self assembly structure of polymer **6.15** (ORTEP drawn with 50% thermal ellipsoid)

From here, it may be pointed out that in each case the solvents are different; accordingly ancillary ligands are also different, thus the two factors the ancillary ligand and the solvent play a crucial role in giving rise to different types of structures. The sulfur atoms of a ligand may or may not participate in weak interactions but provide orientation to the naphthalene rings; such factors are also decisive in the dimensionality of these coordination polymers.

Table 6.7. The hydrogen bond parameters for polymer **6.15**				
D−H···A	D−H (Å)	H···A (Å)	D···A (Å)	<D−H···A(°)
C58−H58C···O2	0.959	2.551	3.386	145.57
C30−H30C··· π_{C48}	0.960	2.675	3.531	
C30−H30C··· π_{C49}	0.960	2.819	3.720	
C30−H30B··· π_{C36}	0.960	2.831	3.706	
C52−H52··· π_{C3}	0.930	2.863	3.753	
C33−H33A··· S4	0.971	2.920	3.636	131.43

The zinc coordination polymer **6.16** derived from **LH2** with the aryl group as the 4-methylphenyl group and having pyridine, has a composition similar to that of **6.13** (**scheme 6.4**). However, in this case we have observed the two aromatic rings in the coordination polymer namely the pyridine ring and the ring attached as the arylsulfanyl groups are disordered.

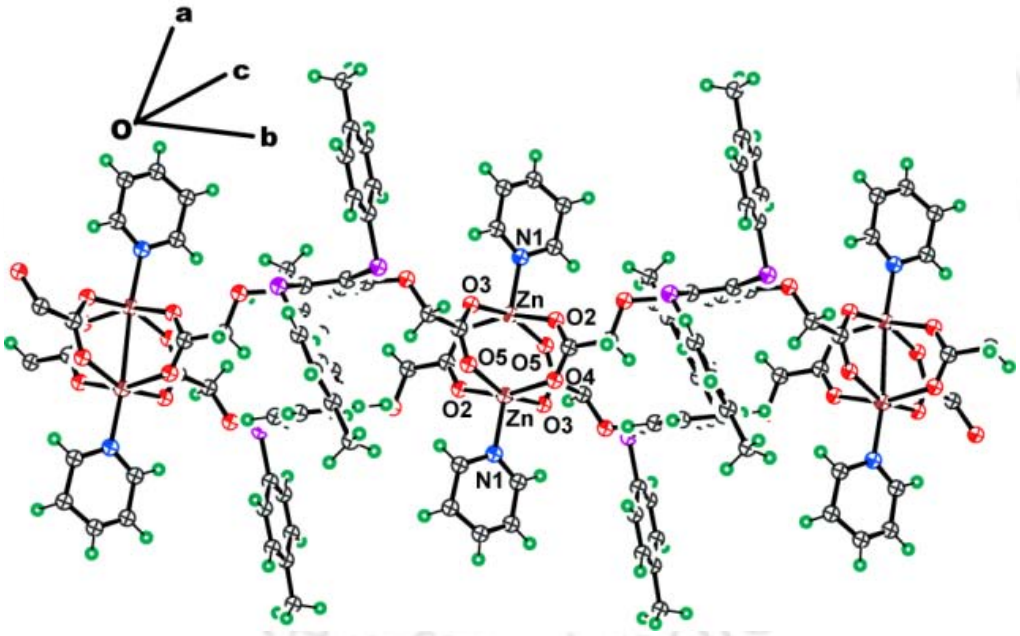

Fig. 6.16 Crystal structure of repeated unit of coordination polymer **6.16** (the disordered atoms are remove for clarity; ORTEP drawn with 30% thermal ellipsoid)

The structure of the coordination polymer **6.16** is shown in **fig. 6.16**. The bond distances and bond angles involving zinc ions are given in **table 6.8**. The complex has distorted square pyramidal geometry around each zinc ion. Although the coordination polymer self assembles through weak interaction due to the disorder in the rings discussion on them has only qualitative value. In solid state FT-IR spectra the complex shows a stretching frequency around at 1619 cm^{-1} for C=O of the carboxylate groups.

Table 6.8 Selected metal-ligand bond distances (Å) and angles (º) of coordination polymers **6.16**

Polymer 6.16			
Bonds	Bond distances (Å)	Bonds	Bond angles (º)
O2-Zn1	2.07(4)	O4-Zn1-O5	90.3(1)
O3-Zn1	2.05(4)	O4-Zn1-N1	101.4(4)
O4-Zn1	2.03(4)	O5-Zn1-O2	103.0(3)
O5-Zn1	2.04(4)	O5-Zn1-N1	86.4(1)
N1-Zn1	2.04(8)	O5-Zn1-O3	158.1(1)
Zn1-Zn1	2.99(1)	N1-Zn1-O2	100.3(4)
Bonds	Bond angles (º)	N1-Zn1-O3	98.9(3)
O4-Zn1-O2	158.3(1)	O3-Zn1-O2	88.8(1)
O4-Zn1-O3	86.2(1)		

From the above discussion, the coordination polymers of zinc with dicarboxylate ligand having flexible methylene groups as tether and depending on the ancillary ligand it adopts different types of structures. In each case paddle wheel structures are formed around each pair of zinc ions, which expand as one or two dimensional polymers. These polymers make supramolecular assemblies through C–H···π, C–H···O and π···π interactions. Pyridine as the ancillary ligand leads to a one dimensional polymer; whereas, dimethylformamide leads to a two dimensional polymer. The presence of dimethylformamide and water as ancillary ligands at two sites of the paddle wheel leads to one-dimensional polymers. The formation of each of these polymers depends on the preferential arrangements of the arylsulfanyl groups in the lattice; which provides the required geometry to the naphthalene rings controlling the dimensionality of the coordination polymer and the process is dependent on the solvents.

6.4 Coordination polymers of cadmium (II) carboxylate

The coordination chemistry of cadmium is interesting due to its ability to form complexes with different coordination numbers.[451-456] The multiple possibilities of coordination numbers make cadmium complexes suitable for structural variations by providing steric factors of ancillary ligands and substituents, and variations between

trigonal prismatic and severely distorted octahedral coordination are observed in cadmium compounds.[457-458] Depending on the compositions and on the ancillary ligands, cadmium complexes adopt a variety of structures. There is good amount of interest on the use of flexible carboxylate ligands for the synthesis of coordination polymers with various interesting structural features.[459-466]

We have also investigated the reaction of (4-carboxymethoxy-2,3-bis-phenylsulfanylnaphthalene-1-yloxy) acetic acid **6.5** with cadmium(II) acetate and observed a three dimensional coordination polymer **6.17** which encapsulates water and dimethylformamide (**scheme 6.5**). The effect of substituent on the naphthalene rings on the structure of a cadmium complex is reflected in the three dimensional coordination polymer derived from (4-carboxy-methoxy-2,3-bis-phenylsulfanylnaphthalene-1-yloxy) acetic acid **6.5** with cadmium ion in dimethylformamide (**scheme 6.5**).

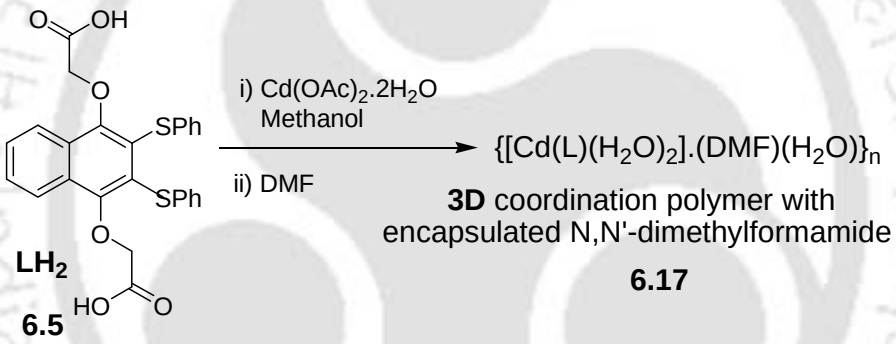

Scheme 6.5 Reaction of cadmium(II) acetate with (4-carboxy-methoxy-2,3-bis-phenylsulfanylnaphthalene-1-yloxy) acetic acid **6.5**.

The three dimensional coordination polymer **6.17** is crystallizes as colorless block in chiral $P2_12_12_1$ space group. The coordination polymer is constructed by cadmium ions in seven coordination geometry. The pictorial representation and the crystal structure of repeated unit in the three dimensional coordination polymer **6.17** is shown in **fig. 6.17**. Each cadmium ion is connected to three ligand molecules through carboxylates, the central metal atom do not bear additional charge and are in (+2) oxidation state.

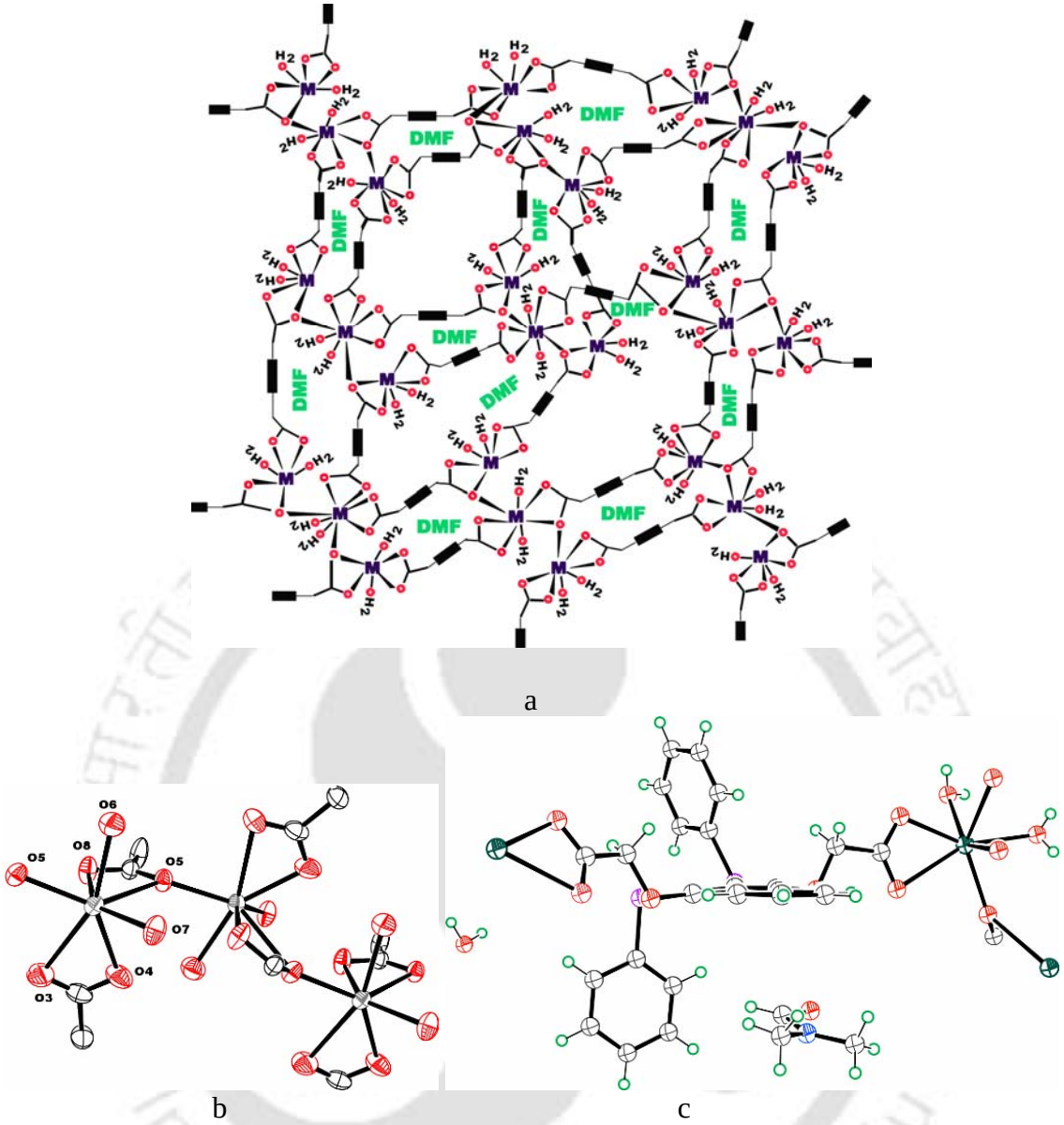

a b c

Fig. 6.17 a) Pictorial representation of three dimensional coordination polymer **6.17**; b) A segment of the polymer backbone to show coordination geometry around cadmium; c) Structure of repeated units of coordination polymer **6.17** (ORTEP drawn with 50% thermal ellipsoids).

The coordination polymer has two perpendicular chelating types of carboxylates and two water molecules coordinated to the metal center. The seventh coordination site is occupied by oxygen of a chelating carboxylate at cadmium. Among the two chelating carboxylate also serves as a bridging ligand. These oxy-bridges adds the extra dimension to the two dimensional networks. Thus, two chelating ligands that makes the chain to grow in perpendicular direction whereas there is another set of chelating carboxylate on neighboring cadmium ions that serves as bridge to make a three

dimensional networks. Some of the important metal-ligand bond distances and angles of compound **6.17** are listed in **table 6.9**.

Table 6.9 Selected metal-ligand bond distances (Å) and angles (º) of compound **6.17**

Polymer 6.17					
Bond	Distance	Bond	Angle	Bond	Angle
Cd1- O3	2.635(2)	O5-Cd1-O7	128.57(8)	O8-Cd1-O3	85.69(8)
Cd1-O4	2.302(2)	O5-Cd1-O4	131.05(8)	O6-Cd1-O3	156.41(10)
Cd1- O5	2.248(8)	O7-Cd1-O4	80.19(9)	O5-Cd1-O5	132.74(3)
Cd1- O6	2.344(3)	O5-Cd1-O8	85.43(7)	O7-Cd1-O5	89.12(7)
Cd1- O7	2.275(2)	O7-Cd1-O8	140.93(8)	O4-Cd1-O5	75.59(7)
Cd1- O8	2.336(19)	O4-Cd1-O8	90.93(8)	O8-Cd1-O5	51.91(6)
Cd1- O5	2.644(17)	O5-Cd1-O6	77.98(9)	O6-Cd1-O5	79.44(9)
Bond	Angle	O7-Cd1-O6	83.96(10)	O3-Cd1-O5	111.84(7)
C26-O8-Cd1	99.59(16)	O4-Cd1-O6	150.48(10)	Cd1-O5-Cd1	134.71(8)
C26-O5-Cd1	133.25(16)	O8-Cd1-O6	85.86(9)	C24-O3-Cd1	85.40(19)
C26-O5-Cd1	85.26(14)	O5-Cd1-O3	79.42(8)	C24-O4-Cd1	100.4(2)
O4-Cd1-O3	51.64(8)	O7-Cd1-O3	115.84(9)		

The powder X-ray diffraction patterns of bulk samples of each of the coordination polymers **6.17** is determined and compared with the theoritical powder X-ray diffraction pattern. **Fig. 6.18** shows the powder X-ray diffraction patterns of three dimensional coordination polymer **6.17** (black line = experimental; blue line = theoretical).

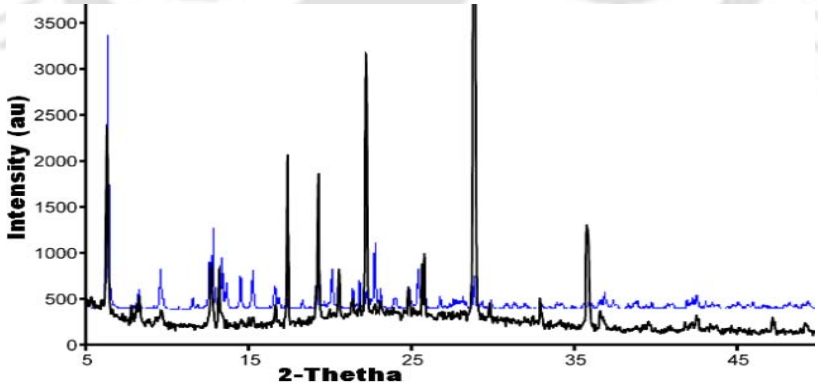

Fig. 6.18 Powder diffraction pattern of polymer **6. 17** (black line = experimental; blue line = theoretical)

We had also synthesized the 4-(carboxymethoxynaphthalen-1-yloxy) acetic acid **6.19** by functionalizing the 1,4-dihydroxy naphthalene as shown in **scheme 6.6**. In this

dicarboxylic acid ligand, the two arylsulphanyl groups are not present as it has in the cases of the dicarboxylic acid ligands **6.5-6.8**.

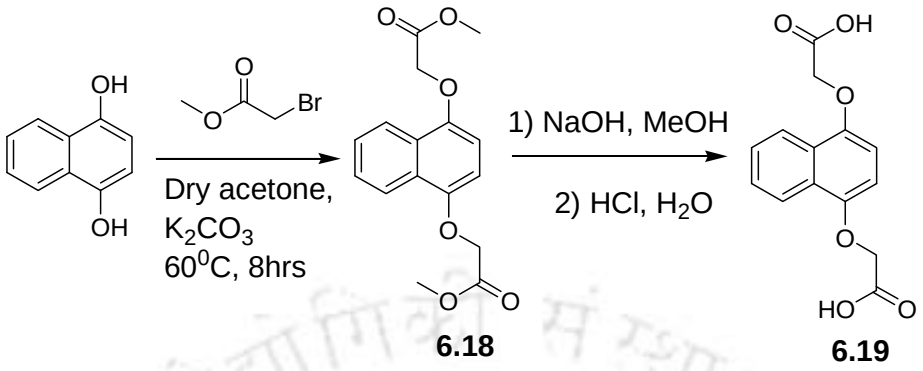

Scheme 6.6 Synthesis of dicarboxylic acid ligand **6.19**

The 4-(carboxymethoxy-naphthalen-1-yloxy) acetic acid **6.19** reacts with cadmium(II) acetate dihydrate in the presence of 1,10-phenanthroline to give an one dimensional polymer **6.20** (**scheme 6.7**). The coordination polymer **6.20** is crystallizes as colorless block in centrosymmetric monoclinic C2/c space group. The polymer has a seven coordination numbers with distorted pentagonal bipyramid geometry.

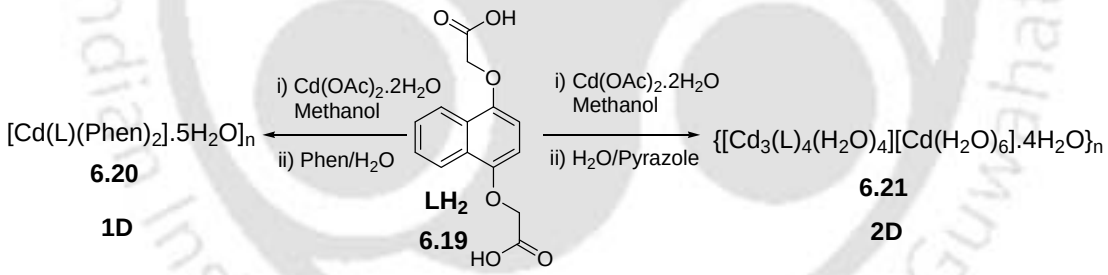

Scheme 6.7 Synthesis of 1D and 2D coordination polymers of cadmium

The basal plane of the pentagonal bipyramid geometry is formed by a bridging carboxylate, two chelating nitrogen donors of one 1,10-phenanthroline and one nitrogen from another 1,10-phenanthroline.

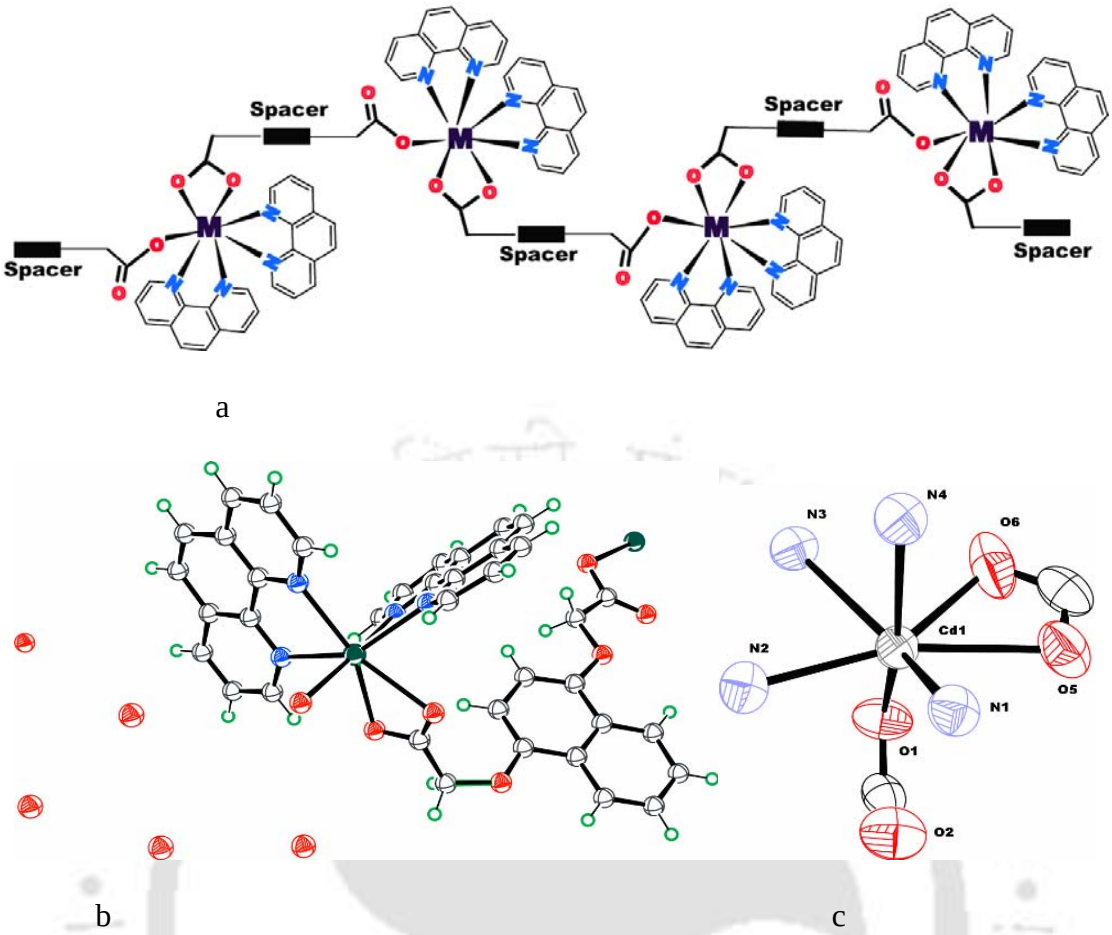

Fig. 6.19 a) Pictorial representation of one dimensional coordination polymer **6.20**; b) Crystal structure of repeated units of coordination polymer **6.20**; c) The coordination environment around cadmium (ORTEP drawn with 50% thermal ellipsoids)

The axial positions are occupied by monodentate carboxylate oxygen of another dicarboxylic acid molecule, and the nitrogen atom of the 1,10-phenanthroline molecule perpendicular to the basal plane. Further to this, each cadmium ion has five molecules of water of crystallization. The pictorial representation and crystal structure of repeated units in the coordination polymer are shown in **fig. 6.19**. The structure of the one dimensional coordination polymer **6.20** is not unusual as the phenylenediacetate complex of cadmium having pyridine as ancillary ligands is a one dimensional coordination polymer[5]. Some of the important metal-ligand bond distances and angles of compound **6.20** is listed in **table 6.10**.

Table 6.10 Selected metal-ligand bond distances (Å) and angles (º) of compound **6.20**

Polymer 6.20					
Bond	Distance	Bond	Angle	Bond	Angle
Cd1-O1	2.294(3)	O1-Cd1-O6	85.2(13)	N1-Cd1-N3	88.6(11)
Cd1-O5	2.524(12)	O1-Cd1-N1	126.3(12)	N1-Cd1-N4	142.2(12)
Cd1-O6	2.322(5)	O1-Cd1-N3	90.7(12)	N1-Cd1-N2	68.9(11)
Cd1-N1	2.367(3)	O1-Cd1-N4	85.7(13)	N1-Cd1-O5	73.1(4)
Cd1-N3	2.398(3)	O1-Cd1-N2	164.8(13)	N2-Cd1-O5	91.2(5)
Cd1- N4	2.428(3)	O1-Cd1-O5	93.5(5)	N3-Cd1-N4	69.3(12)
Cd1-N2	2.511(4)	O6-Cd1-N1	116.2(13)	N3-Cd1-N2	89.9(11)
Bond	Angle	O6-Cd1-N3	151.8(14)	N3-Cd1-O5	159.8(4)
N4-Cd1-O5	130.7(4)	O6-Cd1-N4	82.6(14)	N4-Cd1-N2	80.3(11)
C14-O5-Cd1	95.3(8)	O6-Cd1-N2	87.2(12)	O6-Cd1-O5	48.4(4)

Similar reaction of 4-(carboxymethoxy naphthalen-1-yloxy) acetic acid **6.19** with cadmium(II) acetate were attempted with pyrazole, but we did not get a pyrazole containing complex; instead we obtained a two dimensional anionic polymer **6.21** (**scheme 6.7**).

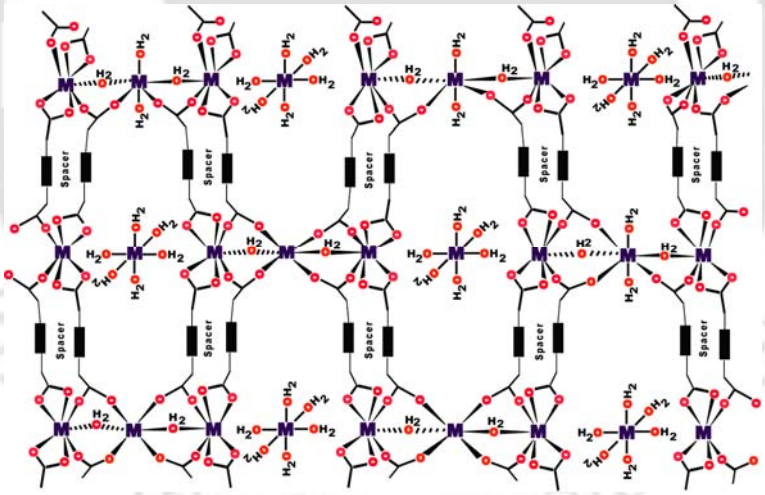

a

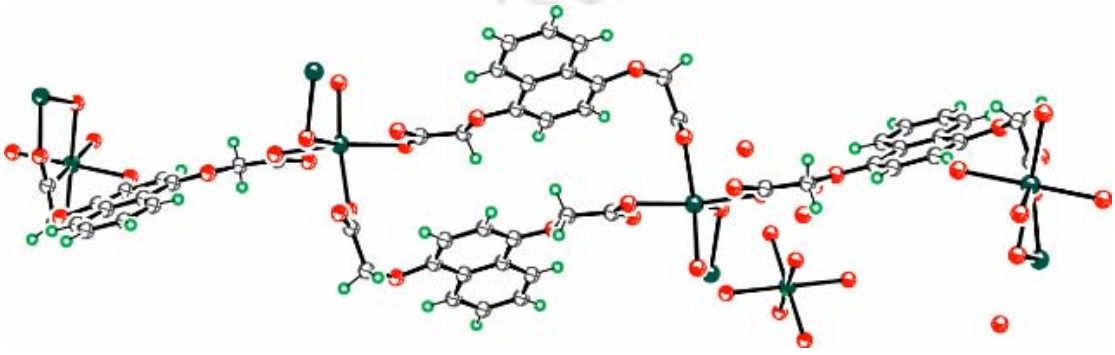

b

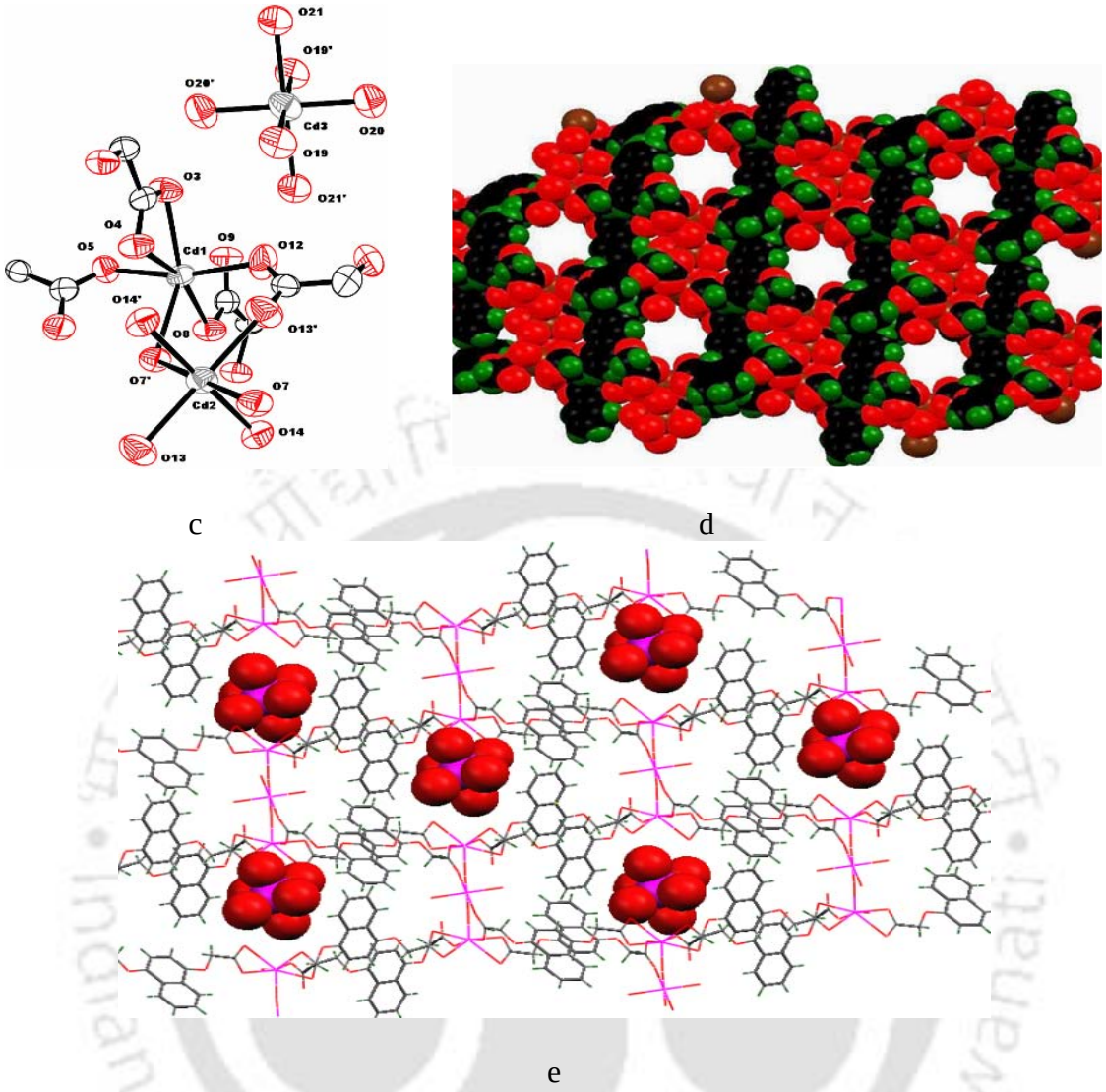

Fig. 6.20 a) Pictorial representation of two dimensional network of **6.21** encapsulating $[Cd(H_2O)_6]^{2+}$; b) Structure of coordination polymer **6.21**; c) segment of the polymer to show coordination geometries around the cadmium centers (ORTEP drawn with 50% thermal ellipsoids); d) Spacefill model of two dimensional polymer **6.21**; e) Encapsulation of hexa-aqua cadmium dications

The two dimensional coordination polymer **6.21** is crystallizes as colorless block in centrosymmetric triclinic P-1 space group. This coordination polymer is unique as it encapsulates hexaaqua cadmium(II) cation (**fig. 6.20**). The polymer could not be prepared without pyrazole suggests that the pyrazole reacted with the acetic acid formed in the reaction. We could not obtain any acetic acid or pyrazole as solvent of crystallization.

The polymer has an aqua bridged and a carboxylate bridge to hold two cadmium ions. These cadmium ions are further held by chelating carboxylate groups. Each cadmium sites in the polymer network is of seven coordination numbers with distorted pentagonal bipyramid geometry. The base of the pentagonal bipyramid comprises of two chelating carboxylates of two independent ligands and a water molecule which serves as bridge between two cadmium centers and allows the polymer to grow parallel to bc-plane. The two axial positions are occupied by oxygen atoms of two independent carboxylate ligands. These two carboxylates serves as bridges to alternating cadmium ions to make the chain grow along the y-axis which is complemented by aqua bridges. The polymer is grown perpendicular to the bc-plane with the help of the chelating carboxylate groups at two ends of the ligands to hold the cadmium ions.

Table 6.11 Selected metal ligand bond distances (Å) and angles (º) of compound **6.21**

Polymer 6.21					
Bond	Distance	Bond	Angle	Bond	Angle
Cd1-O3	2.309(6)	O3-Cd1-O4	54.5(17)	O13-Cd2-O7	86.2(2)
Cd1-O4	2.487(5)	O3-Cd1-O7	132.4(19)	O14-Cd2-O14	180.0(2)
Cd1-O5	2.246(6)	O5-Cd1-O8	91.8(2)	O14-Cd2-O7	88.7(2)
Cd1-O7	2.410(5)	O5-Cd1-O3	84.1(2)	O14-Cd2-O7	91.3(2)
Cd1-O8	2.277(6)	O5-Cd1-O7	90.7(19)	O19-Cd3-O19	180.0(1)
Cd1-O12	2.240(6)	O5-Cd1-O4	88.7(2)	O19-Cd3-O20	96.2(2)
Cd2-O7	2.359(5)	O7-Cd1-O4	78.1(18)	O19-Cd3-O20	83.8(2)
Cd2-O13	2.240(6)	O8-Cd1-O4	157.6(18)	O19-Cd3-O20	96.2(2)
Cd2-O14	2.271(6)	O8-Cd1-O3	147.8(18)	O20-Cd3-O20	180.0(1)
Cd3-O19	2.225(5)	O8-Cd1-O7	79.5(19)	O21-Cd3-O21	180.0(1)
Cd3-O20	2.296(6)	O12-Cd1-O5	164.7(2)	O21-Cd3-O20	92.3(3)
Cd3-O21	2.208(7)	O12-Cd1-O8	91.2(2)	O21-Cd3-O20	87.7(3)
Bond	Angle	O12-Cd1-O3	85.4(2)	O21-Cd3-O19	93.6(2)
C15-O8-Cd1	104.6(5)	O12-Cd1-O7	104.6(2)	O21-Cd3-O19	86.4(2)
C13-O4-Cd1	88.3(5)	O12-Cd1-O4	94.1(2)	Cd2-O7-Cd1	110.7(2)
C13-O3-Cd1	95.8(4)	O7-Cd2-O7	180.0(3)	C14-O5-Cd1	126.1(5)
C28-O12-Cd1	124.7(6)	O13-Cd2-O13	180.0(5)	O13-Cd2-O14	92.4(2)
C28-O13-Cd2	143.7(6)	O13-Cd2-O14	87.6(2)	O13-Cd2-O7	93.8(2)

This growth makes a two dimensional network and making grid like structures. Thus, it is clear that each of the cadmium ions is coordinated by four independent dicarboxylate ligands. This makes each of the cadmium in the chains to have a cationic charge. To compensate these charges, the coordination polymer uses cationic hexa-aqua cadmium dication. These complex dications are held in the interstices to make a rare example of

relatively large size cationic complex inclusion into a coordination polymer. Conventionally macrocyclic type of ligands is used for inclusion of alkali metal ion or transition metal complex hexa-aquated cations. Some of the important metal-ligand bond distances and angles of compound **6.21** is listed in **table 6.11**.

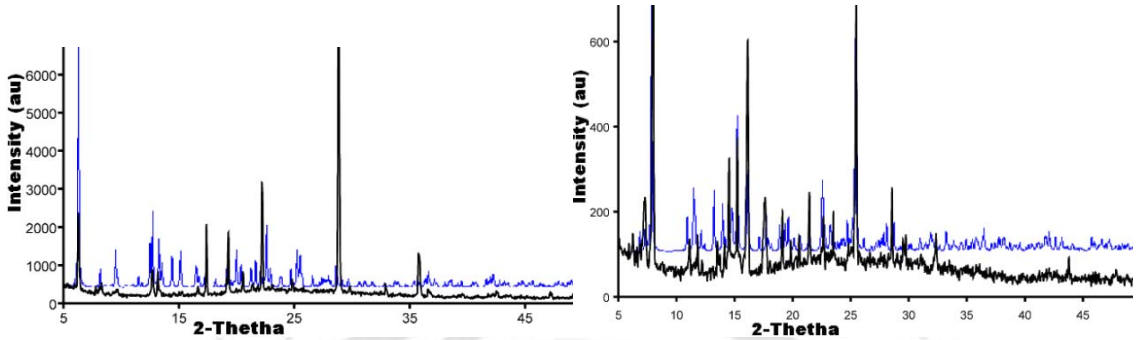

a b

Fig. 6.21 Powder diffraction pattern of polymers a) **6. 20**; b) **6.21** (black line = experimental; blue line = theoretical)

The powder X-ray diffraction patterns of bulk samples of each of the coordination polymers **6.20** and **6.21** were determined and compared with the theoritical powder X-ray diffraction pattern (**fig. 6.21**). A fair amount of additional peaks are observed in the simulated spectra, suggesting differences in the bulk material to the crystals. This is attributed to loss of solvent molecules making the system amorphous. We also could not locate some of the labile hydrogen atoms in the structure determined by single crystal diffraction. Further to this, the bulk samples did not show satisfactory elemental analysis. We checked the thermogravimetry of the coordination polymers and found that they lose the coordinated as well as interstitial water upon heating to 250º C; beyond this temperature the coordination polymers degraded.

6.5 Photoluminescence properties of polymer 6.20 and 6.21

The coordination polymers **6.20** and **6.21** show visible absorptions in the solid state at 480 and 485 nm respectively. Based on the reported observations of absorptions of cadmium complexes with aromatic-donor ligands, these absorptions are assigned to occur from ligand to metal charge transfer transition.[467-468] There is considerable interest on the fluorescence emission of metal organic frameworks that are built with d^{10} metals.[464, 469-471]

In the solid state these two polymers **6.20** and **6.21** shows fluorescence emission at 609 and 638 nm respectively upon excitation at 470 nm (**fig. 6.22**). The relative intensity of emission from the coordination polymer **6.20** is about five times lower than that of the coordination polymer **6.21**.

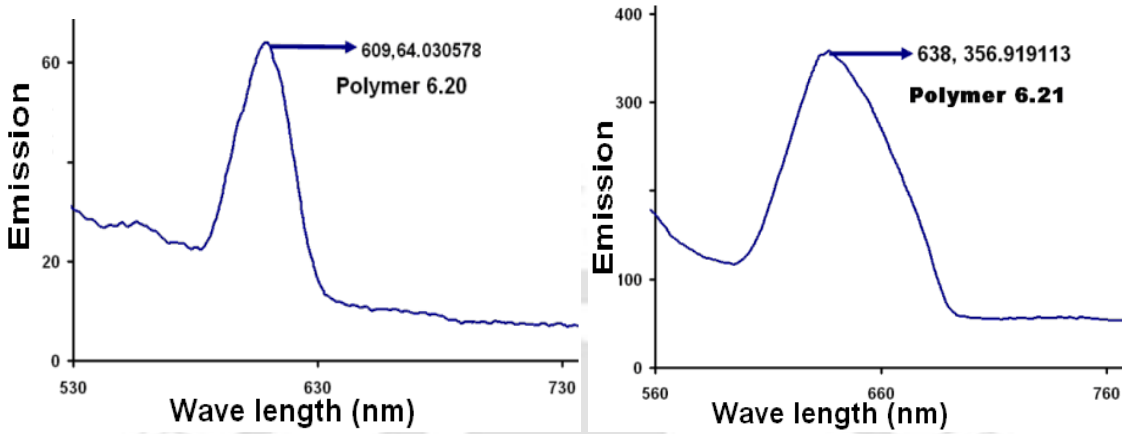

a b

Fig. 6.22 Solid state photoluminescence spectra of coordination polymers a) **6.20**; b) **6.21**

In both the cases we did not observed any shoulder in neither at the longer wavelength side nor at the shorter wavelength side of emission of the parent linker. In addition, the free dicarboxylic acid and 1,10-phenanthroline ligand does not emit any luminescence in the range 500-700 nm and the d-orbital in zinc(II) and cadmium(II) are core like orbital.[472] In polymer **6.20**, all the cadmium(II) ions have same coordination environment, therefore the fluorescence emission at 609 nm may be assigned to the linker to metal charge transfer (LMCT) and/or π–π* transition of the ligand. In polymer **6.21**, it has three cadmium centers with different coordination environment, thus the fluorescence emission at 638 nm might be attributable to a combined contribution of the three metal centers and/or ligand to metal charge-transfer (LMCT).[467-468] The strong fluorescent emissions of the polymers **6.20** and **6.21** make them potentially useful photoactive materials.

The crystal data and refinement parameters of compound **6.9-6.17** and **6.20-6.21** are listed in **table 6.12**.

Table 6.12 Crystallographic parameter of compounds **6.9-6.17** and **6.20-6.21**

Compound No.	**6.9**	**6.10**	**6.11**	**6.12**
Formulae	$C_{76}H_{66}N_4O_{13}S_4Mn_2$	$C_{101}H_{89}N_9O_{12}S_4Cu_2$	$C_{101}H_{89}N_9O_{16}S_4Cu_2$	$C_{97}H_{77}N_9O_{12}S_4Br_4Cu_2$
Mol. wt.	1481.45	1876.13	1940.13	2135.64
Crystal system	Triclinic	Orthorhombic	Orthorhombic	Orthorhombic
Space group	P-1	Pnna	Pnna	Pnna
a (Å)	14.0615(19)	15.9691	15.9667(2)	15.9305
b (Å)	17.151(2)	54.4728	54.5343(7)	54.404
c (Å)	18.125(2)	10.4636	10.57280(10)	10.6095
α/°	62.780(8)	90.00	90.00	90.00
β/°	72.952(8)	90.00	90.00	90.00
γ/°	69.964(9)	90.00	90.00	90.00
V (Å ^{3})	3602.8(8)	9102.1	9206.08(19)	9195.1
Z	2	4	4	4
Density/Mgm^{-3}	1.366	1.369	1.400	1.543
Abs. Coeff. /mm-1	0.532	0.627	0.626	2.359
Abs. correction	none	none	none	none
F(000)	1536	3904	4032	4320
Total no. of reflections	35267	89779	89348	113715
Reflections, I > 2σ(I)	13821	11271	11573	11254
Max. 2θ/°	52.00	56.72	56.86	56.66
Ranges (h, k, l)	-17 ≤ h ≤ 16 -21 ≤ k ≤ 21 -19 ≤ l ≤ 22	-20 ≤ h ≤ 20 -65 ≤ k ≤ 72 -13 ≤ l ≤ 11	-21 ≤ h ≤ 19 -72 ≤ k ≤ 60 -12 ≤ l ≤ 14	-20 ≤ h ≤ 21 -70 ≤ k ≤ 69 -13 ≤ l ≤ 14
Complete to 2θ (%)		99.1	99.8	98.0
Data/ Restraints/Parameters	13821 /0/904	11271/0/583	11573/0/601	11254/0/581
Goof (F2)	1.017	1.110	0.813	1.029
R indices [I > 2σ(I)]	0.0703	0.0784	0.0488	0.0540
R indices (all data)	0.1432	0.1234	0.1456	0.1277

Compound No.	**6.13**	**6.14**	**6.15**	**6.16**
Formulae	$C_{31}H_{23}NO_6S_2Zn$	$C_{29}H_{25}NO_8S_2Zn$	$C_{58}H_{52}N_2O_{16}S_4Zn_2$	$C_{33}H_{27}NO_6S_2Zn$
Mol. wt.	634.990	644.99	1292.00	663.05
Crystal system	Triclinic	Monoclinic	Triclinic	Triclinic
Space group	P-1	$P2_1/c$	P-1	P-1
a (Å)	10.3255(18)	10.9449(3)	10.329(5)	11.8512(5)
b (Å)	12.302(2)	10.8468(3)	15.393(7)	12.7441(6)
c (Å)	12.901(2)	25.1629(8)	18.958(9)	13.0361(6)
α/°	65.031(12)	90.00	94.935(8)	63.497(2)
β/°	73.605(13)	97.845(2)	96.422(8)	65.669(2)
γ/°	87.517(13)	90.00	99.363(10)	68.600(2)
V (Å ^{3})	1419.6(4)	2959.31(15)	2939(2)	1565.42(12)

Z	2	4	2	2
Density/Mgm^{-3}	1.485	1.448	1.460	1.407
Abs. Coeff. /mm^{-1}	1.058	1.021	1.028	0.963
Abs. correction	none	none	none	none
F(000)	652	1328	1332	684
Total no. of	15778	24505	17239	16117
Reflections, I > 2σ(I)	5135	5482	10504	7553
Max. 2θ/°	51.0	51.0	51.0	56.48
Ranges (h, k, l)	-12 ≤ h ≤ 12 -14 ≤ k ≤ 14 -15 ≤ l ≤ 15	-13 ≤ h ≤ 12 -13 ≤ k ≤ 13 -30 ≤ l ≤ 29	-12 ≤ h ≤ 4 -16 ≤ k ≤ 18 -22 ≤ l ≤ 22	-15 ≤ h ≤ 15 -16 ≤ k ≤ 12 -15 ≤ l ≤ 17
Complete to 2θ (%)	97.2	99.3	95.9	97.7
Data/ Restraints/Parameters	5135 / 0 / 370	5482 / 0 / 376	10504/0/751	7553 / 0 / 337
Goof (F2)	0.974	1.033	0.983	1.149
R indices [I > 2σ(I)]	0.0659	0.0381	0.0702	0.0727
R indices (all data)	0.1586	0.0513	0.1467	0.1677
wR indices	0.1961	0.1173	0.2098	0.2204

Compound No.	**6.17**	**6.20**	**6.21**
Formulae	$C_{29}H_{31}CdN_{10}S_2$	$C_{76}H_{52}Cd_2NO_{21}$	$C_{56}H_{40}Cd_4O_{41}$
Mol. wt.	730.07	1638.06	1818.48
Crystal system	Orthorhombic	Monoclinic	Triclinic
Space group	$P2_12_12_1$	C2/c	P-1
a (Å)	8.1523(2)	20.1888(4)	8.7264(8)
b (Å)	18.0510(3)	16.0041(4)	14.2760(13)
c (Å)	21.2912(4)	23.7012(5)	15.1949(14)
α/°	90.00	90.00	65.861(5)
β/°	90.00	92.152(2)	79.139(6)
γ/°	90.00	90.00	76.007(6)
V (Å ^{3})	3133.15(11)	7652.5(3)	1667.6(3)
Z	4	4	1
Density/Mgm^{-3}	1.548	1.422	1.811
Abs. Coeff. /mm^{-1}	0.886	0.633	1.363
Abs. correction	none	none	none
F(000)	1488	3312	896
Total no. of reflections	39347	57726	16084
Reflections, I > 2σ(I)	7661	9879	6072
Max. 2θ/°	56.74	57.64	51.00
Ranges (h, k, l)	-10 ≤ h ≤ 10 -23 ≤ k ≤ 24 -28 ≤ l ≤ 27	-27 ≤ h ≤ 27 -21 ≤ k ≤ 21 -32 ≤ l ≤ 31	-10 ≤ h ≤ 10 -17 ≤ k ≤ 16 -18 ≤ l ≤ 18
Complete to 2θ (%)	98.2	98.6	97.6
Data/Restraints/Parameters	7661 / 0 / 434	9879 / 0 / 493	6072 / 0 / 460
Goof (F2)	1.034	1.046	0.911

R indices [I > 2σ(I)]	0.0287	0.0523	0.0595
R indices (all data)	0.0316	0.0705	0.0967
wR indices	0.0726	0.1843	0.1832

6.6 Experimental

Materials and physical measurement as described in **Chapter 2**, **Section 2.41** and **Section 2.42**.

6.6.1 General procedure for the synthesis of compounds 6.1-6.8

Bis-2,-arylsulfanyl 1,4-naphthalene 1,4-diols (5 mmol), bromomethylacetate (1.82 g, 12 mmol) and anhydrous K_2CO_3 (1.65 g, 12 mmol) were taken in a round bottom flask and then dry acetone (25 ml) was added into it under nitrogen atmosphere. The reaction mixture was stirred for 12 hrs at 60^0 C (The reaction progress was monitored at regular intervals using TLC). After completion of the reaction, the reaction mixture was filtered off (to remove unreacted K_2CO_3) and washed it with acetone. The solvent was removed under reduced pressure. The isolated crude products were washed with 3% sodium hydroxide solution in water and then the product was extracted with dichloromethane .The organic extracts were collected over anhydrous sodium sulphate; subsequent removal of the solvent and recrystallization from acetone gave the pure (4-methoxycarbonylmethoxy-2,3-*bis*-arylsulfanylnapthalene-1-yloxy)acetic acid methylester products **6.1-6.4**.

The (4-methoxycarbonylmethoxy-2,3-*bis*-arylsulfanylnapthalene-1-yloxy) acetic acid methylesters **6.1-6.4** (4 mmol) and sodium hydroxide (0.40 g, 10 mmol) were dissolved independently in methanol (25 ml). The reaction mixtures were stirred for 2 hrs at room temperature. White precipitate formed were filtered, washed with methanol, and dried. The precipitates were redissolved in milli-Q water (20 ml) and the solution was acidified with dilute hydrochloric acid solution (10% v/v). On complete acidification white solid was obtained. The products (4-carboxymethoxy-2,3-*bis*-arylsulfanylnaphthalene-1-yloxy) acetic acids **6.5-6.8** were filtered and washed properly with water until free from acid. Due to the less solubility of the dicarboxylic acids **6.5-6.8** characterization of these compounds were done from their corresponding disodium salts.

6.6.2 Spectroscopic data for the compounds 6.1-6.8

Compound 6.1:

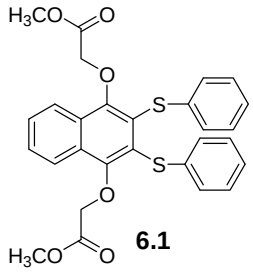

6.1

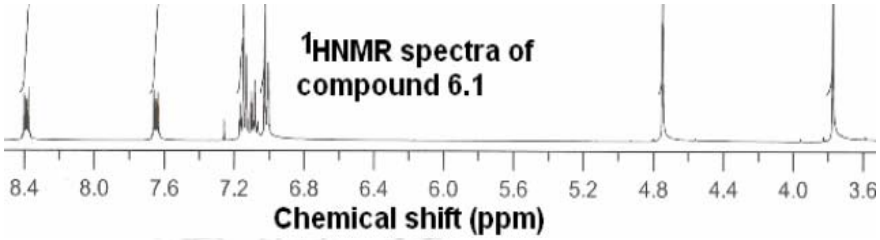

Isolated yield: 89%, IR (KBr, cm^{-1}): 3454 (bm), 2952 (m), 1767 (bs), 1626 (m), 1600 (m), 1511 (s), 1414 (w), 1292 (s), 1315 (s), 1218 (s), 1102 (s), 845 (w), 819 (s), 770 (s), 740 (s), 577 (w). ^{1}HNMR ($CDCl_3$, 400 MHz): 8.40 (dd, J = 8.2, 3.4Hz, 2H), 7.66 (dd, J = 8.2, 3.4Hz, 2H), 7.15 (t, J = 6.8Hz, 4H), 7.10 (t, J = 6.8Hz, 2H), 7.01 (d, J = 8.6Hz, 4H), 4.77 (s, 4H), 3.87 (s, 6H).

Compound 6.2:

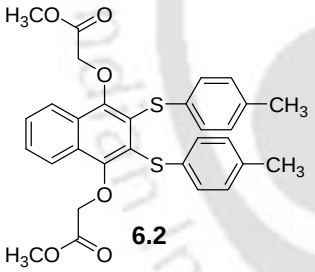

6.2

Isolated yield: 91%; IR (KBr, cm^{-1}) : 3464 (m), 3011 (w), 2954 (m), 2125 (w), 1747 (m), 1631 (s), 1602 (s), 1584 (s), 1513 (s), 1434 (s), 1384 (m), 1316 (m), 1292 (s), 1251 (w), 1216 (w), 1178 (w), 1146 (m), 1079 (s), 1013 (m), 962 (s), 907 (m), 882 (s), 856 (s), 831 (s), 788 (s), 752 (m), 726 (s), 709 (w), 603 (s); ^{1}HNMR ($CDCl_3$, 400 MHz): 8.38 (dd, J = 8.2, 3.4Hz, 2H), 7.65 (dd, J = 8.6, 3.4Hz, 2H), 7.26 (d, J = 8.8Hz, 4H), 6.95 (d, J = 8.8Hz, 4H), 4.76 (s, 4H), 3.78 (s, 6H), 2.25 (s, 6H).

Compound 6.3:

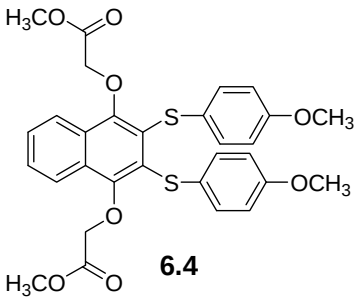

6.4

Isolated yield: 90%; IR (KBr, cm^{-1}) : 3448 (w), 2960 (m), 2920 (m), 2760 (s), 1630 (s), 1605 (w), 1519 (s), 1467 (w), 1434 (s), 1389 (s), 1261 (w), 1209 (s), 1170 (w), 1129 (m), 1079 (s), 1013 (s), 980 (s), 958 (w), 905 (w), 859 (s), 842 (s), 824 (s), 705 (s), 630 (w); ^{1}H NMR ($CDCl_3$, 400 MHz): 8.40 (dd, J = 8.6, 3.6Hz, 2H), 7.64 (dd, J = 8.6, 3.6Hz, 2H), 7.16 (d, J = 7.8Hz, 4H), 7.00 (d, J = 7.8Hz, 4H), 4.75 (s, 4H), 3.78 (s, 6H), 3.72 (s, 6H).

Compound 6.4:

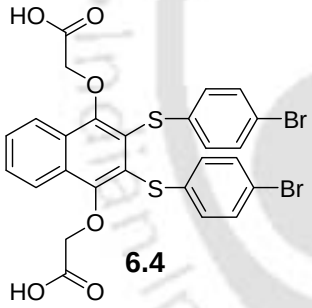

6.4

Isolated yield: 88%; 3455 (w), 2954 (s), 2914 (m), 1755 (s), 1597 (s), 1507 (s), 1439 (s), 1406 (s), 1387 (s), 1337 (w), 1265 (s), 1229 (s), 1210 (s), 1173 (m), 1113 (s), 1073 (w), 994 (w), 932 (s), 887 (s), 791 (m), 724 (s), 602 (m); ^{1}H NMR ($CDCl_3$, 400 MHz): 8.39 (dd, J = 8.6, 3.6Hz, 2H), 7.64 (dd, J = 8.6, 3.6Hz, 2H), 7.22 (d, J = 7.8Hz, 4H), 7.08 (d, J = 7.8Hz, 4H), 4.76 (s, 4H), 3.80 (s, 6H).

Compound 6.5:

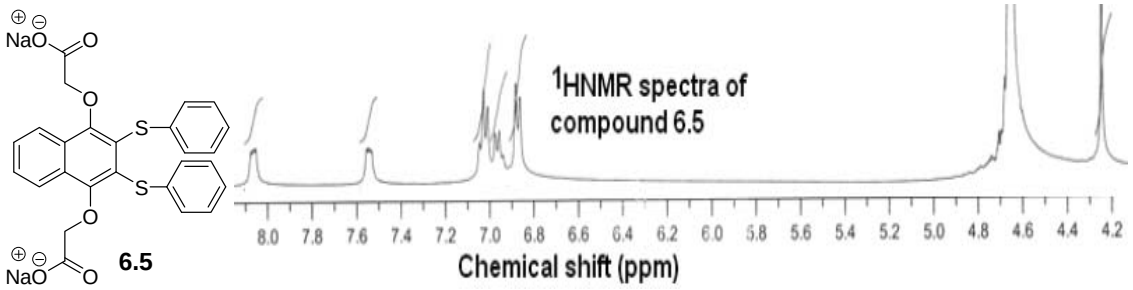

IR (KBr, cm^{-1}): 3409 (bs), 2912 (w), 1606 (s), 1474 (m), 1418 (s), 1368 (w), 1313 (s), 1256 (w), 1116 (w), 1085 (s), 1027 (s), 939 (w), 891 (m), 848 (m), 734 (s); ^{1}H NMR (D_2O, 400 MHz): 8.07 (dd, J = 7.8, 3.2 Hz, 2H), 7.54 (dd, J = 7.8, 4.8 Hz, 2H), 7.03 (t, J = 8.8Hz, 4H), 6.97 (t, J = 8.8Hz, 2H), 6.88 (t, J = 8.8Hz, 4H), 4.22 (s, 6H).

Compound 6.6:

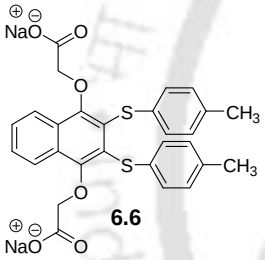

IR (KBr, cm^{-1}): 3434 (bs), 2918 (w), 1606 (s), 1491 (w), 1418 (s), 1312 (s), 1086 (w), 1017 (w), 705 (w); ^{1}H NMR (D_2O, 400 MHz): 8.06 (dd, J = 6.8, 3.2Hz, 2H), 7.54 (dd, J = 7.2, 4.8Hz, 2H), 7.02 (d, J = 7.6Hz, 4H), 6.77 (d, J = 7.8Hz, 4H), 4.24 (s, 4H), 2.01 (s, 6H).

Compound 6.7:

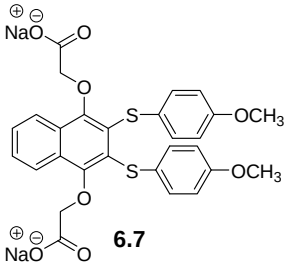

IR (KBr, cm^{-1}): 3396 (bs), 2916 (w), 1605 (s), 1491 (m), 1420 (s), 1368 (w), 1314 (s), 1246 (m), 1172 (w), 1086 (s), 1018 (s), 938 (w), 892 (m), 801 (w), 777 (m); ^{1}H NMR

(D_2O, 400 MHz): 8.04 (dd, J = 6.8, 3.2 Hz, 2H), 7.52 (dd, J = 6.8, 4.8 Hz, 2H), 6.81 (d, J = 8.6 Hz, 2H), 6.52 (d, J = 8.6 Hz, 4H), 4.65 (s, 4H), 4.23 (s, 6H).

Compound 6.8:

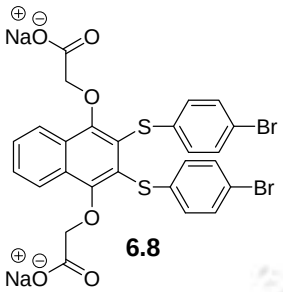

6.8

IR (KBr, cm^{-1}): 3422 (bs), 2926 (w), 1607 (s), 1492 (m), 1422 (s), 1368 (w), 1314 (s), 1246 (m), 1164 (w), 1086 (s), 1027 (s), 1018 (s), 939 (w), 891 (m), 848 (m), 734 (s); ^1H NMR (D_2O, 400 MHz): 8.04 (dd, J = 6.8, 3.2Hz, 2H), 7.52 (dd, J = 6.8, 4.2Hz, 2H), 6.81 (d, J = 8.6Hz, 2H), 6.52 (d, J = 8.6Hz, 4H), 4.65 (s, 4H).

6.6.3 General procedure for the synthesis of complexes 6.9

The disodium salt of (4-carboxymethoxy-2,3-*bis*-*p*-methylphenylsulfanylnaphthalene-1-yloxy)acetic acid **6.6** (0.25 mmol, 0.14 g) was dissolved in milli-Q water (8 ml) and to this solution manganese(II) chloride tetra hydrate (0.25 mmol, 0.048 g) was added. A white precipitate was observed. The precipitate was filtered and was dissolved in pyridine/water (1:3 ratios, 6 ml) solvent mixture and kept it for crystallization. After three days the complex **6.9** was obtained as white crystals.

Compound 6.9:

Isolated Yield: 56%; Elemental anal calcd. for $C_{76}H_{66}Mn_2N_4O_{13}S_4$: C, 61.56; H, 4.46; found C, 61.55, H, 4.48; IR (KBr, cm^{-1}): 3432 (bs), 2920 (w), 1635 (s), 1489 (w), 1445 (s), 1425 (s), 1369 (w), 1315 (s), 1166 (w), 1088 (s), 1033 (w), 704 (s).

6.6.4 General procedure for the synthesis of complexes 6.10-6.12

The disodium salt of (4-carboxymethoxy-2,3-*bis*-arylsulfanylnaphthalene-1-yloxy) acetic acid (0.25 mmol) were dissolved independently in 8 ml of milli-Q water and to the corresponding solution cupric(II) chloride (0.043 g, 0.25 mmol) were added. After

stirring for half an hour, corresponding green precipitate were obtained. The precipitate was filtered and were dissolved in 10 ml pyridine/water (1:10 v/v) solvent and kept it for crystallization. Upon crystallization complexes **6.10-12** were obtained in pure form.

6.6.5 Spectroscopic data for the compounds 6.10-6.12

Complex 6.10:

Isolated Yield: 67%; Elemetal anal. calcd. for $C_{101}H_{89}Cu_2N_9O_{12}S_4$: C, 64.60; H, 4.74; found C, 64.89, H, 4.78; IR (KBr, cm^{-1}): 3428 (bs), 2923 (w), 1633 (s), 1490 (w), 1447 (w), 1411 (w), 1369 (w), 1316 (s), 1218 (w), 1166 (w), 1088 (s), 1025 (w), 700 (s). Magnetic moment (RT) 1.78 BM.

Complex 6.11:

Isolated Yield: 68%; Elemetal anal. calcd. for $C_{101}H_{89}Cu_2N_9O_{16}S_4$: C, 62.47; H, 4.59; found C, 62.51; H, 4.62; IR (KBr, cm^{-1}): 3434 (bs), 3068 (w), 1599 (s), 1491 (s), 1448 (s), 1402 (w), 1368 (w), 1311 (s), 1245 (w), 1169 (w), 1088 (s), 1031 (w), 700 (s). Magnetic moment (RT) 1.78 BM.

Complex 6.12:

Isolated Yield: 72%; Elemental anal. calcd. for $C_{97}H_{77}Br_4Cu_2N_9O_{12}S_4$: C, 54.50; H, 3.61; found C, 54.55; H, 3.67; IR (KBr, cm^{-1}): 3430 (bs), 1607 (s), 1471 (w), 1445 (w), 1408 (s), 1366 (w), 1314 (s), 1259 (w), 1218 (w), 1166 (w), 1088 (s), 1006 (s), 699 (s).

6.6.6 General procedure for the synthesis of complexes 6.13-6.16

The disodium salt of 2,2′-(2,3-*bis*-phenylsulfanylnaphthalene-1,4-yloxy) acetic acid **6.5** (**LH2**) (0.125 g, 0.25 mmol) was dissolved in milli-Q water-methanol mixture (1:1 v/v; 10 ml) and to this solution zinc(II) acetate dihydrate (0.055 g, 0.25 mmol) was added. After stirring for 10 mins, a white precipitate was formed. Crystallization of the precipitate from pyridine/dimethylformamide (1:5 v/v) gave **6.13**, while crystallization from dimethylformamide gave **6.14**. The complex **6.15** was obtained serendipitously by crystallization of the white solid from 10 ml of pyrazine solution (0.16 g, 2 mmol) dissolved in *N*,*N*′-dimethylformamide. Complex **6.16** was prepared from the disodium

salt of 2,2′-(2, 3-*bis*-*p*-methylphenylsulfanylnaphthalene-1,4-yloxy) acetic acid **6.6** by a procedure similar to the synthesis of complex **6.13**.

6.6.7 Spectroscopic data for the compounds 6.13-6.16

Compound 6.13:

Isolated Yield: 79%; Elemental anal calcd for $C_{31}H_{23}NO_6S_2Zn$: C, 58.58; H., 3.62; found C, 58.49; H, 3.75; IR (KBr, cm^{-1}): 3438 (bw), 2919 (w), 1619 (s), 1490 (s), 1448 (m), 1403 (s), 1317 (m), 1165 (w), 1088 (s), 1015 (m), 805 (m), 702 (s) 629 (w).

Compound 6.14:

Isolated Yield: 42%; Elemental anal calcd for $C_{29}H_{25}NO_8S_2Zn$: C, 53.95; H., 3.88; found C, 52.72; H, 3.78; IR (KBr, cm^{-1}): 3435 (bw), 2908 (w), 1660 (s), 1477 (m), 1443 (m), 1418 (s), 1368 (m), 1313 (s), 1162 (w), 1092 (s), 1023 (m), 737 (m), 689 (s).

Compound 6.15:

Isolated Yield: 36%; Elemental anal calcd for $C_{58}H_{52}N_2O_{16}S_4Zn_2$: C, 53.86; H., 4.02; found C, 53.45; H, 3.91; IR (KBr, cm^{-1}): 3366 (w), 3238 (w), 2915 (w), 1653 (s), 1475 (m), 1441 (m), 1418 (s), 1367 (m), 1316 (s), 1162 (m), 1091 (s), 1023 (s), 738 (m), 692 (m),

Compound 6.16:

Isolated Yield: 68%; Elemental anal calcd for $C_{33}H_{27}NO_6S_2Zn$: C, 59.72; H., 4.07; found C, 57.23; H, 4.18; IR (KBr, cm^{-1}): 3438 (bw), 2919 (w), 1619 (s), 1490 (s), 1448 (m), 1403 (s), 1317 (m), 1165 (w), 1088 (s), 1015 (m), 805 (m), 702 (s), 629 (w).

6.6.8 General procedure for the synthesis of complexes 6.17

The disodium salt of (4-carboxymethoxy-2,3-*bis*-phenylsulfanylnaphthalene-1-yloxy) acetic acid **6.5** (0.25 mmol) was dissolved in 15 ml milli-Q water-methanol mixture (1:1 ratio) and to this solution cadmium(II) acetate (0.066 g, 0.25 mmol in 5 ml) was added. After stirring for 10 mins, the resulting white precipitate was collected by filtration. It was dissolved in DMF and was concentrated to 10 ml and left it

undisturbed for crystallization. Upon crystallization complex **6.17** was obtained in pure form.

Compound 6.17:

Isolated Yield: 67%; IR (KBr, cm^{-1}): 3429 (bs), 2923 (w), 1644 (s), 1429 (m), 1418 (s), 1369 (m), 1315 (s), 1164 (m), 1089 (s), 1039 (m), 1022 (m), 843 (w), 744 (m), 699 (s).

6.6.9 General procedure for the synthesis of (4-carboxymethoxy-naphthalen-1-yloxy) acetic acid 6.19

Naphthalene-1, 4-diol (1.60 g, 10 mmol) and methyl bromoacetate (3.04 g, 20 mmol) were dissolved in dry acetone (30 ml) in a round bottle flask. To this solution anhydrous K_2CO_3 (3.3 g, 22 mmol) was added and stirred at 65^0C. After 8 hrs, the reaction mixture was filtered and washed with 5 ml of acetone. The solvent was removed from the resulting filtrate under reduced pressure and the residue was extracted with dichloromethane and allowed to stand to get product (4-methoxycarbonylmethoxy-naphthalen-1yloxy) acetic acid methyl ester **6.18** which was further purified by crystallizing from acetone.

The (4-methoxycarbonylmethoxy naphthalen-1yloxy) acetic acid methyl ester **6.18** (1.52 g, 5 mmol) and NaOH (0.48 g, 12 mmol) were dissolved in 20 ml of methanol and it allowed to stirred at 65^0C for 1h. During this process the resulting salt of dicarboxylic acid gets precipitated. This precipitate was filtered and was dissolved in 30 ml of water and the solution was acidified with dilute hydrochloric acid (10 % solution). On acidification a red brown solid was obtained, which was filtered and washed with water until it got free from acid. The resulting solid was allowed to dry to obtain the (4-carboxymethoxynaphthalen-1-yloxy) acetic acid **6.19**.

6.6.10 Spectroscopic data for the compounds 6.18-6.19

Compound 6.18:

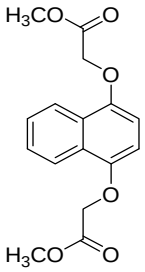

6.18

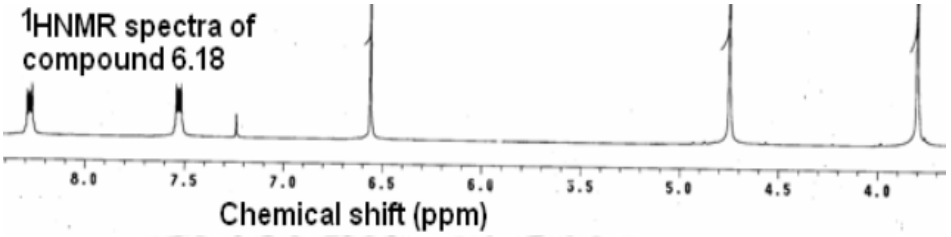

Isolated yield: 91%; IR (KBr, cm^{-1}): 3436 (bw), 2956 (w), 1766 (s), 1755 (s), 1599 (m), 1470 (m), 1438 (s), 1286 (s), 1263 (w), 1213 (s), 1179 (m), 1156 (m), 1120 (s), 1035 (w), 811 (m), 772 (m). ^{1}H NMR ($CDCl_3$, 400 MHz): 8.29 (dd, J = 6.4, 2.8 Hz, 2H), 7.54 (dd, J = 6.4, 2.8 Hz, 2H), 6.56 (s, 2H), 4.75 (s, 4H), 3.80 (s, 6H). ^{13}C NMR ($CDCl_3$, 100 MHz): 169.8, 148.8, 126.7, 126.6, 122.2, 104.8, 66.3, 52.5.

Compound 6.19:

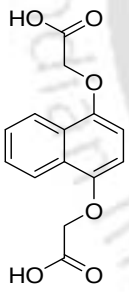

6.19

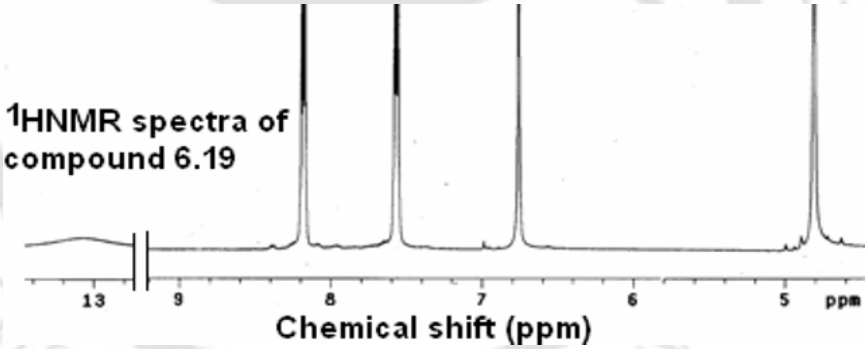

Isolated yield: 89%; IR (KBr, cm^{-1}): 3444 (bw), 3267 (bm), 2908 (m), 1731 (s), 1633 (w), 1600 (s), 1474 (m), 1440 (m), 1425 (m), 1399 (s), 1308 (m), 1269 (s), 1238 (s), 1161 (s), 1121 (s), 1029 (w), 919 (m), 824 (w), 765 (m). ^{1}H NMR (DMSO-d_6, 400 MHz): 8.19 (dd, J = 7.2, 3.2Hz, 2H), 7.55 (dd, J = 7.2, 3.2Hz, 2H), 6.75 (s, 2H), 4.79 (s, 4H). ^{13}C NMR (DMSO-d_6, 100 MHz): 170.3, 147.5, 126.1, 125.7, 121.6, 104.9, 65.2.

6.6.11 General procedure for the synthesis of complex 6.20

4-Carboxymethoxy naphthalen-1-yloxy) acetic acid (0.276 g, 1 mmol) was dissolved in 15 ml of methanol and to this solution cadmium(II) acetate (0.665 g, 1 mmol, in 5 ml) was added. The above solution was stirred for 15 mins and the resulting white precipitate was collected by filtration. The precipitate was redissolved in a solution of 1, 10-phenanthrolin (0.360 g, 2 mmol) in 20 ml of milli-Q water and kept it for crystallization.

Compound 6.20:

Isolated Yield: 72%; IR (KBr, cm^{-1}): 3417 (bs), 2917 (w), 1593 (s), 1413 (m), 1465 (w), 1426 (s), 1343 (w), 1316 (w), 1272 (m), 1234 (m), 1100 (s), 844 (s), 729 (s), 636 (m).

6.6.12 General procedure for the synthesis of complex 6.21

4-Carboxymethoxy naphthalen-1-yloxy) acetic acid (0.276 g, 1 mmol) was dissolved in 15 ml methanol and to this solution cadmium(II) acetate (0.665 g, 1 mmol, in 5 ml) was added. The above solution was stirred for 15 minutes and the resulting white precipitate was collected by filtration. The precipitate was redissolved in a solution of pyrazol (0.136 g, 2 mmol) in 20 ml of milli-Q water and again it was heated at boiling temperature for 10 mins. On slow evaporation of this solution at room temperature gave the complex **6.21** as colorless crystals.

Compound 6.21:

Isolated Yield: 69%; IR (KBr, cm^{-1}): 3449 (bs), 2925 (w), 1607 (s), 1466 (s), 1423 (s), 1394 (m), 1337 (m), 1274 (s), 1238 (m), 1238 (m), 1156 (m), 1107 (s), 1024 (w), 770 (m), 703 (w).

Conclusions:

In this work we have synthesized a series of novel quinone derivatives including carboxylic acid ligands. The quinone derivatives are chracterised by conventional spectroscopic techniques and X-ray crystallography. The utility of these ligands in cancer, polymorphism, host-guest system, molecular self-assembly and metal complexation are studied. Several coordination polymers with different dimensions are synthesized and characterised, role of solvent and ancillary ligand in changing the dimentionallity in coordination polymers are shown. Several notable observations are encapsulation of $Cd(H_2O)_6$ cations, inclusion of pyridine molecules as guest molecules, inclusion of N, N′-dimethylformamide molecules as guest molecules in 3-D coordination polymer, aqua bridged dimeric repreated unit containing coordination polymers, synthesis of alternating five and six coordination polymers. A novel C-S bond cleavage reaction is discovered. Some copper complexes prepared through such reactions can not be easily prepared by directly using ligands. As ligands themselves are highly oxidizing and difficult to deal with. Similarly iron catalysed reactions led to iron phenanthroline complexes with large anions. These are catalysts for epoxidation reactions. We have also studied the photoluminescence properties of coordination polymer of cadmium carboxylate complexes.

CIF of the compounds studied in this thesis are compiled with CD in the end of the thesis. Other details of the instruments are given in Appendix.

Appendix

Details of the analytical instruments:

X-Ray Crystallography

X-ray diffraction data were collected on Bruker 3-circle diffractometers with CCD area detectors ProteumM APEX or SMART 6000 or Bruker Nonius Apex 2, using graphite-monochromated Mo-$K\alpha$ radiation (λ = 0.71073 Å) from a 60W microfocus Bede Microsource® with glass polycapillary optics or a sealed tube. In case of the structures that were determined at 120K, the low temperature of the crystals was maintained using Cryostream (Oxford Cryosystems) open-flow N_2 cryostats.

X-ray diffraction data for all crystals were collected using Bruker SMART software. This software was also used for indexing and determination of the unit cell parameters. The structures were solved by direct methods and refined by full-matrix least squares against F^2 of all data, using SHELXTL software.

All non-H atom were refined by full-matrix least squares in anisotropic, all H atoms in isotropic approximation, against F^2 of all reflections. All non-H atoms were refined by full-matrix least squares in the anisotropic approximation and the hydrogen atoms attached to these atoms were treated as 'riding' in calculated positions and in some of the cases the hydrogen atoms have been located on the difference Fourier maps. In all cases the hydrogen atoms attached to polar atoms such as O and N were located on the difference Fourier maps and refined in the final structure in isotropic approximation. The crystallographic tables for all the compounds are given at the end of this section, which includes the crystal parameters and the refinement factors.

UV-visible, Emission and IR Spectroscopy

UV-vis adsorption spectra were recorded using Perkin-Elmer Lambda 25 spectrophotometer equipped with double cell compartments. All the chemicals and solvents used were as obtained from the satndard suppliers such as E.Merck Germany, Sigma Aldrich USA, Ranbaxy India. The solvents for spectroscopic were of HPLC

grade (Aldrich or Merck) and used as obtained. The fluorescence spectra were recorded with a Perkin Elmer LS 55 fluorescence spectrophotometer. The IR spectra were recorded on Perkin-Elmer spectrum one spectrometer.

NMR Spectroscopy

The NMR spectra, ^{1}H, ^{13}C as well as the HOMOCOSY were recorded in a Bruker 400 MHz spectrometer. The chemical shifts in the NMR spectra are all given in ppm and tetramethylsilane as the internal standard. The concentration dependent NMR spectra of compounds were recorded by dissolving calculated amounts of the sample in a fixed amount of appropriate solvent.

Thermogravimetric Studies and Elemental analysis

The thermogravimetric studies were performed using a Mettler Toledo TGA/ STDA 851^{e} and Mettler Toledo DSC^{e} thermal analyser. Typically about 8-10mg of the samples were mounted on platinum crucibles and the TG/DSC profiles recorded at the heating rate of 5°C/min and under nitrogen atmosphere. Elemental analyses were done on a Perkin-Elmer PE 2400 II CHN analyzer 2400.

Cyclic Voltammetry

Cyclic voltammograms are recorded using a Model 263 potentiostat from Princeton Applied Research (USA). All cyclic voltammetric experiments have been performed in dry degassed solvents, under nitrogen atmosphere.

Cyclic voltammograms were measured for 0.01mM solutions of the compound in dry degassed acetonitrile at 298 K. Tetrabutylammonium perchlorate (TBAP) was used as supporting electrolyte and the experimental solution was purged with dry argon before each measurement. The glassy-carbon working electrode, which was used for performing the experiment, was cleaned with electrode polishing materials available from BAS, washed with deionised water and acetone. The non-aqueous Ag/AgCl electrode was used as reference in all the measurements while a Pt-foil ($1cm^2$) was used as counter electrode.

Electron Paramagnetic Resonance Spectroscopy and Magnetic measurements

The ESR experiments were performed using a Bruker X-band spectrometer calibrated with internal teslameter. Simulations of the ESR data were done using standard WinEPR software available from Bruker. The ESR spectrometer magnetic field is calibrated with respect to diphenyl picryl hydazyl radical as the standard and the spectra were recorded at room temperature. Room temperature magnetic susceptibility measurements were made using a EG&G PARC MODEL 155 Vibrating Sample magnetometer while the low temperature magnetic measurements were carried out with 15-20 mg samples in the temperature range 60-300K with a Faraday balance.

Gas Cromatography-Mass Spectroscopy

GC-MS experiments were recorded on a Hewlett-Packard HP6890 series instrument equipped with an HP-5 column. GC analyses were carried out on a Hewlett-Packard HP6890 series instrument equipped with an FID detector and HP7683 series autosampler and injector and analyzed using HP Chemstation software. The column was a 30 m HP-5 (cross-linked 5% PH ME siloxane) capillary column with 0.32 mm inner diameter and 0.25 μm film thickness (inlet pressure = 13.9 psig; column flow = 1.2 mL/min; temperature program for all analyses, initial temp = 50^0 C, initial time = 0 min, rate = 5^0 C/min, final temp) 250^0 C, final time = 15 mins.

References

1. D. E. Ward and J. Shen, *Org. Lett.*, **2007**, 9, 2843.

2. K.-L. Wu, S. Wilkinson, N. O. Reich and T. R. R. Pettus, *Org. Lett.*, **2007**, 9, 5537.

3. B. J. D. Wright, J. Hartung, F. Peng, R. V. de Water, H. Liu, Q.-H. Tan, T.-C. Chou and S. J. Danishefsky, *J. Am. Chem. Soc.*, **2008**, 130, 16786.

4. A. Kuboki, C. Maeda, T. Arishige, K. Kuyama, M. Hamabata and S. Ohira, *Tetrahedron Lett.*, **2008**, 49, 4516.

5. A. Emadi, J. S. Harwood, S. Kohanim and K. W. Stagliano, *Org. Lett.*, 2002, 4, 511.

6. A. Osyezka, C. C. Moser, F. Daldal and P. L. Dutton, *Nature*, **2004**, 427, 607.

7. R. D. Adams and S. Miao, *J. Am. Chem. Soc.*, **2004**, 126, 5056.

8. C.-X. Yin and R. G. Finke, *J. Am. Chem. Soc.*, **2005**, 127, 9003.

9. A. S. Attia and C. G. Pierpont, *Inorg. Chem.*, **1998**, 37, 3051.

10. S. B. Colbran, S. T. Lee, D. G. Lonnon, F. J. D. Maharaj, A. M. McDonagh, K. A. Walker and R. D. Young, *Organometallics*, **2006**, 25, 2216.

11. J.-M. Lu, S. V. Rosokha, I. S. Neretin and J. K. Kochi, *J. Am. Chem. Soc.*, **2006**, 128, 16708.

12. M. Kivala, C. Boudon, J.-P Gisselbrecht, P. Seiler, M. Gross and F, Diederich, *Chem. Commun.*, **2007**, 4731.

13. T. Arimura, S. Ide, H. Sugihara, S. Murata and J. L. Sessler, *New J. Chem.*, **1999**, 23, 977.

14. Z. Zhang, L. Huang, V. M. Shulmeister, K. Young-Inchi, K. Kim, L.- W. Hung, A. R. Crofts, E. A. Berry and S.- H. Kim, *Nature*, **1998**, 392, 677.

15. S. R. Merder, D. W. Bruce and D, O'Hare, *Inorganic Material*, Chichester, **1996**, 2nd edn., 121.

16. R. E. P. Chandrasena, P. D. Edirisinghe, J. L. Bolton and G. R. J. Thatcher, *Chem. Res. Toxicol.*, **2008**, 21, 1324.

17. W. A. Cramer, H. Zhang, J. Yan, G. Kurisu and J. L. Smith, *Biochemistry*, **2004**, 43, 5921.

18. D. M. Tiede, J. Vazquez, J. Cordova and P. A. Marone, *Biochemistry*, **1996**, 35, 10763.

19. L. M. Utschig, M. C. Thurnauer, D. M. Tiede and O. G. Poluektov, *Biochemistry*, **2005**, 44, 14131.

20. A. Patel, F. Liebner, T. Netscher, K. Mereiter and T. Rosenau, *J. Org. Chem.* **2007**, 72, 6504.

21. K. U. Baldenius, L. von dem Bussche-Hunnefeld, E. Hilgemann, P. Hoppe and R. Sturmer, In *Ullmann's Encyclopedia of Industrial Chemistry*; VCH: Weinheim, Germany, **1996**, Vol. A27.

22. K. M. Aubart and C. H. Heathcock, *J. Org. Chem.*, **1999**, 64, 16.

23. O.V. Zalomaeva, O. A. Kholdeeva and A. B. Sorokin, *Green Chem.*, **2006**, 8, 883.

24. T.Takeya, H. Doi, T. Ogata, I. Okamoto and E. Kotani, *Tetrahedron*, **2004**, 60, 9049.

25. M. Chigr, H. Fillion, A. Rougny, M. Berlion, J. Riondel and H. Beriel, *Chem. Pharm. Bull.*, **1990**, 38, 688.

26. K. Chiba, M. Jinno, A. Nozaki and M. Tada, *Chem. Commun*., **1997**, 1403.

27. M. A. Kienzler, S. Suseno and D. Trauner, *J. Am. Chem. Soc.*, **2008**, 130, 8604.

28. M. C. Carreno, M. Ribagorda, A. Somoza and A. Urbano, *Angew. Chem. Int. Ed*., **2002**, 41, 2755.

29. O. Ouerfelli and K. A. Watanabe, *J. Med. Chem.*, **1996**, 39, 2812.

30. I. V. Nechepurenko, E. E. Shults and G. A. Tolstikov, *Russian J. Org. Chem.*, **2001**, 37, 9.

31. M. Alajarn, J. Cabrera, A.Pastor, P. Snchez-Andrada and D. Bautista, *J. Org. Chem.*, **2007**, 72, 2097.

32. K. Chiba, M. Jinno, A. Nozaki and M. Tada, *Chem. Commun*., 1**997**, 1403.

33. A. M. Castro, *Chem. Rev*., **2004**, 104, 2939.

34. L. M. Harwood, A. J. Oxford and C. J. Thomson, *Chem. Commun*., **1991**, 1303.

35. M. Hiersemann and L. Abraham, *Eur. J. Org. Chem*., **2002**, 1461.

36. S. Kotha, K. Mandal, A. C. Deb and S. Banerjee, *Tetrahedron Lett.*, **2004**, 45, 9603.

37. A. P. Kostikov and V. V. Popik, *J. Org. Chem.* **2007**, 72, 9190.

38. S.-T. Huang, H.-S. Kuo, C.-L. Hsiao and Y.-L. Lin, *Bioorg. Med. Chem*., **2002**, 10, 1947.

39. I. K. Boddy, R. C. Cambie, G. Dixon, P. S. Rutledge and P. D. Woodgate, *Aust. J. Chem.*, **1983**, 36, 803.

40. S. H. Reich, M. Melnick, M. J. Pino, M. A. M. Fuhry, A. J. Trippe, K. Appelt, J. F. Davies, B. W. Wu, II and L. Musick, *J. Med. Chem.*, **1996**, 39, 2781.

41. K. Krohn and S. Bernhard, *Synthesis,* **1996**, 699.

42. F. Dumur, N. Gautier, N. Gallego-Planas, Y. Suahin, E. Levillain, N. Mercier, P. Hudhomme, M. Masino, A. Girlando, V. Lloveras, J. Vidal-Gancedo, J. Veciana and C. Rovira, *J. Org. Chem.*, **2004**, 69, 2164.

43. C. Boulle, O. Desmars, N. Gautier, P. Hudhomme, M. Cariou and A. Gorgues, *Chem. Commun.*, **1998**, 2197.

44. S. S. H Davarani, A. R. Fakhari, A. Shaabani, H. Ahmar, A. Maleki and N. S. Fumani, *Tetrahedron Lett.,* **2008**, 49, 5622.

45. H. S. Mason, *Nature* **1955**, 175, 771.

46. P. A. Cranwell and R. D. Haworth, *Tetrahedron*, **1971**, 27, 1831.

47. P. Asenjo, F. Farina, M. V. Martin, M. C. Paredes and J. J. Soto, *Tetrahedron lett.,* **1995**, 36, 319.

48. A. Digga, S. Gracheva, C. Livingstone and J. Davis, *Electrochem. Commun.*, **2003**, 5, 732.

49. T. Wina and S. Bittner, *Tetrahedron Lett.,* **2005**, 46, 3229.

50. J. S. Yadav, T. Swamy, B. V. S. Reddy and D. K. Rao, *J. Mol. Catal. A: Chem.* **2007**, 274, 116.

51. E. Katz and I. Willner, *Chem. Commun.,* **2005**, 5641.

52. M. E. Peover, In *Electroanalytical Chemistry*; A. J. Bard, Ed.; Dekker, New York, 1967; pp 1-51.

53. A. Heller and B. Feldman, *Chem. Rev.,* **2008**, 108, 2482.

54. C. Costentin, *Chem. Rev.*, **2008**, 108, 2149**.**

55. M. Albrecht, O. Schneider and A. Sxhimidt, *Org . Biomol. Chem.*, **2009**, 7, 1445.

56. Y. Ge, R. R. Lilienthal and D. K. Smith *J. Am. Chem. Soc.*, **1996**, 118, 3976.

57. Y. Ge and D. K. Smith, *Anal. Chem.,* **2000**, 72, 1860.

58. Y. Ge, L. Miller, T. Ouimet and Diane K. Smith *J. Org. Chem.,* **2000**, 65, 26.

59. C. Costentin, M. Robert and J.-M. Saveant, *J. Am. Chem. Soc.,* **2006**, 28, 8726.

60. J. Q. Chambers, in *The Chemistry of the Quinonoid Compounds*; S. Patai, Z. Rappoport, Eds.; Wiley: New York, **1974**; Vol. I, Chapter 14, pp 737-791; **1988**; Vol. II, Chapter 12, pp 719-757.

61. A. J. Swallow, in *Function of Quinones in Energy Conserving Systems*; Trumpower, B. L., Ed.; Academic Press: New York, **1982**; Chapter 3, p 66.

62. V. Sundstrom, *Prog. Quantum Electron.*, **2000**, 24, 187.

63. N. P. Redmore, I. V. Rubtsov and M. J. Therien, *J. Am. Chem. Soc.*, **2003**, 125, 8769.

64. A. Dreuw, G. A. Worth, L. S. Cederbaum and M. Head-Gordon, *J. Phys. Chem. B*, **2004**, 108, 19049.

65. J. Springer, G. Kodis, L. de la Garza, A. L. Moore, T. A. Moore and Devens Gust, *J. Phys. Chem. A*, **2003**, 107, 3567.

66. F. D'Souza and G. R. Deviprasad, *J. Org. Chem.*, **2001**, 66, 4601.

67. X. Shi, S. R. Amin, and L. S. Liebeskind, *J. Org. Chem.*, **2000**, 65, 1650.

68. F. D'Souza, *J. Am. Chem. Soc.*, **1996**, 118, 923.

69. P. Rothemund and A. R. Mennotti, *J. Am. Chem. Soc*., **1941**, 63, 267.

70. D. Kuciauskas, P. A. Liddell, S.-C. Hung, S. Lin, S. Stone, G. R. Seely, A. L. Moore, T. A. Moore and Devens Gust, *J. Phys. Chem. B*, **1997**, 101, 429.

71. G. Arsenault, E. Bullock and S. MacDonald, *J. Am. Chem. Soc.*, **1960**, 82, 4384.

72. J. A. S. Cavaleiro, G. W. Kenner and K. M. Smith, *J. Chem. Soc., Perkin Trans.*, **1974**, 1, 1771.

73. T. Iyoda, T. Saika, K. Honda and T. Shimidzu, *Tetrahedron Lett.*, **1989**, 30, 5429.

74. G. De Santis, L. Fabbrizzi, M. Licchelli, N. Sardone and A. H. Velders, *Chem.Eur. J.*, **1996**, 2, 1243.

75. R. Bergonzi, L. Fabbrizzi, N. Licchelli and C. Mangano, *Coord. Chem. Rev.*, **1998**, 170, 31.

76. R. A. Illos, E. Harlev and S. Bittner, *Tetrahedron Lett.*, **2005**, 46, 8427.

77. R. A. Illos, D. Shamir, L. J. W. Shimon, I. Zilbermann and S. Bittner, *Tetrahedron Lett.*, **2006**, 47, 5543.

78. C. G. Pierpont and C. W. Lange, *Prog. Inorg. Chem.*, **1994**, 41, 331.

79. M. Ruf, W. S. Durfee and C. G. Pierpont, *Chem. Commun.*, **2004**,1022.

80. P. Anzenbacher, Jr., M. A. Palacios, K. Jursıkova and M. Marquez, *Org. Lett.*, **2005**, 7, 5027.

81. K. C. Nicolaou and W. M. Dai, *Angew. Chem. Int. Ed.*, **1991**, 103, 1453.

82. P. Chen, *Angew. Chem. Int. Ed.*, **1996**, 108, 1584.

83. G. Jones and X. Qian, *J. Phys. Chem. A*, **1998**, 102, 2555.

84. C. E. Aldiaturi, V. Otero, F. Anzola and F. Rosillo, *Acta Cient Venez.*, **1982**, 33, 348.

85. I. S. Ioffe and Z. Y. Khavin, *Zh. Obshch. Khim.*, **1954**, 54, 521.

86. R. Foster, N. Kulevsky, S. *J.* Wanigasekera, *J. Chem. Soc., Perkin Trans*, **1974**, 1, 1318.

87. Y. Chen and M.G. Steinmetz, *Org. Lett.*, **2005**, 7, 17.

88. A. Kost, L. Tutt, M. B. Klein, T. K. Dougherty and W. E. Elias, *Opt. Lett.*, **1993**, 18, 334.

89. A. Itaya, I. Suzuki, Y. Tsuboi, and H. Miyasaaka, *J. Phys. Chem. B*, **1997**, 101, 334.

90. N. Kamanina and I. Denisyuk, *Opt. Commun.*, **2004**, 235, 361.

91. R. Quintero-Torres and M. Thakur, *Appl. Phys. Lett.*, **1995**, 66, 1310.

92. M. Bakarezos, M. A. Camacho, I. J. Blewett, A. K. Kar, B. S. Wherrett, H. Matsuda, T. Fukuda, S. Yamada, R. Rangel-Rojo, H. Katagi, H. Kasai, S. Okada and H. Nakanishi, *Electron. Lett.*, **1999**, 35, 1078.

93. R. Rangel-Rojo, L. Stranges, A. K. Kar, M. A. Mendez-Rojas and W. H. Watson *Opt. Commun.*, **2002**, 203, 385.

94. M. Mendez-Rojas, S. G. Bodige and W. H. Watson, *J. Chem. Cryst.*, **1999**, 29, 1225.

95. I. Fuks-Janczarek, J. Luc, B. Sahraoui, F. Dumur, P. Hudhomme, J. Berdowski, and I. V. Kityk, *J. Phys. Chem. B*, **2005**, 109, 10179.

96. M. Iyoda, F. Sultana, S. Sasaki and M. Yoshida, *Chem. Commun.*, **1994**, 1929.

97. M. Iyoda, S. Sasaki, F. Sultana, M. Yoshida, Y. Kuwatani and S. Nagase, *Tetrahedron Lett.*, **1996**, 37, 7987.

98. B. M. Illescas, N. Martın, C. Seoane, P. de la Cruz, F. Langa, and F. Wudl, *Tetrahedron Lett.*, **1995**, 36, 8307.

99. B. M. Illescas, N. Martın, C. Seoane, E. Ortı, P. M. Viruela, R. Viruela and A.de la Hoz, *J. Org. Chem.*, **1997**, 62, 7585.

100. A. M. Castano and J.- E. Backvall, *J. Am. Chem. Soc.*, **1995**, 117, 560.

101. K. Bergstad, H. Grennberg and J.-E. Backvall, *Organometallics*, **1998**, 17, 45.

102. H. Grennberg, A. Gogoll and J.-E. Backvall, *Organometallics*, **1993**, 12, 1790.

103. J. D. Scott and R. M. Williams, *Chem. Rev.*, **2002**, 102, 1669.

104. V. K. Tandon, D. B. Yadav, R. V. Singh, M. Vaish, A. K. Chaturvedi and P. K. Shukla, *Bioorg. Med. Chem. Lett.*, **2005**, 15, 3463.

105. C.-K. Ryu, J.-Y. Shim, M. J. Chae, I. H. Choi, J.-Y. Han, O.-J. Jung, J. Y. Lee, and S. H. Jeong, *Eur. J. Med. Chem.*, **2005**, 40, 438.

106. G. Errante, G. L. Motta, C. Lagana, V. Wittebolle, M.- E. Sarciron and R. Barret, *Eur. J. Med. Chem.*, **2006**, 41, 773.

107. V. K. Tandon, H. K. Maurya, D. B. Yadav, A. Tripathi, M. Kumar and P. K. Shukla, *Bioorg. Med. Chem. Lett*., **2006**, 16, 5883.

108. V. K. Tandon, D. B. Yadav, A. K. Chaturvedi and P. K. Shukla, *Bioorg. Med. Chem. Lett*., **2005**, 15, 3288.

109. S. Y. Hung, K. H. Chung, H. J. You, I. H. Choi, M. J. Chae, J. Y. Han, O. J. Jung, S. J. Kang and C. K. Ryu, *Bioorg. Med. Chem. Lett.*, **2004**, 14, 3563.

110. K. Ushiyama, N. Tanaka, H. Ono and H. Ogato, *Jpn. J. Anribiot.*, **1971**, 24 , 197.

111. D. Barasch, O. Zipori, I. Ringel, I. Ginsberg, A. Samuni and J. Katzhendler, *Eur. J. Med. Chem.*, **1999**, 34, 597.

112. D. L. Boger and R. M. Garbaccio, *J. Org. Chem.*, **1999**, 64, 8350.

113. L. F. Tietze, K. M. Gericke, R. R. Singidi and I. Schuberth, *Org. Biomol. Chem.*, **2007**, 5, 1191.

114. E. Champeil, M. M. Paz, S. Ladwa, C. C. Clement, A. Zatorski and M. Tomasz, *J. Am. Chem. Soc*., **2008**, 130, 9556.

115. J. Yoo, H.- S. Choi, C.-H. Choi, Y. Chung, B. Hee Kim and H. Cho, *Arch. Pharm. Res.*, **2008**, 31, 142.

116. Y. Ikeda, Y. Shimada, K. Honjo, T. Okumoto and T. Munakata, *J. Antibiot.*, **1983**, 36, 1290.

117. T. Okumoto, M. Kawana, I. Nakamura, Y. Ikeda and K. Isagai, *J. Antibiot.*, **1985**, 38, 767.

118. Y. Fan, E. M. Schreiber, A. Giorgianni, J. C. Yalowich and B. W. Day, *Chem. Res. Toxicol.*, **2006**, 19, 937.

119. D. L. Boger and R. M. Garbaccio, *J. Org. Chem.*, **1999**, 64, 8350.

120. N. M. Kogan, R. Rabinowitz, P. Levi, D. Gibson, P. Sandor, M. Schlesinger and R. Mechoulam, *J. Med. Chem.*, **2004**, 47, 3800.

121. P. J. O'Brien, *Chem. Biol. Interact.*, **1991**, 80, 1.

122. C. Asche, *Mini –Rev. Med. Chem.*, **2005**, 5, 449.

123. A. Srikrishna, B. V. Lakshmi and P. C. Ravikumar, *Tetrahedron Lett.,* **2006**, 47, 1277.

124. S. J. Gould, *Chem. Rev.*, **1997**, 97, 2499.

125. N. Chen, M. B. Carriere, R. S. Laufer, N. J. Taylor and G. I. Dmitrienko, *Org. Lett.*, **2008**,10, 381.

126. M. A. Brimble, E. Ireland and S. J. Phythian, *Tetrahedron Lett.*, **1991**, 32. 6417.

127. K. Ushiyama, N. Tanaka, H. Ono and H. Ogato, *Jpn. J. Anribiot.*, **1971**, 24 , 197.

128. H. W. Moore and R. Czemiak, *Med. Res. Rev.*, **1981**, 1, 249.

129. M. Das Sarma, R. Ghosh, A. Patra, R. Chowdhury, K. Chaudhuri and B. Hazra, *Org. Biomol. Chem.*, **2007**, 5, 3115.

130. T. S. Wu, H. C. Hsu, P. L. Wu, C. M. Teng and Y. C. Wu, *Phytochemistry*, **1998**, 49, 2001.

131. N. Kongkathip, S. Luangkamin, B. Kongkathip, C. Sangma, R. Grigg, P. Kongsaeree, S. Prabpai, N. Pradidphol, S. Piyaviriyagul and P. Siripong, *J. Med. Chem.*, **2004**, 47, 4427.

132. T. Arai, K. Takahashi and A. Kubo, *J. Antibiot.*, **1977**, 30, 1015.

133. J. D. Scott and R. M. Williams, *Chem. Rev.*, **2002**, 102, 1669.

134. Y. Mikami, K. Yokoyama, H. Tabeta, K. Nakagaki and T. Arai, *J. Pharm. Dyn.*, **1981**, 4, 282.

135. T. Asaoka, K. Yazawa, Y. Mikami, T. Arai and K. Takahashi, *J. Antibiot.*, **1982**, 35, 1708.

136. T. Arai, K. Takahashi, K. Ishiguro and K. Yazawa, *J. Antibiot.*, **1980**, 3, 951.

137. J. D. Dunitz, *Pure Appl. Chem.*, **1991**, 63, 177.

138. J. D. Dunitz and J. Bernstein, *Acc. Chem. Res.*, **1995**, 28, 193.

139. J. D. Dunitz, *Acta Cryst. Sect. B.*, **1995**, 51, 619.

140. J. Bernstein, R. J. Davey and J.-O. Henck, *Angew. Chem. Int. Ed.*, **1999**, 38, 3441.

141. J. Bernstein, *Polymorphism in Molecular Crystals*; Oxford University Press: Oxford, **2002**.

142. R. J. Davey, *Chem. Commun.*, **2003**, 1463.

143. J. Bernstein, *Chem. Commun.*, **2005**, 5007.

144. S. R. Bryn, R. R. Pfeiffer and J. G. Stowell, *Solid-State Chemistry of Drugs*, SSCI: West Lafayette, IN, **1999**.

145. M. L. Peterson, S. L. Morissette, C. McNulty, A. Goldsweig, P. Shaw, M. LeQuesne, J. Monagle, N. Encina, J. Marchionna, A. Johnson, J. Gonzalez-Zugasti, A. V. Lemmo, S. J. Ellis, M. J. Cima and O. Almarsson, *J. Am. Chem. Soc.*, **2002**, 124, 10958.

146. C. P. Price, A. L. Grzesiak and A. J. Matzger, *J. Am. Chem. Soc.*, **2005**, 127, 5512.

147. S. Roy, R. Banerjee, A. Nangia and G. J. Kruger, *Chem. Eur. J.*, **2006**, 12, 3777.

148. J. Bernstein, R. J. Davey and J.-O. Henck, *Angew. Chem. Int. Ed.*, **1999**, 38, 3440.

149. R. P. Kashyap, D. Sun and W. H. Watson, *J. Chem. Cryst.*, **1995**, 25, 339.

150. G. R. Desiraju, *J. Chem. Soc. Perkin Trans.*, **1983**, 2, 1025.

151. S. K. Chandran, N. K. Nath, S. Roy, and A. Nangia, *Cryst. Growth. Des.*, **2008**, 8, 140.

152. T. W. Lewis, D. Y. Curtin and I. C. Paul, *J. Am. Chem. Soc.*, **1979**, 101, 5717.

153. H.-D. Becker, *J. Org. Chem.*, **1967**, 32, 2943.

154. Y. Imai, T. Kinuta, K. Nagasaki, T. Harada, T. Sato, Y. N. Tajima, Y. Sasaki, R. Kuroda and Y. Matsubara, C*rystEngComm*, **2009**, 11, 1223 .

155. J. Fajer, K. M. Barkigia, D. Melamed, R. M. Sweet, H. Kurreck, J. Von Gersdorff, M. Plato, H.-C. Rohland, G. Elger and K. Mo1bius, *J. Phys. Chem. B*, **1996**, 100, 14236.

156. H. A. Staab, M. Tercel, R. Fischer and C. Krieger, *Angew. Chem., Int. Ed.*, **1994**, 33, 1463.

157. C. Krieger, J. Weiser and H. A. Staab, *Tetrahedron Lett.*, **1985**, 26, 6055.

158. J. L. Sessler, M. R. Johnson, S. E. Creager, J. C. Fettinger and J. A. Ibers, *J. Am. Chem. Soc.*, **1990**, 112, 9310.

159. Y. Aoyama, K. Endo, T. Anzai, Y. Yamaguchi, T. Sawaki, K. Kobayashi, N. Kanehisa, H. Hashimoto, Y. Kai and H. Masuda, *J. Am. Chem. Soc.*, **1996**, 118, 5562.

160. P. R. Bangal, *Chem. Phys. Lett.*, **2005**, 401, 200.

161. M. Bouvet, B. Malezieux, P. Herson and F. Villain, *Helvet. Chim. Acta*, **2009**, 92, 453.

162. A. Tsuda, C. Fukumoto and T. Oshima, *J. Am. Chem. Soc.*, **2003**, 125, 5811.

163. M. Hashimoto, H. Takagi and K. Yamamura, *Tetrahedron Lett.*, **1999**, 40 6037.

164. G. Lenaz, Ed. Coenzyme Q: Biochemistry, Bioenergetics and Clinical Applications of Ubiquinone; Wiley: New York, **1985**.

165. M. Oh, G. B. Carpenter and D. A. Sweigart, *Angew. Chem. Int. Ed.*, **2002**, 41, 3650.

166. M. Oh, G. B. Carpenter and D. A. Sweigart, *Angew. Chem. Int. Ed.*, **2003**, 42, 2026.

167. M. Oh, G. B. Carpenter and D.A. Sweigart, *Chem. Commun.*, **2002**, 2168.

168. M. Oh, G. B. Carpenter and D. A. Sweigart, *Organometallics*, **2003**, 22, 2364.

169. H. Schumqnn, A. M. Arif and T.G. Richmond, *Polyhedron***, 1990**, 9, 1677.

170. Y.-S. Huang, S. Sabo-Etienne, X.-D. He and B. Chaudret, *Organometallics*, **1992**, 11, 3031.

171. J. L. Bras, H. Amouri and J. Vaissermann, *Organometallics*, **1998**, 17, 1116.

172. H. Amouri and J. Le Bras, *Acc. Chem. Res.*, **2002**, 35, 501.

173. S. Sun, G. B. Carpenter and D. A. Sweigart, *J. Organomet. Chem.*, **1996**, 512, 257.

174. M. Oh, J. A. Reingold, G. B. Carpenter and D. A. Sweigart, *Coord. Chem. Rev.*, **2004**, 248, 561.

175. M. Oh, G. B. Carpenter and D. A Sweigart, *Organometallics,* **2002**, 21, 1290.

176. M. Oh, G. B. Carpenter and D. A. Sweigart, *Angew. Chem., Int. Ed.*, **2001**, 40, 3191.

177. C. G. Pierpont, *Coord. Chem. Rev.*, **2001,** 216, 99.

178. C. G. Pierpont and R. M. Buchanan, *Coord. Chem. Rev.*, **1981**, 38, 45.

179. C. G. Pierpont and C. W. Lange, *Prog. Inorg. Chem.*, **1994**, 41, 331.

180. F. Rohrscheid, A. L. Balch and R. H. Holm, *Inorg. Chem.*, **1966**, 5, 1542.

181.R. M. Buchanan and C. G. Pierpont, *J. Am. Chem. Soc.*, **1980**,102, 4951.

182. R.M. Buchanan and C.G. Pierpont, *Inorg. Chem.*, **1979**, 18, 3439.

183. A. S. Attia and C. G. Pierpont, *Inorg. Chem.*, **1997**, 36, 6184.

184. A. S. Attia and C. G. Pierpont, *Inorg. Chem.*, **1995**, 34, 1172.

185. A. S. Attia, O.-S. Jung and C. G. Pierpont, *Inorg. Chim. Acta*, **1994**, 226, 91.

186. O.-S. Jung and C. G. Pierpont, *J. Am. Chem. Soc.*, **1994**, 116, 2229.

187. D. M. Adams, A. Dei, A. L. Rheingold and D. N. Hendrickson, *J. Am. Chem. Soc.*, **1993**, 115, 8221.

188. P. Gutlich and A. Dei, *Angew. Chem. Int. Ed.*, **1997**, 37, 2734.

189. D. M. Adams and D. N. Hendrickson, *J. Am. Chem. Soc.*, **1996**, 118, 11515.

190. O.-S. Jung, D. H. Jo, Y.-A Lee, Y. S. Sohn and C. G. Pierpont, *Inorg. Chem.*, **1998**, 37, 5875.

191. D. M. Adams, L. Noodleman and D. N. Hendrickson, *Inorg. Chem.*, **1997**, 36, 3966.

192. A. S. Attia, S. Bhattacharya and C. G. Pierpont, *Inorg. Chem.*, **1995**, 34, 4427.

193. M. W. Lynch, D. N. Hendrickson, B. J. Fitzgerald and C. G. Pierpont, *J. Am. Chem. Soc.*, **1984**,106, 2041.

194. W. S. Durfee and C. G. Pierpont, *Inorg. Chem.*, **1993**, 32, 493.

195. K. Yamada, S. Yagishita, H. Tanaka, K. Tohyama, K. Adachi, S. Kaizaki, H. Kumagai, K. Inoue, R. Kitaura, H.-C. Chang, S. Kitagawa and S. Kawata, *Chem. Eur. J.*, **2004**, 10, 2647.

196. E. Katz and I. Willner, *Electrochem. Commun.*, **2006**, 8. 879.

197. E. Katz and H.-L. Schmidt, *J. Electroanal. Chem.*, 1993, 360, 337.

198. E. Katz and I. Willner, *Langmuir*, **1997**, 13, 3364.

199. E. Katz and I. Willner, *Chem. Commun.*, **2005**, 5641.

200. F. Vogtle, *Supramolecular Chemistry*, Wiley: Chichester, **1991**, 313.

201. J. W. Steed and J. L. Atwood, *Supramolecular Chemistry*, 2nd edition. Wiley: Chichester, **2009**, 707-775.

202. H. Wu, D. Zhang, L. Su, K. Ohkubo, C. Zhang, S. Yin, L. Mao, Z. Shuai, S. Fukuzumi and D. Zhu, *J. Am. Chem. Soc.*, **2007**, 129, 6839.

203. E. F. Elslager, M. L. Werbel and D. F. Worth, *J. Med. Chem.*, **1970**, 13,104.

204. H. J. Kallmayer and C. Tappe, *Pharm. Acta Helv.*, **1987**, 62, 2.

205. F. J. Bullock, J. F. Tweedie, D. D. McRitchie and D. Aurther, *J. Chem. Soc. C*, **1969**, 1799.

206. R. A. William and K.-L. Anja, *Trends Biochem. Sci.*, **2001**, 26, 648.

207. J. H. R. Tucker and S. R. Collinson, *Chem. Soc. Rev.*, **2002**, 31, 147.

208. D. Summerer, S. Chen, N. Wu, A. Deiters, J. W. Chin and P. G. Schultz, *Proc. Nat. Acad. of Sci. USA*, **2006**,103, 9785.

209. C-K. Ryu, J.-Y. Shim, M. J. Chae, I. H. Choi, J.-Y. Han, O.-J. Jung, J. Y. Lee and S. H. Jeong, *Eur. J. Med. Chem.*, **2005**, 40, 438.

210. Y. Sutovsky, G. I. Likhtenshtein and S. Bittner, *Tetrahedron*, **2003**, 59, 2939.

211. C. D. Gabbutt, J. D. Hepworth and B. M. Heron, *Tetrahedron*, **1994**, 50, 7865.

212. P. Asenjo, F. Farina, M. V. Martin, M. C. Paredes and J. J. Soto, *Tetrahedron lett.*, **1995**, 36, 319.

213. T. C. McKenzie, W. Hassen and S. J. F. Macdonald, *Tetrahedron Lett.,* **1987**, 28, 5435.

214. M. A. Brimble, E. Ireland and S. J. Phythian, *Tetrahedron Lett.*, **1991**, 32, 6417.

215. G. A. Kraus and J. A. Walling, *Tetrahedron Lett.*, **1986**, 27, 1873.

216. R. A. Illos, E. Harlev and S. Bittner, *Tetrahedron Lett.*, **2005**, 46, 8427.

217. M. Iwao and T. Kuraishi, *Tetrahedron Lett.*, **1985**, 26, 6213.

218. M. A. Brimble, O. Laita and J. E. Robinson, *Tetrahedron*, **2006**, 62, 3021.

219. R. A. Illos, D. Shamir, L. J. W. Shimon, I. Zilbermannc and S. Bittner, *Tetrahedron Lett.*, **2006**, 47, 5543.

220. A. Schmidt, M. Topp, T. Mordhorsta and O. Schneider, *Tetrahedron*, **2007**, 63, 1842.

221. J. S. Yadav, B. V. S. Reddy, T. Swamy and N. Ramireddy, *Synthesis*, **2004**, 1849.

222. F. H. Fry, A. L. Holme, N. M. Giles, G. I. Giles, C. Collins, K. Holt, S. Pariagh, T. Gelbrich, M. B. Hursthouse, N. J. Gutowski and C. Jacob, *Org. Biomol. Chem.*, **2005**, 3, 2579.

223. A. Decken, A. Mailman, S. M. Mattar and J. Passmore, *Chem. Commun.*, **2005**, 2366.

224. S. G. Polonik, P. S. Dmitrenok, V. V. Makhankov, V. F. Anufriev and N. Vorozhtsov, *Russ J. Org. Chem.,* **2006**, 42, 302.

225. W.-D. Rudorf, D. Loos, J. Wybraniec, N. Pronayova, R, Gawinecki and Z. Sustekova, *Coll. Czech. Chem. Commun.*, **2006**, 71, 59.

226. D. Frederic, G. Nicolas, G.-P. Nuria, S. Yuecel, L. Eric, M. Nicolas, H. Pietrick, M. Matteo, G. Alberto, L. Vega, V.-G. Jose, V. Jaume and R. Concepcio, *J. Org. Chem.*, **2004**, 69, 2164.

227. R. Adams, B. H. Braun and S. H. Pomerantz, *J. Am.Chem. Soc.*, **1953**, 75, 642.

228. C. Blackburn, *Tetrahedron Lett.*, **2005**, 46 , 1405.

229. M. V. Stasevych, M. Y. Plotnikov, M. O. Platonov, S. I. Sabat, R. Y. Musyanovych and V. P. Novikov, *Heteroatom Chem.*, **2005**, 16, 587.

230. V. Wittebolle, S. Lemriss, G. L. Morella, J. Errante, P. Boiron, R. Barret and M. E. Sarciron, *Mycoses*, **2006**, 49, 169.

231. M. P. Soriaga and A. T. Hubbard, *J. Am. Chem. Soc.*, **1982**, 104, 2737.

232. T. Sakamoto, H. Yonehara and C. Pac, *J. Org. Chem.*, **1997**, 62, 3194.

233. A. Puzari and J. B. Baruah, *J. Mol. Catal. A: Chem.*, **2002**, 187, 149.

234. S. Sharma, N. Barooah and J. B. Baruah, *J. Mol. Catal. A: Chem.*, **2005**, 229, 171.

235 E. Bosch, R. Rathore and J. K. Kochi, *J. Org. Chem.*, **1994**, 59, 2529.

236. R. Rathore, E. Bosch, J. K. Kochi, *Tetrahedron Lett.*, **1994**, 35, 1335.

237. D. E. Van Sickle, G. L. Myers, W. D. Nottingham and G. C. Jones, US Patent 5118823, **1992**.

238. D. Villemin, M. Hammadi and M. M. Hachemi, *Synth. Commun.*, **2002**, 32, 1501.

239. D. R. Hwang, C. Y. Chu, S. K.Wang and B. J. Uang, *Synlett*, **1999**, 77.

240. B. Sain, P. S. Murthy, T. V. Rao, T. S. R. P. Rao and G. C. Joshi, *Tetrahedron Lett.*, **1994**, 35, 5083.

241. I. A. Owsik and B. N. Kolarz, *Catalysis Today*, 2004, 91, 199.

242. H. Zhou, Z. Q. Pan, Q. H. Luo, G. Q. Mei, D. L. Long and J. T. Chen, *Chin. J. Chem.*, **2005**, 23, 835.

243. K. Sakai, T. Tsubomura and K. Matsumoto, *Inorg. Chim. Acta*, **1995**, 234, 157.

244. K. Sakata, T. Kikutake, Y. Shigaki and M. Hashimoto, *Inorg. Chim. Acta*, **1988**, 144, 1.

245. S. Fujibayashi, K. Nakayama, Y. Nishiyama and Y. Ishii, *Chem. Lett.*, **1994**, 1345.

246. P. A. Ganeshpure, A. Sudalai, and S. Satish, *Tetrahedron Lett.*, **1989**, 30, 5929.

247. S. Muralidharan and H. Freiser, *J. Mol. Catal. A: Chem.*, **1989**, 50, 181.

248. H. Miyamura, M. Shiramizu, R. Matsubara and S. Kobayashi, *Angew. Chem. Int. Ed.*, **2008**, 120, 8213.

249. H. Miyamura, M. Shiramizu, R. Matsubara and S. Kobayashi, *Chem. Lett.*, **2008**, 37, 360.

250. S. Padhye, S. Banerjee, A. M. Ahmad and R. Sarkar. *Cancer. Ther.*, **2008**, 6, 495.

251. S. Banerjee, A. O. Kaseb and Z. Wang, *Cancer. Res.*, 2009, 69, 5575.

252. R. S. Ryan. *Anticancer Res.*, **2005**, 25, 2199.

253. A. M. Shoieb, M. Elgayyar, P. S. Dudrick, J. L. Bell and P. K. Tithof, *Int. J. Oncol.*, **2003**, 22,107.

254. H. Gali-Muhtasib, M. Diab-Assaf and C. Boltze, *Int J Oncol.*, **2004**, 25, 857.

255. M. Roepke, A. Diestel and K. Bajbouj, *Cancer Biol. Ther.*, **2007**, 6, 160.

256. L. S. Boulas and M. H. N. Arsanious, *Synth. Commun.*, **2002**, 32, 2779.

257. M. Aguilar-Martinez, G. Cuevas, M. Jimenez-Estrada, I. Gonzalez, B. Lotina-Hennsen and N. Macias-Ruvalcaba, *J. Org. Chem.*, **1999**, 64, 3684.

258. N. R. Sperandeo and R. Brun, *Chem. Bio. Chem.*, **2003**, 4, 69.

259. W. M. Horspool, P. I. Smith and J. M. Tedder, *J. Chem. Soc., Perkin Trans. 1*, **1972**, 1024.

260. Vogel's Textbook of Practical Organic Chemistry, 5th ed, revised by B. S. Furniss, A. J. Hannaford, P. W. G. Smith and A. Tatchell, Longmann Scientific & Technical, UK, **1989**.

261. G. M. Sheldrick, SHELXS97, *Program for the Solution of Crystal Structures*, Univ. of Gottingen, Germany, **1997**.

262. G. M. Sheldrick, SHELXL97, *Program for the Refinement of Crystal Structures*. Univ. of Gottingen, Germany, **1997**.

263. SHELXTL Release 5.10; *The Complete Software Package for Single Crystal Structure Determination*. Bruker AXS Inc., Madison, WI 53719-1173, **1997**.

264. L. L. Shen, J. Baranowski and A. G. Pernet, *Biochemistry*, **1989**, 28, 3879.

265. X. Chen and B. Ramakrishnan, *J. Mol. Biol.*, **1997**, 267, 1157.

266. Y. Umezawa and M. Nishio, *Biopolymers*, **2005**, 79, 248.

267. G. R. Desiraju, *Science*, **1997**, 278, 404.

268. D. Braga, L. Maini, C. Fagnano, P. Taddei, M. R. Chierotti and R. Gobetto, *Eur. J. Chem.*, **2007**, 13, 1222.

269. A. M. Bittner, P. Behrens and E. Baeuerlein, *Handbook of Biomineralization: Biomimetic and Bioinspired Chemistry*, **2007**, 335.

270. A. Kalman, L. Fabian, G. Argay, G. BernPth and Z. Gyarmati, *J. Am. Chem. Soc.*, **2003**, 125, 34.

271. I. Weissbuch, V. Y. Torbeev, L. Leiserowitz and M. Lahav, *Angew. Chem. Int. Ed.*, **2005**, 117, 3290.

272. M. Morimoto, S. Kobatake and M. Irie, *Chem. Eur. J.*, **2003**, 9, 621.

273. P. Raiteri, R. Martooak and M. Parrinello, *Angew. Chem. Int. Ed.*, **2005**, 117, 3835.

274. P. K. Thallapally, R. K. R. Jetti, A. K. Katz, H. L. Carrell, K. Singh, K. Lahiri, S. Kotha, R. Boese and G. R. Desiraju, *Angew. Chem. Int. Ed.*, **2004**, 116, 1169.

275. G. R. Desiraju, *Angew. Chem. Int. Ed.*, **1995**, 107, 2541.

276. R. J. Davey, *Chem. Commun.*, **2003**, 1463.

277. N. Blagden and R. J. Davey, *Cryst. Growth Des.*, **2003**, 3, 873.

278. P. Erk, H. Hengelsberg, M. F. Haddow, R. van Gelder, *CrystEngComm*, **2004**, 6, 474.

279. J. Bernstein, *Chem. Commun*., **2005**, 5007.

280. S. R. Bryn, R. R. Pfeiffer and J. G. Stowell, *Solid-State Chemistry of Drugs*, SSCI, West Lafayette IN, **1999**.

281. V. N. Nesterov, V. V. Nesterov, *Acta Cryst. C*, **2004**, 60, 781.

282. J. Pacifico, H. Stoeckli-Evans, *Acta Cryst. C*, **2004**, 60, 152.

283. F. A. Tabellion, S. R. Seidel, A. M. Arif and P. J. Stang, *J. Am. Chem. Soc.*, **2001**, 123, 7740.

284. K. Kobayashi, R. Shimaoka, M. Kawahata, M. Yamanaka and K. Yamaguchi, *Org. Lett.*, **2006**, 8, 2385.

285. W. Anker, G. W. Bushnell, R. H. Mitchell, *Can. J. Chem.*, **1979**, 57, 3080.

286. F. Bottino, S. Foti, S. Pappalardo, P. Finocchiaro and M. Ferrugia, *J. Chem. Soc. Perkin Trans. I*, **1979**, 198.

287. F. Bottino and S. Pappalardo, *Tetrahedron Lett.*, **1980**, 36, 3095.

288. W. M. Wolf, *Acta Cryst. B*, **2001**, 7, 806.

289. X. He, U. J. Griesser, J. G. Stowell, T. B. Borchardt and S. R. Byrn, *J. Pharm. Sci.*, **2001**, 90, 371.

290. G. Hogarth and I. Richards, *Inorg. Chem. Commun.*, **2007**, 10, 66.

291. K. Okamoto, H. Umehara and J. Hidaka, *Bull. Chem. Soc. Japan*, **1987**, 60, 2875.

292. L. Ma, S. Liu, H. Zhu and J. Zubieta, *Polyhedron*, **1989**, 8, 669.

293. P. Li, M. Wang, C. He, G. Li, X. Liu, C. Chen, B. Akermark and L. Sun, *Eur. J. Inorg. Chem.*, **2005**, 2506.

294. R. S. Morgan and J. M. McAdon, *Int. J. Peptide and Protein Res.*, **1980**, 15, 177.

295. F. I. Adam, G. Hogarth, I. Richards and B. E. Sanchez, *J. Chem. Soc. Dalton Trans.*, **2007**, 2495.

296. A. Nangia and G. R. Desiraju, in: E. Weber (Ed.), *Supramolecular Synthons and Pattern Recognition: Design of Organic Solids*, Springer-Verlag, Berlin, **1998**

295. C.-L. Lin, C.-C. Lai, Y.-H. Liu, S.-M. Peng and S.-H. Chiu, *Chem. A. Eur. J.* **2007**, 13, 4350.

296. H. J. Schneider, *Angew. Chem., Int. Ed.*, **1991**, 30, 1417.

297. J. C. MacDonald and G. M. Whitesides, *Chem. Rev.*, **1994**, 94, 2383.

298. T. Suzuki, H. Fuji, T. Miyashi and Y. Yamashita, *J. Org. Chem.*, **1992**, 57, 6744.

299. S. H. Dale, M. R. J. Elsegood and A. E. L. Cooombs, *CrystEngComm*, **2004**, 6, 328.

300. S. Subramanian and M. J. Zawarotko, *Coord. Chem. Rev.*, **1994**, 137, 357.

301. D. Braga, F. Grepioni and G. R. Desiraju, *Chem.Rev.*, **1998**, 98, 1375.

302. P. Chakrabarti and U. Samanta, *J. Mol. Biol.*, **1995**, 251, 9.

303. A. Ghosh and M. Bansal, *Acta Crystallogr. Sect. D: Biol. Crystallogr.*, **1999**, 55, 2005.

304. M. Harigai, M. Kataoka and Y. Imamoto, *J. Am. Chem. Soc.*, **2006**, 128, 10646.

305. L. Jiang and L. Lai, *J. Biol. Chem.*, **2002**, 277, 37732.

306. S. Scheiner, T. Kar and Y. Gu, *J. Biol. Chem.*, **2001**, 276, 9832

307. G. R. Desiraju, *Acc. Chem. Res.*, **1991**, 24, 290.

308. H. Yoshida, T. Harada, K. Ohno and H. Matsuura, *Chem. Commun.*, **1997**, 2213.

309. Y. Gu and T. Kar, *J. Am. Chem. Soc.*, **1999**, 121, 9411.

310. J. B. Baruah, A. Karmakar and N. Barooah, *CrystEngComm*, **2008**, 10, 151.

311. J. A. Potenza, T. J. Emge, J. Albaneze, S. Knapp and H. J. Schugar, *Acta Cryst. C*, **2000**, 56, 1494.

312. J. Ireta, J. Neugebauer and M. Scheffler, *J. Phys. Chem. A*, **2004**, 108, 5692.

313. P. Hohenberg and W. Kohn, *Phys. Rev. B*, **1964**, 136, 864.

314. A. D. Becke, *J. Chem. Phys.*, **1993**, 98, 5648.

315. C. Lee, W. Yang and R. G. Parr, *Phys. Rev. B*, **1988**, 37, 785.

316. A. Dkhissi, L. Adamowicz and G. Maes, *J. Phys. Chem. A*, **2000**, 104, 2112.

317. A. Dkhissi, L. Adamowicz and G. Maes, *Chem. Phys. Lett.*, **2000**, 324, 127.

318. D. E. Woon and T. H. Jr. Dunning, *J. Chem. Phys.*, **1993**, 98, 1358.

319. GAUSSIAN03, *Revision B.05; Gaussian, Inc.: Pittsburgh, PA*, **2003**.

320. GAUSSIAN03, *Revision B.05; Gaussian, Inc.: Pittsburgh, PA*, **2003**.

321. G. Chalasinski and M. Szczesniak, *Chem. Rev.*, **1994**, 94, 1723.

322. G. M. Whitesides, E. E. Simanek, J. P. Mathias, C. T. Seto, D. N. Chin, M. Mammen and D. M. Gordon, *Acc. Chem. Res.*, **1995**, 28, 37.

323. R. B. Grossman, K. Hattori, S. Parkin, B. O. Patrick and M. A. Varner, *J. Am. Chem. Soc.*, **2002**, 124, 13686.

324. J. Bernstein, R. E. Davis, L. Shimoni and N. L. Chang, *Angew. Chem. Int. Ed.*, **1995**, 34, 1555.

325. D. Braga, F. Grepioni and G. Desiraju, *Chem. Rev.*, **1998**, 98, 1375.

326. S. H. Druker and M. D. Curtis, *J. Am. Chem. Soc.*, **1995**, 117, 6366.

327. W. D. Jones, R. M. Chin and C. L. Hoaglin, *Organometallics*, **1999**, 18, 1786.

328. L. Lefort, T. W. Crane, M. D. Farwell, D. M. Baruch, J. A. Kaeuper, R. J. Lachicotte and W. D. Jones, *Organometallics*, **1998**, 17, 3889.

329. D. A. Vicic and W. D. Jones, *Organometallics*, **1999**, 18, 134.

330. C. Bianchini and A. Meli, *Acc. Chem. Res.*, **1998**, 31, 109.

331. T. V. Choudhary, J. Malandra, J. Green, S. Parrott and B. Johnson, *Angew. Chem. Int. Ed.*, **2006**, 45, 3299.

332. K. Fujisawa, Y. Moro-oka and N. Kitajima, *Chem. Commun.*, **1994**, 623.

333. L. Han, M. Hong, R. Wang, B. Wu, Y. Xu, B. Lou, Z. Lin, *Chem. Commun.*, **2004**, 2578.

334. D. Shimizu, N. Takeda and N. Tokitoh, *Chem. Commun.*, **2006**, 177.

335. M. Li, A. Ellern and J. H. Espenson, *Angew Chem. Int Ed.*, **2004**, 43, 5837.

336. E. Lopez-Torres, M. A. Mendiola and C. J. Pastor, *Inorg. Chem.*, **2006**, 45, 3103.

337. S. C. Schuman and H. Shalit, *Catal. Rev.*, **1970**, 4, 245.

338. R. J. Angelici, *Acc. Chem. Res.*, **1988**, 21, 387.

339. N. N. Sauer, E. J. Markel, G. L. Schrader and R. J. Angelici, *J. Catal.*, **1989**, 117, 295.

340. W. D. Jones, D. A. Vicic, R. M. Chin, J. H. Roache and A. W. Myers, *Polyhedron*, **1997**, 16, 3115.

341. X.-L Geng, Z. Wang, X.-Q. Li and C. Zhang, *J. Org. Chem.*, **2005**, 70, 9610.

342. M. Wu, B. Wang, S. Wang, C. Xia and W. Sun, *Org. Lett.*, **2009**, 11, 3625.

343. M. A. Reynolds, I. A. Guzei and R. J. Angelici, *Inorg. Chem.*, **2003**, 42, 2191.

344. D. Coucouvanis, A. Hadjikyriacou, R. Lester and M. G. Kanatzidis, *Inorg. Chem.*, **1994**, 33, 3645.

345. T.-Y. Luh and Z.-J. Ni, *Synthesis*, **1999**, 89.

346. D. A. Vicic and W. D. Jones, *J. Am. Chem. Soc.*, **1999**, 121, 7606.

347. W. D. Jones, K. A. Reynolds, C. K. Sperry, R. J. Lachicotte, S. A. Godleski and R. Valente, *Organometallics*, **2000**, 191, 661.

348. P. Chaudhuri, M. Hess, U. Florke and K. Weghardt, *Angew. Chem. Int Ed.*, **1998**, 37, 2217.

349. H.-J. Kruger, *Angew. Chem. Int. Ed.*, **1999**, 38, 627.

350. R. C. Pratt and T. D. P. Stack, *J. Am. Chem. Soc.*, **2003**, 123, 8716.

351. D. Shimizu, N. Takeda and N. Tokitoh, *Chem. Commun.*, **2006**, 177.

352. M. Li, A. Ellern and J. H. Espenson, *Angew. Chem. Int. Ed.*, **2004**, 43, 5837.

353. M. Li, A. Ellern and J. H. Espenson, *J. Am. Chem. Soc.*, **2005**, 127, 10436.

354. T. D. Tullius, P. Frank and K. O. Hodgson, *Proc. Natl. Acad. Sci.*, **1978**, 75, 4069.

355. J. A. Halfen, S. Mahapatra, E. G. Wilkinson, S. Kadeerli, V. G. Young Jr., Lawrence Que Jr., A. Zuberbuhler and W. B. Tolman, *Science*, **1996**, 271, 1397.

356. S. Reinoso, P. Vitoria, L.S. Felices, A. Montero, L. Lezama and J. M. Gutiérrez-Zorrilla, *Inorg. Chem.*, **2007**, 46, 1237.

357. M. Kodera, H. Shimakoshi, Y. Tachi, K. Katyama and K. Kano, *Chem. Lett.*, **1998**, 441.

358. E. C. Constable, *Chem. Ind.*, **1994**, 56.

359. C. Huang, S. Gou, H. Zhu and W. Huang, *Inorg. Chem.*, **2007**, 46, 5537.

360. H. Alper, and F. Sibtain, *J. Organomet. Chem.*, **1985**, 285, 225.

361. C. T. Ng, X. Wang and T.-Y. Luh, *J. Org. Chem.*, **1988**, 53, 2536.

362. H. Alper, F. Sibtain and J. Haveling, *Tetrahedron Lett.*, **1983**, 24, 5329.

363. J. Simaan, S. Poussereau, G. Blondin, J. J. Girerd, D. Defaye, C. Philouze, J. Guilhem and L. Tchertanov, *Inorg. Chim. Acta*, **2000**, 299, 221.

364. K. J. Lee, I. Yoon, S. S. Lee, B. Y. Lee, *Bull. Korean Chem. Soc.*, **2002**, 23, 399.

365. W. M. Singh and J. B. Baruah, *Synth Commun.*, **2009**, 39, 325.

366. Z. Jixiong, Z. Yingjun, H. Maochun, S. Daofeng, S. Qian and C. Rong, *Chem. lett.*, **2002**, 31, 484.

367. K. A. Jorgensen, *Chem. Rev.*, **1989**, 89, 431.

368. Q.-H. Xia, H.-Q. Ge, C.-P. Ye, Z.-M. Liu and K.-X. Su, *Chem. Rev.*, **2005**, 105, 1603.

369. G. Dubois, A. Murphy and T. D. P. Stack, *Org. Letters*, **2003**, 5, 2469.

370. B. S. Lane and K. Burgess, *Chem. Rev.*, **2003**, 103, 2457.

371. L. Que Jr. and B.T. William, *Nature*, **2008**, 455, 333.

372. J.-E. Backvall, Ed. *Modern Oxidation Methods*; Wiley-VCH: Weinheim, Germany, **2004**.

373. F. G. Gelacha, B. Bitterlich, G. Anilkumar, M. K. Tse and M. Beller, *Angew. Chem. Int. Ed.*, **2007**, 46, 7293.

374. M. B. Francis and E. N. Jacobsen, *Angew. Chem. Int. Ed.*, **1999**, 38, 937.

375. O. F. Cheng, X. Y. Xu, W. X. Ma, S. J. Yang and T. P. You, *Chin. Chem. Lett.*, **2005**, 16, 1467.

376. M. Costas, M. P. Mehn, M. P. Jensen and Jr. L. Que, *Chem. Rev.*, **2004**, 104, 939.

377. J. W. De Boer, W. R. Browne, J. Brinksma, P. L. Alsters, R. Hage and B. L. Feringa, *Inorg. Chem.*, **2007**, 46, 6353.

378. M. C. White, A. G. Doyle and E. N. Jacobsen, *J. Am. Chem. Soc.*, **2001**, 123, 7194.

379. B. Bitterlich, G. Anilkumar, F. G. Gelalcha, B. Spilker, A. Grotevendt, R. Jackstell, M. K. Tse and M. Beller, *Chem. Asian J.*, **2007**, 2, 521.

380. S. Taktak, W. Ye, A. M. Herrera and E. V. Rybak-Akimova, *Inorg. Chem.*, **2007**, 46, 2929.

381. K. A. Srinivas, A. Kumar and S. M. S. Chauhan, *Chem. Commun.*, **2002**, 2456.

382. W. Nam, H. J. Lee, S.-Y. Oh, C. Kim and H. G. Jang, *J. Inorg. Biochem.*, **2000**, 80, 219.

383. J. Wahlen, D. E. de Vos and P. A. Jacobs, *Organic Lett.*, 2003, 5, 1777.

384. L. L. Koh, Y. Xu, A. K. Hsieh, B. Song, F. Wu and L. Ji, *Acta Cryst.*, **1994**, C50, 884.

385. F. H Allen, *Acta Cryst.*, **2002**, B58, 380.

386. V. C. R. Payne, R. T. Stibrany and A. A. Holder, *Anal. Science*, **2007**, 23, 169.

387. M. G. Ondrus and G. Gordon, *Inorg. Chem.*, **1971**, 10, 474.

388. T. J. Terry, G. Dubois, A. Murphy and T. D. P. Stack, *Angew. Chem. Int. Ed.*, **2007**, 46, 945.

389. B. Meunier, *Chem. Rev.*, **1992**, 92, 1411.

390. D. Dolphin, T. Taylor and G. Xie, *Acc. Chem. Res.*, **1997**, 30, 251.

391. J. P. Collman, X. Zhang, V. J. Lee, E. S. Uffelman and J. I. Brauman, *Science*, **1993**, 261, 1404.

392. C. Janiak, *J. Chem. Soc. Dalton Trans.*, **2003**, 2781.

393. M. Nishio, *CrystEngComm*, **2004**, 6, 130.

394. M. Nishio, M. Hirota, and Y. Umezawa, *The CH/*p *interaction (Evidence, Nature and consequences)*, Wiley-VCH, **1998**.

395. C. Janiak, S. Temizdemir, S. Dechert, W. Deck, F. Girgsdies, J. Heinze, M. J. Kolm, T. G. Scharmann and O. M. Zipffel, *Eur. J. Inorg. Chem.*, **2000**, 1229.

396. R. Robson, B. F. Abrahams, S. R. Batten, R. W. Gable, B. F. Hoskins and J. P. Liu, *ACS Symp. Ser.*, **1992**, 499, 256.

397. S. Kitagawa and S. Noro, *Compreh. Coord. Chem.*, **2004**, *7*, 231.

398. F. A. Cotton, C. Lin and C. A. Murillo, *Acc. Chem. Res.*, **2001**, 34, 759.

399. R. Murugavel, M. G. Walawalkar, M. Dan, H. W. Roesky and C. N. R. Rao, *Acc. Chem. Res.*, **2004**, 37, 763.

400. L. Brammer, M. D. Burgard, M. D. Eddleston, C. S. Rodger, N. P. Rath and H. Adams, *CrystEngComm*, **2002**, 4, 239.

401. L. Brammer, M. D. Burgard, C. S. Rodger, J. K. Swearingen and N. P. Rath, *Chem. Commun.*, **2001**, 2468.

402. C. M. Rivas and L. Brammer, *Coord. Chem. Rev.*, **1999**, 183, 43.

403. A. Messerschmidt, A. Huber, T. Poulos and K. Wieghardt (Eds.), *Handbook of Metalloproteins*, Wiley, Chichester, UK, **2001**.

404. J. T. Groves and L. Ann Baron, *J. Am. Chem. Soc.*, **1989**, 111, 5442.

405. H. Shim and F. M. Raushel, *Biochemistry*, **2000**, 39, 7357.

406. R. C. Holz, *Coord. Chem. Rev.*, **2002**, 232, 5.

407. Y.-H. Liu, H.-L. Tsai, Y.-L. Lu, Y.-S. Wen, J.-C. Wang and K.-L. Lu, *Inorg. Chem.*, **2001**, 40, 6426.

408. R. A. Reynolds III, W. R. Dunham and D. Coucouvanis, *Inorg. Chem.*, **1998**, 37, 1232.

409. R. Lachicotte, A. Kitaygorodskiy and K. S. Hagen, *J. Am. Chem. Soc.*, **1993**, 115, 8883.

410. D. M. Kurtz, *Chem. Rev.*, **1996**, 96, 585.

411. C. He and S. J. Lippard, *J. Am. Chem. Soc.*, **1998**, 120, 105.

412. A. M. Barrios and S. J. Lippard, *J. Am. Chem. Soc.*, **2000**, 122, 9172.

413. D. Lee, P.-L. Hung, B. Spingler and S. J. Lippard, *Inorg. Chem.*, **2002**, 41, 521.

414. A. Caneschi, F. Ferraro, D. Gatteschi, M. C. Melandri, P. Rey and R. Sessoli, *Angew. Chem., Int. Ed.*, **1989**, 42, 4409.

415. S.-B. Yu, S. J. Lippard, I. Shweky and A. Bino, *Inorg. Chem.*, **1992**, 31, 3502.

416. M. Alexiou, C. Dendinou-Samara, A. Karagianni, S. Biswas, C. M. Zaleski, J. Kampf, D. Yoder, J. E. Penner-Hann, V. L. Pecoraro and D. P. Kessissoglou, *Inorg. Chem.*, **2003**, 42, 2185.

417. V. L. Pecoraro, M. J. Baldwin, M. T. Caudle, W.-Y. Hsieh and N. A. Law, *Pure Appl. Chem.*, **1998**, 70, 925.

418. N. A. Law, T. Caudle and V. L. Pecoraro, *Adv. Inorg. Chem.*, **1999**, 46, 305.

419. C. E. Dube, R. Sessoli, M. P. Hendrich, D. Gatteschi and W. A. Amstrong, *J. Am. Chem. Soc.*, **1999**, 121, 3537.

420. R. Herchel, R. Boca, M. Gembicky, K. Falk, H. Fuess, W. Haase and I. Svoboda, *Inorg. Chem.*, **2007**, 46, 1544.

421. D. Maspoch, J. Gomez-Segura, N. Domingo, D. Ruiz-Molina, K. Wurst, C. Rovira, J. Tejada and J. Veciana, *Inorg. Chem.*, **2005**, 44, 6936.

422. R. D. Poulsen, A. Bentien, M. Chevalier and B. B. Iversen, *J. Am. Chem. Soc.*, **2005**, 127, 9156.

423. Z. Wang, V. Ch. Kravtsov and M. J. Zaworotko, *Angew. Chem., Int. Ed.*, **2005**, 44, 2877.

424. Y. Cui, O. R. Evans, H. L. Ngo, P. S. White and W. Lin, *Angew. Chem., Int. Ed.*, **2002**, 41, 1159.

425. S. Wang, H. Xing, Y. Li, J. Bai, Y. Pan, M. Sheer and X. You, *Eur. J. Inorg. Chem.*, **2006**, 3041.

426. C. Mellot-Draznieks and G. Ferey, Prog. *Solid State Chem.*, **2005**, 33, 187.

427. F. M. Tabellion, S. R. Siedel, A. M. Arif and P. J. Strang, *J. Am. Chem. Soc.*, **2001**, 123, 7740.

428. J. Moncol, P. Segla, D. Miklos, M. Mazur, M. Melnik, T. Glowiak, M. Valko and M. Koman, *Polyhedron*, **2006**, 25, 1561.

429. B. Moulton and M. J. Zaworotko, *Chem. Rev.*, **2001**, 101, 1629.

430. Y. Rodirigues-Martin, M. Haernadez-Molina, F. S. Delgado, J. Pasan, C. Ruiz-Perez, J. Sanchiz, F. Lloret and M. Julve, *CrystEngComm*, **2002**, 4, 522.

431. A. Erxleben, *Coord. Chem. Rev.*, **2003**, 246, 203.

432. S. Hu, H.-H. Zou, M.-H. Zeng, Q.-X. Wang and H. Liang, *Cryst. Growth Des.*, **2008**, 8, 2346.

433. S. Jung and M. Oh, *Angew. Chem., Int. Ed.*, **2008**, 47, 2049.

434. Y. Gong, R. Wang, D. Yuan, W. Su, Y. Huang, C. Yue, F. Jiang and M. Hong, *Polyhedron*, **2007**, 26, 5309.

435. P. D. C. Dietzel, R. Blom and H. Fjellvag, *J. Chem. Soc., Dalton Trans.*, **2006**, 586.

436. Y. Wei, H. Hou, L. Li, Y. Fan and Y. Zhu, *Cryst. Growth Des.*, **2005**, 5, 1405.

437. K.-L. Lu, Y.-F. Chen, Y.-H. Liu, Y.-W. Cheng, R.-T. Liao and Y.-S. Wen, *Cryst. Growth Des.*, **2005**, 5, 403.

438. M. Rombach, M. Gelinsky and H. Vahrenkamp, *Inorg. Chim. Acta*, **2002**, 334, 25.

439. N. Lalioti, C. P. Raptopoulou, A. Terzis, A. Panagiotopoulos, S. P. Perlepes and E. Manessi-Zoupa, *J. Chem. Soc., Dalton Trans.*, **1998**, 1327.

440. S. G. Baca, I. G. Filippova, N. V. Gerbeleu, Y. A. Simonov, M. Gdaniec, G. A. Timco, O. A. Gherco and Y. L. Malaestean, *Inorg. Chim. Acta*, **2003**, 344, 109.

441. H. A. Habib, J. Sanchiz and C. Janiak, *J. Chem. Soc., Dalton Trans.*, **2008**, 1734.

442. H. A. Habib, J. Sanchiz and C. Janiak, *J. Chem. Soc., Dalton Trans.*, **2008**, 4877.

443. B. Wisser, A.-C. Chamayou, R. Miller, W. Scherer and C. Janiak, *CrystEngComm*, **2008**, 10, 461.

444. M. Domagata, S. J. Grabowski, K. Ubrbaniak and G. Mloston, *J. Phys. Chem., B,* **2003**, 107, 2730.

445. J. J. Novoa, M. C. Rovira,C. Rovira, J. Veciana and J. Tarres, *Adv. Mater.*, **1995**, 7, 233.

446. Z. R. Zhou, W. Xu, Y. Xia, Q. R. Wang, Z. B. Ding, M. Q. Chen, Z. Y. Hua and F. G. Tao, *Acta Cryst.*, **2001**, C57, 471.

447. I. Brito, A. Mundaca, A. Cardenas and M. Lopez-Rodriguez, *Acta Cryst.*, **2008**, E64, o102.

448. M. Chen, X.-D. Chen and M. Du, *Acta Cryst.*, **2007**, C63, m570.

449. X.-P. Li, M. Pan, S.-R. Zheng, Y.-R. Liu, Q.-T. He, B.-S. Kang and C.-Y. Su, *Cryst. Growth Des.*, **2007**, 7, 2481.

450. C. Janiak, *J. Chem. Soc., Dalton Trans.*, **2000**, 3885.

451. A. Michaelides, C. D. Papadimitriou, J. C. Plakatouras, S. Skoulika and P. G. Veltsistas, *Polyhedron*, **2004**, 23, 2587.

452. B. Barszcz, S. Hodorowicz, A. Jablonska-Wawrzycka and K. Stadnicka, *J. Coord. Chem.*, **2005**, 58, 203.

453. Z.-F. Chen, R.-G. Xiong, B. F. Abrahams, X.-Z. You and C.-M. Che, *J. Chem. Soc., Dalton Trans.*, **2001**, 2453.

454. X.-L. Wang, C. Qin, E.-B. Wang and Z.-M. Su, *Chem. Eur. J.*, **2006**, 12, 2680.

455. H. C. LopezSadovel, N. Barbabehrens, S. Bernes, N. FarfanGarcia and H. Hoplf, *J. Chem. Soc., Dalton Trans.*, **1997**, 3415.

456. S. Sen, M. K. Saha, P. Kundu, S. Mitra, C. Kruger and J. Bruckmann, *Inorg. Chim. Acta*, **1999**, 288,118.

457. S. Banerjee, A. Ghosh, B. Wu, P.-G. Lassahn and C. Janiak, *Polyhedron*, **2005**, 24, 593.

458. S. Banerjee, P.-G. Lassahn, C. Janiak and A. Ghosh, *Polyhedron,* **2005**, 24, 2963.

459. C. Aakeröy, N. Champness and C. Janiak, *CrystEngComm*, **2010**, 12, 22.

460. H. A. Habib, J. Sanchiz and C. Janiak, *Inorg. Chim. Acta,* **2009**, 362, 2452.

461. S. K. Henninger, H. A. Habib and C. Janiak, J. *Am. Chem. Soc.*, **2009**, 131, 2776.

462. H. A. Habib, A. Hoffmann, H. A. Höppe and C. Janiak, *J. Chem. Soc., Dalton Trans.*, **2009**, 1742.

463. J. Yang, J.-F. Ma, Y.-Y. Liu and S. R. Batten, *CrystEngComm,* **2009**, 11, 151.

464. M. Du, Z.-H. Zhang, X.-G. Wang, L.-F. Tang and X.-J. Zhao, *CrystEngComm*, **2008**, 10, 1855.

465. Y.-Q. Lan, S.-L. Li, Y.-M. Fu, Y.-H. Xu, L. Li, Z.-M. Su and Q. Fu, *J. Chem. Soc., Dalton Trans.*, **2008**, 6796.

466. P. Ren, M.-L. Liu, J. Zhang, W. Shi, P. Cheng, D.-Z. Liao and S.-P. Yan, *J. Chem. Soc., Dalton Trans.*, **2008**, 4711.

467. A. Meijerink, G. Blasse and M. Glasbeek, *J. Phys. Condens. Matter*, **1990**, 2, 6303.

468. R. Bertoncello, M. Bettinelli, M. Cassrin, A. Gulino, E. Tondello and A. Vittadini, *Inorg. Chem.*, **1992**, 31, 1558.

469. S. Zang, Y. Su, Y-Z. Li, J. Lin, X. Duan, Q. Meng and S. Gao, *CrystEngComm*, **2009**, 11,122.

470. P. Ren, M.-L. Liu, J. Zhang, W. Shi, P. Cheng, D.-Z. Liao and S.-P. Yan, *J. Chem. Soc., Dalton Trans.*, **2008**, 4711.

471. W. Liu, L. Ye, X. Liu, L. Yuan, J. Jiang and C. Yan, *CrystEngComm*, **2008**, 10, 1395.

472. M. D. Allendorf, C. A. Bauer, R. K. Bhakta and R. J. T. Houka, *Chem. Soc. Rev.*, **2009**, 38, 1330.

List of Publications:

Articles/Papers based on this study have appeared in:

1. W. M. Singh and J. B. Baruah, *Inorg. Chem. Commun.*, **2010**, 13, 899-903.

2. S. Banerjee, A. S. Azmi, S. Padhye, W. M. Singh, J. B. Baruah, P. A. Philip, F. H. Sarkar and R. M. Mohammad, *Pharm. Res.*, **2010**, 27, 1146-1158.

3. P. R. Dandawate, A. C. Vyas, S. B. Padhye, M. W. Singh and J. B. Baruah, *Mini Rev. Med. Chem.*, **2010**, 10, 436-454.

4. W. M. Singh, J. B. Baruah, *Polyhedron*, **2010**, 29, 1543-1550.

5. W. M. Singh and J. B. Baruah, *J. Mol. Struct.*, **2009**, 931, 82-86.

6. W. M. Singh and J. B. Baruah, *Dalton Trans.*, **2009**, 2352-2358.

7. W. M. Singh and J. B. Baruah, *Synth. Commun.*, **2009**, 39, 1433-1442.

8. P. Mondal, A. Karmakar, W. M. Singh and J. B. Baruah, *CrystEngComm*, **2008**, 10, 1550-1559.

9. J. B. Baruah, W. M. Singh and A. Karmakar; *J. Mol. Struct.*, **2008**, 892, 84-87.

10. W. M. Singh, A. Karmakar and J. B. Baruah, *Inorg. Chem. Commun.*, **2008**, 11, 576-579.

11. W. M. Singh, A. Karmakar, N. Barooah and J. B. Baruah, *Beil. J. Org. Chem.*, **2007**, 3, 10.

12. W.M. Singh, J.B.Baruah, Characterization of molecular complexes of 1, 4-naphthoquinone derivatives, *J. Chem. Crystal.*, **2011** in press.

13. B. R. Jali, W.M. Singh and J.B.Baruah, Polymorphs of aromatic thiolato 1, 2 or 1,4-naphthoquinones, CrystEngComm., **2011**, 13, 763.